# DESIGN AND IMPLEMENTATION OF A CLOSED-LOOP BLOOD GLUCOSE CONTROL SYSTEM IN PATIENTS WITH TYPE 1 DIABETES

**Fabian Mauricio LEÓN VARGAS**

**Dipòsit legal: Gi. 1566-2013**
http://hdl.handle.net/10803/125007

Universitat de Girona

**DOCTORAL THESIS**

# Design and implementation of a closed-loop blood glucose control system in patients with type 1 diabetes

Fabian Mauricio León Vargas

2013

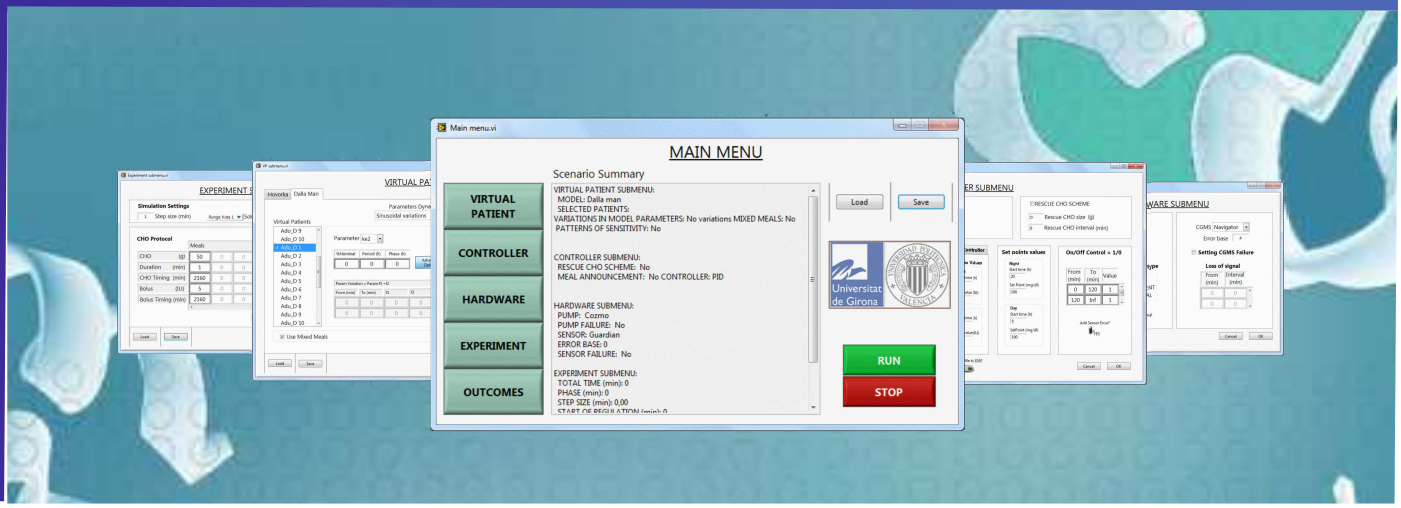

DOCTORAL THESIS

# Design and implementation of a closed-loop blood glucose control system in patients with type 1 diabetes

**Fabian Mauricio León Vargas**

2013

Doctoral Programme in Technology

Advisor:
Prof. Josep Vehí

Thesis submitted in partial fulfillment of the requirements for the degree of Doctor of Philosophy.

# Design and implementation of a closed-loop blood glucose control system in patients with type 1 diabetes

Doctoral Programme in Technology

A dissertation submitted to the University of Girona in partial fulfillment of the requirements for the degree of Doctor of Philosophy


Fabian Mauricio León Vargas
Author

Prof. Josep Vehí
Advisor



Girona, Spain
September, 2013

*A mi madre Luzmila, mi padre Hermes y mi hermana Katherine.*
*Este es un pequeño homenaje a su apoyo*
*y amor incondicional.*

*A mi esposa Maira y mi hijo Joan Felipe.*
*Por ser mi fuente de alegría e inspiración,*
*por ser parte de mi vida.*

# Agradecimientos

El emprendimiento de un nuevo reto marca el camino de nuestras posibilidades y nos hace crecer cualquiera sea el resultado final. Gracias a la calidad de personas que he tenido la fortuna de conocer durante esta investigación y de quienes he recibido los medios, los conocimientos, las experiencias, y mucho más, he podido concretar satisfactoriamente esta etapa de mi vida. Quisiera agradecer a todos y cada uno de aquellos implicados de manera directa o indirecta en la consecución de esta meta.

En primer lugar agradezco el apoyo que he recibido del Prof. Josep Vehí, su experiencia en la dirección de grandes proyectos y su gran capacidad de materializar nuevas oportunidades han propiciado que yo pudiese realizar esta investigación y con su ayuda superar en lo posible las no pocas limitaciones que me he encontrado en el camino.

Durante el transcurso de esta tesis fue muy grato trabajar tanto en Girona como en La Plata, junto a personas de la más alta calidad científica como el Dr. Fabricio Garelli y el Dr. Hernán de Battista, cuya aún mayor calidad personal los precede. Agradezco especialmente al Dr. Jorge Bondia por su acompañamiento durante importantes etapas de esta investigación y su minuciosa labor en el diseño de pruebas y documentación respectiva, garantizando así la calidad del resultado. Con especial afecto también agradezco a la Dra. Remei Calm por sus sabios aportes y dedicación en trabajos de gran dificultad técnica y creativa, sin su paciencia y participación no hubiera sido posible concluirlos exitosamente. De igual forma, durante el inicio de esta tesis trabajé con personas como Guillermo Prados, cuyo apoyo incondicional y soporte técnico propició un avance significativo en los resultados obtenidos.

El buen ánimo de charlas, cenas, consultas y discusiones con los compañeros del grupo Modal Intervals and Control Engineering (MICELab) lo valoro enormemente. Su integración y compañerismo se ha evidenciado en todo momento tanto a nivel académico como personal. A los miembros del proyecto INSULAID2 y CLOSEDLOOP4MEAL les estoy agradecido por sus contribuciones y valiosa colaboración.

Todas aquellas personas que han hecho parte de mi vida durante estos años y con quienes he tenido la fortuna de compartir grandes momentos. Aquellos quienes además me han brindado su aliento cuando la adversidad parecía mayor al deseo de seguir. A Yenny, Crisos, Mauricio, Fabian, Claudia, Anna, Eduard, Yeimy, Doña Pilar, mil gracias por su ayuda, confianza y los innumerables momentos compartidos, por su amistad y por hacer parte de este proceso. Un agradecimiento muy especial a Magda, Luis, Andrea, Ronald, Sabik, Dayan, y los peques Esteban, Alejandro, Violeta, Sergio y Camilo, por recibirme como un integrante más de la familia, por brindarme su hogar y su cariño. Su respaldo me hizo sentir como en casa.

Esta lista tan larga en realidad se queda corta sin antes dedicar un par de frases a mi familia. A mi madre por su infinito amor y apoyo, por ser el motor que impulsa mi vida, por sus enormes sacrificios y sus sabios consejos, los logros de mi vida en realidad son los suyos, gracias mamita. A mi padre por su inagotable disposición a ayudar y velar en cada etapa de mi vida, por su respaldo y cariño de siempre. A mi hermana y mejor amiga, porque siempre he contado con su apoyo y a quien no podré compensar mi ausencia en momentos tan importantes de su vida. A mis tíos, primos, a mi nonita y nonito porque son el pilar de nuestra unión.

Por último y no menos importante, a Dios gracias porque esta aventura me ha bendecido

con la compañía de Maira, mi hermosa mujer, amiga, colega y esposa. No encontraré las gracias suficientes por llenar mi vida con su amor y hacerla completa con su dedicación, con su apoyo e invaluable contribución a esta tesis en todo momento. Por ser la fuerza que dirige la brújula de mi rumbo a la felicidad, la mayor alegría y orgullo de mi vida, mi hijo Joan Felipe, gracias pues su presencia ha llenado de luz e ilusiones nuestra vida como nunca.

A todos gracias... totales.

*Fabian M. León Vargas*
*Girona, España*
*Septiembre 2013*

# Publications

## Journals

**F. León-Vargas**, F. Garelli, H. de Battista, J. Vehí. (2013) "Safe Tuning and Improvement of the Postprandial Response in Closed-Loop Blood Glucose Controllers." *Biomedical Signal Processing and Control.* Submitted.

**F. León-Vargas**, F. Garelli, H. de Battista, J. Vehí. (2013) "Postprandial Blood Glucose Control using a Hybrid Adaptive PD Controller with Insulin-on-Board Limitation." *Biomedical Signal Processing and Control.* 8:724-732.

**F. León-Vargas**, R. Calm, J. Bondia, J. Vehí. (2012) "Improving the Computational Effort of Set-Inversion-Based Prandial Insulin Delivery for Its Integration in Insulin Pumps." *Journal of Diabetes Science and Technology.* 6(6):1420-1428.

## Conferences

**F. León-Vargas**, F. Garelli, H. de Battista, J. Vehí. (2013) "Hypoglycemia Reduction via Hybrid Blood Glucose Control with Insulin-on-Board Constraints". In *XV Workshop on Information Processing and Control RPIC.* September 16-20, San Carlos de Bariloche, Argentina.

**F. León-Vargas**, J. Bondía, J. Vehí. (2012) "Metodología para Generación de Pacientes Virtuales con Diabetes Tipo 1". In *14th International Conference on Energy Efficiency ans Sustainability in Ambient Intelligence.* June 25-27, Tarragona, Spain.

**F. León-Vargas**, G. Prados, J. Bondia, J. Vehí. (2011) "A New Virtual Environment for Testing and Hardware Implementation of Closed-loop Control Algorithms in the Artificial Pancreas". In *33rd Annual International Conference of the IEEE Engineering in Medicine and Biology Society.* August 30-September 3, Boston, USA.

**F. León-Vargas**, G. Prados, J. Bondia, and J. Vehí. (2011) "Platform for rapid prototyping design of closed-loop glycemic controllers in virtual patients of type 1 diabetes mellitus". In *Workshop on Control, Dynamics, Monitoring and Applications.* February 7-9, Caldes de Montbui, Spain.

## Posters

**F. León-Vargas**, A. Carreras, J. Bondia, J. Vehí. (2012) "In-silico evaluation for the outpatient artificial pancreas: emulating day-by-day living". In *5th International Conference on Advanced Treatments & Technologies for Diabetes.* February 8-11, Barcelona, Spain.

**F. León**, G. Prados, J. Bondia, J. Vehí. (2010) "Integrating closed loop algorithms development,

in- silico validation and hardware implementation in a single framework". In *3rd International Conference On Advanced Technologies and Treatments For Diabetes.* February 10-13, Basel, Switzerland.

## Multimedia publications

**F. León-Vargas**, G. Prados, J. Vehí, J. Bondia. (2009) "Plataforma Tecnológica para Control en Tiempo Real de Glucemia en Pacientes Virtuales con Diabetes Tipo 1".
http://sine.ni.com/cs/app/doc/p/id/cs-12640. National Instruments, Spain.

## Technical Documentation

**F. León-Vargas**, A. Carreras, M. García-Jaramillo, J. Bondia, J. Vehí (2013). Documentación presentada ante la Agencia Española de Medicamentos y Productos Sanitarios (AEMPS) para la validación del controlador a usar en la investigación clínica "Mejora de glicemia postprandial mediante un nuevo sistema de control en lazo cerrado". Esta investigación está enmarcado dentro del proyecto CLOSEDLOOP4MEAL.

# Nomenclature

The following acronyms, abbreviations and variables are used in this thesis.

### Acronyms and abbreviations

| | |
|---|---|
| AEMPS | Agencia española de medicamentos y productos sanitarios |
| AIDA | Automated insulin dosage advisor |
| AP | Artificial pancreas |
| APD | Adaptive proportional-derivative |
| ARMA | Autoregressive moving average |
| ARMAX | Autoregressive-moving average with external input |
| ARX | AutoRegresive model with eXternal input |
| AUC | Area under the curve |
| BMI | Body mass index |
| CF | Correction factor |
| CGM | Continuous glucose monitoring |
| CHO | Carbohydrates |
| CSII | Continuous subcutaneous insulin infusion |
| CV | Coefficient of variation |
| CVGA | Control variability grid analysis |
| DCCT | Diabetes Control and Complications Trial Research Group |
| DIA | Duration of insulin action |
| DKA | Diabetic ketoacidosis |
| DM | Diabetes mellitus |
| ePID | external Physiologic insulin delivery |
| ePID-IFB | ePID with insulin feedback |
| FDA | Food and drug administration |
| FMPD | Fading memory proportional derivative |
| GIM | Glucose-insulin model |
| GPC | Generalized predictive control |
| HbA1c | Glycosylated hemoglobin |
| HBGI | High blood glucose index |
| I:CHO | Insulin to CHO ratio |
| IDF | International diabetes federation |
| IIT | Intensive insulin treatment |
| IOB | Insulin on board |
| ISF | Intersticial fluid |
| IU | Insulin units |
| JDRF | Juvenile Diabetes Research Foundation |
| LBGI | Low blood glucose index |
| LMPC | Linear MPC |
| MC | Monte-carlo |
| MDI | Multiple daily injections |
| MMPPC | Multiple model probabilistic predictive control |
| MPC | Model predictive control |

| | |
|---|---|
| NIH | National institute of health |
| NMPC | Nonlinear MPC |
| PG | Plasma glucose |
| PID | Proportional integrative derivative |
| PPBD | Postprandial basal duration |
| qMC | quasi Monte-carlo |
| SAFE | Safety Auxiliary Feedback Element |
| SC | Subcutaneous |
| SIB | Set-inversion-based |
| SIVIA | Set Inversion via Interval Analysis |
| SMBG | Self monitoring blood glucose |
| SMRC | Sliding mode reference conditioning |
| T1D | Type 1 diabetes |
| T2D | Type 2 diabetes |
| TBG | Target for blood glucose |
| TDD | Total daily dose |
| UCAM | University of Cambridge |
| UVa | University of Virginia |

# List of Figures


2.1 Oral glucose tolerance test. The blue line corresponds to a healthy person and the red line to a diabetic patient. . . . 13
2.2 IDF global projections for prevalence of people with diabetes (20–79 years), 2011–2030 (taken from Scully (2012)). . . . 15
2.3 IDF estimations for deaths of diabetes related complications (20–79 years) in 2011 (taken from International Diabetes Federation (2011)). . . . 15
2.4 Total health-care expenditures (USD) due to diabetes (20–79 years) in 2011 (taken from International Diabetes Federation (2011)). . . . 16
2.5 Insulin and glucagon secretion from islet cells, which maintains homeostasis for blood glucose levels (adapted from Campbell et al. (2006)). . . . 19
2.6 Insulin profiles obtained according to the therapy used. In red the bolus insulin dose and in blue the basal insulin dose. Profile obtained from (a) insulin released in non-diabetics, (b) insulin delivery with conventional therapy, (c) insulin delivery with multiple daily injections (MDIs), and (d) insulin delivery with continuous subcutaneous insulin infusion (CSII). The insulin profile from non-diabetics is highlighted in all figures with dashed lines. . . . 21
2.7 Main parts of an insulin pump (obtained from Valla (2010)). . . . 22
2.8 Devices used for insulin delivery: syringe, pen, and pump. . . . 22
2.9 Glucose meter used in a capillary blood test. . . . 23
2.10 Current CGM devices used in home monitoring: the Abbott FreeStyle Navigator® continuous glucose monitoring system, the DexCom SEVEN®, and the Medtronic MiniMed Paradigm® REAL-Time insulin pump and continuous glucose monitoring system. . . . 25
2.11 Bolus insulin profiles available in modern insulin pumps. . . . 28

3.1 Closed-loop components of an artificial pancreas system. . . . 31
3.2 Biphasic insulin response to step increase in glucose of the $\beta-$cells (left), and with the PID control model (right). The shaded regions on the PID response represent each control action (proportional-integral-derivative) obtained. (adapted from Steil et al. (2004)). . . . 35
3.3 MPC. At time step $t_k$, a sequence of $M$ control movements is selected to minimise a performance criterion that involves the predicted output ($y$) over $P$ time steps, which is subject to maximum and minimum constraints on the manipulated input ($u$) (taken from Bequette (2005)). . . . 38
3.4 Structure of UCAM simulator (taken from Chassin (2005)). . . . 46
3.5 Structure of the UCAM subject setup (taken from Chassin (2005)). . . . 47
3.6 UCAM example protocol (taken from Chassin (2005)). . . . 47
3.7 UVa components (taken from Kovatchev et al. (2008)). . . . 48

3.8 UVa user interface (taken from Kovatchev et al. (2008)). . . . . 49

4.1 General scheme of the glucose-insulin system. . . . . 52
4.2 Scheme of gastro-intestinal Dalla Man *et al.* system (adapted from Dalla Man et al. (2007). . . . . 52
4.3 $k_{empt}(t, Q_{sto})$ function, where $D$ is the total glucose quantity of the last meal. . . 53
4.4 Scheme of subcutaneous insulin kinetics proposed by Dalla Man et al. (2007). . . 53
4.5 Scheme of the glucose-insulin system in T1D. Solid lines represent glucose and insulin fluxes; dashed lines represent control signals. Physical activity affects insulin-independent glucose utilization (taken from Dalla Man et al. (2009)). . . . 54
4.6 Scheme of the glucose subsystem (adapted from Dalla Man et al. (2007)). . . . . 55
4.7 Schema of the insulin subsystem (adapted from Dalla Man et al. (2007)). . . . . 57
4.8 Compartment model of subcutaneous insulin absorption proposed by Hovorka et al. (2004a). . . . . 59
4.9 Compartment model of glucose-insulin system (adapted from Hovorka et al. (2004a)). 60
4.10 1000 simulated N(0,1) random values using (a) the Monte Carlo and (b) the quasi-Monte Carlo method. . . . . 63
4.11 Flow diagram of the virtual patient generation. . . . . 64
4.12 The layout of the platform, which includes a virtual patient with proper instrumentation for a closed-loop control scheme and the control algorithm to close the loop. . . . . 66
4.13 Platform main menu. . . . . 67
4.14 Virtual patient submenu. . . . . 67
4.15 Controller submenu. . . . . 68
4.16 Hardware submenu. . . . . 68
4.17 Experiment submenu. . . . . 69
4.18 Outcomes submenu. . . . . 69
4.19 Time profile of rate glucose appearance for mixed meals (a) 1–5 (b) 6–10 (c) 11–15 (d) 16–20 (e) 21–25 and (f) 26–30. . . . . 72
4.20 Time profile of rate glucose appearance for mixed meals (a) 31–35 (b) 36–40 (c) 41–45 (d) 46–50 (e) 51–55 and (f) 56–60. . . . . 73
4.21 Experiment submenu when mixed meals option is on. . . . . 74
4.22 Average hourly basal rate values by age group. The open triangle represents ages 3–10 years of age, the open square depicts ages 11–20 years of age, the solid square represents ages 21–60 years of age, and the solid triangle depicts ages >60 years of age (taken from Scheiner and Boyer (2005)). . . . . 74
4.23 Mean and standard deviation of the variation profile of the insulin sensitivity parameter $V_{mx}$, which was applied to adult virtual patients in the Dalla Man *et al.* model. . . . . 74
4.24 Mean and standard deviation of the basal insulin profile applied to adult virtual patients in the Dalla Man *et al.* model. . . . . 75
4.25 Advanced settings of patterns of sensitivity options from the virtual patient submenu. . . . . 75
4.26 Glucose concentration response of a virtual patient (a), including variation in insulin sensitivity, and (b), according to the basal insulin applied. The blue dashed line denotes a profile of basal insulin and the solid red line denotes a constant value of basal insulin. . . . . 76
4.27 Example of (a) blood glucose signal, and (b) corresponding sensor measure glucose signal. . . . . 79

4.28 Outcomes metrics implemented in the *in silico* platform: (a) CVGA, (b) risk trace, (c) Poincare plot, (d) aggregate blood glucose, (e) histogram, (f) grading system, and (g) available numeric outcomes. . . . . 80
4.29 Rate of glucose appearance of mixed meals from Table 4.11. . . . . 81

5.1 Plot that illustrates the concept of inner and outer subpaving. The dark rectangles represent the inner subpaving and guarantee the fulfillment of the constraints. The outer subpaving is made up of both the dark and the light rectangles. Its complementary set (in white) is guaranteed to contain only nonsolutions that violate some of the constraints. Results in the boundary (light rectangles) are unknown a priori. . . . . 85
5.2 Plot representing: (a) three-dimensional (basal dose, bolus dose, and PPBD) feasible set and (b) its corresponding basal-bolus two-dimensional projection. . . 86
5.3 Basal-bolus space partitioned in a grid for the optimization method. . . . . 87
5.4 Smart search pathway used by the optimization algorithm. If the constraints are met by a basal value less than the nominal value, the solution may be found in checkpoints "[$\mathbf{x}_1$]" or "[$\mathbf{x}_2$]"; otherwise, it will be in "[$\mathbf{x}_4$]", "[$\mathbf{x}_5$]", or beyond. . . 88
5.5 Typical interval glucose response when using the maximum bolus limit. The hypoglycemia constraint is always violated at the initial box "[$\mathbf{x}_0$]". . . . . 89
5.6 Insulin profiles (left) and their corresponding glucose responses (right) for two cases. (a) When a box is below the nominal basal, a shorter PPBD value produces a lower glucose response (blue solid curve) than a longer PPBD value (red dashed curve). (b) When a box is above the nominal basal, those PPBD values imply the opposite action. The dashed green lines area and the solid orange lines area indicates the values of PPBD at which hyperglycemia or hypoglycemia conditions are obtained, respectively. . . . . 90
5.7 tHyper and tHypo dynamics observed in a bolus-PPBD plane. For some cases, no bolus reduction will achieve tHyper $\geq$ tHypo (left); for other cases, it can be achieved (right). . . . . 90
5.8 Flowchart of the optimized version of the iBolus algorithm. Hypo, hypoglycemia constraint; Hyper, hyperglycemia constraint; PPBD, postprandial basal duration. 92

6.1 Estimated time profiles of insulin activity parameterized by DIA. . . . . 99
6.2 Hybrid control scheme for glucose regulation. . . . . 100
6.3 Structure of the hybrid PD controller. . . . . 101
6.4 Block diagram of the adaptation law. . . . . 101
6.5 Two consecutive control periods 10 min each with an internal sample time of 1 min of the adaptive algorithm. (a) shows the switching behaviour of $\omega$ that avoids an excess in $IOB$ (limit fixed to 6.1 IU), and (b) shows the resulting $IOB$ prediction based on such $\omega$ dynamics. (c) shows the $\gamma$ value as the average of $\omega$ in each period, and (d) shows the effective $IOB$ obtained based on such $\gamma$ value. Note that the internal loop of the adaptive algorithm acts in a predictive way on each control period. The time step of this internal loop defines the maximum switching rate of $\omega$, the higher the maximum frequency of $\omega$, the higher the performance of the adaptive algorithm. . . . . 103
6.6 Time response of patient 1 to the hybrid PD controller with and without $\overline{IOB}$ constraint. . . . . 104
6.7 Mean and standard deviation of blood glucose resulting from the optimal open-loop therapy in meal tests of (a) 40 g and (b) 100 g. . . . . 105

6.8 Mean and standard deviation of $IOB$ from optimal open-loop therapy in meal tests of (a) 40g, and (b) 100g. . . . 105
6.9 Mean and standard deviation of blood glucose resulting from closed-loop therapy using as $\overline{IOB}$ limit the $IOB$ value at the (a) $2^{nd}$ and (b) $3^{rd}$ postprandial hour of the optimal open-loop therapy for a meal test of 40 g; while as $\overline{IOB}$ limit the $IOB$ value at the (c) $2^{nd}$ and (d) $3^{rd}$ postprandial hour of the optimal open-loop therapy for a meal test of 100 g. . . . 106
6.10 Lineal regression between $IOB$ values at the $2^{nd}$ and $3^{rd}$ postprandial hour from meal tests of 40 g and 100 g respectively using (a) *in silico* experiment, and (b) clinical data. . . . 109
6.11 Calculation of $\overline{IOB}$ using $IOB$ and blood glucose response. . . . 110
6.12 Mean and standard deviation of blood glucose for (a) PID with insulin feedback (PID-IFB), (b) PID controller with 35% pre-bolus, (c) PD controller with bolus, (d) Hybrid Adaptive PD controller. . . . 112
6.13 CVGA for (a) PID with insulin feedback (PID-IFB), (b) PID controller with 35% pre-bolus, (c) PD controller with bolus, (d) Hybrid Adaptive PD controller. . . . 113
6.14 Basic scheme of a glucose control loop with the SAFE algorithm. . . . 114
6.15 PDBasal Hybrid scheme with implementation of the SAFE method. . . . 115
6.16 PID-IFB scheme with implementation of the SAFE method. The prandial Bolus insulin was not employed in this realisation. . . . 116
6.17 Performance results of patient six of the PDBasal Hybrid with (circle) and without (cross) the SAFE layer using several combinations of the control gain and the size of the prandial bolus. . . . 118
6.18 Performance results of patient six of the PID-IFB algorithm with (circle) and without (cross) the SAFE layer using several combinations of the control gain and the insulin feedback term gamma. . . . 119
6.19 Blood glucose, insulin infusion, and IOB calculation of the MPC (gray) and the MPC-SAFE (black) response for patient five. . . . 121

7.1 Software framework. . . . 126
7.2 Login user. . . . 126
7.3 Execution mode and Connection confirmation. . . . 126
7.4 Information chart of clinical parameters for the patient selected and respective settings of the control algorithm. . . . 127
7.5 Selection of patient and type of study. . . . 127
7.6 Main menu: (1) Patient and study information, (2) glucose data, (3) insulin data, (4) data on sampling times, (5) intake data, (6) incidents, (7) registration, control, and exit options, (8) numeric outputs and temporal scale options of the charts, and (9) glucose and insulin charts. . . . 128
7.7 General scheme of the controller which will be clinically validated in the multi-center trial: the PDBasal Hybrid SAFE algorithm. . . . 129
7.8 Graphical code in LabVIEW used to implement the (a) derivative action, and the (b) SMRC scheme. . . . 130
7.9 CVGA from the test in the (a) open-loop control and (b) closed-loop control; corresponding blood glucose response from the (c) open-loop control and (d) closed-loop control. These results demonstrate better performance of the PDBasal Hybrid SAFE algorithm according to safety and postprandial responses in conventional open-loop therapy. . . . 131
7.10 Real-time validation test of the software application. . . . 132

# List of Tables


2.1 Pharmacokinetics of available insulin products. . . . . 20
2.2 Primary features of insulin pens and insulin pumps. . . . . 24

4.1 Univariate model parameters. . . . . 62
4.2 Multivariate model parameters. . . . . 62
4.3 Mean and standard deviation of clinical parameters for patients with T1D in a Barcelona hospital. . . . . 65
4.4 Mean and standard deviation of clinical parameters from the virtual patients. . . 65
4.5 Library of mixed meals. . . . . 71
4.6 Individualised basal insulin rate (IU/h) for each patient in the cohort. . . . . 75
4.7 Individualised insulin-to-carbohydrate ratio (IU/g) for each patient in the cohort. 75
4.8 Parameter values used for Johnson transformation. . . . . 77
4.9 Display period of glucose measurements of implemented CGM systems. . . . . 77
4.10 Technical features of implemented insulin pumps. . . . . 78
4.11 Nutritional composition of mixed meals (in grams) used for the test scenario. . . 81

5.1 Performance Comparison between the Non- and Optimized iBolus algorithm. For each patient, several tests were conducted using different meal sizes. . . . . 93
5.2 Statistical comparison of the difference between solutions given from optimized and the non-optimized iBolus algorithm. . . . . 93
5.3 Mean Absolute Error using best solution of Monte-Carlo technique for 1% and 5% of all possible with respect to solution of non-optimized iBolus algorithm. . . 94

6.1 IOB model parameter $K_{DIA}$ ($\text{min}^{-1}$) for different durations of insulin action. . . 99
6.2 Optimal open-loop therapies used in conventional Basal/Bolus control . . . . . 104
6.3 $IOB$ values obtained *in silico* at the $2^{nd}$ and $3^{rd}$ postprandial hour from open-loop meal tests of 40g and 100g. . . . . 107
6.4 Minimum glucose values obtained *in silico* per patient for a meal test of 40g. . . 107
6.5 Minimum glucose values obtained *in silico* per patient for a meal test of 100g. . . 108
6.6 Clinical $IOB$ value at the $2^{nd}$ and $3^{rd}$ postprandial hour from open-loop meal test of 40 g and 100 g. . . . . 108
6.7 Controller and other relevant parameters . . . . . 111
6.8 Mean and standard deviation of maximum glucose excursion, number of hypoglycemia events (hypos) and time in hyper (¿180 mg/dL) and hypoglycemia (¡70 mg/dL) . . . . . 112
6.9 Control variability grid analysis for the different controllers . . . . . 113
6.10 Performance results of PDBasal Hybrid and PID-IFB with and without the SAFE layer using nominal-tuning. . . . . 118

6.11 Performance results of the PDBasal Hybrid with and without the SAFE layer regarding to minimal hypoglycaemic events and glucose excursion using the best-tuning. The best tuning of $Kp$ and $I : CHO$ in each case is presented as a percentage change with respect to the nominal value. . . . . 119
6.12 Performance results of PID-IFB with and without the SAFE layer regarding to minimal hypoglycemia events and glucose excursion using the best-tuning. The best tuning of $Kp$ and $\gamma$ in each case is presented as a percentage change with respect to the nominal value. . . . . 120

# Contents

**List of Figures** **xi**

**List of Tables** **xv**

**Contents** **xvii**

**1 Introduction** **7**
1.1 Motivation . . . 7
1.2 Problems and Challenges . . . 8
1.3 Objectives . . . 9
1.4 Thesis Structure . . . 10

**2 Type 1 Diabetes and Blood Glucose Control** **13**
2.1 Diabetes Overview . . . 13
2.1.1 Types of Diabetes . . . 13
2.1.2 Numbers and Estimations . . . 14
2.1.3 Complications . . . 16
2.2 Blood Glucose Control . . . 18
2.2.1 Synopsis of Blood Glucose-Insulin Regulation . . . 18
2.2.2 Diabetes Treatment . . . 18
2.2.3 Intensive Insulin Treatment . . . 20
2.3 Control Devices for Glucose Regulation . . . 21
2.3.1 Insulin Delivery . . . 21
2.3.2 Glucose Monitoring . . . 23
2.4 Postprandial Control . . . 26
2.4.1 Basal-Bolus Therapy . . . 27
2.4.2 Bolus Types and Settings . . . 28
2.5 Summary . . . 29

**3 Artificial Pancreas Research** **31**
3.1 Introduction . . . 31
3.2 Closed-Loop Approaches and Clinical Trials . . . 34
3.2.1 PID controllers . . . 35
3.2.2 MPC controllers . . . 37
3.2.3 Other controllers . . . 41
3.3 Modelling and Simulation . . . 42
3.3.1 Diabetes Related Simulators . . . 42
3.3.2 Artificial Pancreas Simulators . . . 45
3.4 Summary . . . 48

**4 Virtual Environment for Designing and Testing of Glucose Controllers 51**
4.1 Introduction . . . 51
4.2 Virtual Patients . . . 51
4.2.1 Dalla Man *et al.* model . . . 52
4.2.2 Hovorka *et al.* model . . . 58
4.2.3 Representing a Real Patient Cohort . . . 61
4.3 In Silico Platform . . . 66
4.3.1 Overview . . . 66
4.3.2 Mixed Meals . . . 69
4.3.3 Intra-Patient Variability . . . 70
4.3.4 Instrumentation models . . . 76
4.3.5 Outcome Measurements . . . 78
4.4 Constructing a Simulation Scenario for Postprandial Control . . . 79
4.5 Summary . . . 81

**5 Open-Loop Postprandial Control: A Set-Inversion-Based Approach 83**
5.1 Introduction . . . 83
5.2 Interval Analysis and Set Inversion . . . 83
5.3 Prandial Insulin Delivery Algorithm . . . 85
5.4 Optimization Method . . . 86
5.4.1 Algorithm Rationale . . . 88
5.5 Numerical Results . . . 91
5.6 Discussion . . . 93
5.7 Summary . . . 95

**6 Closed-Loop Postprandial Control: Design and In silico Validation 97**
6.1 Introduction . . . 97
6.2 Insulin-on-Board . . . 98
6.2.1 Estimation of Insulin-on-Board . . . 99
6.3 Hybrid Adaptive PD Controller . . . 99
6.3.1 Control Structure . . . 100
6.3.2 Switching Adaption Law . . . 101
6.3.3 Operation Example . . . 102
6.3.4 Determination of Insulin-on-Board Constraint . . . 103
6.3.5 Controller Tuning . . . 110
6.3.6 Performance Results . . . 110
6.4 Safety Auxiliary Feedback Element Evaluation . . . 113
6.4.1 SAFE Method . . . 114
6.4.2 Switching SAFE Law . . . 115
6.4.3 Glucose Controllers . . . 115
6.4.4 Performance Results . . . 117
6.4.5 Optimal Tuning . . . 117
6.4.6 SAFE in other control schemes (MPC) . . . 119
6.5 Summary . . . 121

**7 Control Software Application: Implementation and Validation for use in Clinical Trials 123**
7.1 Introduction . . . 123
7.2 Study Protocol Summary . . . 123

7.3 Software Description . . . . . 125
7.3.1 System Requirements . . . . . 125
7.3.2 Software Framework . . . . . 125
7.4 Implementation and Validation . . . . . 128
7.5 Technical Documentation . . . . . 130

**8 Conclusions and Future Work** **133**
8.1 Contributions . . . . . 133
8.2 Future Research . . . . . 134

**Bibliography** **135**

Universitat de Girona
Departament d'Enginyeria Elèctrica, Electrònica i Automàtica

# Resum

La diabetis és una malaltia crònica que es caracteritza per nivells elevats de glucosa en sang a causa de la destrucció irreversible de les cèl·lules del pàncrees (diabetis tipus 1), que són responsables de la excreció d'insulina, o degut a una combinació de resistència a la acció de la insulina i una secreció d'insulina compensatòria inadequada (diabetis tipus 2). La diabetis pot conduir a complicacions micro o macrovasculars a llarg termini amb conseqüències potencialment perilloses per a la vida. S'estima que el nombre de persones en edat de 20 a 79 anys amb diabetis, augmentarà de 79 milions al 2012 a 371 milions al 2030. Les conseqüències econòmiques de la diabetis a Europa són significatives, amb costos anuals de 138.8 milions d'euros el 2012.

La diabetis és una de les malalties més greus que han de ser regulades artificialment. El tractament convencional amb insulina es basa en múltiples injeccions diàries o amb infusió subcutània contínua mitjançant bombes d'insulina. Tot i que aquesta última teràpia és la millor opció disponible en l'actualitat, encara presenta diversos inconvenients per mantenir els nivells de glucosa en sang prop de la normoglicèmia. En les últimes dècades s'han produït avenços significatius en el camp dels dispositius terapèutics per a la diabetis tipus 1. Això ha promogut el desenvolupament del pàncrees artificial, també conegut com un sistema d'administració d'insulina de llaç tancat, per administrar insulina de forma automatitzada i contínuament d'acord amb els nivells de glucosa mesurats en temps real. S'han proposat diverses estratègies de regulació durant la última decada per fer front a diferents condicions dels pacients, algunes ja han estat provades en assajos clínics.

En aquesta investigació, es desenvolupen estratègies de control en llaç obert i llaç tancat encaminades a superar els principals problemes de control al periode postprandial. En primer lloc, es va desenvolupar un nou algoritme de control basat en models per a la regulació de glucosa postprandial en llaç obert basat en la tecnologia d'inversió de conjunts. Aquest coordina automàticament els valors d'insulina basal-bol d'una manera eficient per tal d'aconseguir certs objectius de control predefinits. L'algoritme va ser dissenyat per permetre la seva integració en bombes d'insulina intel·ligents. Finalment, es van implementar estratègies de regulació basades en tècniques de control en mode lliscant i limitacions de la insulina a bord, per reduir el risc d'episodis d'hipoglucèmia tardana per tal d'aconseguir un acompliment més segur sense augmentar el temps a hiperglucèmia. La robustesa dels controladors va ser demostrada mitjançant una àmplia evaluació i validació en un entorn virtual integral especificament dissenyat i implementat en aquesta tesi per permetre simulacions realistes. Una metodologia pràctica per "virtualitzar" una cohort real de pacients diabètics tipus 1 també va ser desenvolupada. D'altra banda, s'espera que un algoritme de control de glucosa en sang de llaç tancat, dissenyat i desenvolupat en aquesta tesi, sigui validat en un assaig clínic multicèntric.

Universitat de Girona
Departament d'Enginyeria Elèctrica, Electrònica i Automàtica

# Resumen

La diabetes es una enfermedad crónica que se caracteriza por niveles elevados de glucosa en sangre debido a la destrucción irreversible de las células $\beta$ del páncreas (diabetes tipo 1), que son responsables de la excreción de insulina, o debido a una combinación de resistencia a la acción de la insulina y una secreción de insulina compensatoria inadecuada (diabetes tipo 2). La diabetes puede conducir a complicaciones micro o macrovasculares a largo plazo con consecuencias potencialmente peligrosas para la vida. Se estima que el número de personas en edad de 20 a 79 años con diabetes, aumentará de 79 millones en el 2012 a 371 millones en el 2030. Las consecuencias económicas de la diabetes en Europa son significativas, con costos anuales de 138.8 mil millones de euros en 2012.

La diabetes es una de las enfermedades más graves que han de ser reguladas artificialmente. El tratamiento convencional con insulina se basa en múltiples inyecciones diarias o con infusión subcutánea continua mediante bombas de insulina. Aunque esta última terapia es la mejor opción disponible en la actualidad, aún presenta varios inconvenientes para mantener los niveles de glucosa en sangre cerca de la normoglucemia. En las últimas décadas se han producido avances significativos en el campo de los dispositivos terapéuticos para la diabetes tipo 1. Esto ha promovido el desarrollo del páncreas artificial, también conocido como un sistema de administración de insulina de lazo cerrado, para administrar insulina de forma automatizada y continuamente de acuerdo con los niveles de glucosa medidos en tiempo real. Se han propuesto varias estrategias de regulación durante la última década para hacer frente a diferentes condiciones de los pacientes, algunas ya han sido probadas en ensayos clínicos.

En esta investigación, se desarrollan estrategias de control en lazo abierto y lazo cerrado encaminadas a superar los principales problemas de control en el período postprandial. En primer lugar, se desarrolló un nuevo algoritmo de control basado en modelos para la regulación de glucosa postprandial en lazo abierto basado en la tecnología de inversión de conjuntos. Éste coordina automáticamente los valores de insulina basal-bolo de una manera eficiente a fin de lograr ciertos objetivos de control predefinidos. El algoritmo fue diseñado para permitir su integración en bombas de insulina inteligentes. Por último, se implementaron estrategias de regulación basadas en técnicas de control en modo deslizante con limitaciones de la insulina a bordo para reducir el riesgo de episodios de hipoglucemia tardía a fin de conseguir un desempeño más seguro sin aumentar el tiempo en hiperglucemia. La robustez de los controladores fue demostrada mediante una amplia evaluación y validación en un entorno virtual integral específicamente diseñado e implementado en esta tesis para permitir simulaciones realistas. Una metodología práctica para "virtualizar" una cohorte real de pacientes diabéticos tipo 1 también fue desarrollada. Por otra parte, se espera que un algoritmo de control de glucosa en sangre de lazo cerrado, diseñado y desarrollado en esta tesis, sea validado en un ensayo clínico multicéntrico.

Universitat de Girona
Departament d'Enginyeria Elèctrica, Electrònica i Automàtica

# Abstract

Diabetes is a chronic disease characterised by elevated plasma glucose levels due to the irreversible destruction of $\beta-$cells in the pancreas (Type 1 diabetes), which are responsible for the excretion of insulin or a combination of resistance to insulin action and an inadequate compensatory insulin secretory response (Type 2 diabetes). Diabetes can cause long-term micro- or macrovascular complications with potentially life-threatening consequences. The total number of people with diabetes in the age range of 20–79 is projected to increase from 371 million in 2012 to 552 million in 2030. The economic consequences of diabetes in Europe are profound, with annual costs of 138.8 billion EUR in 2012.

Diabetes is a serious disease that must be artificially regulated. Conventional insulin treatment is based on multiple daily injections (MDI) or continuous subcutaneous insulin infusion (CSII) pumps. Although CSII therapy is currently the best available option for diabetic patients, this method presents several drawbacks regarding the maintenance of blood glucose levels near normoglycaemia. Significant advances in the field of therapeutic devices for Type 1 diabetes have been achieved over the last decade. This has promoted the development of the artificial pancreas, which is also known as the closed-loop insulin delivery system, to deliver insulin in an automated and continuous manner according to real-time sensor glucose levels. Several closed-loop control strategies have been proposed during the last decade to address different patient conditions, some of which have already been tested in clinical trials.

In the work presented in this dissertation, open-loop and closed-loop control strategies that were aimed at resolving major control problems in the postprandial period were developed. A new model-based control algorithm for postprandial glucose regulation in open-loop, which is based on set-inversion technology, was developed. It automatically and efficiently coordinates the values of basal-bolus insulin to achieve certain predefined control objectives. The algorithm was designed to enable integration into existing smart insulin pumps. Closed-loop control strategies based on sliding mode techniques and insulin-on-board constraints were implemented to reduce the risk of late hypoglycaemic events and to obtain safer controller performance without increasing the period of hyperglycaemia. Extensive evaluation and validation of the control robustness was performed in a comprehensive virtual environment that was specifically designed and implemented to facilitate realistic simulations. A practical methodology to "virtualise" a cohort of real Type 1 diabetic patients was also developed. A closed-loop blood glucose control algorithm was also designed and developed in this thesis and is expected to be validated in a multicentre clinical trial.

# Chapter 1

# Introduction

This chapter presents an overview of the dissertation and considers the motivations of the research. The challenges, objectives, and methodology of this study are briefly explained. A description of the structure and content of the thesis is also presented.

## 1.1 Motivation

Diabetes mellitus (DM) is a disease characterised by absolute or relative insulin deficiency (Type 1 diabetes – T1D and Type 2 diabetes – T2D, respectively). It is currently one of the most common chronic conditions and has a significant impact on European public health and economy. The International Diabetes Federation estimates that more than 8.4% of the European population in the age range of 20–79, that is, approximately 55 million European citizens, currently suffer from diabetes; this number is expected to increase to 64 million by the year 2030. The economic consequences of diabetes in Europe, with annual costs of 138.8 billion EUR in 2012 (International Diabetes Federation, 2011), are profound. Approximately 10% of diabetic patients are affected by T1D, and Europe has the highest global prevalence rate of T1D in children.

Diabetes constitutes serious risks for the health and life of citizens. Previously, people affected with DM died from a diabetic coma. However, the discovery of insulin in 1921 has minimised the risk of this acute complication and has transformed diabetes into a chronic condition. Currently, T2D (previously referred to as noninsulin-dependent diabetes mellitus) can be effectively treated with oral medicine. Conversely, the external administration of insulin is required for the survival of patients with T1D (also known as insulin-dependent diabetes mellitus or juvenile diabetes). With the availability of miniature glucometers, which are easy to use and provide affordable point-of-care, self-monitoring of glucose levels is prevalent. By creating an opportunity for self-management, glucometers enable patients to actively participate in their treatment. Compared with multiple daily injections of insulin therapy, continuous subcutaneous insulin infusion treatment using an insulin pump has proven to be effective for reducing HbA1c (an index of mean glycaemic control) in patients with T1D (Doyle , Boland; Retnakaran et al., 2004); however, hypoglycaemic episodes have not been reduced.

In the last two decades, technological progress has fuelled research on closed-loop glucose control systems (artificial pancreas), which combine an insulin pump and a continuous glucose monitor (CGM) for a more effective treatment of T1D subjects. Although satisfactory clinical results have been reported for overnight glucose control (Sherr et al., 2013; Elleri et al., 2011b),

several challenges for effectively realising an optimal postprandial (post-meal) closed-loop control of blood glucose are evident. The lack of accuracy for existing continuous glucose monitors in the hypoglycaemic range, the safety of insulin pumps, the disturbances during large meals, stress and physical exercise, a patient's variability and the delays in the subcutaneous route have been identified as limiting factors in the development of an artificial pancreas for ambulatory use.

Different approaches have been suggested to address meal disturbances in closed-loop glucose controllers. Fully closed-loop systems, in which information about meal size and timing are not provided in advance to the system, have demonstrated poor performance with unacceptably high postprandial glucose and low post-meal nadir glucose (Steil et al., 2006, 2011). These results have promoted less-ambitious approaches, in which meals are announced to the system by the generation of feed-forward action, such as a prandial insulin bolus (semi-closed loop). Hybrid approaches have also been proposed, in which a percentage of the prandial bolus is applied and the remainder of the prandial bolus is provided to the closed-loop controller (Hovorka, 2011). Clinical studies have compared the efficacy of these solutions for reducing postprandial excursions during closed-loop control systems with the efficacy of fully closed-loop systems (Weinzimer et al., 2008a). The results indicate that the first generation of an artificial pancreas will require the announcement of meals. However, the prevention of overcorrection remains the primary drawback of control algorithms. Aggressive tuning for a low post-prandial glucose peak may cause an accumulation of insulin and produce late hypoglycaemia. This possibility imposes the consideration of constraints on residual insulin activity (insulin-on-board) in Proportional-Integral-Derivative (PID) (Steil et al., 2006, 2011; Ruiz et al., 2012) and Model-Predictive-Control (MPC)-based systems (Ellingsen et al., 2009; Percival et al., 2011). However, clinical results of the few existing prototypes of automated glycaemic control during a meal with PID and MPC have not been satisfactory (Steil et al., 2011; Kovatchev et al., 2010; Dassau et al., 2013). Some emerging approaches using dual hormonal schemes to reduce severe hypoglycaemia have also been examined with PID and MPC control algorithms (El Youssef et al., 2011; El-Khatib et al., 2010).

Despite control strategies with meal announcement and the inclusion of constraints on residual insulin activity, the prevention of overcorrection, which causes hypoglycaemia episodes, remains a significant challenge for control algorithms. Therefore, innovative strategies are needed for efficient and safe post-meal glucose control. Improvements in control algorithms, measurement accuracy, and fault-detection systems will deliver the required performance and safety for automated post-meal control in T1D.

## 1.2 Problems and Challenges

A list of the primary challenges for the development of artificial pancreas systems are outlined as follows:

- **Inter- and intra-patient variability**: Due to the large inter-subject variability of glucose regulation, which requires tuning of the system, an artificial pancreas system must be patient-specific. Factors affecting inter-patient variability include hormonal changes, stress, illness, and activity levels. An artificial pancreas must also address intra-patient variability (Wilinska et al., 2010; Rossetti et al., 2012). It must consider variations in insulin sensitivity produced by circadian rhythms and changes in insulin absorption as well as meal absorption (Heinemann, 2002; Scholtz et al., 2005).

- **Coping with disturbances and uncertainty**: An artificial pancreas system is affected by numerous disturbances, such as meals, stress and exercise, which are sources of uncertainty. In fully closed-loop systems, information about a meal is not introduced into the system. In other approaches, information about meals is introduced into the system (meal announcement), which generates advice about a prandial insulin bolus. Food intake is an important source of uncertainty as accurate estimates are difficult to construct for a mixed meal and errors can occur when counting carbohydrates (Graff et al., 2000; Brazeau et al., 2013).

- **Extensive physiological delays in the subcutaneous route**: In healthy people, insulin is delivered from the $\beta$-cells in the pancreas to the portal circulation. In this case, the delay in insulin action is approximately 30 min (Hovorka, 2006). When the subcutaneous route is used to deliver insulin, the delay in insulin action is approximately 90 min from the time of infusion, even when rapid-acting insulin analogues are used. Additional delay is attributable to glucose sensing in the subcutaneous route due to the transport of glucose from blood to the interstitial fluid. These delays may result in the overdosing of insulin and insulin stacking, which increases the risk of hypoglycaemia. To minimise the risk of insulin-stacking, appropriate control methods must be used and control actions must be constrained based on robust estimations of the insulin-on-board.

- **The accuracy and reliability of existing CGM systems**: The lack of accuracy and reliability of CGM systems has technologically hindered the automation of insulin delivery. Relative errors greater than 20% have been reported in different CGM systems, which produce challenges for a closed-loop controller, especially when the temporal patterns of the errors are presented in the form of bias. To improve their reliability, CGM systems should contain an embedded self-monitoring capacity and should possess the ability to detect abrupt faults and malfunctions (Mazze et al., 2009).

- **The safety of insulin pumps**: Although insulin pumps are highly developed and can be integrated into an artificial pancreas, their reliability requires improvement. The failure of most infusion systems involve the infusion set components and the subcutaneous infusion site, e.g., obstruction of the infusion set, infection of the infusion site, leakage from the infusion site or leakage at the infusion set connection (Guilhem et al., 2006).

## 1.3 Objectives

The general objective of this research is to develop efficient and safe open and closed-loop strategies for postprandial glucose control in T1D patients.

To achieve this objective, the study addressed the following specific issues:

1. To develop a virtual environment for intensive and realistic preclinical testing and validation of blood glucose controllers. The definition of realistic scenarios will be performed in a simple manner, including intra-patient circadian variation in insulin sensitivity, easy-to-import dynamic profile features of model parameters, estimated rate of glucose appearance from mixed meals, representative models and failures of insulin pumps and continuous glucose monitoring systems, and several outcome metrics.

2. To develop a new postprandial control algorithm that can be efficiently implemented into smart insulin pumps. Analysis of interval simulations, physiological assumptions, and search domain contractions will be used to enable efficient implementation.

3. To develop and extensively evaluate closed-loop postprandial control algorithms that exhibit appropriate postprandial responses whilst maintaining safety by limiting the risk of late hypoglycaemic events. Sliding mode techniques will be used to include insulin-on-board constraints to prevent hypoglycaemia.

4. To implement and validate the developed closed-loop postprandial glucose controller for use in clinical trials and subsequent acceptance by the regulatory agency.

## 1.4 Thesis Structure

This dissertation is organised as follows:

- **Chapter 1** introduces the motivation for this research, outlines the main challenges of the development of the artificial pancreas and presents the research objectives.

- **Chapter 2** presents an overview of T1D and the complications and health-care costs for diabetic patients. It describes conventional methods used for blood glucose control and the postprandial control therapies that are currently performed in home-care systems. The devices involved in blood glucose control are also presented.

- **Chapter 3** details artificial pancreas research and major advances by leader teams in this field. Different closed-loop control approaches for glucose regulation, which have been evaluated in clinical trials and *in silico* experiments, are addressed. Simulators that are extensively used to facilitate the development of artificial pancreas systems are also described in this chapter.

- **Chapter 4** describes the simulator that was designed to develop more realistic testing scenarios for the improvement and validation of glucose controller designs. First, models of the glucose insulin system, which are part of the virtual environment, are presented. Second, a practical procedure to represent a real cohort of T1D subjects *in silico* is also described. Last, all elements that comprise the virtual environment and a test scenario, including all realistic features with challenging intra-patient variations, are presented.

- **Chapter 5** addresses the problem of the computational performance of a new open-loop postprandial control approach envisioned to be practically implemented. First, a brief review of the interval analysis and set inversion technology, on which the methodology is based, is presented. Second, the non-optimised version of this control approach and the proposed optimisation algorithm are described. Last, to demonstrate the feasibility of the proposed method, a performance comparison, according to several specific solutions and practical issues, is presented.

- **Chapter 6** is dedicated to the design and validation of a closed-loop control approach for the postprandial period based on sliding mode techniques. This approach enables the reduction of late hypoglycaemic events without increasing the period of hyperglycaemia. Realistic simulations used to evaluate this control approach are addressed to demonstrate the robustness with regards to overcorrection of hyper- and hypoglycaemia under challenging conditions. Different glucose controllers, which utilise a safety layer based on insulin-on-board constraints, are presented to compare the effects on control performance.

- **Chapter 7** presents the software application designed to clinically validate a closed-loop control algorithm for the postprandial period, which was developed based on simulation results obtained in chapter 6. This chapter also includes a description of the study protocol and provides information about the technical documentation required by the national regulatory agency prior to the initiation of clinical trials.

- **Chapter 8** outlines the conclusions and contributions of this research and future studies.

The framework of this thesis is the coordinated project DPI2010-20764-C02, "Nuevas estrategias de control glucémico postprandial mediante terapia con bomba de insulina en diabetes tipo 1" (CLOSEDLOOP4MEAL).

# Chapter 2

# Type 1 Diabetes and Blood Glucose Control

## 2.1 Diabetes Overview

Diabetes mellitus (DM) is a metabolic disease characterised by elevated blood glucose concentration where pancreas either no longer produces enough insulin or cells do not properly uptake glucose in the plasma. Figure 2.1 presents a blood glucose response from a healthy and a diabetic patient when ingests 1 g/kg glucose in a oral glucose tolerance test. The blood glucose resultant for a diabetic patient is higher and takes 3–4 h more to return to baseline.

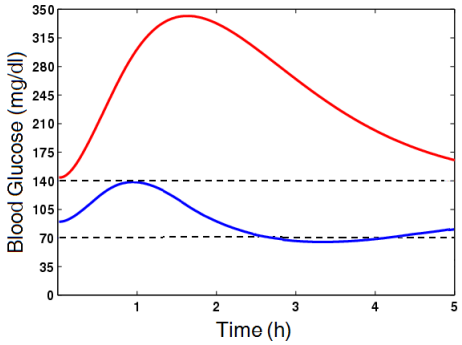


Figure 2.1: Oral glucose tolerance test. The blue line corresponds to a healthy person and the red line to a diabetic patient.

### 2.1.1 Types of Diabetes

#### Type 1 diabetes

Type 1 diabetes mellitus (T1D, known also as insulin-dependent or childhood-onset diabetes) is a chronic and autoimmune disease characterized by the irreversible destruction of the $\beta-$cells in the islets of Langerhans of the pancreas, which are responsible for the excretion of insulin. The inability of the diabetic organism to produce insulin leads to hyperglycemia, which may cause severe diseases in the long-term. Without insulin, glucose remains in the bloodstream, so blood glucose levels increase, especially after meals (Hanas, 2007). The glucose is then passed out of

the body in the urine.

Although T1D can develop at any age, it typically appears during childhood or adolescence. Most common symptoms of T1D include tiredness, hunger, and loss of weight. Untreated hyperglycaemia can lead to serious complications, including cardiovascular diseases, kidney failure, blindness, and stroke. When hypoglycaemia is untreated, it will worsen and cause confusion, clumsiness, or fainting. Severe hypoglycaemia can lead to seizures, coma, and even death.

Early in 1993, the Diabetes Control and Complications Trial Research Group (DCCT) reported the relation among hyperglycemia and the risk of chronic micro and macro vascular complications (Diabetes Control and Complications Trial Research Group, 1993; Reichard et al., 1993). DCCT showed that an intensive insulin treatment keeping blood glucose levels near normoglycemia can significantly reduce the risk of the chronic complications associated with diabetes. Today, the treatment required to achieve this glucose control objective involves the administration of insulin into the body, exercise, and a healthy diet. These treatments in turn increase the risk of severe hypoglycaemia, with all its consequences. Regrettably, a universal, efficient, and safe system of normalizing the glucose levels of T1D patients is still lacking.

#### Type 2 diabetes

Type 2 diabetes (T2D, known also as noninsulin-dependent or adult-onset diabetes) is characterised by a relative lack of insulin secretion and sensitivity. Over time, the number of $\beta-$cells starts to decline and the T2D patient must be treated with insulin, like the T1D, to maintain his/her blood sugar at normal levels. T2D is very insidious and can develop over years before being diagnosed as it is a more gradual process than that of T1D. It is usually found in people over 40 years old, and accounts approximately 90–95% of diabetic patients population worldwide.

T2D is the more common type, can develop at any age and is often preventable. It is believed that the origin of T2D is multifactorial. The risk of developing this form of diabetes increases with age, obesity, lack of physical activity, and some nutritional related factors (American Diabetes Association, 2012). Most common symptoms include thirst, urination, and tiredness. The same disease process can cause impaired fasting glucose and/or impaired glucose tolerance without fulfilling the criteria for a diagnosis of diabetes.

### 2.1.2 Numbers and Estimations

Diabetes mellitus is one of the most common worldwide chronic diseases with continued and growing socio-economic impact. According to the latest data from the *International Diabetes Federation* (IDF), the number of people living with diabetes was more than 371 million in 2012, and it will increase to 552 million by 2030. Between 2011 and 2030, the number of adults with diabetes is expected to increase a 92% in low-income countries, followed by 57% in lower-middle income countries, 46% in upper-middle income countries, and 25% in higher income countries (Shaw et al., 2010; Whiting et al., 2011). The prevalence of diabetes is increasing in every country and half of people with diabetes are unaware of their condition (see Figure 2.2). This increase of worldwide prevalence is mainly attributable to an aging population, the growth in population size, urbanization, and a high prevalence of obesity and sedentary lifestyles.

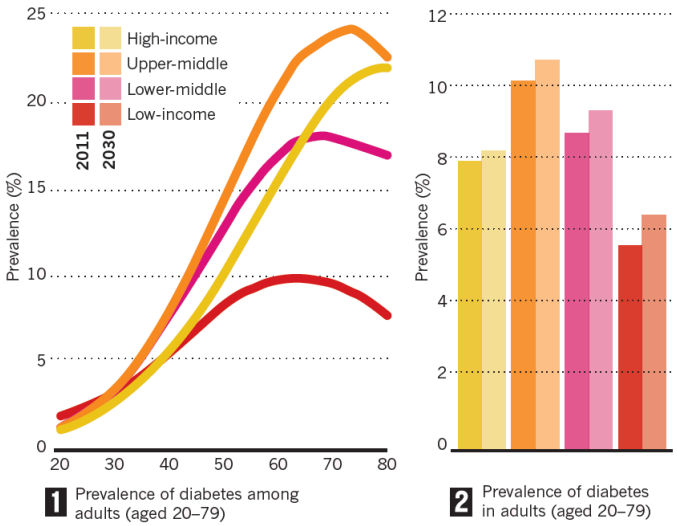


Figure 2.2: IDF global projections for prevalence of people with diabetes (20–79 years), 2011–2030 (taken from Scully (2012)).

Diabetes mellitus and its complications are largely responsible for early death worldwide. More than 4.6 million people (20–79 years) died from diabetes in 2011, accounting for 8.2% of global all-cause mortality of people in this age group (International Diabetes Federation, 2011). Figure 2.3 shows an estimation of the number of deaths attributable to diabetes.

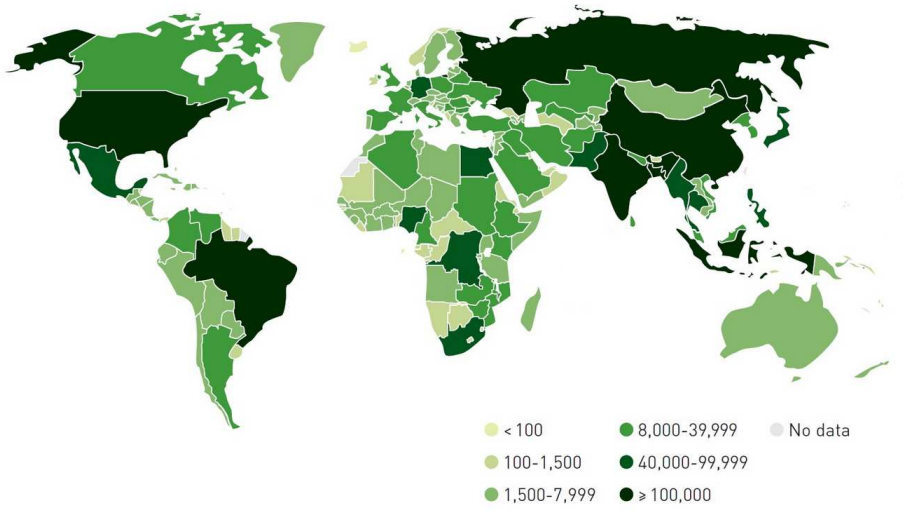


Figure 2.3: IDF estimations for deaths of diabetes related complications (20–79 years) in 2011 (taken from International Diabetes Federation (2011)).

The health-care costs of diabetic people are double the costs incurred by people without diabetes (R=2). Estimated global health-care expenditures to treat diabetes and prevent complications totalled at least US dollars (USD) 465 billion in 2011. By 2030, this number is projected to

exceed some USD 595 billion. Health-care expenditures due to diabetes account for 11% of the total health-care expenditures in the world in 2011 (International Diabetes Federation, 2011). Figure 2.4 shows the estimated expenditure for diabetes by IDF for 2011, assuming R=2. It is clear that there are economic and social benefits in identifying effective therapies for diabetes.

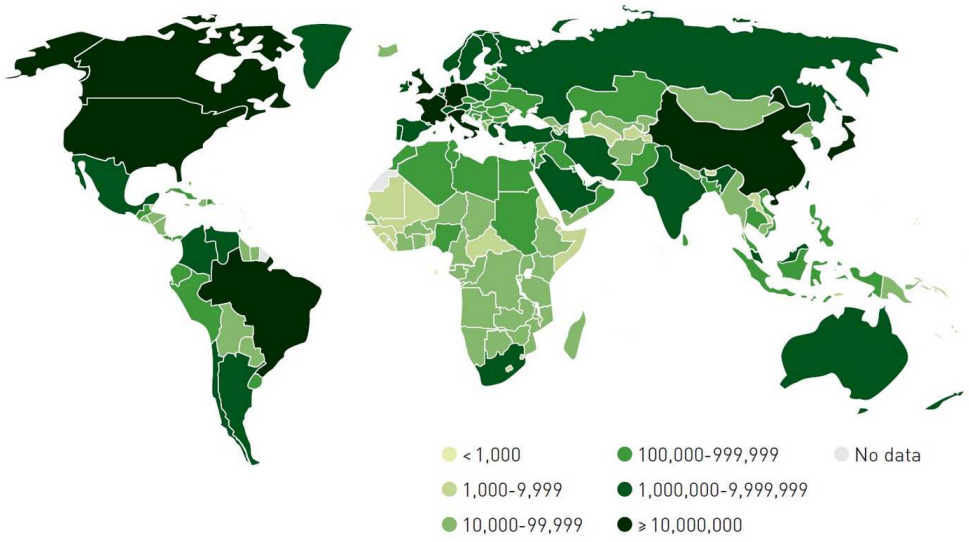


Figure 2.4: Total health-care expenditures (USD) due to diabetes (20–79 years) in 2011 (taken from International Diabetes Federation (2011)).

### 2.1.3 Complications

Diabetes complications may be disabling or even life-threatening. Insulin deficiency and subsequent high blood sugar levels eventually damage blood vessels, nerves, and organ systems in the body. The potentially debilitating complications arising with diabetes may initiate in the short- or long-term.

#### Short-term complications

Short-term complications are the day-to-day problems that can appear without warning. Hypoglycemia and hyperglycemia are considered short-term complications, and the symptoms vary depending on how much the glucose levels are reduced or elevated. Both T1D and T2D may develop the same complications. Some people, especially those with prediabetes or T2D, may not experience symptoms initially. In T1D, symptoms tend to come on quickly and be more severe. Some of the signs and symptoms of T1D and T2D include:

- Increased thirst
- Blurred vision
- Extreme hunger

- Unexplained weight loss
- Fatigue
- Slow-healing sores
- Frequent urination
- High blood pressure
- Weakness or shakiness
- Nervousness
- Frequent infections, such as gums or skin infections and vaginal or bladder infections

Prolonged hyperglycaemia can lead to a condition called "ketoacidosis", which is caused by high levels of ketones in the blood and urine. Ketones are a byproduct of the breakdown of muscle and fat that happens when there is not enough insulin. This can lead to acidosis or "diabetic ketoacidosis" (DKA), a condition in which the blood is too acidic. DKA is an emergency situation that requires immediate care, otherwise it may induce a diabetic coma.

### Long-term complications

Diabetes is a chronic illness with no cure, and it is progressive. High blood sugar levels eventually damage blood vessels, nerves, and organ systems in the body. Many of the complications of diabetes do not show up until after many years of having the disease.

Glycosylated hemoglobin (HbA1c) is the "gold standard" in the management of diabetes and it is commonly used to assess long-term blood glucose control. The normal range for the HbA1c test is 4–6% for people without diabetes. Above this range, the higher the HbA1c value, the greater long-term risk of complications associated with diabetes. These chronic complications can be classified as macro-vascular, or as micro-vascular. Among the potential complications are:

**Cardiovascular disease** Diabetes dramatically increases the risk of several cardiovascular problems, including coronary artery disease with chest pain (angina), heart attack, stroke and narrowing of arteries (atherosclerosis). People with diabetes are more likely to have high cholesterol and hypertension, both of which cause damage to the cells lining the artery walls. Cardiovascular disease is one of the leading causes of death for people with diabetes and can account for 50% or more of deaths due to diabetes.

**Nerve damage (neuropathy)** The impact of diabetic neuropathy in the nerve damage can range from slight inconvenience as loss of feeling, pain and weakness in the feet, legs, hands, and arms, to major disability and even death. Excess sugar can injure the walls of the tiny blood vessels (capillaries) that nourish the nerves. Neuropathy affects more than 60% of T1D people.

**Kidney damage (nephropathy)** Diabetic kidney disease is one of the most common and most devastating complications of diabetes. The kidneys contain millions of tiny blood vessel clusters (glomeruli) that filter waste from the blood. Diabetes can damage this delicate filtering system. Severe damage can lead to kidney failure or irreversible end-stage renal disease. About one third of T1D people develop nephropathy.

**Eye damage (retinopathy)** Diabetic retinopathy is the most common and serious eye-related complication of diabetes. It is a progressive disease that can destroys small blood vessels of the retina, potentially leading to blindness. Diabetes also increases the risk of other serious vision conditions, such as cataracts and glaucoma. Nearly all T1D people show some symptoms of diabetic retinopathy, usually after about 20 years of living with diabetes; approximately 20% to 30% of them develop the advanced form.

**Erectile Dysfunction** Diabetes is one of the primary causes of erectile dysfunction. An erection occurs when nerves send a message to the muscles of the corpus cavernosa in the penis to relax so that the spongy tissue can fill with blood. With diabetes, the nerve impulses are impaired, so the muscles do not relax adequately, and the circulation to the corpus cavernosa may be impaired as well so that the tissue can not fill with blood.

**Foot damage** Nerve damage in the feet or poor blood flow to the feet increases the risk of various foot complications. Left untreated, cuts and blisters can become serious infections. Severe damage might require toe, foot or even leg amputation.

**Skin and mouth conditions** Diabetes may leave skin problems, including bacterial and fungal infections. Gum infections also may be a concern, especially with a history of poor dental hygiene.

## 2.2 Blood Glucose Control

### 2.2.1 Synopsis of Blood Glucose-Insulin Regulation

An appropriate regulation of blood glucose concentration is generally performed with insulin to reduce high glycaemia and with glucagon to counteract and maintain glycaemia within a normoglycaemic range (70–109 mg/dl or 3.9–6.04 mmol/l). Both hormones are secreted by the pancreatic islets of Langerhands and are critical to the regulation of carbohydrate, protein and lipid metabolism. Figure 2.5 illustrates the feedback loop, in which the two hormones maintain homeostasis for blood glucose levels. The basic mechanism for blood glucose regulation can be explained by two metabolic conditions. When a person consumes a meal, his/her glucose level increases, which is referred to as hyperglycaemia, and the $\beta-$cells of the pancreas respond by secreting insulin to consume the glucose in the plasma and cease glucose production in the liver. When a person exercises, his/her glucose level decreases, which is referred to as hypoglycaemia, and the $\alpha-$cells of the pancreas respond by releasing glucagon and the liver converts glucagon and glycogen to glucose. Exogenous factors that affect blood glucose concentration include food intake, physical activity, illness, stress, and reproductive state.

### 2.2.2 Diabetes Treatment

Diabetes mellitus treatment has progressively evolved since the discovery and isolation of insulin and its subsequent purification in 1921 (Bliss, 2007). Prior to 1921, people with diabetes were treated using strict diet control to achieve smooth blood glucose peaks and to prevent death. In 1978, the synthetic version of human insulin subsequently led to current diabetes treatment. Insulin enables diabetic patients to live with a chronic disease according to basic considerations of insulin therapy. Presently, the most common treatment for T1D patients is performed subcutaneously through injections or infusion of insulin.

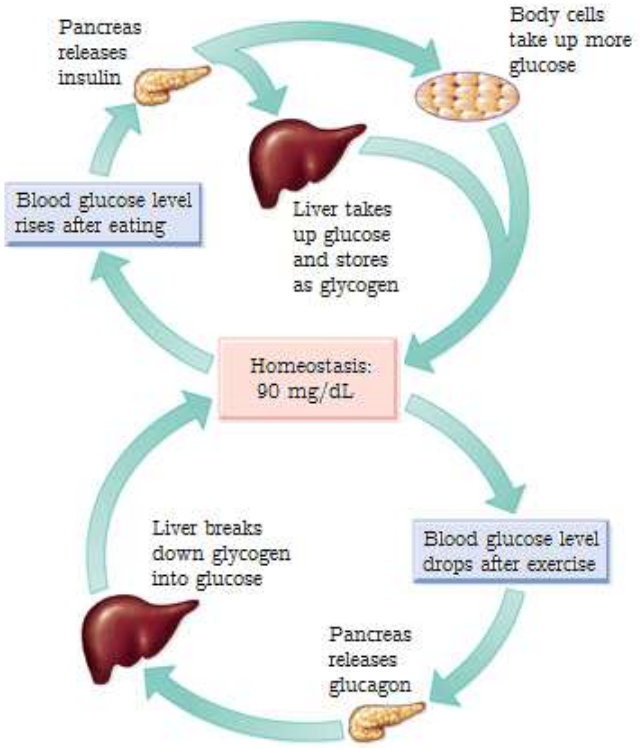


Figure 2.5: Insulin and glucagon secretion from islet cells, which maintains homeostasis for blood glucose levels (adapted from Campbell et al. (2006)).

Alternatives, such as islet transplantation, offers the advantages of safety and stability and a potential remedy as no reservoir of insulin is required. However, the high risk of graft rejection, which is potentially carcinogenic, is a deterrent to the use of islet transplantation (Senior et al., 2012). As the side effects can be significant, it is often performed in conjunction with a kidney transplant. Therefore, this alternative is typically reserved for patients who exhibit serious diabetes complications. Until stem cells for the regeneration of pancreatic $\beta-$cells become available (Soria et al., 2001), T1D management using insulin therapy can improve a person's quality of life.

The use of synthetic insulin to counteract $\beta-$cell destruction and subsequent genetic manipulation of its structure creates an extensive range of insulin analogues with unique pharmacologic features. Each type of insulin is characterised as follows:

- Onset - when the effects of insulin are detected;
- Peak - when the effects of insulin achieve optimum performance;
- Duration - the length of time during which the effects of insulin are exhibited.

Available insulin analogues are classified according to their period of action, as shown in Table 2.1. In some cases, pre-mixed insulin –a combination of specific proportions of intermediate-acting, short-acting or rapid-acting insulin in one bottle or insulin pen– is an option.

| Insulin type | Generic and brand name | Onset of action | Peak effect | Duration |
|---|---|---|---|---|
| rapid-acting | Lispro (Humalog) | 5-15 minutes | 30-90 minutes | 3-5 hours |
| | Aspart (NovoLog) | 10-20 minutes | 1-3 hours | 3-5 hours |
| short-acting | Regular (Humulin R, Novolog R) | 30-60 minutes | 1-5 hours | 6-10 hours |
| intermediate-acting | NPH human (Humulin N) | 1-2 hours | 6-14 hours | 16-24 hours |
| long-acting | Glargine (Lantus) | 1.1 hours | None | ∼24 hours |

Table 2.1: Pharmacokinetics of available insulin products.

### 2.2.3 Intensive Insulin Treatment

Conventional treatment conducted with insulin analogues is administered daily in one to three fixed doses of insulin using a mixture of intermediate- and short-acting insulin. This regime is minimally intrusive for diabetics with a normal lifestyle (i.e., consuming approximately the same amount of food at the same time each day and maintaining the same daily level of activity) to match the insulin dose. However, the use of several insulin doses per day to achieve blood glucose levels that are similar to the blood glucose levels of nondiabetic people has been shown to minimise the risk of long-term complications associated with hyperglycaemia (Diabetes Control and Complications Trial Research Group, 1993). This treatment is referred to as intensive insulin therapy (IIT). IIT typically employs the subcutaneous route and involves a continual supply of insulin to serve as basal insulin, a supply of meal insulin in doses that are proportional to the nutritional load of the meals (also known as bolus insulin), and a supply of extra insulin when needed to correct high glucose levels.

Insulin analogues with different physiologic pharmacokinetic properties were used to obtain optimised intensive insulin therapies (Diabetes Control and Complications Trial Research Group, 1993; Hirsch, 2005). An IIT performed with multiple daily injections (MDI) is implemented with long-acting insulin analogues for basal insulin, which are expected to produce a daily flat profile of plasma insulin concentration, and rapid-acting insulin formulations for bolus insulin, which is expected to exhibit rapid onset of action to overcome postprandial hyperglycaemia or high glucose concentrations (Shetty and Wolpert, 2010).

An IIT performed with continuous subcutaneous insulin infusion (CSII), which is implemented by an insulin pump using short- or rapid-acting insulin analogues, is used for basal and bolus dosages. In CSII therapy, basal infusion rates are programmed with time-varying profiles over a 24-h period to account for circadian variations of a patient's insulin sensitivity and activity. Figure 2.6 shows the insulin profiles obtained from mentioned insulin therapies.

Modern insulin pumps for CSII therapy contain an electronic drive mechanism that enables the delivery of small amounts of insulin or microboluses from a reservoir, as shown in Figure 2.7. To emulate basal insulin, the pump varies the delivery frequency of microboluses according to the insulin rate programmed by the user. This mechanism enables greater flexibility and more effective glycaemic control. Several studies have shown that diabetes patients who undergo intensive insulin treatments with CSII using insulin pumps exhibit improvements in glycaemic control compared with MDI, especially in patients with a history of poor glycaemic control (Bell and Ovalle, 2000; Pickup et al., 2002; Retnakaran et al., 2004; Nimri et al., 2006; Buse et al., 2011).

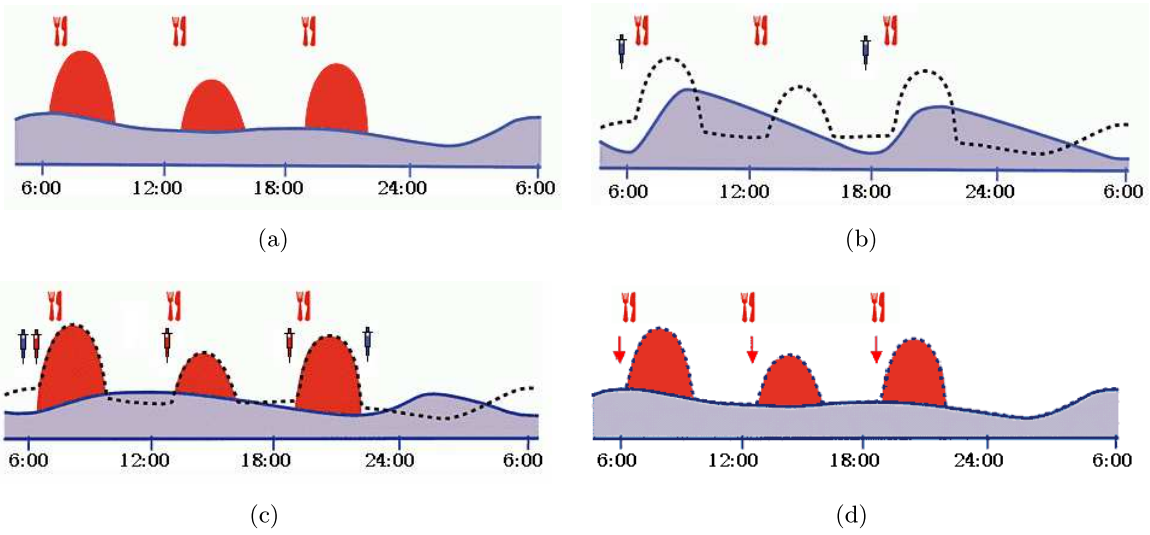


Figure 2.6: Insulin profiles obtained according to the therapy used. In red the bolus insulin dose and in blue the basal insulin dose. Profile obtained from (a) insulin released in non-diabetics, (b) insulin delivery with conventional therapy, (c) insulin delivery with multiple daily injections (MDIs), and (d) insulin delivery with continuous subcutaneous insulin infusion (CSII). The insulin profile from non-diabetics is highlighted in all figures with dashed lines.

For the MDI or CSII methods, IIT requires self-monitoring of blood glucose to achieve optimal blood glucose regulation. The patient must frequently check his/her glucose levels and consider an estimation of their carbohydrate intake, their insulin sensitivity, and the amount of insulin previously administered as well as other considerations. According to blood tests in typical cases, insulin injections are supplied subcutaneously three or four times daily.

The major benefits of IIT include prevention or reduction of the progression of long-term diabetes complications. In 1993, the Diabetes Complications Research Group reported that the strict control of blood sugar levels reduces the risk of diabetes-related heart attacks and strokes by more than 50%, reduces the risk of eye damage by more than 75%, reduces the risk of nerve damage by 60%, and prevents or slows the progression of kidney disease by 50% (Diabetes Control and Complications Trial Research Group, 1993; Reichard et al., 1993).

## 2.3 Control Devices for Glucose Regulation

### 2.3.1 Insulin Delivery

Several options of insulin delivery to perform intensive insulin therapies (IIT) are available (Takahashi et al., 2008). Due to its rapid delivery capabilities, rapid-acting insulin is commonly used with subcutaneous injection to comprise the bolus supply of endogenous insulin during meal intake. In particular, the subcutaneous injection of Lispro insulin has been proven to take effect within approximately the same time frame as intravenous-injected regular (normal) insulin (Bellazzi et al., 2001). This finding enables the control of patient glucose levels with home monitoring that is similar to the control of patient glucose levels with intravenous management but in a less invasive and painful manner.

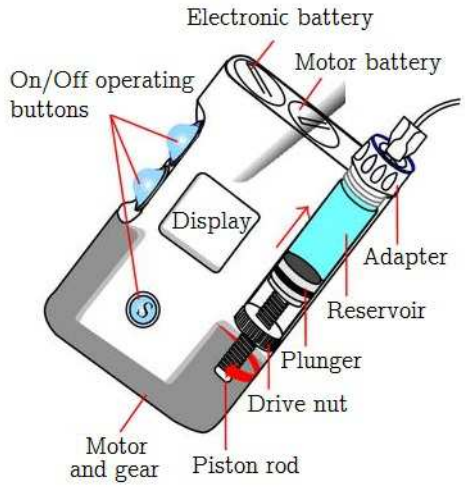


Figure 2.7: Main parts of an insulin pump (obtained from Valla (2010)).

The majority of people who take insulin use a needle and syringe to subcutaneously inject insulin. Common alternatives for delivering insulin consist of insulin pens and insulin pumps. Using a syringe, insulin pen or insulin pump, the subcutaneous insulin supply is usually administered in the fat under the skin. Figure 2.8 shows examples of these devices. Injection ports, injection aids, and insulin jet injectors are also available.

Figure 2.8: Devices used for insulin delivery: syringe, pen, and pump.

For insulin injections with a syringe or an insulin pen, basal supply is performed by slow-acting insulin as it achieves a longer effect than other types of insulin. In addition to the prandial bolus, each shot in IIT is devised such that the effect of the insulin dosage can be maintained for as long as possible. An insulin pump continuously supplies a small amount of rapid-acting insulin analogues as basal doses (Bode, 2011). The bolus dose during mealtime is supplied by increasing the rate of insulin to adjust high blood glucose concentrations. Of all treatments, insulin pump therapy is the treatment that closely simulates the action of a healthy pancreas.

Some important features about insulin pens and insulin pumps are described as follows:

**Insulin pens** are convenient and simple ways of injecting insulin and are considered less painful than a standard needle or syringe. An insulin pen resembles a pen with a cartridge. Some insulin pens contain cartridges of insulin that are inserted into the pens, whereas other

pens are pre-filled with insulin and discarded after the insulin has been exhausted.

**Insulin pumps** are approximately the size and weight of a cell phone. They comprise a disposable insulin reservoir, a small battery-operated motor that is linked to a computerised control mechanism module with a display, and a subcutaneous infusion set (cannula and tubing system). Integrated systems, such as the MiniMed Paradigm REAL-Time System, represents the first step in combining glucose monitoring and insulin delivery systems and employs the most advanced technology available.

Table 2.2 lists pros and cons of insulin pens and insulin pumps in comparison with conventional syringes.

### 2.3.2 Glucose Monitoring

#### Glucometers

The first patent for a blood glucose monitor for health-care use in diabetic patients was filed in 1971 in the USA by Anton Clemens. New versions of the sensor were subsequently developed. The first studies with this home blood glucose monitoring, which demonstrated a dramatic improvement in glycaemic control in 10 T1D patients, revealed a mean glycated haemoglobin (HbA1c) of 5.4% at the endpoint compared with a baseline of 10.3% (Peterson et al., 1978).

To adjust diabetes treatment, point samples are predominantly used to check the level of glucose from capillary blood measured with a glucometer. Self-monitoring of blood glucose (SMBG) can be performed anywhere, such as at home or work. The process involves pricking a fingertip to collect a drop of blood, absorbing the blood with a test strip, and inserting the test strip into an electronic glucose monitor, which displays a number on a screen. Figure 2.9 shows a typical device used to perform capillary blood tests.


Figure 2.9: Glucose meter used in a capillary blood test.

SMBG has been described as one of the most important advancements in diabetes management since the invention of insulin. Capillary blood glucose levels at the fingertip have been shown to correlate with systemic arterial blood glucose levels (Koschinsky et al., 2003). Recent advances in glucose sensor technology for measuring interstitial glucose concentrations have challenged the dominance of glucose meters in diabetes management (Cengiz and Tamborlane, 2009). Nearly all commercially available glucose sensors share the subcutaneous interstitial fluid (ISF) compartment as their preferred implantation site. Numerous technologies are pursued to develop novel glucose sensors, including invasive, non-invasive or minimally invasive sensors.

| Insulin pens | |
|---|---|
| Pros | Cons |
| · They are portable, discreet, and convenient for remotely administered injections. | · Insulin in pens and cartridges are frequently more expensive than insulin in bottles for use in syringes. |
| · The extraction of insulin from a bottle is not necessary, it is already pre-filled in the self-contained cartridge. | · Some types of insulin are not available for use in insulin pen cartridges. |
| · They usually allow a patient to set an accurate dose by the simple turn of a dosage dial. | · Some insulin is wasted when pens are used, one to two units of insulin are wasted when the pen is primed prior to each injection. |
| · Their design and compact size enable simple and convenient insulin delivery. | · The mixing of different types of insulin is prevented, if an insulin mixture is required, it is not available as a pre-mix. |
| · Possible single-dose amounts range from 0.5 to 80 units, depending on the pen. | · Some patients may also require two insulin pens if their treatment involves two different types of insulin. |
| **Insulin pumps** | |
| Pros | Cons |
| · Delivers insulin in precise units, a minimum of 0.05 units, that can be closely matched to the needs of a patient. | · Can cause weight gain. |
| · Facilitates matching of insulin to the lifestyle of a patient rather than adjusting the lifestyle of a patient to his/her body's response to insulin injections. | · Can be bothersome as the patient is frequently attached to the pump. |
| · Reminders and alerts on pumps can be customised for safety to improve control and reduce the frequency of hypoglycaemia. | · Increases the risk of diabetes ketoacidosis, if insulin delivery is disrupted for any reason, blood glucose will increase and rapidly increase the risk of ketoacidosis. |
| · Eliminates the inconvenience of multiple daily injections and the unpredictable effects of associated intermediate- or long-acting insulin. | · May be expensive, the pump costs approximately $7000 and the supplies cost approximately $1500 per year. |
| · Enables a patient to exercise without having to consume large amounts of carbohydrates. | |
| · Includes bolus advisors that assist the patient and delivers special meal boluses that correspond to the delayed absorption of certain foods. | · Can malfunction and deliver too much or too little insulin. |

Table 2.2: Primary features of insulin pens and insulin pumps.

According to these technologies, measurements may depend on transdermal, sampling of blood or ISF. Please see Takahashi et al. (2008); Oliver et al. (2009) for a comprehensive review of the topic.

### Continuous Glucose Monitoring

Existing continuous glucose monitoring (CGM) systems have the advantage of direct insertion of electrochemical sensors into the subcutaneous space rather than having to transport of the sampled fluid outside the body to detect glucose concentrations. Commercially available CGM systems that are approved by the Food and Drug Administration (FDA) have been introduced over the last decade. The first system on the market was the MiniMed (Northridge, CA) continuous glucose monitoring system, which stored glucose readings every 5 min for a maximum of 3 days (Tavris and Shoaibi, 2004). However, sensor glucose values were only available retrospectively after downloading of the sensor data.

The advent of real-time glucose sensing has been crucial to glucose monitoring technology. In contrast with former retrospective analysis systems, real-time glucose monitoring enables a patients to rapidly adjust their insulin doses, food intake and physical activity by inspecting glucose values and trends and by responding to low and high glucose alarms.

The main value of CGM in clinical practice involves the identification of trends of glucose values and the reduction in the frequency and severity of hypoglycaemic events. In previous years, three continuous glucose monitors have appeared on the market: the Abbott FreeStyle Navigator® continuous glucose monitoring system, the DexCom SEVEN®, and the Medtronic MiniMed Paradigm® REAL-Time insulin pump and continuous glucose monitoring system. The devices display a new glucose reading every 1 to 5 minutes for a maximum of seven days of continuous wear per sensor insertion. Figure 2.10 shows currently available CGM systems.


Figure 2.10: Current CGM devices used in home monitoring: the Abbott FreeStyle Navigator® continuous glucose monitoring system, the DexCom SEVEN®, and the Medtronic MiniMed Paradigm® REAL-Time insulin pump and continuous glucose monitoring system.

As continuous glucose sensor manufacturing has not progressed to the accuracy and precision of blood glucose meter strips, sensor glucose signals must be calibrated against corresponding blood glucose meter levels. Although sensor levels may trail glucose levels by 5–10 min, the most important effect on lag is the introduction of error during calibration, which affects long-term sensor performance. The effect of sensor lag on performance is evident during periods of rapid glucose rate of change (increase or decrease). Software programs have been designed to accommodate the lag in subcutaneous glucose readings (Stout et al., 2004). Biocompatibility problems, such as biofouling and degeneration, contribute to drift in sensor signals over time and affect sensor functionality (Mang et al., 2005).

The continuous glucose sensor is a critical component of closed-loop insulin delivery systems and must be selective, reliable, durable, wearable, rapid, predictable and acceptable for continuous patient use. CGM systems are expected to become more suitable devices that encourage

improvements in future applications.

## 2.4 Postprandial Control

Advances, such as the discovery of insulin and modern diabetes technology, have generated significant improvements in the quality of life of diabetes patients. However, hypoglycaemia remains the most feared complication of insulin therapy by prescribers and patients. Although modern rapid-acting insulin analogues suppress glucose increases either by meals or variations in sensitivity, it requires 90–120 minutes for subcutaneously delivered insulin analogues to attain their maximum glucose-lowering capacities.

A primary challenge that entail the delays associated of the absorption of subcutaneously delivered insulin is the postprandial period. Using insulin infusion to compensate for meals, particularly unannounced meals, can cause late postprandial hypoglycaemia as open- or closed-loop systems may deliver too much insulin as a way to correct high postprandial glucose levels.

This problem can be significantly reduced by the intravenous route, which offers several benefits compared with other routes of insulin injection. For example, intravenous infusion of insulin acts more rapidly and reaches the bloodstream more effectively, which enables management of an insulin overdose. Subcutaneous insulin injection is preferred to facilitate continuous glucose management as it is much more agreeable and safer to conduct during home monitoring. In addition, the subcutaneous route exhibits a minimal risk of infection and, compared with conventional single injections, a subcutaneous infusion of insulin improves the administration of the glycaemic profile. Intraperitoneal insulin infusion is rapidly effective and is less likely to produce hypoglycaemia than subcutaneously infusion due to rapid uptake and metabolic activity, but requires invasive procedures to install and maintain.

Regardless of the route, an important limitation of insulin therapy in postprandial control is its one-way action, i.e., insulin cannot be removed from the body once it is supplied. Research on dual-hormone therapies that considers the administration of insulin and glucagon to reduce the risk of hypoglycaemia are in progress (Castle et al., 2010; El-Khatib et al., 2010). However, commercially available glucagon is not likely to be suitable for extended pump use as it does not maintain its liquid form at room temperature after the powder and solution are combined (Jackson et al., 2012). Research is underway to develop more stable formulations of the hormone (Haidar et al., 2013). Thus, physicians and patients should carefully select the type and amount of insulin to use in their daily control therapies.

Insulin pumps used for CSII therapy offer more advantages over MDI and facilitate a more comfortable lifestyle. Modern insulin pumps incorporate bolus advisors that help patients to calculate prandial bolus, which is a customisable basal insulin flow that is sensitive to daily changes and custom alarms. (Walsh and Roberts, 2006; Zisser et al., 2008a). Similarly to support intensive insulin therapy (IIT), industry investment and research progress in more reliable CGM systems has enabled the development of corrective actions by improving the performance of open-loop treatments. They are currently combined in decision support systems or sensor-augmented insulin pumps.

Although subcutaneous insulin infusion is expected to follow complex real hormone secretion, conventional insulin therapy does not sufficiently follow the complex metabolism of a nondiabetic

person. The majority of existing problems in postprandial control refer to insulin dynamics, take too long to begin and last too long for most meals. This undesired imbalance, which is usually represented by poorly controlled T1D patients, produces short-term hyperglycaemia and late-term episodes of hypoglycaemia (Walsh and Roberts, 2006). Imprecise estimation of the amount of ingested carbohydrates, metabolic changes in the glucose-insulin system, and sources of variability, such as stress and physical activity, are also prone to hypoglycaemia in the late postprandial period (Diabetes Control and Complications Trial Research Group, 1993; Reichard et al., 1993; Fatourechi et al., 2008).

### 2.4.1 Basal-Bolus Therapy

The suggested bolus dose to be performed using MDI or CSII therapy is calculated based on several patient's parameters as the insulin-to-carbohydrate ratio ($I:CHO$), the correction factor ($CF$), and the insulin-on-board ($IOB$) to prevent insulin stacking (Zisser et al., 2008a). The bolus dose is typically calculated as follows:

$$Bolus = I:CHO \times CHO + \frac{pBG - TBG}{CF} - IOB \tag{2.1}$$

where $I:CHO$ in units of IU/g, $CHO$ is the meal in units of g, $pBG$ is the preprandial blood glucose value in units of mg/dL, $TBG$ is the target for glucose concentration in units of mg/dL, and the $CF$ is in units of mg/dL/IU. The $IOB$ value is commonly calculated according to some predefined curves that are used to estimate the remaining active insulin in the body (Walsh and Roberts, 2006). In addition to prandial boluses, the correction factor $CF$ is also used with occasional fingerstick glucose measurements in IIT to trigger corrective actions in order to react to deviations from the nominal profile expected to produce with the control therapy. These correction actions are more suitable when a continuous glucose monitoring system is involved.

Regarding the basal dose, the first step is to determine the total daily dose ($TDD$) of insulin:

$$TDD = K \times W \tag{2.2}$$

where $W$ is the subject's weight and $K$ is a subject-specific constant that is dependent on the sensitivity exhibited by each patient. The units of $W$ are in kilograms and the range of $K$ is typically 0.5 to 2.0 IU/kg (Walsh and Roberts, 2006). The basal insulin requirement is approximately 50% of the $TDD$; thus, the resulting basic basal rate (IU/h) should be expressed as follows:

$$Basal = 0.5 \left( \frac{TDD}{24} \right) \tag{2.3}$$

Insulin sensitivity changes throughout the day due to circadian variation of hormone levels. During a single 24-h cycle, basal insulin requirements are relatively high during the early morning period and subsequently decrease during the remainder of the day and night.

### 2.4.2 Bolus Types and Settings

In CSII therapy, bolus insulin infusion can be delivered via different profiles to distribute the meal-related insulin infusion in a manner that optimises postprandial glycaemic control. Normal, square wave, and dual wave boluses are currently embedded into commercial insulin pumps as part of automatic bolus calculators or bolus advisors to address different meal compositions or other circumstances, such as stress, exercise and foods, which vary in glycaemic index or in fat and protein content (Chase et al., 2002; Zisser et al., 2010b; Klonoff, 2012). Figure 2.11 shows the types of bolus profiles currently found in insulin pumps.

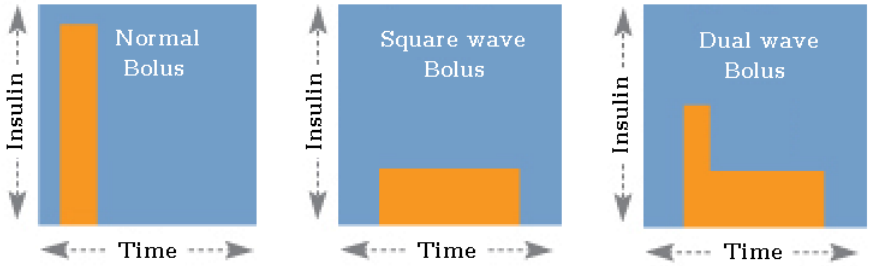


Figure 2.11: Bolus insulin profiles available in modern insulin pumps.

Insulin pump settings are commonly adjusted by the healthcare provider to calculate appropriate basal and bolus doses. Whichever method is used to calculate parameters, it is generally considered a starting point and should be refined as needed as insulin resistances may vary from person to person and/or over time.

Several guidelines for optimal bolus calculator settings from formulas based on individual measurements have been investigated to minimise frequent hypoglycaemia and lower elevated mean glucose levels (Davidson et al., 2008; Shashaj et al., 2008; Scheiner et al., 2009; Walsh et al., 2010, 2011). Even when parameters like $I : CHO$, $CF$, $IOB$, and basal doses from $TDD$ are accurately and appropriately used, situational dose modifications by users will always be required for changes in activity, weight, stress, and other variables.

Despite the development of bolus advisors and associated guidelines to obtain appropriate settings, the optimisation of postprandial control remains an empiric process based on the experience of the physician and the patient; it does not offer complete solutions to the primary concerns of T1D patients and only partially satisfies IDF guidelines for postmeal control (no hypoglycemia and 2-h postprandial glucose below 140 mg/dL) (International Diabetes Federation, 2007). A critical evaluation of several clinical trials, which were performed to determine the impact of the different types of boluses on postprandial metabolic control, revealed fundamental shortcomings in the study design and performance of the majority of the trials (Heinemann, 2009). Therefore, the benefits of different bolus profiles included in modern insulin pumps, such as the combination/dual-wave bolus, need to be carefully accepted until better evidence is obtained.

*In silico* studies have also been conducted to improve the process of tuning parameters involved in conventional schemes and to test new open-loop control schemes. Run-to-run optimisation methods have been presented by Zisser et al. (2005) and Palerm et al. (2007) to adjust $I : CHO$ based on user evaluation of $CHO$ amount and several blood glucose measurements.

The best-fitting basal insulin injection doses were implemented by dividing the day into four segments. This repetitive blood glucose control strategy was focused on the adaptation of the basal insulin infusion rate in order to reduce the risk of hypoglycemia, and converged within approximately six days of simulation without hypoglycemia events. However, it can not respond to a rapid change in glucose concentration (meals) which may cause severe hyperglycemia (Palerm et al., 2008).

A prandial insulin delivery method using a set-inversion-based (SIB) algorithm based on mathematically guaranteed techniques (interval analysis) was presented in Bondia et al. (2009); Revert et al. (2011). The algorithm calculates the optimal prandial basal-bolus combination from a pre-prandial glucose measurement and a patient's prediction model which may account for intra-patient variability. SIB algorithm, also called iBolus algorithm, revealed the need of a temporal basal decrement at mealtime combined with an equivalent increase in the meal bolus (a generalization of the superbolus concept introduced by Walsh and Roberts (2006)). This alternative bolus profile achieves good postprandial performance when the carbohydrate content is high, such as in meals that contain grams of carbohydrates equal to or greater than the person's weight (kg). The iBolus algorithm allows for a decrease in a meal bolus combined with an equivalent increase in basal delivery. Compared to traditional bolus administration mode, one of the major advantages of this new approach is that it allows the patient be more aggressive and flexible with prandial insulin doses without increasing the risk for late-term hypoglycemia.

## 2.5 Summary

In this chapter, a brief overview of diabetes, the short- and long-term complications of diabetes, and the associated socio-economic impacts are described. Traditional and modern therapies, which are employed as part of intensive insulin therapy to improve the blood glucose control of diabetic patients, have also been addressed. The most considerable advance in intensive insulin therapy involves modern devices of diabetes technology, which enable the patient to be more effective in their daily treatment. Existing devices for insulin delivery and glucose measurement are presented with a special focus on subcutaneous insulin pumps and continuous glucose monitoring systems. Finally, the control methods most extensively used for postprandial glucose regulation in T1D are also described.

# Chapter 3

# Artificial Pancreas Research

## 3.1 Introduction

Improving glycaemic control and overcoming drawbacks of traditional therapies, which are likely to produce abnormal glucose levels and present inappropriate burdens for patients, was envisioned with the concept of glycaemic control in a "closed-loop"; in diabetes technology, this is also referred to as the artificial pancreas (AP). The AP is an engineering solution that can simulate the endocrine function of a healthy pancreas to provide fully automated glycaemic control. It consists of a continuous glucose monitoring (CGM) system, which provides real-time measurements to an automatic closed-loop controller that is responsible for calculating and administering the proper dose to infuse using an insulin pump without (or with minimal) human intervention. Figure 3.1 shows a schematic design of automatic glycaemic control or AP.

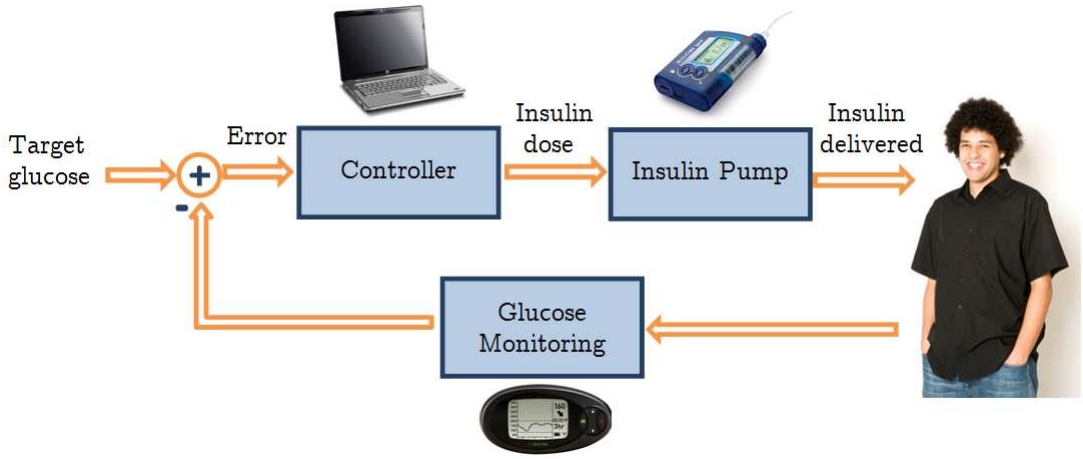


Figure 3.1: Closed-loop components of an artificial pancreas system.

Utilising current insulin pump and glucose sensor technology, closed-loop systems present a promising method of addressing the complications of hypoglycaemia and hyperglycaemia, whilst simultaneously maintaining recommended levels of HbA1c by experts (Weinstock, 2011).

However, the control of postprandial glycaemia excursions is a barrier to AP development. Meals comprise the main challenge of existing clinical validations of the few existing prototypes

of automated glycaemic control. For safety and regulatory reasons, automatic closed-loop therapies have only been administered with intensive supervision (Hovorka et al., 2010; El-Khatib et al., 2010; Kovatchev et al., 2010; Cobelli et al., 2011; Breton et al., 2012). Some deployments of a wearable AP for outpatient trials, including a smartphone computational platform for ambulatory use, are underway (Cobelli et al., 2012). Unfortunately, robust and reliable automatic control systems that are capable of providing satisfactory performance for different patient conditions, including the postprandial period, have not yet been realised.

From a control standpoint, the design of a control algorithm for the AP encounters the following challenges:

- Slow dynamic response to the control action.
- Nonlinear, uncertain and time-varying models.
- Large disturbances, such as meals, stress and exercise.
- Non-negative actuation.
- Measurement errors, including noise, drift and bias.

In recent years, numerous research teams have worked to develop artificial pancreas systems (Weinzimer et al., 2008b; Kovatchev et al., 2009; Buckingham et al., 2010; Kovatchev, 2011; Hovorka et al., 2011; Heinemann et al., 2011; Ward et al., 2011; Nimri et al., 2012). Improvements in continuous glucose monitors, such as improved sensors (more reliable and more precise) and more accurate calibration algorithms, represent significant progress. However, the development of reliable, effective and robust control algorithms that consider all problems of the subcutaneous route and safety issues, remains a major concern.

One of the most significant global advances in the field of the AP was accomplished by the Juvenile Diabetes Research Foundation (JDRF) Artificial Pancreas Consortium, which launched in 2006 to validate the effectiveness of new technologies in continuous glucose monitoring and to promote the development of simulators for preclinical testing that enable "close the loop" by linking continuous glucose monitors with insulin pumps. This research extends previous studies that were funded by JDRF at Yale, which demonstrated that patients with T1D, who used closed-loop systems in a hospital, frequently measured in the normal glucose range. The consortium has funded multiple sites coordinated by the Jaeb Centre for Health Research to assess the feasibility, efficacy and safety of various automated closed-loop glucose control systems and to improve their effectiveness in real-world situations, such as meals, exercise, and stress. Although initial research has been conducted in hospital-based clinical settings, the initiative is also testing AP systems in settings representative of daily life, such as at home or school. Consortium participants include Cambridge University, Boston University, the Oregon Health and Science University, the Sansum Diabetes Research Institute, Stanford University, the University of Colorado, the University of Virginia, and Yale University. Groups from Italy and France also participate.

In addition to JDRF's aggressive campaign, which is focused on accelerating the development, regulatory approval, clinician adoption, and health insurance coverage of an artificial pancreas and its components, AP research is one of the critical path initiatives of the Food and Drug Administration (FDA). The FDA aims to accelerate the development and availability of a

safe and effective artificial pancreas for the treatment of diabetes mellitus. In partnership with the National Institutes of Health (NIH), the FDA has established a multidisciplinary group of scientists and clinicians to address the clinical, scientific and regulatory challenges related to this unique medical product.

The Diabetes wiREless Artificial pancreas consortiuM (DREAM) project (Nimri et al., 2012) is an international collaborative research project that consists of teams from Schneider Children's, the Department of Pediatric Endocrinology and Diabetes at Kinderkrankenhaus auf der Bult in Hannover, Germany, and the Department of Pediatric Endocrinology, Diabetes and Metabolism at University Children's Hospital in Ljubljana, Slovenia. In this project, an artificial pancreas trial was conducted outside of the hospital as a prospective crossover study within the framework of the 3-day DREAM Camp for Children with Diabetes at a hotel near Jerusalem. The camp was composed of 18 children between the ages of 12 and 15 years. A team of engineers and medical staff remained in the control room in the hotel during both nights, where they supervised the trial by remote control and monitored the glucose levels of the children.

The Artificial Pancreas At Home (AP@home) consortium is a European project that commenced in February 2010. The consortium consists of 12 partners in seven European countries. In the first phase of the AP@home project, the available AP algorithms were tested with CGM systems and insulin pumps that were available on the market using a "two-port" approach with two skin punctures to attach the glucose monitor and the insulin pump. In that stage, the aim was to improve the accuracy of the glucose sensors and the safety and effectiveness of the algorithms that relate insulin delivery to blood glucose levels. Innovative AP systems that combine an insulin pump and a CGM system into a single device, which uses only one access point through the skin, were also developed. In the final year of the 4-year project, the performance of the newly created AP system, including remote monitoring facilities, was compared with standard daily intensive insulin therapy in a multinational controlled trial. The AP@home consortium combines world-renowned experts in the fields of medical device development, clinical studies and modelling and control algorithms. Consortium participants include seven academic partners (the University of Cambridge, the University of Padova, the University of Pavia, the University Hospital of Amsterdam, the University of Montpellier, the Medical University Graz, and EPF Lausanne) and five industrial partners (Profil Institut für Stoffwechselforschung GmbH, Triteq Ltd, Sensile Medical AG, STMicroelectronics and 4a engineering GmbH). The project was funded by the European Commission's Framework Programme 7.

Medtronic manufactured the first AP controllers in the United States. Although their controllers cannot be considered fully closed-loop controllers, they are first-generation partially automated systems of AP systems that link CGM measurements with insulin pumps, which automatically stop insulin delivery (shutting off) in response to pending low blood glucose levels. Shutting off the flow of insulin occurs in healthy people in response to low blood sugar. The results of several studies performed at Stanford and in Denver indicated that the device reduced the total number of low blood sugar episodes in diabetics by 31.8% compared with the total number of low blood sugar episodes experienced by diabetics using an insulin pump without a shutoff feature. The study results also showed that the device had no impact on the long-term control of blood sugar (A1c). Medtronic has presented the study results to the FDA and received an approval letter for its next-generation pump device, which includes the shutting off feature; the device can be approved provided the company satisfies certain conditions. Currently, Medtronic and other companies, including Johnson & Johnson's Animas unit, are designing next-generation devices that include additional automated features, that is, a system

designed to predict when diabetics are in danger of low blood sugar levels and that implements pre-emptive measures, such as decreasing the amount of insulin the pump delivers. The initial studies conducted at night with 19 adults with T1D revealed that the software control program helped people stay within a target range 90% of the time.

This chapter outlines the postprandial control approaches in closed-loop systems and emphasises the approaches previously tested in clinical trials. Relevant software tools that have been implemented to support glycaemic control design for educational purposes or directed to AP development are also presented.

## 3.2 Closed-Loop Approaches and Clinical Trials

One of the distinctive challenges of blood glucose control for closed-loop systems is the effect of the meal "disturbance", which is particularly difficult as the meal triggers a rapid increase in glucose that is substantially faster than the time required for insulin absorption and action. Inherent delays of the subcutaneous route may result in overadministration of insulin to compensate for the meal and, consequently, low secondary glucose levels after a few hours (late hypoglycaemia).

This control task is currently being addressed by the control community in two different ways. The first approach is based on proportional-integral-derivative (PID) techniques, which are well-established, reliable, robust, contain few parameters, demonstrate intuitive tuning, and applied extensively in industry (Clemens, 1979; Steil et al., 2006; Weinzimer et al., 2008b; Castle et al., 2010; Steil et al., 2011; Ruiz et al., 2012; Sherr et al., 2013). The second approach is based on model predictive control (MPC), which entails an on-line optimisation procedure that determines an optimal control signal for a given model (Hovorka et al., 2004b; Schaller et al., 2006; Kovatchev et al., 2010; El-Khatib et al., 2010; Elleri et al., 2011a; Devries et al., 2012; Elleri et al., 2013; Turksoy et al., 2013b; Dassau et al., 2013). Fuzzy logic control is another algorithmic approach, which approximates reasoning to replicate conventional insulin-dosing instructions by diabetes practitioners (Atlas et al., 2010; Nimri et al., 2012).

However, fully automated schemes of closed-loop control have not been completely successful in addressing insulin needs during mealtime (Steil et al., 2006; Hovorka et al., 2004a). All artificial pancreas trials reported a significant peak in postprandial glucose above the normal range (Cobelli et al., 2011). Due to large disturbances (meals) and long delays (subcutaneous route), a semi-automatic control with meal announcement usually performs better than fully automatic controls, particularly for patients with low sensitivity to insulin (Weinzimer et al., 2008b; Elleri et al., 2011a). In the semi-automatic scheme, the most challenging control problem is the prevention of late postprandial hypoglycaemia, which is typically caused by controller over-reaction whilst maintaining a reasonable postprandial peak. Different proposals for limiting insulin administration have been published in both PID and MPC control approaches (Steil et al., 2011; Ellingsen et al., 2009).

In this section, special attention to PID and MPC controllers that have been implemented in experimental or clinical trials are considered. Other approaches that have been experimentally or extensively evaluated *in silico* are also presented.

### 3.2.1 PID controllers

The PID algorithm is expressed by the following mathematical representation

$$u(t) = k_p \left[ e(t) + \frac{1}{\tau_I} \int e(t)dt + \tau_D \frac{de(t)}{dt} \right] \tag{3.1}$$

where $e = r - y$ is the error (difference between the set point and measured output; e.g., difference between the desired and measured glucose concentration) and $u$ is the manipulated input (e.g., insulin infusion rate). The three tuning parameters are $k_p$, which is the proportional gain; $\tau_I$, which is the integral time; and $\tau_D$, which is the derivative time. These PID tuning parameters are related to biometric parameters of the patient (Steil et al., 2004).

A PID control strategy is attractive for glucose control as it simulates the first-phase and second-phase responses of nondiabetic individuals, which are used by the pancreas $\beta-$cells to secrete insulin in response to the continuously sensed glucose (Steil et al., 2004). Figure 3.2 shows the analogous behaviour of insulin response from the $\beta-$cell and the PID control.

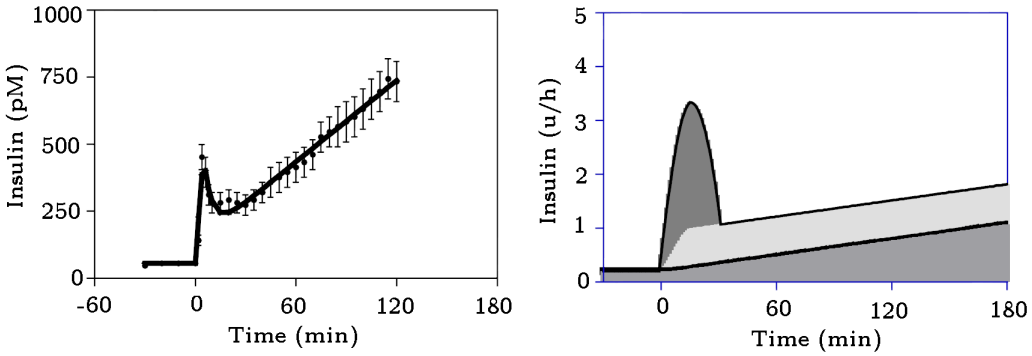


Figure 3.2: Biphasic insulin response to step increase in glucose of the $\beta-$cells (left), and with the PID control model (right). The shaded regions on the PID response represent each control action (proportional-integral-derivative) obtained. (adapted from Steil et al. (2004)).

The first significant clinical result regarding the fully automated closed loop was obtained by Medtronic Inc. In Steil et al. (2006), the feasibility of a fully automated closed loop system was demonstrated in 10 adults with T1D using a subcutaneous external pump and sensor and a controller, known as an external physiologic insulin delivery (ePID) algorithm, in reference to the employed PID control technique. The mean peaks of the postprandial glucose levels were higher than the ideal peaks, with average glucose levels of 189 mg/dL, 172 mg/dL and 225 mg/dL for the food, dinner and breakfast, respectively, measured two hours after each meal. PID controllers have also been used for intravascular and subcutaneous glucose sensing and insulin delivery (Shimoda et al., 1997; Steil et al., 2004; Renard et al., 2006) and during intraperitoneal insulin delivery (Renard et al., 2010).

Due to the presence of substantial delays in the subcutaneous insulin-to-glucose route, PID control may react less rapidly and effectively to meals than the usual pre-meal boluses of conventional therapy. To improve the performance of the PID in postprandial glycaemic control,

a feed-forward action (using a regular bolus), which was conducted approximately 15 min prior to a meal, was added to the fully closed-loop version to create a hybrid scheme for meal compensation as demonstrated by Weinzimer et al. (2008b). Although both settings were shown to effectively prevent glucose variations, the hybrid control was more effective than the fully closed-loop in terms of minimising post-meal glycaemic excursions.

Recently, Steil et al. (2011) a negative feedback of the estimated plasma insulin was added to the PID action in the ePID-IFB algorithm. This feedback involves model-based feedback of insulin concentration, which creates a cascade type of strategy to mitigate hypoglycaemic events (Palerm, 2011). The PID algorithm with insulin feedback is modelled as

$$u(t) = k_p \left[ e(t) + \frac{1}{\tau_I} \int e(t)dt + \tau_D \frac{de(t)}{dt} \right] - \gamma I_p(t) \tag{3.2}$$

where $\gamma I_p$ is the feedback component. In the first clinical assessment of the ePID-IFB algorithm, a meal bolus of 2 IU was included (Steil et al., 2011), regardless of the meal size. The results revealed a mean peak of postprandial glucose of 172 mg/dL, 150 mg/dL and 173 mg/dL for lunch, dinner and breakfast, respectively. These levels are below the recommended maximum glucose level of 180 mg/dL but above the ideal level of 150 mg/dL. In a recent clinical trial with four T1D patients, a crossover study that compared the use of a version of the ePID-IFB algorithm without pre-meal manual bolus versus the PID was performed (Ruiz et al., 2012)). The control results showed similar postmeal blood glucose excursions of 114 ± 28 versus 114 ± 47 mg/dl and the total insulin delivery averaged 57 ± 20 IU with PID versus 45 ± 13 IU with ePID-IFB. However, eight hypoglycaemic events occurred during PID control versus no PID control during ePID-IFB. Although several studies effectively demonstrate the benefits of ePID-IFB to mitigate hypoglycaemia, significant benefits of mitigating postprandial hyperglycaemia remain inconclusive. Some concerns involve estimation of the control gain. The ePID-IFB algorithm has proven to be effective in reducing the risk of nocturnal hypoglycaemia whilst increasing the percentage of time spent in the target range, regardless of activity levels during mid-afternoon (Sherr et al., 2013).

In another PID based algorithm, Marchetti et al. (2008b) proposed to switch off the PID controller prior to ingestion; the re-start time was a function of the current blood glucose concentration and the rate of change. The control performance was successful with respect to differing patient body weights and initial glucose values in simulations conducted over a 30-day period. As the switching criteria are dependent on direct blood glucose measurements, this control algorithm requires modification prior to application in a subcutaneous control system. Subsequently, a feedforward controller was included to accommodate the glucose rate of appearance according to meal size (Marchetti et al., 2008a). However, as the control action is dependent on the rate of appearance of meal-derived glucose, a control scheme including a library of mixed meals is required to adapt this methodology to a practical application.

An asymmetric PID control algorithm without the derivative term was designed to account for different risks associated with hypo- and hyperglycaemia variations (Gantt et al., 2007). The proportional gain is adapted as a function of the output error in a scheme of subcutaneous glucose measurement and insulin delivery. Although abnormal negative glucose variations (hypoglycaemia) are treated more aggressively than positive variations, simulation performances showed that hypoglycaemic events can be reduced but not prevented. The control algorithm

has to be improved to completely impede hypoglycaemia and improve the postprandial blood glucose to normoglycaemia using a more aggressive insulin reaction.

#### PID with a Dual Hormone Scheme

An algorithm named the fading memory proportional derivative (FMPD), which is based on the PID control system without an integration component, was designed for insulin delivery (El Youssef et al., 2009). Instead of using integration to arrive at basal- and duration-related insulin delivery rates, the FMPD applies a "fading memory" of the proportional and derivative components to utilise the duration of abnormal glycaemia. The "fading memory" designation refers to weighting recent errors more heavily than remote errors. This method was successfully applied to rats with T1D (Gopakumaran et al., 2005; Ward et al., 2005) and was recently implemented to deliver glucagon in a dual-hormonal control scheme with T1D patients (Castle et al., 2010). In the latter implementation, the proportional and derivative error gain factors for glucagon were negative, such that negative proportional and derivative errors prompted an increase in the glucagon rate. Although effective for reducing the risk of hypoglycaemia, results presented by Castle et al. (2010) show that glucagon cannot be fully relied upon to reverse the effect of insulin overdelivery.

In El Youssef et al. (2011), insulin-on-board was continually estimated to minimise hypoglycaemia using a model derived from data published by Holmes et al. (2005). The insulin infusion was discontinued if the estimated insulin-on-board reached 20% of the subject's estimated total daily insulin requirement. Oral hydrocortisone was repeatedly administered to create insulin resistance to compare the FMPD algorithm with an adaptive proportional-derivative (APD) algorithm, which adapted FMPD parameters as a function of an estimated insulin sensitivity. Although results for the APD algorithm showed elevated insulin infusion rates, which led to lower glucose levels than the observed glucose levels during the comparable period of the FMPD algorithm, the APD algorithm did not increase the incidence of hypoglycaemia compared with the FMPD algorithm.

### 3.2.2 MPC controllers

The basic approach to MPC is shown in Figure 3.3, in which a model is used to predict the effect of current and future control movements (insulin infusion rates) on future outputs (glucose concentration). An optimiser determines the best set of current and future control moves to maintain the desired outputs for this future prediction horizon. This control approach enables constraints on the state and control variables to be satisfied (Camacho and Bordons, 1999). As MPC requires the repeated solving of an optimisation problem, computational cost has been a frequent deterrent to its application for all systems, with the exception of systems with extremely slow dynamics.

Generally, the MPC approach functions by comparing the model-predicted glucose levels with the actual glucose levels, updating the model, and calculating future insulin infusion rates to minimise the difference between the model-predicted glucose concentration and the target glucose concentration. This approach simply accommodates delays associated with insulin absorption and also accounts for meal intake and prandial insulin boluses. The basic framework of MPC involves many different types of models and objective functions.

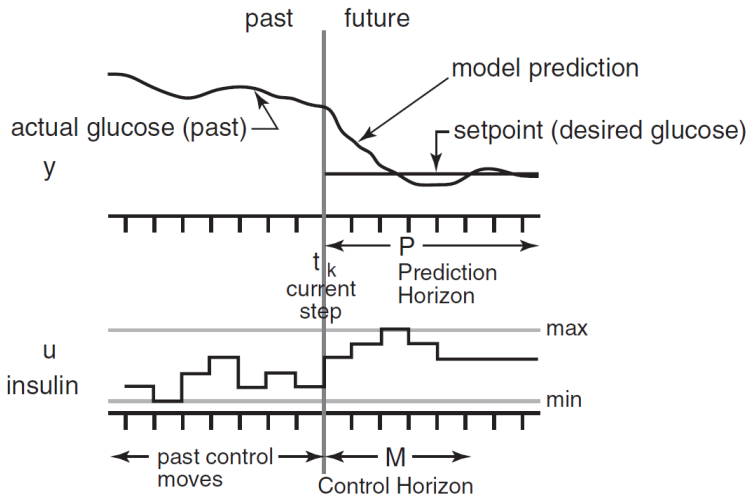


Figure 3.3: MPC. At time step $t_k$, a sequence of $M$ control movements is selected to minimise a performance criterion that involves the predicted output ($y$) over $P$ time steps, which is subject to maximum and minimum constraints on the manipulated input ($u$) (taken from Bequette (2005)).

A basic approach of MPC is an unconstrained linear scheme, which neglects constraints and employs a linear model an input-output form, such as an ARX-type or ARMAX-type model, instead of a state-space model, to prevent the need for a state observer. In Magni et al. (2007), a basic unconstrained MPC strategy was implemented, in which the model is a linearisation of the glucose-insulin model of Dalla Man et al. (2006) obtained at an average value of the population parameters. The results of simulation studies of the linear MPC (LMPC) indicate that a single parameter, such as the weighting on the output predictions in the objective function, can be tuned for each individual for improved performance. Data used to tailor this unconstrained LMPC include the patient's individual body weight, the average total daily insulin use, the typical insulin-to-carbohydrate ratio, and the typical insulin infusion basal rate. In Soru et al. (2012), techniques for meal compensation from conventional insulin therapy and individualisation of linear models for improved performance were implemented in simulation studies involving four different scenarios and 100 subjects. In this study, two implementable strategies were compared: a single adjustable parameter based on clinical parameters without an individualised model and low-order models to produce a more realistic model based on patient-specific information.

First, commercial realisations of an artificial pancreas are expected to include the unconstrained LMPC scheme due to its simplification. The following clinical trials have been conducted using unconstrained LMPC:

- Bruttomesso et al. (2009): Unconstrained LMPC in a preliminary clinical trial with six subjects was performed at two clinical investigation centres. The results demonstrate the feasibility of this control approach during 22 h of overnight hospital admissions. A sample time of 15 min in the control action and a prediction horizon of 240 min were employed.
- Clarke et al. (2009): Unconstrained LMPC using individualised models based on weight, total daily insulin dose, and correction factor was performed with eight subjects in an

overnight study following a standardised meal. Overnight hypoglycaemic events were significantly reduced, whereas the occurrence of postprandial blood glucose excursions was similar during closed-loop and open-loop control.

- Kovatchev et al. (2010): Unconstrained LMPC performance reports from a pilot study involving 20 adults. A one-min sensor sample time and a 15-min actuator sample time were utilised. The design of the control algorithm was performed entirely *in silico* (less than 6 months). Nocturnal hypoglycaemic events were reduced from 23 to 5 and the amount of time within the target range increased from 64% to 78%, compared with standard open-loop treatment.

- Devries et al. (2012): Unconstrained LMPC algorithm by Soru et al. (2012) and the nonlinear MPC algorithm by Hovorka et al. (2010) were examined in trials involving 47 patients in six centres. Each closed-loop algorithm exhibited a higher mean glucose level than mean glucose levels using open-loop control; however, both resulted in shorter incidences of hypoglycaemia than open-loop control.

In the constrained LMPC approach, which is also referred to as explicit multiparametric MPC, the existence of a closed-form solution can be computed offline under the piecewise constant control law. An application to blood glucose control in a virtual subject was reported in Dua et al. (2006). An online optimal solution via quadratic programming methods was implemented by Lee et al. (2009) and presented as a computationally advantageous alternative to constrained LMPC. In Ellingsen et al. (2009), a strong dynamic $IOB$ constraint was incorporated in the optimisation problem of a constrained LMPC based on ARX models. The $IOB$ constraint was designed to be shaped as a function of meal size to prevent violation. Thus, the $IOB$ constraint was employed to embed certain safety factors that already existed within the real-time control module. In Lee and Bequette (2009), subspace identification techniques to develop discrete state space models and $IOB$ constraints were incorporated. Features such as a pump shut-off algorithm to prevent hypoglycaemia and meal detection with size estimation algorithms to handle unannounced meals were also included. In Percival et al. (2011), low-order models based on clinical parameters were used to design a multi-parametric MPC strategy with an insulin-on-board algorithm, which enables the constrained optimisation problem to be solved using a lookup table. The use of a lookup table significantly reduces the computational requirements. A pilot clinical trial evaluation of this fully automated artificial pancreas was conducted using commercial devices in 17 subjects (Dassau et al., 2013). The results showed that blood glucose was maintained in the near-normal range (80-180 mg/dL) for an average of 70% of the trial time. In Cameron et al. (2011, 2012), a multiple model probabilistic predictive control (MMPPC) strategy that minimises an asymmetric risk function subject to satisfying hypoglycaemic constraints was designed. In this implementation, MMPPC was forced to be more conservative when uncertainties were high. Clinical studies are underway to test the feasibility of MMPPC that incorporates meal detection, meal size estimation, and insulin-on-board constraints for closed-loop insulin delivery in a carefully monitored inpatient clinical research environment. In Eren-Oruklu et al. (2009), an adaptive generalised predictive control (GPC) strategy for regulating estimated blood glucose levels based on CGM measurements was implemented. This strategy was compared with linear quadratic control in simulation studies based on the glucose-insulin system of Hovorka et al. (2004a) and Glucosim models (Agar et al., 2005). In Eren-Oruklu et al. (2009), an adaptive Generalized Predictive Control (GPC) strategy, a type of input-output unconstrained LMPC, was used to regulate the estimated blood glucose levels based on CGM measurements. This was compared with Linear Quadratic Control in simulation studies based on the glucose-insulin system of Hovorka et al. (2004a) and Glucosim models

(Agar et al., 2005). In Turksoy et al. (2013a), a multivariable adaptive GPC was employed with physiological signals such as energy expenditure and galvanic skin response, obtained from a multisensory armband, and glucose measurements, obtained from a CGM system, to generate a multiple-input-single-output model for predicting future glucose concentrations. Insulin-on-board predictions were also designed to control the blood glucose of patients with T1D. The controllers were tested in a pilot clinical trial, which comprised seven cases with three different patients, for 32 or 60 h without any meal or activity announcements.

In Hovorka et al. (2004a), a nonlinear model predictive control (NMPC) was designed using the glucose-insulin model of Hovorka et al. (2002). The need for an individual model was addressed by online recursive identification of model parameters within a Bayesian setting. Thus, parameters which describe insulin sensitivity were re-estimated at each control step depending on the current plasma glucose measurement. In addition, Magni et al. (2009b) demonstrated a distinct improvement of NMPC over linear MPC for the average virtual subject of the glucose-insulin model from Dalla Man et al. (2006). The following experiments on real patients were performed using NMPC:

- Hovorka et al. (2004b); Schaller et al. (2006): NMPC based on intra venous measurements, which were delayed 30 min to simulate the time lag associated with the subcutaneous route, was employed in clinical studies with 10 T1D patients under fasting conditions. This scheme demonstrated potential feasibility.
- Hovorka et al. (2010); Elleri et al. (2011b): NMPC was employed in overnight studies in which CGM data were entered manually in the algorithm and the results were transferred to a pump in 15-min intervals. A reduction in nocturnal hypoglycaemia was achieved compared with standard pump treatment. Application after a standard evening meal and late-afternoon exercise resulted in 20% improvement in the number of glucose levels within a target range for children and adolescents. Results showed no significative difference of the closed-loop performance when the controller is initiated at different start times.
- Hovorka et al. (2011); Hovorka (2011): NMPC based on a fully automated strategy, which incorporated a time sample of 15-min, was used in overnight studies with adults. It was initiated immediately after dinner or a late night snack accompanied by alcohol. Results suggested that closed loop delivery of insulin may improve overnight control of glucose levels respect to conventional insulin therapy, and reduce the risk of nocturnal hypoglycaemia.
- Elleri et al. (2011a): NMPC used with pre-meal bolus doses was evaluated in a multinational study to reduce the frequency of nocturnal and after breakfast hypoglycaemic events. The controller achieved glucose levels as effectively as patient-directed conventional insulin pump therapy.
- Murphy et al. (2011a,b): NMPC was used in women with T1D throughout different stages of pregnancy. Near-optimal nocturnal glycaemic control was obtained in early and late pregnancy stages.
- Elleri et al. (2013): NMPC was used in adolescents with T1D to maintain glycaemic control after meals, physical exercise, and with snacks not announced to the algorithm. The percentage of glucose was in the target range of 84%, and the mean plasma glucose level was 128 mg/dL compared with a glucose percentage of 49% and a mean plasma glucose level of 165 mg/dL for conventional insulin pump therapy. Hypoglycaemia occurred during 10 control visits and 9 NMPC executions.

#### MPC with a Dual-Hormone Scheme

The GPC control strategy was initially experimented in studies involving diabetic swine using both insulin and glucagon to improve control at lower blood glucose levels (El-Khatib et al., 2007, 2009). An adaptive GPC algorithm based on a discrete-time second-order model with model parameters adapted on line was designed to employ insulin or glucagon, depending on the sign of the difference between the measured glycaemia and its target value (El-Khatib et al., 2007). A prediction of the insulin concentration was included in the objective function to prevent problems associated with $IOB$. In the human clinical studies, this adaptive GPC was used to compute the insulin rate, whereas a PD controller that was active under certain glucose concentrations was used for glucagon delivery (El-Khatib et al., 2010). In this implementation, a prediction horizon of one was used in the adaptive GPC, which resulted in an adaptive PID controller. Constraints on insulin were imposed by clamping and were not part of the control algorithm. A 5-min sample time was used for the sensor measurements.

### 3.2.3 Other controllers

Fuzzy logic employs graded membership for given variables (e.g., blood glucose and derived signals as the rate of change) and a defined interaction between the variables. Rules such as *if (blood glucose is too high) and (rate is low) then (dosage is little)* are used in this scheme, which yield an exact number using defuzzification techniques (Trajanoski and Wach, 1996). A fuzzy logic control algorithm for delivery insulin developed by Atlas et al. (2010) was tested in a trial of seven adults. This approach is part of the MD-Logic artificial pancreas system and uses a combination of control-to-range and meal detection system with a 5-min sample time. In Miller et al. (2011), a learning algorithm that extends the MD-Logic strategy to improve interpatient variability, was simulated. Automated overnight closed-loop studies in seven patients of the MD-Logic system were presented by Nimri et al. (2012).

Chen et al. (2008) implemented a fuzzy control scheme that uses blood glucose and the rate-of-change *in silico* based on ten rules. In the fuzzy logic controller designed by Mauseth et al. (2010), blood glucose acceleration was also used and the algorithm was tuned based on a personalisation factor. In Campos-Delgado et al. (2006), a fuzzy-based controller including subcutaneous glucose measurements and insulin delivery was implemented to consider associated delay.

In Wang et al. (2010a), iterative learning control was implemented to improve the closed-loop performance of an MPC strategy in simulation studies over several days. Fewer than 10 days were required to regulate the glucose levels of an individual within the desired range of glucose values. In Magni et al. (2009a), a run-to-run approach for implementing day-by-day tuning of an unconstrained MPC algorithm was implemented. The aggressiveness of the closed-loop control law was effectively auto-tuned regardless of the meal variation and slow parameter variations, such as daily insulin sensitivity. Some strategies based on continuous glucose monitoring, as proposed by Wang et al. (2009), vary the basal insulin delivery depending on the glucose trend and certain heuristic assumptions. Based on current blood glucose levels and the rate of change, the basal rate is adapted using a gain multiplier, which is determined by a basal gain mosaic. A bolus design combined with this basal therapy was involved for treating severe hyperglycaemia (Wang et al., 2010b). In this approach, a bolus is automatically delivered to compensate for the influence of meals and to correct for hyperglycaemia. The “optimal” bolus size is determined according to the blood glucose level, the target blood glucose, the insulin-to-carbohydrate ratio, the correction factor, and a final component of $IOB$ to prevent insulin stacking, which may lead

to hypoglycaemia. This strategy is dependent on an accurate estimate of the ingested $CHO$ and, therefore, appears to be more feasible in a scheme with meal announcement.

Other model-based but robust techniques such as $\mathcal{H}_\infty$ for perfect tracking and disturbance rejection of meals (Parker et al., 2000; Ruiz-Velázquez et al., 2004; Kienitz and Yoneyama, 1993; Chee et al., 2005; Kovacs et al., 2013), sliding mode control with prediction of glucose after meals and feedforward action (Abu-Rmileh et al., 2010; Kaveh and Shtessel, 2008), as well as control based on neural networks (de Canete et al., 2012; Trajanoski and Wach, 1998; Alamaireh, 2006; El-Jabali, 2005; Dazzi et al., 2001), have also been explored.

## 3.3 Modelling and Simulation

*In silico* diabetes simulators are used to optimise clinical designs and improve the performance of control algorithms prior to application to actual patients. Simulators can show the behaviour exhibited by the glucose dynamics of diabetic patients using a mathematical model of the interactions in the glucose-insulin system. A comprehensive model of the glucose-insulin system describes the processes of insulin pharmacokinetics and pharmacodynamics, carbohydrate absorption, and glucose transport and elimination. Many models of glucose regulation have been proposed in recent decades. A review of glucose-insulin dynamics has been presented by Nucci and Cobelli (2000); Mari (2002); Makroglou et al. (2006); Wilinska and Hovorka (2008); García-Jaramillo (2011). Two of the most relevant and comprehensive mathematical models of the glucose-insulin system are described in detail in section 4.2

The simulator may include particular devices involved in glycaemic control. Features about glucose measurement sensors or the infusion pump used to deliver exogenous insulin are commonly included in simulators intended for control design. Most simulators are created as educational tools of diabetes and are used by T1D patients and medical staff to evaluate traditional therapies.

AP research requires testing of closed-loop control algorithms in animals or humans with the approval of regulatory agencies, which involves several constraints related to resource demand and ethical issues. However, few *in silico* diabetes simulators are intended for AP research. In addition to a comprehensive mathematical model of the glucose-insulin system, a simulator to accelerate AP development also requires a virtual population of T1D patients to extensively test the designed control algorithms. High robustness, safety, feasibility and practical implementation, as well other imperative issues, must be satisfied by the AP.

A discussion of different simulators used as educational and research tools in the field of diabetes technologies and an overview of the most relevant simulators designed specifically for AP development are included in the following section.

### 3.3.1 Diabetes Related Simulators

**AIDA** (automated insulin dosage advisor) is one of the most popular diabetes simulators. The AIDA was developed by Lehmann and Deutsch in 1992 (Lehmann and Deutsch, 1992a) and was originally designed as a simulator to teach diabetic patients and clinical staff about glucose-insulin interaction, insulin dosage, and dietary adjustments to perform more effective diabetes therapies (Wilson, 1999). The AIDA has been continuously upgraded through integration of new

models of subcutaneous insulin absorption and carbohydrate digestion and absorption. Some of the models that comprise the AIDA structure describe the kinetics of meal glucose appearance in the plasma (Lehmann and Deutsch, 1992b) and the subcutaneous insulin plasma rate of the appearance of several insulin analogues (Berger and Rodbard, 1989). The model of Tarin et al. (2005) is used to describe rapidly acting insulin analogues, short-acting (regular) insulin preparations, intermediate-acting insulin, and long-acting insulin analogues (Lehmann et al., 2009). The subsystems of insulin action and glucose kinetics has remained unchanged since the first version was developed (Lehmann and Deutsch, 1992b).

Although the AIDA is a freeware educational simulator program with numerous downloads (Lehmann, 1999, 2001), insufficient information of refined individual simulations render it unfeasible for realistic simulations.

**GLUCOSIM** was developed by Agar in 2005 (Agar et al., 2005). The main purpose of the GLUCOSIM is to assist medical and engineering students with the visualisation of glucose-insulin dynamics and the response to external perturbations, such as meal intake and the supply of insulin. The GLUCOSIM employs the Puket model (Puckett, 1992) to describe the dynamics of insulin and glucose levels in the blood of healthy individuals and T1D patients. This compartmental model represents the transport of glucose and insulin through the major vessels to the capillaries according to actual body regions. The main disadvantages of these models is the lack of consideration of personal variations in physiological parameters and the average model output values.

This simulator contains two modes: a "healthy person" mode, in which the user can modify the body weight and the meal protocol during a 24 h simulation, and a "T1D person" mode, in which the user can select conventional treatment or well-established closed-loop strategies. However, the design and testing of new control strategies is not viable.

**GIM** (glucose-insulin model) is an interactive diabetes simulator developed by Dalla Man in 2007 (Dalla Man et al., 2007). The purpose of the GIM is to provide a user-friendly interface for investigators, who do not possess specific modelling experience, to compare healthy people with insulin-resistant people or open-loop versus closed-loop treatments for T1D patients. The GIM uses the model of the glucose-insulin system described by Cobellis's group (Dalla Man et al., 2006; Dalla Man et al., 2007). The model for healthy subjects is composed of glucose and insulin subsystems linked by the control of glucose on insulin secretion and by insulin on glucose utilisation and endogenous production. The T1D subject is simulated by substituting the insulin secretion module with a subcutaneous insulin infusion module. This model is presented in section 4.2.1.

This simulator has a graphical user interface to facilitate the adjustment of menu options, which vary according to normal or T1D subjects. Open- and closed-loop options are available and, according to the end use (educational or research), inclusion of new control algorithms may be allowed. However, the inclusion of more realistic conditions, such as insulin sensitivity variation or a virtual cohort of T1D patients to perform individual assessment, do not exist in this simulator.

**JEDMA** (java educational diabetes management advisor) is an educational simulator that was developed by Hernández-Ordoñez in 2007 (Hernández-Ordoñez et al., 2007). The purpose of the JEDMA is to provide an educational diabetes simulator with enhancements based on options from other simulators, such as the AIDA and the GLUCOSIM. The JEDMA includes three models, which describe glucose-insulin dynamics using a compartmental model proposed by Sorensen (1985) and an extended version that considers exercise periods, including important metabolic effects related to glucose regulation gastric (Hernandez-Ordonez and Campos-Delgado., 2006): the model of glucose absorption by the intestine proposed by Lehmann and Deutsch (1992b) and the model of subcutaneous insulin absorption of several insulin analogues for MDI therapy proposed by Berger and Rodbard (1989).

This simulator enables the user to include MDI or CSII intensive therapies for which different predefined control algorithms can be tested. However, the design concept of the final realisation does not enable inclusion of additional control strategies or a virtual patient cohort for control assessment.

**Archimides** is a simulator used for educational and research purposes. It was developed by Eddy and Schlessinger (Eddy and Schlessinger, 2003) at Kaiser Permanente Southern California in 2003. The purpose of Archimides is to realistically simulate what occurs in health care systems and address research challenges for which empirical studies may be impractical due to factors, such as high cost, extensive follow-up periods, large sample sizes, lack of participation by vendors or customers, or the rapid pace of technological change. In a typical application of the simulator, hundreds of patients can be simulated, each patient possesses an individual anatomy and physiology disorders can be simulated using different medical care facilities, tests and treatments by medical staff can be simulated, and the output measures can be simulated.

The Archimides model includes organic systems with the continuous interaction of more than 50 biological variables (Schlessinger and Eddy, 2002). The level of detail and realism was determined by medical considerations, the need to differentiate clinically relevant variables, and the level of detail required to conduct clinical trials. The full Archimedes model is designed to be comprehensive and includes not only patients but also other important aspects of a health care system, such as health care personnel, facilities, equipment, supplies, policies and procedures, regulations, utilities, and costs.

The Archimedes simulator supports decisions by clinicians and administrators regarding several issues related to clinical trials in health care systems. However, this type of simulator is not suitable for the development of new treatments for T1D patients due to the inability to predict outcomes for a particular patient. Instead, Archimides predicts average trends with conventional treatments.

The Archimides simulators are based on population models; as a result, their capabilities are limited to the prediction of population averages. For the development of the artificial pancreas, a different type of system that is capable of simulating the glucose-insulin dynamics of a particular person is needed.

### 3.3.2 Artificial Pancreas Simulators

The baseline requirements include a comprehensive model of the glucose-insulin system, a cohort of virtual patients who represent a target population of real T1D patients, and models of the instrumentation used in a practical implementation of the artificial pancreas. Additional features, such as instrumentation failures, diurnal and daily variability, mixed meal perturbations, and several outcome measurements, are employed to improve the functionality and realism of the simulator.

Although most comprehensive models do not completely reflect realistic behaviour as they do not consider important physiological variables, such as stress and physical activity, they are useful for eliminating or improving inappropriate control designs. The Hovorka *et al.* model (Hovorka et al., 2004a) has been used for both simulation and experimental control purposes (Hovorka et al., 2007) in the UCAM (University of Cambridge) simulator (Chassin, 2005). Similarly, the DallaMan *et al.* model developed by Cobelli's group in Padova, Italy (Dalla Man et al., 2007) has been used in the UVa (University of Virginia) simulator, which was accepted as a substitute for animal trials in the preclinical testing of closed-loop control in T1D (Kovatchev et al., 2009).

The Hovorka *et al.* and Dalla man *et al.* model have been primarily used for control in development of the AP. These models are described in section 4.2. Additional hardware-in-the-loop implementations, as presented by Dassau et al. (2009) and in which the instrumentation models are replaced with real devices, are used to perform clinical trials. This implementation incorporates a CGM system and an insulin pump to communicate the control algorithm with real in/out signals from T1D patients.

The UCAM and UVa simulators, which illustrate the features currently used to promote the development of AP prototypes, are described as follows:

**UCAM simulator** The main components included in this simulator are the subjects, the glucose sensor, the insulin pump, the glucose controller, and the experimental protocol, as shown in Figure 3.4. A simulated human is represented by the simulation model of the glucose-insulin system described by Hovorka *et al.*, and the corresponding individual parameters set. This simulator have a cohort of 18 virtual patients with T1D.

A remarkable difference with respect to the UVa simulator is the within-subject variability. The inter- and intra-subject variability is established for each individual subject. Diurnal variations and unmodelled effects of intra- or within-subject variability are implemented using certain time-variant parameters. However, only sinusoidal oscillations with amplitudes of 5% and 3h periods can be performed using nominal values of the time-varying parameters. A single parameter that represents a reduction in plasma glucose concentration is employed to include the effect of physical exercise on glucose homeostasis. Figure 3.5 includes an example for the setup of the subject in this simulator.

The model of measurement error and calibration error in the glucose sensor is a generic representation consisting of two parameters, the coefficient of variation (CV) of the measurement error and the CV of the calibration error. The sensor error signal can also be derived from a specific data-based representation of a real CGM system. The model of error in insulin pump

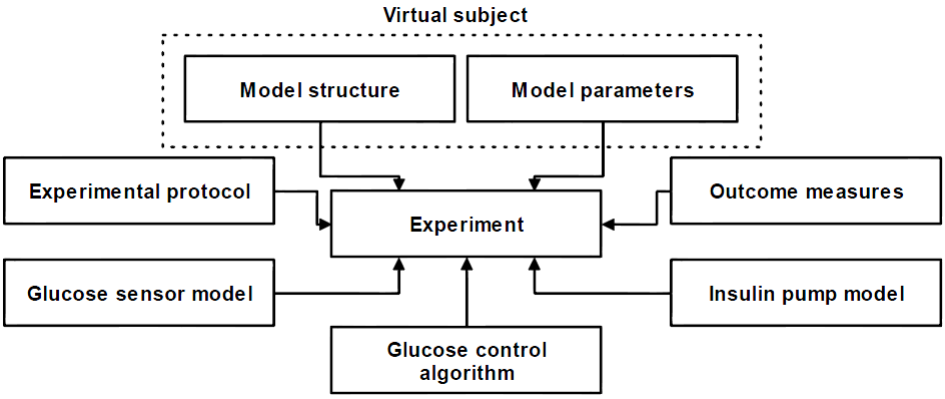


Figure 3.4: Structure of UCAM simulator (taken from Chassin (2005)).

delivery comprises three parameters: the infusion type (intravenous or subcutaneous), the error CV of continuous infusion, and the error CV of an insulin bolus.

The experimental protocol includes the details of the *in silico* experiment, as shown in Figure 3.6. Basic information regarding scenario configuration, the administration of meals, the proposed insulin route, the rescue CHO option, the exercise sessions characteristics, the disturbance or unannounced events, the system failures in adjusting the insulin pump occlusion or loss of sensor signal, the beginning glucose and the target glucose range are included.

The outcome measures of this simulator comprise 32 built-in functions for processing the response signals. The functions include the mean value, the percentage of time spent in the target glucose range, the number of all hypoglycaemia events, the root mean square error, and the area under the curve. The UCAM simulator was implemented using Matlab 7.8.

**UVa simulator** The components, which are organised as shown in Figure 3.7, include a cohort of virtual patients with T1D, a sensor error model capable of reproducing the time lag, calibration bias, and random noise, and a model of the insulin pump that considers engineering limitations.

Figure 3.8 presents the main user interface window of this simulator, which enables the definition of a test scenario, the selection of subjects, the selection of the CGM sensor and insulin pump, and the selection of a set of outcome metrics.

The simulated human is represented in this simulator by the mathematical model of the glucose-insulin system as described by Dalla man *et al.* The UVa simulator have a large cohort of *in silico* subjects, which are based on real individual data that spans the observed variability of key parameters in the general population. The cohort of virtual patients includes 100 adults, 100 adolescents, and 100 children, which reflects an important inter-subject variability of information. However, intra-subject variability is not defined or assumed in this implementation.

The sensor simulation model is described by Breton and Kovatchev (2008) and is based on sensor-reference glucose data pairs. In this model, the decomposition of sensor errors was

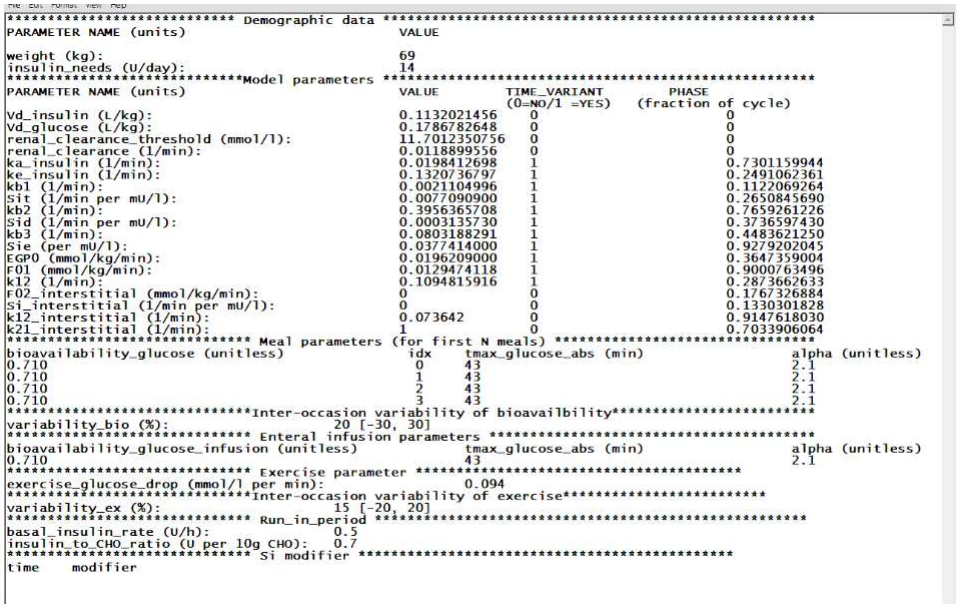

```
********** Demographic data **********
PARAMETER NAME (units)                          VALUE

weight (kg):                                    69
insulin_needs (U/day):                          14
**********Model parameters **********
PARAMETER NAME (units)                          VALUE          TIME_VARIANT        PHASE
                                                               (0=NO/1 =YES)    (fraction of cycle)
Vd_insulin (L/kg):                              0.1132021456    0                   0
Vd_glucose (L/kg):                              0.1786782648    0                   0
renal_clearance_threshold (mmol/l):             11.7012350756   0                   0
renal_clearance (1/min):                        0.0118899556    0                   0
ka_insulin (1/min):                             0.0198412698    1                   0.7301159944
ke_insulin (1/min):                             0.1320736797    1                   0.2491062361
kb1 (1/min):                                    0.0021104996    1                   0.1122069264
Sit (1/min per mU/l):                           0.0077090900    1                   0.2650845690
kb2 (1/min):                                    0.3956365708    1                   0.7659261226
Sid (1/min per mU/l):                           0.0003135730    1                   0.3736597430
kb3 (1/min):                                    0.0803188291    1                   0.4483621250
Sie (per mU/l):                                 0.0377414000    1                   0.9279202045
EGP0 (mmol/kg/min):                             0.0196209000    1                   0.3647359004
F01 (mmol/kg/min):                              0.0129474118    1                   0.9000763496
k12 (1/min):                                    0.1094815916    1                   0.2873662633
F02_interstitial (mmol/kg/min):                 0               0                   0.1767326884
Si_interstitial (1/min per mU/l):               0               0                   0.1330301828
k12_interstitial (1/min):                       0.073642        0                   0.9147618030
k21_interstitial (1/min):                       1               0                   0.7033906064
********** Meal parameters (for first N meals) **********
bioavailability_glucose (unitless)      idx    tmax_glucose_abs (min)                alpha (unitless)
0.710                                    0     43                                    2.1
0.710                                    1     43                                    2.1
0.710                                    2     43                                    2.1
0.710                                    3     43                                    2.1
**********Inter-occasion variability of bioavailbility**********
variability_bio (%):                    20 [-30, 30]
********** Enteral infusion parameters **********
bioavailability_glucose_infusion (unitless)     tmax_glucose_abs (min)                alpha (unitless)
0.710                                           43                                    2.1
********** Exercise parameter **********
exercise_glucose_drop (mmol/l per min):         0.094
**********Inter-occasion variability of exercise**********
variability_ex (%):                     15 [-20, 20]
********** Run_in_period **********
basal_insulin_rate (U/h):               0.5
insulin_to_CHO_ratio (U per 10g CHO):   0.7
********** Si modifier **********
time    modifier
```

Figure 3.5: Structure of the UCAM subject setup (taken from Chassin (2005)).

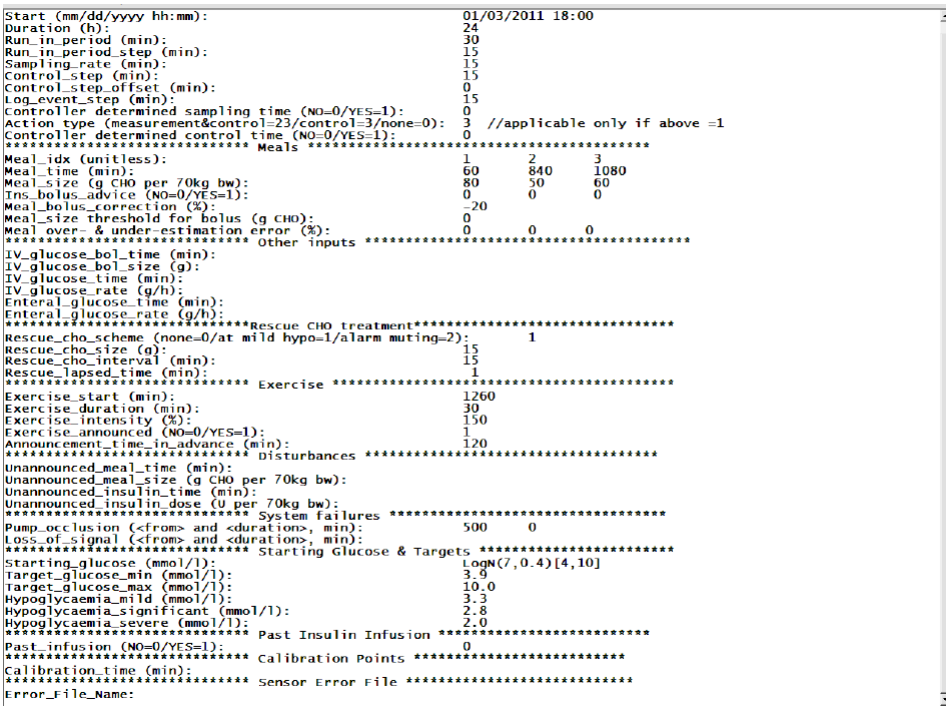

```
Start (mm/dd/yyyy hh:mm):                       01/03/2011 18:00
Duration (h):                                   24
Run_in_period (min):                            30
Run_in_period_step (min):                       15
Sampling_rate (min):                            15
Control_step (min):                             15
Control_step_offset (min):                      0
Log_event_step (min):                           15
Controller_determined_sampling_time (NO=0/YES=1):   0
Action_type (measurement&control=23/control=3/none=0):  3  //applicable only if above =1
Controller_determined_control_time (NO=0/YES=1):    0
********** Meals **********
Meal_idx (unitless):                            1       2       3
Meal_time (min):                                60      840     1080
Meal_size (g CHO per 70kg bw):                  80      50      60
Ins_bolus_advice (NO=0/YES=1):                  0       0       0
Meal_bolus_correction (%):                      -20
Meal_size threshold for bolus (g CHO):          0
Meal over- & under-estimation error (%):        0       0       0
********** Other inputs **********
IV_glucose_bol_time (min):
IV_glucose_bol_size (g):
IV_glucose_time (min):
IV_glucose_rate (g/h):
Enteral_glucose_time (min):
Enteral_glucose_rate (g/h):
**********Rescue CHO treatment**********
Rescue_cho_scheme (none=0/at mild hypo=1/alarm muting=2):    1
Rescue_cho_size (g):                            15
Rescue_cho_interval (min):                      15
Rescue_lapsed_time (min):                       1
********** Exercise **********
Exercise_start (min):                           1260
Exercise_duration (min):                        30
Exercise_intensity (%):                         150
Exercise_announced (NO=0/YES=1):                1
Announcement_time_in_advance (min):             120
********** Disturbances **********
Unannounced_meal_time (min):
Unannounced_meal_size (g CHO per 70kg bw):
Unannounced_insulin_time (min):
Unannounced_insulin_dose (U per 70kg bw):
********** System failures **********
Pump_occlusion (<from> and <duration>, min):    500     0
Loss_of_signal (<from> and <duration>, min):
********** Starting Glucose & Targets **********
Starting_glucose (mmol/l):                      LogN(7,0.4)[4,10]
Target_glucose_min (mmol/l):                    3.9
Target_glucose_max (mmol/l):                    10.0
Hypoglycaemia_mild (mmol/l):                    3.3
Hypoglycaemia_significant (mmol/l):             2.8
Hypoglycaemia_severe (mmol/l):                  2.0
********** Past Insulin Infusion **********
Past_infusion (NO=0/YES=1):                     0
********** Calibration Points **********
Calibration_time (min):
********** Sensor Error File **********
Error_File_Name:
```

Figure 3.6: UCAM example protocol (taken from Chassin (2005)).

performed as errors due to calibration, blood-to-interstitial glucose transfer, and random noise. The features of three CGM system devices are included: Freestyle Navigator$^{TM}$, Guardian RT, and Dexcom STS$^{TM}$. The model of insulin pump is defined as the period and dynamics of insulin transport from subcutaneous tissue to blood as described by Dalla Man et al. (2007) and

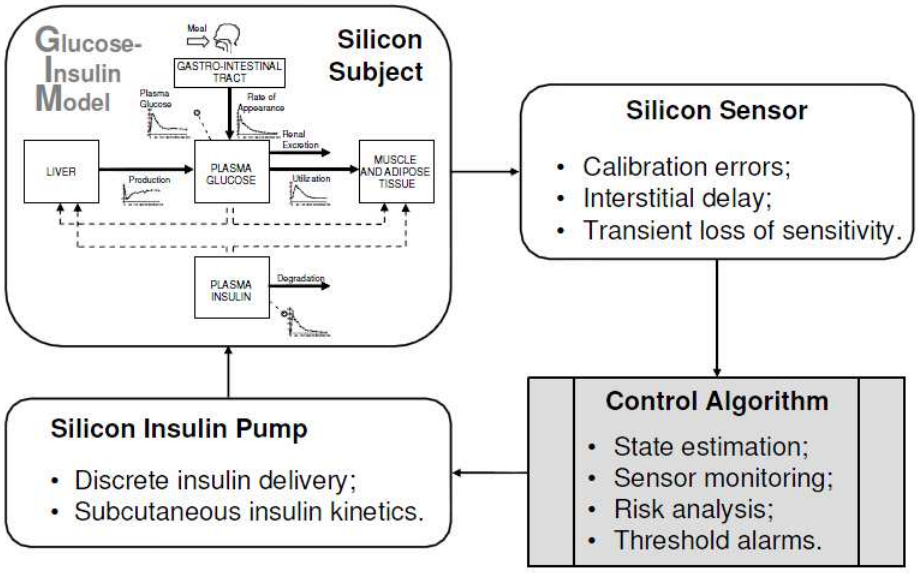


Figure 3.7: UVa components (taken from Kovatchev et al. (2008)).

discrete insulin infusion corresponding to stepwise basal pump rate and insulin boluses. The technical limitations of two devices are included: the Omnipod Insulin Management System and Deltec Cozmo®. However, additional system failures features are not included in this simulator.

The set of metrics of glucose control implemented within the simulation environment includes several measures of average glycaemia, temporal glucose variability, and associated risks for hypoglycaemia and hyperglycaemia. These measures include the mean blood glucose; the percentage of time spent within the target range; the area under the curve per gram $CHO$; graphical metrics, such as a histogram of blood glucose rate of change; or a control variability grid analysis (CVGA). The UVa simulator was implemented using Matlab and Simulink platforms.

## 3.4 Summary

In this chapter, a brief review of the current state of artificial pancreas research is introduced. Modern devices for home-monitoring are used in conjunction with control algorithms in closed-loop, which determines the amount of insulin to infuse at each moment. The main AP control approaches, which were performed experimentally or in clinical trials, are addressed. Different simulators, which were implemented to improve and/or support glycaemic control design with educational and artificial pancreas research, and the implementation of physiological models to perform simulations, are discussed.

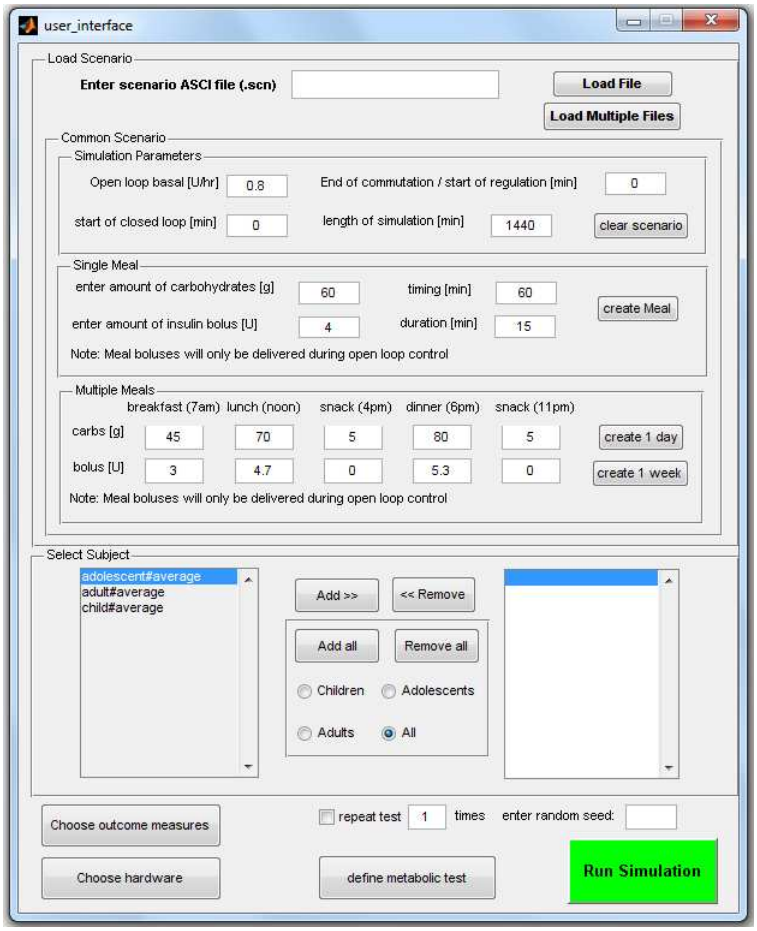


Figure 3.8: UVa user interface (taken from Kovatchev et al. (2008)).

# Chapter 4

# Virtual Environment for Designing and Testing of Glucose Controllers

## 4.1 Introduction

This chapter is devoted to a detailed description of the design and simulation platform used in this thesis (León-Vargas et al., 2011a). The platform corresponds to a virtual environment composed of several stages to support the development of closed-loop insulin delivery systems for T1D. This platform enables the user to define an experiment as simple or as complex as required in a practical and intuitive manner (León-Vargas et al., 2010, 2011b, 2012c). After the controller is extensively tested, it can be directly integrated into an electronic control unit that reuses the entire code and facilitates a rapid prototyping design (León-Vargas, 2009).

This chapter is organised as follows: First, the models of the virtual patients used in the platform and the proposed method for representing *in silico* a real patient cohort is described. Second, an overview of the components of the virtual environment and a detailed description of prominent features that represent realistic scenarios is provided. Last, a realistic test experiment for the evaluation and validation of several closed-loop glucose controllers in the remaining chapters is presented.

## 4.2 Virtual Patients

Virtual patients are extensively employed in diabetes research as a substitute for the glucose-insulin system of real patients. This research is conducted using mathematical models of subcutaneous insulin absorption, carbohydrates digestion and absorption, and the control of insulin on glucose utilisation and endogenous production. Figure 4.1 illustrates the relationships amongst these processes.

The primary reason for using virtual patients is to develop extensive preclinical testing of control strategies in artificial pancreas studies. Several clinical trials have been supported by *in silico* studies, in which a comprehensive assessment of individuals and virtual populations have become a prerequisite.

In this section, the model of Dalla Man *et* al. and Hovorka *et* al., which represent the glucose-insulin system, are described. Both models are used extensively for control and have been integrated into the platform. This section also discusses a method to "virtualise" a real

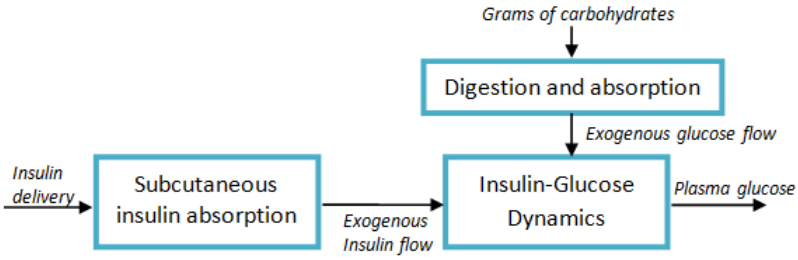


Figure 4.1: General scheme of the glucose-insulin system.

patient cohort by considering clinical parameters to obtain information about the expected performance of real glycaemic control studies.

### 4.2.1 Dalla Man *et al.* model

*Carbohydrate digestion and absorption*: Dalla Man et al. (2006) proposed a three-compartment nonlinear model (see Figure 4.2), two for the glucose in the stomach solid $Q_{sto1}$ (mg) and liquid $Q_{sto2}$ (mg), and one for the glucose in the intestinal tract $Q_{gut}$ (mg). The meal is digested in the stomach with a grinding coefficient $k_{gri}$ ($\text{min}^{-1}$); then the chyme (partially-digested food) enters the intestine with fractional coefficient of transfer $k_{empt}$ ($\text{min}^{-1}$) and finally glucose is absorbed and enters the bloodstream.

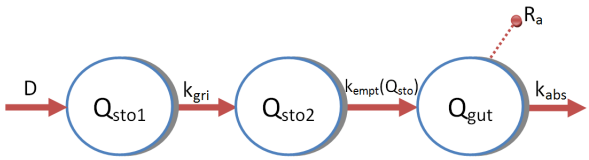


Figure 4.2: Scheme of gastro-intestinal Dalla Man *et al.* system (adapted from Dalla Man et al. (2007).

The rate of appearance $R_a$ (mg $\text{kg}^{-1}$ $\text{min}^{-1}$) describes glucose transit through the stomach and intestine:

$$\begin{aligned}
Q_{sto}(t) &= Q_{sto1}(t) + Q_{sto2}(t) && Q_{sto}(0) = 0 \\
\frac{\mathrm{d}Q_{sto1}(t)}{dt} &= -k_{gri}\, Q_{sto1}(t) + D\, \delta(t) && Q_{sto1}(0) = 0 \\
\frac{\mathrm{d}Q_{sto2}(t)}{dt} &= -k_{empt}(t, Q_{sto})\, Q_{sto2}(t) + k_{gri}\, Q_{sto1}(t) && Q_{sto2}(0) = 0 \\
\frac{Q_{gut}(t)}{dt} &= -k_{abs}\, Q_{gut}(t) + k_{empt}(t, Q_{sto})\, Q_{sto2}(t) && Q_{gut}(0) = 0 \\
R_a(t) &= \frac{f\, k_{abs}\, Q_{gut}(t)}{BW} && R_a(0) = 0
\end{aligned} \tag{4.1}$$

In order to guarantee model identifiability, $k_{gri}$ is fixed and equal to $k_{max}$ ($\text{min}^{-1}$). Further-

more, $f$ is the fraction of intestinal absorption which actually appears in plasma (90%), $k_{abs}$ ($\text{min}^{-1}$) is the rate constant of intestinal absorption, $D$ (mg) is the amount of carbohydrate to be ingested, $\delta(t)$ is the impulse function, and $BW$ (kg) is the body weight.

The coefficient of gastric emptying $k_{empt}$ is a time-variant nonlinear function of $Q_{sto}$ as shown in Figure 4.3.

$$k_{empt}(t, Q_{sto}) = k_{min} + \frac{k_{max} - k_{min}}{2} \{tanh(\alpha(Q_{sto}(t) - b\ D)) - tanh(\beta(Q_{sto}(t) - d\ D)) + 2\} \quad (4.2)$$

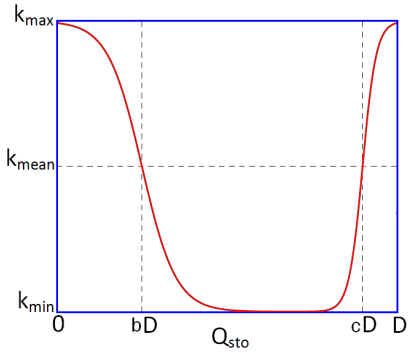


Figure 4.3: $k_{empt}(t, Q_{sto})$ function, where $D$ is the total glucose quantity of the last meal.

The parameters $\alpha$ and $\beta$ are constraints in order to $k_{empt}(t, Q_{sto}) = k_{max}$ for $Q_{sto}(t) = D$ and $Q_{sto}(t) = 0$, as follows:

$$\alpha = \frac{5}{2\ D\ (1 - b)}, \qquad \beta = \frac{5}{2\ D\ c}$$

where $k_{min}$ and $k_{max}$ are the minimum and maximum rate of gastric emptying respectively, $b$ is the percentage of the dose for which the rate of gastric emptying decreases at $k_{mean}$, and $c$ is the percentage of the dose for which the rate of gastric emptying is back to $k_{mean}$.

*Subcutaneous insulin absorption*: The model formulated by Dalla Man et al. (2007) to describe the subcutaneous insulin absorption uses two-compartments: $S_1$ and $S_2$ (pmol $\text{kg}^{-1}$) to represent the polymeric and the monomeric insulin in the subcutaneous tissue respectively (see Figure 4.4).

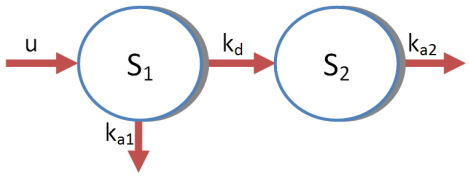


Figure 4.4: Scheme of subcutaneous insulin kinetics proposed by Dalla Man et al. (2007).

The model is represented by the following equations:

$$\begin{aligned} \frac{\mathrm{d}S_1(t)}{dt} &= u(t) - (k_{a1} + k_d)S_1(t) & S_1(0) &= \frac{u(0)}{k_d + k_{a1}} \\ \frac{\mathrm{d}S_2(t)}{dt} &= k_d\, S_1(t) - k_{a2}S_2(t) & S_2(0) &= \frac{k_d\, S_1(0)}{k_{a2}} \\ S(t) &= k_{a1}\, S_1(t) + k_{a2}\, S_2(t) & S(0) &= S_b \end{aligned} \tag{4.3}$$

where $u$ (pmol kg$^{-1}$ min$^{-1}$) represents injected insulin flow, $k_d$ (min$^{-1}$) is called degradation constant, $k_{a1}$ and $k_{a2}$ (min$^{-1}$) are absorption constants. The quantity $S_b$ (pmol min$^{-1}$) represents insulin infusion to maintain diabetic patient at basal steady state and $S$ (pmol kg$^{-1}$ min$^{-1}$) is the rate of appearance of insulin in plasma.

*Insulin action and glucose kinetics*: Some modifications to model of Dalla Man et al. (2007), regarding to $\beta-$cells insulin secretion, were presented by Magni et al. (2007) to simulate the specific metabolism of T1D. This model is composed of one glucose and one insulin subsystem linked by the control of insulin on glucose utilization and endogenous production, as can be seen in Figure 4.5.

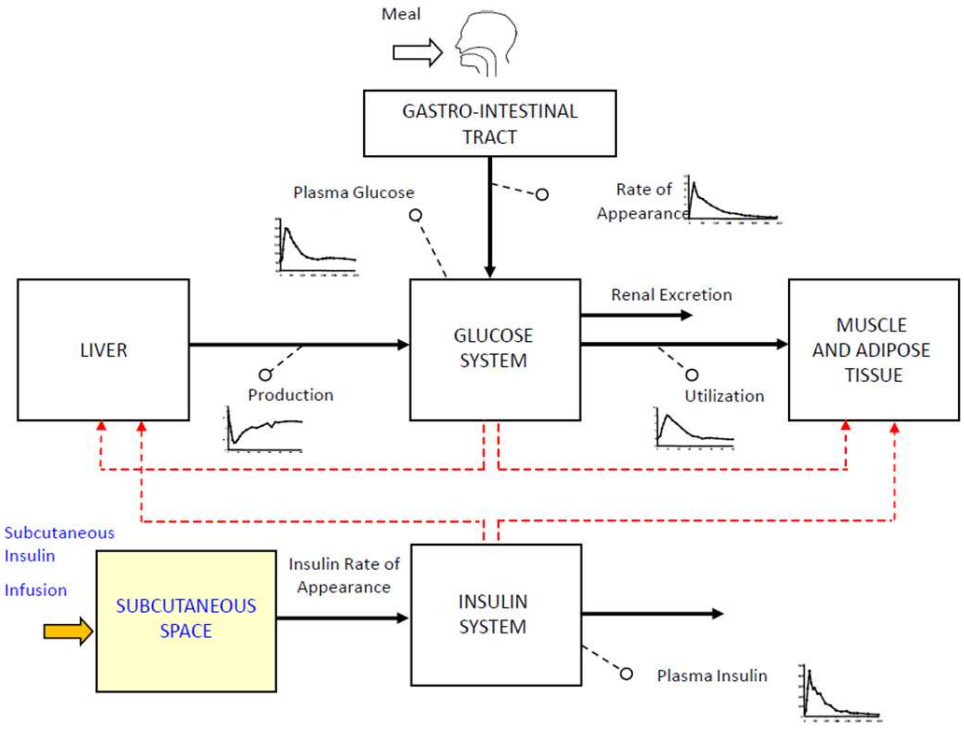


Figure 4.5: Scheme of the glucose-insulin system in T1D. Solid lines represent glucose and insulin fluxes; dashed lines represent control signals. Physical activity affects insulin-independent glucose utilization (taken from Dalla Man et al. (2009)).

Next, the sub-models corresponding to each one of the subsystems are described.

*Glucose Subsystem*: Dalla Man et al. (2007) used a two-compartment model to describe glucose kinetics, as can be seen in Figure 4.6.

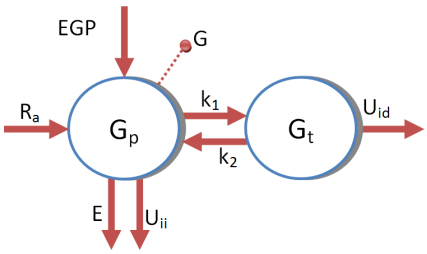


Figure 4.6: Scheme of the glucose subsystem (adapted from Dalla Man et al. (2007)).

The model equations are:

$$\begin{aligned}
\frac{\mathrm{d}G_p(t)}{\mathrm{d}t} &= EGP(t) + R_a(t) - U_{ii}(t) - E(t) - k_1 G_p(t) + k_2 G_t(t) && G_p(0) = G_{pb} \\
\frac{\mathrm{d}G_t(t)}{\mathrm{d}t} &= -U_{id}(t) + k_1 G_p(t) - k_2 G_t(t) && G_t(0) = G_{tb} \\
G(t) &= \frac{G_p(t)}{V_g} && G(0) = G_b
\end{aligned} \tag{4.4}$$

where $G_p$ and $G_t$ (mg kg$^{-1}$) are glucose masses in plasma and rapidly-equilibrating tissues, and in slowly equilibrating tissues, respectively, $G$ (mg dL$^{-1}$) plasma glucose concentration, with the suffix $b$ denoting the basal state. $EGP$ (mg kg$^{-1}$ min$^{-1}$) is the endogenous glucose production, $R_a$ (mg kg$^{-1}$ min$^{-1}$) is the glucose rate of appearance in plasma, $E$ (mg kg$^{-1}$ min$^{-1}$) is renal excretion, $U_{ii}$ and $U_{id}$ are the insulin independent and dependent glucose utilizations, respectively. $V_g$ (dL kg$^{-1}$) is the distribution volume of glucose and $k_1$ and $k_2$ (min$^{-1}$) are the rate parameters.

At basal steady-state endogenous production $EGP_b$ equals glucose disappearance, i.e. the sum of glucose utilization and renal excretion (which is zero in the normal subject), $U_b + E_b$:

$$EGP_b = U_b + E_b \tag{4.5}$$

The glucose renal excretion $E$ is modeled by a linear relationship with plasma glucose

$$E(t) = \begin{cases} k_{e1}\,(G_p(t) - k_{e2}) & \text{if } G_p(t) > k_{e2} \\ 0 & \text{if } G_p(t) \leq k_{e2} \end{cases}$$

where $k_{e1}$ (min$^{-1}$) is the glomerular filtration rate and $k_{e2}$ (mg kg$^{-1}$) is the renal threshold of glucose.

*Endogenous glucose production subsystem*: This model incorporates the notion that a portal insulin signal controls the rapid suppression of EGP. Since the portal insulin signal is an anticipated version of plasma insulin, it was approximated with a portal-like derivative of insulin

concentration signal.

The endogenous glucose production, is described as:

$$EGP(t) = k_{p1} - k_{p2}G_p(t) - k_{p3}I_d(t) \qquad EGP(0) = EGP_b \tag{4.6}$$

where $k_{p1}$ (mg kg$^{-1}$ min$^{-1}$) is the extrapolated $EGP$ at zero glucose and insulin, $k_{p2}$ (min$^{-1}$) liver glucose effectiveness, and $k_{p3}$ (mg kg$^{-1}$ min$^{-1}$ per pmol L$^{-1}$) parameter governing amplitude of insulin action on the liver. $I_d$ is a delayed insulin signal realized with a chain of two compartments:

$$\begin{aligned} \frac{\mathrm{d}I_1(t)}{\mathrm{d}t} &= -k_i(I_1(t) - I(t)) \qquad I_1(0) = I_b \\ \frac{\mathrm{d}I_d(t)}{\mathrm{d}t} &= -k_i(I_d(t) - I_1(t)) \qquad I_d(0) = I_b \end{aligned} \tag{4.7}$$

where $k_i$ (min$^{-1}$) is the rate parameter accounting for delay between insulin signal and insulin action. $EGP$ is also constrained to be non-negative.

At basal steady state, one has,

$$k_{p1} = EGP_b + k_{p2}G_{pb} + k_{p3}I_b$$

so,

$$EGP(t) = EGP_b + k_{p2}(G_{pb} - G_p(t)) + k_{p3}(I_b - I_d(t)) \tag{4.8}$$

*Glucose utilization subsystem*: The model of glucose utilization by body tissues during a meal assumes that glucose utilization is made up of two components: insulin-independent and insulin dependent.

$$U(t) = U_{ii}(t) + U_{id}(t) \tag{4.9}$$

Insulin-independent utilization takes place in the first compartment, is constant, and represents glucose uptake by the brain and erythrocytes ($F_{cns}$):

$$U_{ii}(t) = F_{cns}$$

Insulin-dependent utilization takes place in the remote compartment and depends nonlinearly (Michaelis Menten) upon glucose in the tissues:

$$U_{id}(t) = \frac{V_m(X(t))\, G_t(t)}{K_m(X(t)) + G_t(t)} \tag{4.10}$$

where $V_m(X(t))$ (mg kg$^{-1}$ min$^{-1}$ per pmol L$^{-1}$), and $K_m(X(t))$ (mg kg$^{-1}$ per pmol L$^{-1}$) are assumed to be linearly dependent upon a remote insulin, $X$ (pmol L$^{-1}$):

$$\begin{aligned} V_m(X(t)) &= V_{m0} + V_{mx}\ X(t) \\ K_m(X(t)) &= K_{m0} \end{aligned} \tag{4.11}$$

which depends from insulinemia in the following way

$$\frac{\mathrm{d}X(t)}{\mathrm{d}t} = -p_{2U}\ X(t) + p_{2U}(I(t) - I_b) \qquad X(0) = 0 \tag{4.12}$$

where $I$ is plasma insulin, and $p_{2U}$ (min$^{-1}$) is a rate constant defining insulin action on peripheral glucose utilization. $V_{m0}$ (mg kg$^{-1}$ min$^{-1}$), and $K_{m0}$ (mg kg$^{-1}$) are the Michaelis-Menten parameter of glucose utilization at zero insulin action, and $V_{mx}$ (mg kg$^{-1}$ min$^{-1}$ per pmol L$^{-1}$) is the disposal of insulin sensitivity.

In the basal steady state one has:

$$\begin{aligned} G_{tb} &= \frac{F_{cns} - EGP_b + k_1 G_{pb}}{k_2} \\ U_b &= EGP_b = F_{cns} + \frac{V_{m0} G_{tb}}{K_{m0} + G_{tb}} \end{aligned}$$

from which

$$V_{m0} = \frac{(EGP_b - F_{cns})(K_{m0} + G_{tb})}{G_{tb}}$$

*Insulin subsystem*: Insulin flow $S$, coming from the subcutaneous compartments, enters the bloodstream and is degraded in the liver and in the periphery. The two-compartment model used to describe insulin kinetics can be seen in Figure 4.7.

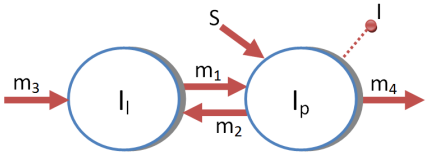


Figure 4.7: Schema of the insulin subsystem (adapted from Dalla Man et al. (2007)).

The model equations are:

$$\begin{aligned}
\frac{\mathrm{d}I_l(t)}{\mathrm{d}t} &= -I_l(t)(m_1 + m_3) + m_2\ I_p(t) && I_l(0) = I_{lb} \\
\frac{\mathrm{d}I_p(t)}{\mathrm{d}t} &= -I_p(t)(m_2 + m_4) + m_1\ I_l(t) + S(t) && I_p(0) = I_{pb} \\
\frac{\mathrm{d}I(t)}{\mathrm{d}t} &= \frac{I_p(t)}{V_i} && I(0) = I_b
\end{aligned} \tag{4.13}$$

where $I_p$ and $I_l$ (pmol kg$^{-1}$) are insulin masses in plasma and in liver respectively, $I$ (pmol L$^{-1}$) is plasma insulin concentration, $V_i$ (L kg$^{-1}$) is the distribution volume of insulin, $m_1$, $m_2$, $m_3$, and $m_4$ (min$^{-1}$) are rate parameters, and $m_2$, $m_3$, and $m_4$ depend on $m_1$ in the following way:

$$\begin{aligned}
m_2 &= 0.6\frac{CL}{HE_b\ V_i\ BW} \\
m_3 &= m_1\frac{HE_b}{1 - HE_b} \\
m_4 &= 0.4\frac{CL}{V_i\ BW}
\end{aligned} \tag{4.14}$$

where $HE_b$ is the basal hepatic insulin extraction and was fixed to 0.6, $CL$ (min$^{-1}$) is the insulin clearance.

At basal one has

$$I_{lb} = \frac{I_{pb}\ m_2}{m_1 + m_3} \qquad I_{pb} = I_b\ V_i \tag{4.15}$$

where $I_{lb}$ and $I_{pb}$ corresponds with to the basal steady state of insulin masses in plasma and in liver respectively.

*Subcutaneous Glucose Kinetics*: In Magni et al. (2007), the subcutaneous glucose concentration $G_M$ (mg/dl) is obtained as:

$$\frac{\mathrm{d}G_M(t)}{\mathrm{d}t} = -k_{sc}G_M(t) + k_{sc}G(t) \tag{4.16}$$

where $k_{sc}$ is a transfer-rate constant.

### 4.2.2 Hovorka *et al.* model

*Carbohydrate digestion and absorption*: In Hovorka et al. (2004a) and Wilinska et al. (2010), carbohydrates catabolism to monosaccharide (mostly glucose) taking place during meal digestion, as well as intestinal absorption is described. The glucose absorption rate $U_G(t)$ (mg min$^{-1}$) is represented by:

$$\begin{aligned}
\frac{\mathrm{d}G_1(t)}{\mathrm{d}t} &= -\frac{\mathrm{d}G_1(t)}{\mathrm{d}t} + Bio * D(t) \qquad G_1(0) = 0 \\
\frac{\mathrm{d}G_2(t)}{\mathrm{d}t} &= \frac{G_1(t)}{t_{max}} - \frac{G_2(t)}{t_{max}} \\
U_G &= \frac{G_2(t)}{t_{max}}
\end{aligned} \tag{4.17}$$

being $D(t)$ (mg) the amount of CHO ingested at time t, $Bio$ (dimensionless) is the bioavailability of the meal and $t_{\max}$ (min) is the time-of-maximum appearance rate of glucose in plasma.

*Subcutaneous insulin absorption*: Hovorka *et al.* (Hovorka et al., 2004a; Wilinska et al., 2010) described two-compartments that represents the absorption of subcutaneously administered rapid-acting insulin (see Figure 4.8).

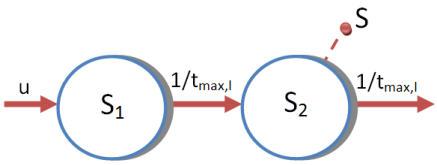


Figure 4.8: Compartment model of subcutaneous insulin absorption proposed by Hovorka et al. (2004a).

The model is represented by the following equations:

$$\begin{aligned}
\frac{\mathrm{d}S_1(t)}{dt} &= u(t) - k_a S_1(t) \qquad S_1(0) = \tfrac{u(0)}{k_a} \\
\frac{\mathrm{d}S_2(t)}{dt} &= k_a S_1(t) - k_a S_2(t) \qquad S_2(0) = S_1(0) \\
\frac{\mathrm{d}I}{dt} &= \frac{k_a S_2(t)}{V_I} - k_e I(t)
\end{aligned} \tag{4.18}$$

where $S_1$ and $S_2$ (mU) represents insulin masses in the accessible and nonaccessible compartments, $u$ (mU min$^{-1}$) represents administration (bolus and infusion) of rapid-acting insulin, $k_a$ (min$^{-1}$) is insulin absorption rate constant, $V_I$ (L kg$^{-1}$) is the volume of distribution of rapid-acting insulin, $I$ (mU kg L$^{-1}$) is the insulin concentration in plasma, and $k_e$ (min$^{-1}$) represents the fractional elimination rate from plasma.

*Insulin action and glucose kinetics*: In Hovorka et al. (2002), the model regards separately at each action of insulin on different phenomena with its final effect on blood glucose. The relation between insulin in plasma, every virtual compartment representing insulin actions and the two compartments for glucose are shown in Figure 4.9.

Two compartments representing kinetics of native glucose:

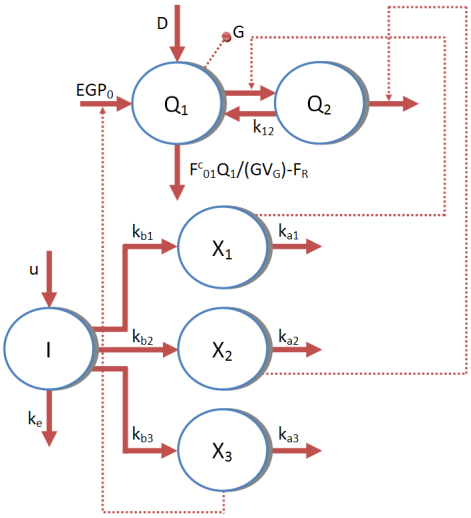


Figure 4.9: Compartment model of glucose-insulin system (adapted from Hovorka et al. (2004a)).

$$
\begin{aligned}
\frac{\mathrm{d}Q_1(t)}{\mathrm{d}t} &= -x_1(t)Q_1(t) + k_{12}Q_2(t) - F_{01}^c(t) - F_R(t) + U_G(t) \\
&\quad +\mathrm{EGP}_0(1 - x_3(t)) && Q_1(0) = G(0)\, V_g \\
\frac{\mathrm{d}Q_2(t)}{\mathrm{d}t} &= x_1(t)Q_1(t) - (k_{12} + x_2(t))Q_2(t) && Q_2(0) = \frac{Q_1(0)x_1(0)}{k_{12} + x_2(0)} \\
G(t) &= \frac{Q_1(t)}{V_G} && G(0) = G_b
\end{aligned}
\tag{4.19}
$$

where $Q_1$ and $Q_2$ (mmol) represents the masses of glucose in the accessible and non-accessible compartments, $k_{12}$ (min$^{-1}$) represents the transfer rate constant from the non-accessible to the accessible compartment, $V_G$ (L kg$^{-1}$) represents the distribution volume of the accessible compartment, $G$ (mmol L$^{-1}$) is the glucose concentration in plasma and $\mathrm{EGP}_0$ (mmol min$^{-1}$) represents endogenous glucose production extrapolated to the zero insulin concentration. $F_{01}^c$ (mmol min$^{-1}$) is the total non-insulin-dependent glucose disposal, and $F_R$ is the renal glucose clearance above the glucose threshold of $R_{thr}$ (mmol L$^{-1}$):

$$
F_{01}^c(t) = \frac{F_{01}G(t)}{0.85(G(t) + 1)} \tag{4.20}
$$

$$
F_R(t) = \begin{cases} R_{cl}(G(t) - R_{thr})V_G & \text{if} \quad G(t) \geq R_{thr} \\ 0 & \text{if} \quad G(t) < R_{thr} \end{cases} \tag{4.21}
$$

where $R_{cl}$ is the renal clearance constant.

The model adds a new compartment for every action of insulin, and there are three considered events: insulin increases the flow of glucose from blood to the tissues, insulin increases the glucose uptake by muscles and adipose tissue, and insulin inhibits production of glucose in the liver. These three influences are reflected in the model as virtual compartments (see Figure 4.9).

The insulin actions are modelled as first-order processes:

$$\begin{aligned}
\frac{\mathrm{d}x_1(t)}{\mathrm{d}t} &= -k_{a1}x_1(t) + k_{a1}S_{IT}I(t) \qquad x_1(0) = S_{IT}\ I(0) \\
\frac{\mathrm{d}x_2(t)}{\mathrm{d}t} &= -k_{a2}x_2(t) + k_{a2}S_{ID}I(t) \qquad x_2(0) = S_{ID}\ I(0) \\
\frac{\mathrm{d}x_3(t)}{\mathrm{d}t} &= -k_{a3}x_3(t) + k_{a3}S_{IE}I(t) \qquad x_3(0) = S_{IE}\ I(0)
\end{aligned} \tag{4.22}$$

where $x_1$ ($\mathrm{min}^{-1}$) represents the effects of insulin on glucose distribution/transport, $x_2$ ($\mathrm{min}^{-1}$) represents the effect on glucose disposal, and $x_3$ ($\mathrm{min}^{-1}$) the effect on endogenous glucose production; $k_{ai}$, $i = 1, \ldots, 3$ are deactivation rate constants, and $S_{IT}$, $S_{ID}$ and $S_{IE}$ ($\mathrm{min}^{-1}$ per mU $\mathrm{L}^{-1}$) are insulin sensitivities to transport, disposal, and endogenous glucose production, respectively.

*Subcutaneous Glucose Kinetics*: The model of the interstitial glucose kinetics uses a simple diffusion model:

$$\frac{\mathrm{d}C(t)}{\mathrm{d}t} = -k_{a\_int}[G(t) - C(t)] \tag{4.23}$$

where $C$ is glucose concentration in the subcutaneous tissue, $G$ is glucose concentration in the plasma, and $k_{a\_int}$ is the transfer-rate constant.

### 4.2.3 Representing a Real Patient Cohort

A conventional procedure for virtualising a real patient cohort involves the identification of individual parameters of a representative model of the glucose-insulin system. Signals, such as glucose or insulin concentration, are obtained from specific clinical tests, including the oral glucose tolerant test or the intravenous glucose tolerant test as well as other tracer signals in the identification process. Population values associated with well-known metabolic processes are reused in most identification procedures to reduce complexity and promote a better fit (Hovorka et al., 2002; Dalla Man et al., 2006). Data fitting software, such as SAAM II, return optimal parameter estimation and associated statistics (Barrett et al., 1998).

However, this identification procedure is expensive with regards to the associated cost-benefits, as the number of virtual patients is equivalent to the number of real patients. For this reason, information about the model parameters from clinical studies have been adapted to additional approaches. Virtual patients included in the FDA-approved UVa simulator were derived from probability distribution functions associated with the model parameters of Dalla Man *et al.* (Kovatchev et al., 2009). Virtual patients included in the UCAM simulator were derived from the conventional procedure, whereas the virtual cohort was validated by comparing the outcomes obtained from real closed-loop tests with the results obtained in the *in silico* version of similar tests (Wilinska et al., 2010).

The approach implemented and described in this section is conducted from the statistical data of the model parameters of Hovorka *et al.*, and a discarding method related to the common

clinical parameters of T1D patients (León-Vargas et al., 2012a).

Probability distributions of model parameters were extracted from Chassin (2005). Tables 4.1 and 4.2 show the univariate and multivariate parameters, respectively, from the Hovorka *et al.* model respectively.

| Symbol | Units | Distribution | Limits |
|---|---|---|---|
| $V_G$ | liter kg$^{-1}$ | exp($V_G$) $\sim N$(ln(0.15),0.23$^2$) | [0.09-0.25] |
| $R_{\_thr}$ | mmol liter$^{-1}$ | $R_{\_thr} \sim N$(9,1.5$^2$) | [7.5-15] |
| $R_{\_cl}$ | min$^{-1}$ | $R_{\_cl} \sim N$(0.01,0.025$^2$) | [0.003-0.03] |
| $V_I$ | liter kg$^{-1}$ | $V_I \sim N$(0.12,0.012$^2$) | [0.08-0.180] |
| $k_a$ | min$^{-1}$ | $k_a \sim N$(0.018,0.0045$^2$) | [0.005-0.060] |
| $k_e$ | min$^{-1}$ | $k_e \sim N$(0.14,0.035$^2$) | [0.050-0.300] |
| $Bio$ | % | $Bio \sim U$(70,120) | - |
| $t_{max}$ | min | exp(1/$t_{max}$) $\sim N$(-3.689,0.25$^2$) | [0.010-0.040] |
| $k_{a\_int}$ | min$^{-1}$ | exp($k_{a\_int}$) $\sim N$(-2.372,1.092$^2$) | - |
| $k_{12}$ | min$^{-1}$ | exp($k_{12}$) $\sim N$(-2.813,0.43$^2$) | [0.01-0.2] |
| $k_{a1}$ | min$^{-1}$ | exp($k_{a1}$) $\sim N$(-5.684,1.0$^2$) | [0.0002-0.0500] |
| $k_{a2}$ | min$^{-1}$ | exp($k_{a2}$) $\sim N$(-2.882,0.75$^2$) | [0.0050-0.4000] |
| $k_{a3}$ | min$^{-1}$ | exp($k_{a3}$) $\sim N$(-3.730,0.75$^2$) | [0.0030-0.1000] |

Table 4.1: Univariate model parameters.

| Symbol | Units | Mean |
|---|---|---|
| $F_{01}$ | $\mu$mol kg$^{-1}$ min$^{-1}$ | 11.1 |
| $EGP_0$ | $\mu$mol kg$^{-1}$ min$^{-1}$ | 16.9 |
| $S_{ID}$ | min$^{-1}$ per mU liter$^{-1}$ | 5.05 x 10$^{-4}$ |
| $S_{IE}$ | per mU liter$^{-1}$ | 0.019 |
| $S_{IT}$ | min$^{-1}$ per mU liter$^{-1}$ | 18.41 x 10$^{-4}$ |

Table 4.2: Multivariate model parameters.

The sampling procedure for extracting parameter vectors was performed using the quasi-Monte Carlo (qMC) method (Niederreiter, 1978). The conventional Monte Carlo (MC) method is also available. However, the qMC method stratifies the random generation of values through a quasi-random sequence, which ensures a better distributed sampling than the pseudo-random sequences in the MC method. The difference between the conventional MC and the qMC methods is illustrated by Figure 4.10, which compares two random sequences in one dimension.

In the case of multivariate parameters, the covariance matrix is employed for sampling the probability distribution. The covariance matrix is obtained using parameter data from Chassin (2005), which were previously transformed to be normally distributed, as shown in Eq. 4.24.

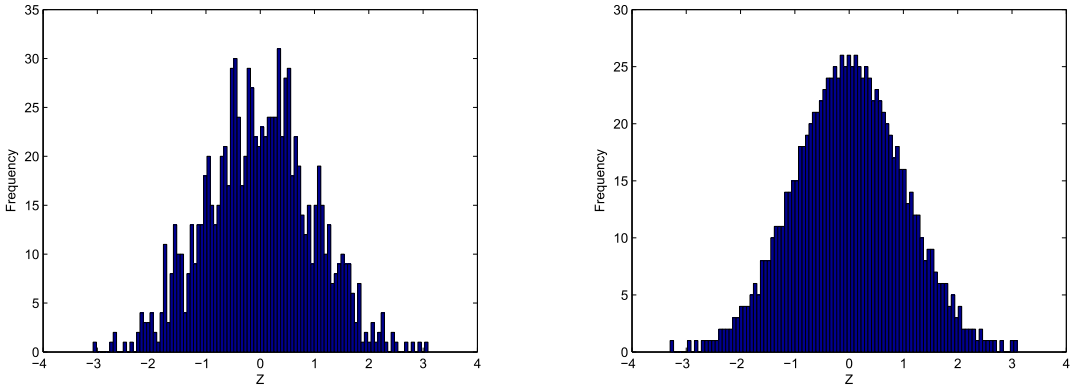


(a) (b)

Figure 4.10: 1000 simulated N(0,1) random values using (a) the Monte Carlo and (b) the quasi-Monte Carlo method.

$$\left|\begin{array}{ccccc} 0.221 & 0.053 & -0.283 & -0.024 & 0.242 \\ 0.053 & 0.155 & -0.177 & 0.221 & 0.158 \\ -0.283 & -0.177 & 0.830 & -0.072 & -0.269 \\ -0.024 & 0.221 & -0.072 & 0.410 & 0.148 \\ 0.242 & 0.158 & -0.269 & 0.148 & 0.446 \end{array}\right| \tag{4.24}$$

Once the sampling procedure is completed, the raw cohort of virtual patients is obtained by antitransformation. The discard method to eliminating incorrect virtual patients is divided into the following two stages:

- First, virtual patients with parameter values beyond an allowable range or with an insulin-independent glucose utilisation greater than the endogenous glucose production are omitted.
- Second, virtual patients with clinical parameter values beyond the target range are omitted. All virtual patients are assessed using open-loop tests to calculate the clinical parameters. The target range is defined according to the requirements of the *in silico* experiment.

The process for representing a real patient cohort is summarised in Figure 4.11.

As an illustration of generation methodology, a virtual cohort based on clinical parameters of a real cohort is developed. Table 4.3 lists the clinical parameters from a real patient cohort. The target range of values for the virtual patients is defined by $\pm 2SD$ from the mean of the clinical parameters in the discard method.

A list of clinical parameters for the discard method may contain the total daily basal, the total daily bolus, the total daily dose, the insulin-to-carbohydrate ratio, and the duration of insulin action (DIA). The corresponding tests used to calculate these clinical parameters are described as follows:

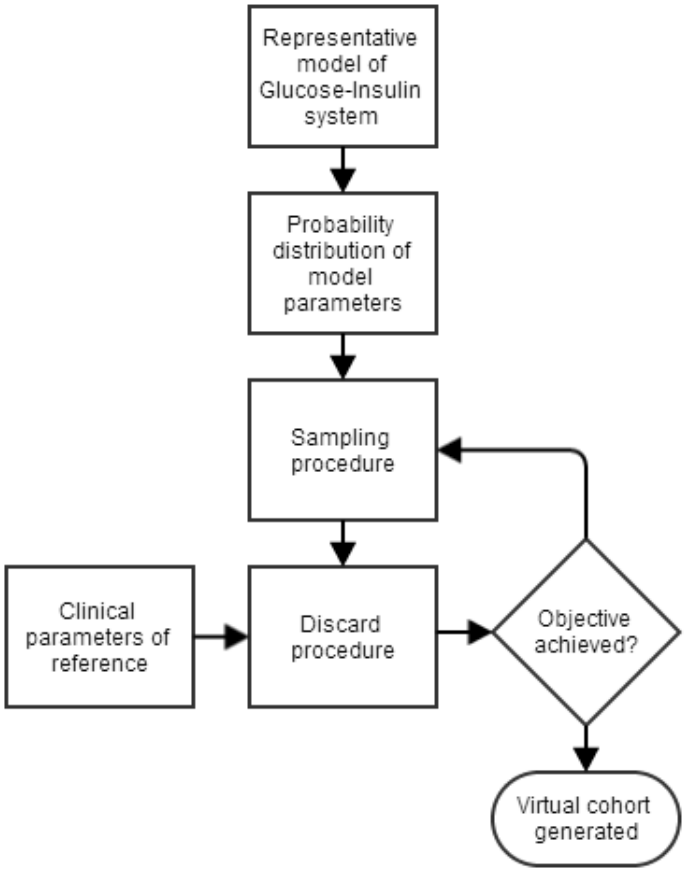


Figure 4.11: Flow diagram of the virtual patient generation.

*Basal insulin*: In the Hovorka *et al.* model, some equations can be combined and reformulated to yield the following expressions:

$$I_p = \frac{-b \pm \sqrt{b^2 - 4ac}}{2a} \tag{4.25}$$

where $I_p$ is the plasma insulin, and the remaining terms are:

$$\begin{aligned} a &= (G_b V_G S_{IT} + EGP_0 S_{IE}) S_{ID} \\ b &= EGP_0 S_{IE} k_{12} + (F_{01}^c(0) + F_R(0) - U_G(0) - EGP_0) S_{ID} \\ c &= (F_{01}^c(0) + F_R(0) - U_G(0) - EGP_0) k_{12} \end{aligned} \tag{4.26}$$

where $G_b$ corresponds to the basal glucose value obtained with basal insulin in a steady state. The corresponding insulin infusion $U_{2SS}$ is subsequently obtained from the subcutaneous insulin absorption model as follows:

$$U_{2SS} = V_I k_e I_p \tag{4.27}$$

| Basal dose (U) | Bolus dose (U) | Total daily dose (U) | I/CHO (U/g) | Mean blood glucose (mg/dl) | DIA* (h) |
|---|---|---|---|---|---|
| 20.8±8.4 | 20.1±10.3 | 40.9±15.0 | 0.13±0.04 | 158.2±20.1 | 4±0 |

* DIA stands for Duration of Insulin Action

Table 4.3: Mean and standard deviation of clinical parameters for patients with T1D in a Barcelona hospital.

*Total daily dose of insulin and Insulin-to-carbohydrate ratio*: Both parameters are estimated from an open-loop test using 3 meals per day and a meal size according to the daily calorie requirements of each virtual patient. The corresponding basal insulin to maintain plasma glucose over 100 mg/dl in a steady state is used in this test. The goal is to establish a bolus size that produces a maximum period of normoglycaemia. Daily calorie $C_D$ and carbohydrates $CHO_D$ are calculated as:

$$\begin{aligned} C_D &= Weight \cdot CalorieFactor \\ CHO_D &= \frac{C_D}{10} \end{aligned} \tag{4.28}$$

where $C_D$ is divided by 10 to reflect 40% of calories obtained from carbohydrates. $CalorieFactor$ is adjusted to 14, which represents a carbohydrate requirement associated with a moderate activity level (Walsh and Roberts, 2006). The open-loop protocol is breakfast, lunch and dinner at 08:00, 13:00 and 20:00 respectively, and a corresponding prandial bolus is administered 20 min prior to a meal.

*Duration of insulin action*: This test begins with a high blood sugar (in the range of hyperglycaemia) and minimal bolus on board acting. An accurate correction bolus and a correct duration of insulin action will return a high blood sugar to the target ragÂ¡nge by the end of the duration time period with no additional lowering of the blood sugar during the 2 hours beyond this time (Walsh and Roberts, 2006). In this case, each virtual patient is brought to hyperglycaemia by suspending the insulin infusion and attaining a reduction in glucose of 100 mg/dl as a target.

As a result, given the 100 virtual patients generated by sampling the probability distributions, only 17% have approved the proposed discard method. In the first filter 53% of virtual patients were dismissed. Of the 47% admitted in this filter, 36% satisfied the requirements of the second filter. The clinical parameters resulting from this test are shown in Table 4.4.

| Basal dose (U) | Bolus dose (U) | Total daily dose (U) | I/CHO (U/g) | Mean blood glucose (mg/dl) | DIA (h) |
|---|---|---|---|---|---|
| 22.6±8.2 | 24.2±6.2 | 46.7±11.3 | 0.12±0.02 | 131.7±0.9 | 6.1±1.5 |

Table 4.4: Mean and standard deviation of clinical parameters from the virtual patients.

One of the main advantages of the generation process is the flexibility of the simulation procedure. This method reuses collected statistical data from previous clinical studies to satisfy actual conditions of open-loop control tests. In this manner, a cohort of real patients who will be used in a clinical trial has a virtual counterpart that satisfies the same clinical parameters without identifying the individual parameters values of the model used. Although the proposed method can be easily and practically implemented, acquiring a virtual counterpart for a specific

patient may require a considerable amount of computation; however, this option is also valid. The use of virtual counterparts for T1D patients involved in an actual clinical study facilitates the optimisation of glycaemic control, which improves the effectiveness of the resources invested in development and subsequent clinical implementation. Although only open-loop control metrics have been proposed in this implementation, the use of closed-loop control metrics is also feasible. Due to the complexity of this procedure, the initial use of the discard method, which considers common clinical parameters, may be more appropriate.

## 4.3 In Silico Platform

### 4.3.1 Overview

The layout of the platform is shown in Figure 4.12. The closed-loop control scheme comprises the virtual patient, the instrumentation, and the controller block. The platform requires metadata to set up each block and configure the experimental design. An additional block is employed to configure parameters settings, such as the sample period, the differential equation solver, and the experiment protocol. The last block contains the outcomes used to assess the control performance. This platform environment and the graphic user interface is implemented in LabVIEW$^{TM}$. Each platform element is described as follows:

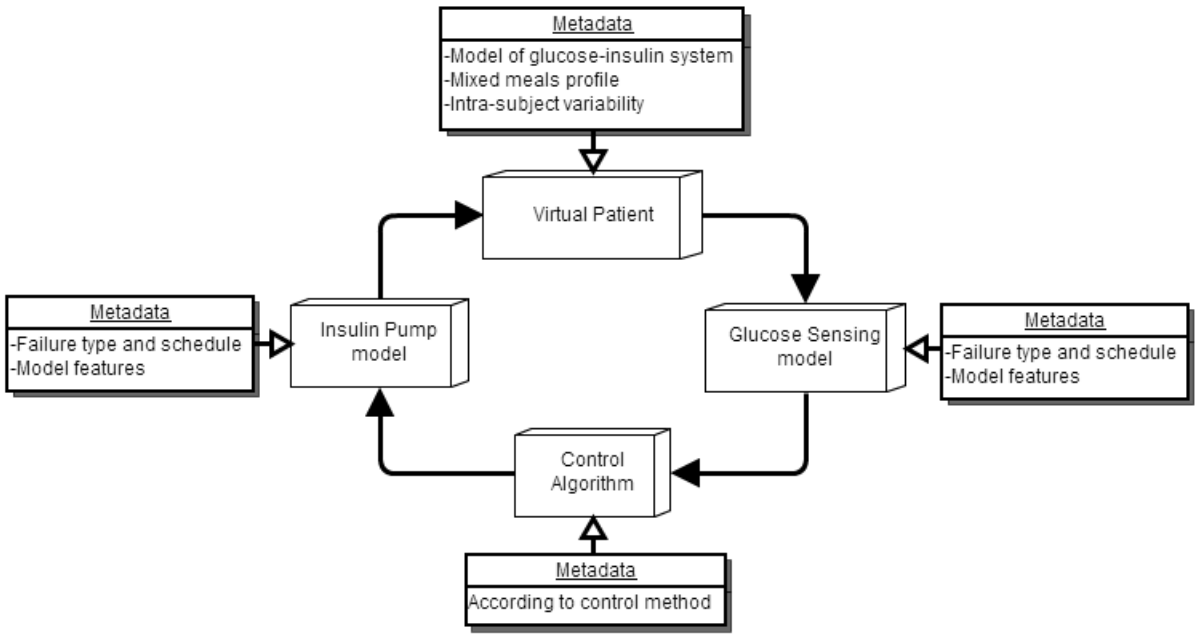


Figure 4.12: The layout of the platform, which includes a virtual patient with proper instrumentation for a closed-loop control scheme and the control algorithm to close the loop.

The main menu for the platform is shown in Figure 4.13. All configuration blocks are accessed using this menu. It also includes a scenario summary window, options to load and save, and control buttons to run or stop the simulation.

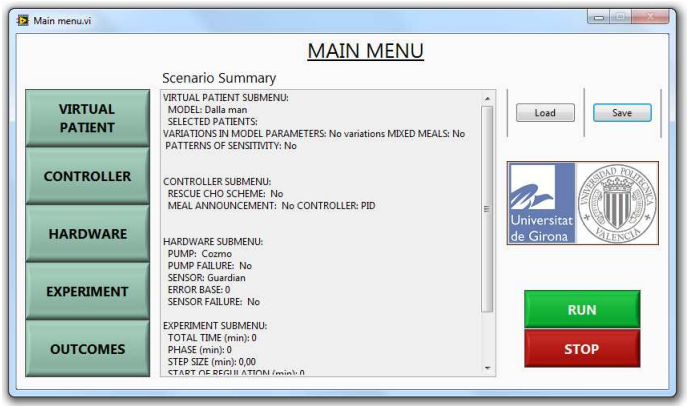


Figure 4.13: Platform main menu.

The virtual patient submenu is shown in Figure 4.14. The model of the glucose-insulin system by Hovorka *et al.* or Dalla Man *et al.* is selected and a list of virtual patients are available. The option of *parameters dynamics* allows a user to define sinusoidal variations or import customised variations over model parameters. In addition, an option designed to include and customise patterns of circadian variability to sensitivity parameters is also available. The last option for defining whether the virtual patient will work with profiles of rate glucose appearance from mixed meals or the corresponding model of carbohydrate absorption is included. A description of intra-patient variability and information about mixed meals is detailed in the following sections.

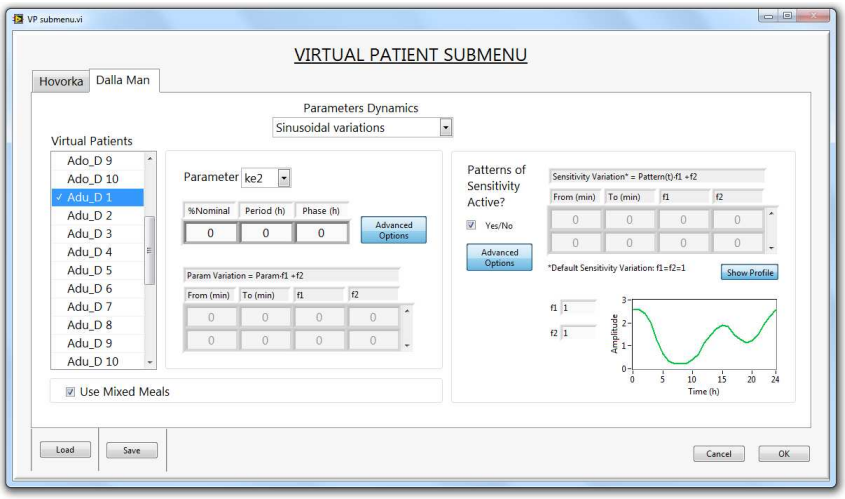


Figure 4.14: Virtual patient submenu.

The controller submenu is shown in Figure 4.15. Meal announcement and CHO rescue are options available to the control algorithm if required. With the meal announcement option, the controller has information about the timing and size of the meal intake. With the rescue option, it is possible to define the CHO size and the interval to check the glucose concentration. It is also possible to configure the turn on/off schedule of the controller during the simulation

duration. The remaining options are configured according to the design of the control algorithm.

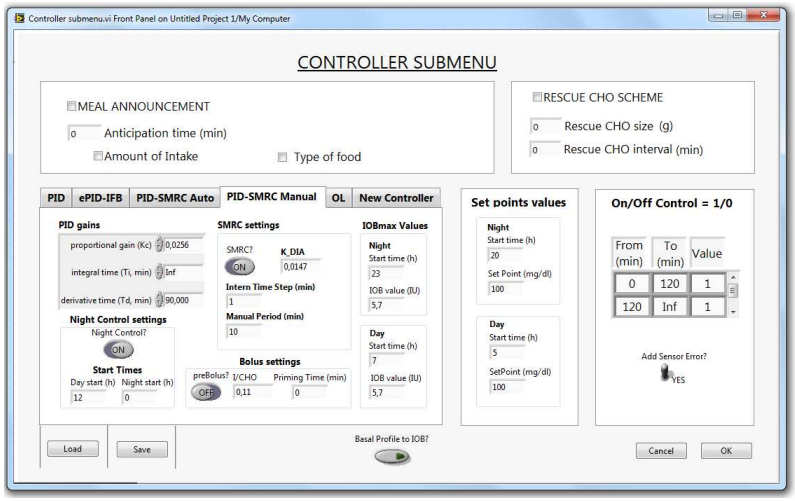


Figure 4.15: Controller submenu.

The hardware submenu is shown in Figure 4.16. This submenu involves the insulin pump and the glucose monitoring system. Features of several devices and representative failures have been included in both cases. For glucose monitoring, a loss of signal can be scheduled; for an insulin pump, a different type of occlusion can be adjusted and scheduled to the simulation. Model devices are described in the following sections.

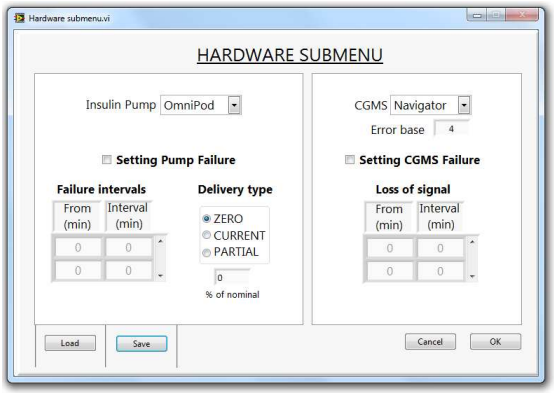


Figure 4.16: Hardware submenu.

The experiment submenu is shown in Figure 4.17. Simulation settings relative to the solver and the corresponding step size are adjusted using this submenu. In addition, the experiment duration and a phase term used to modify the sensitivity patterns can be found. The CHO protocol enables the user to specify the duration and size of meals and the corresponding bolus insulin if required. A profile of basal rate insulin can be defined as a constant, dynamic or default profile.

The outcomes submenu is shown in Figure 4.18. In this menu, several metrics can be selected to evaluate the control algorithm. The period of assessment can be adjusted to a specific simu-

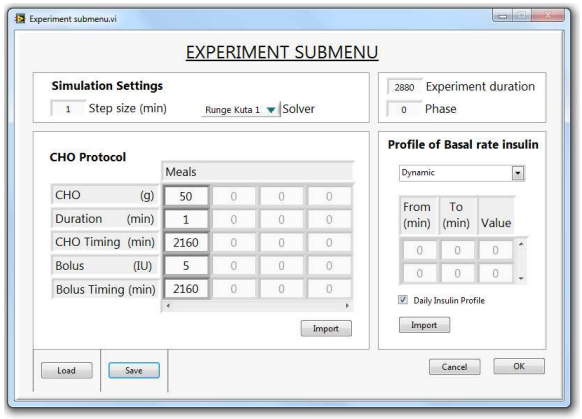


Figure 4.17: Experiment submenu.

lation. Additional information about the provided metrics is detailed in the following sections.

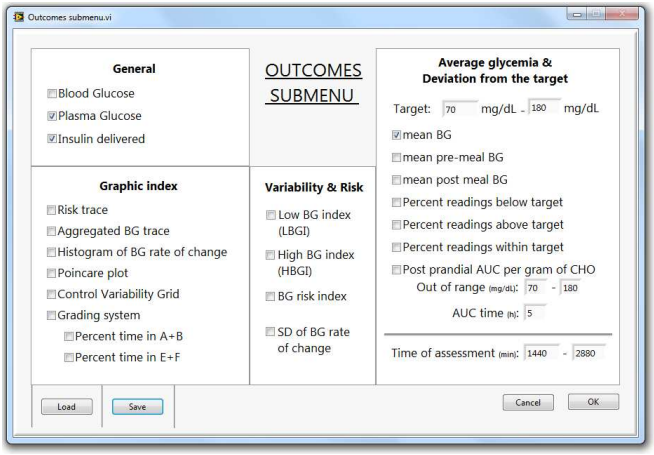


Figure 4.18: Outcomes submenu.

### 4.3.2 Mixed Meals

*In silico* studies of the artificial pancreas require the implementation of complex conditions that reflect real challenges to the control algorithm. Different models of the glucose-insulin system have been developed to explain the complex dynamics involved. However, some processes, such as carbohydrate absorption or insulin action, are modified daily by external disturbances, which have not been modelled and may impair the final performance of control algorithms. In the case of carbohydrate absorption, given a model for a virtual patient, such as Dalla Man *et al.* or Hovorka *et al.*, the glucose appearance response disregards the meal composition and prevents the handling of complex dynamics by the control algorithm.

Intensive in silico trials should be as realistic as possible to evaluate performance and safety. The MICELab group has developed a mixed meals library that contains profiles of the rate

of glucose appearance from several meal compositions using Bayesian identification methods (Barajas-Solano et al., 2012; Herrero et al., 2012). This library is implemented into the platform as an additional feature that enables variability in mixed meals of different sizes and compositions. When a mixed meal is selected for simulation, the carbohydrate absorption model is replaced by the time profile of the corresponding meal. Table 4.5 contains information about the mixed meals library, and Figures 4.19 and 4.20 show their corresponding time profiles. The mixed meal option appears in the platform in the virtual patient submenu, as shown in Figure 4.14. When this option is selected, the experiment submenu displays the corresponding meal codes from the library and the protocol schedule also changes, as illustrated in Figure 4.21.

### 4.3.3 Intra-Patient Variability

Intra-patient variability of insulin sensitivity defines the metabolic balance between insulin concentration and glucose disposal. This variability is present in T1D patients as an individual profile of variation that can be characterised and considered for improved continuous subcutaneous insulin infusion treatment. Several patient-related factors, such as illness, exercise, stress, dawn phenomenon or alcohol, and treatment-related factors, such as medications, can influence insulin sensitivity.

Models with virtual patients, such as patients in the Dalla Man *et al.* model, do not currently consider any intra-patient variability; however, it is reflected in the model description (Dalla Man et al., 2007). Virtual patients in the Hovorka *et al.* model are susceptible to sinusoidal variations in insulin sensitivity (Wilinska et al., 2010). Individualised variations of insulin sensitivity as presented by real patients have not been detailed or applied extensively in virtual patients. The inclusion of this intra-patient variability enables more realistic simulations and enhanced information about patient treatment.

For patients with T1D, patterns of basal insulin are achieved with an insulin pump to compensate variation from insulin sensitivity. Parameters related to insulin sensitivity in the Dalla Man *et al.* model are modified to implement realistic circadian variations. Figure 4.22 shows the patterns found in T1D patients classified by age range. In this thesis, all simulation tests focus on adult patients; the solid square pattern in Figure 4.22 is selected as the baseline for the basal insulin dynamics of virtual patients.

In the Dalla Man *et al.* model, the $V_{mx}$ parameter represents the disposal of insulin sensitivity and is modified accordingly. Figure 4.23 shows the average variation applied to the $V_{mx}$ parameter for adult virtual patients. The individualisation of this variation for each virtual patient enables the reproduction of the basal insulin profile from the selected pattern, as shown in Figure 4.24. Note that the applied variation exhibits inverse dynamics as the basal insulin and the insulin sensitivity have opposing effects.

Table 4.6 summarises the hourly basal insulin values per patient to accommodate the circadian variation in the insulin sensitivity shown in Figure 4.23. Also, Table 4.7 shows the insulin-to-carbohydrate ratio for each patient.

The platform includes a specific option in the virtual patient submenu to set up the inclusion of insulin sensitivity variation. There are two alternatives: clicking the check button of patterns of sensitivity or using the associated advanced options. The advanced options allow the user

| Meal | Ingredients | CHO (g) |
|---|---|---|
| 1 | Milk, white rice, pear, bran-cookies, low-fat cheese, oil | 52.0 |
| 2 | Milk, white rice, pear, bran-cookies, oil | 111.0 |
| 3 | Milk, white bread, low-fat cheese, butter, oil | 52.5 |
| 4 | Milk, white bread, low-fat cheese, butter, oil | 111.0 |
| 5 | Pasta + low content of sunflower oil | 75.0 |
| 6 | Pasta + high content of sunflower oil | 75.0 |
| 7 | Rice pudding, sugar and cinnamon | 50.0 |
| 8 | Kidney benas, wholemeal bread, salami, cheese | 50.0 |
| 9 | Pasta + psyllium low fat | 52.0 |
| 10 | Barley Temp | 25.0 |
| 11 | Oat Tempe | 25.0 |
| 12 | Chocolate Raspberry Bar | 10.0 |
| 13 | Chocolate Daydream shake | 10.0 |
| 14 | Peanut Butter Chocolate Bar | 25.0 |
| 15 | Chocolate Daydream shake fructose | 25.0 |
| 16 | Lightly Salted Soy Protein Chips | 25.0 |
| 17 | Soy Spaghetti | 25.0 |
| 18 | Low GI (250ml of water): Boiled pearl barley | 50.0 |
| 19 | High GI (285ml of water): Mashed potato | 50.0 |
| 20 | Baked potato, gelatin, turkey breast | 45.0 |
| 21 | Boiled rice, corn, turkey breast | 50.0 |
| 22 | White bread, eggs, margarine and orange juice | 50.0 |
| 23 | Powdered nutritional supplement | 50.0 |
| 24 | Pasta and tomato sauce | 50.0 |
| 25 | Pasta and tomato sauce + oil | 50.0 |
| 26 | Pasta and tomato sauce + oil + psyllium | 50.0 |
| 27 | High CHO meal | 93.0 |
| 28 | High fat meal | 27.0 |
| 29 | Pasta + medium content of sunflower oil | 75.0 |
| 30 | Standard breakfast 1 | 120.0 |
| 31 | Standard breakfast 2 | 70.3 |
| 32 | Standard breakfast 3 | 50.0 |
| 33 | Cheese omelet, bread and margarine | 38.0 |
| 34 | Spaghetti with tomato, cheese and lentils | 87.0 |
| 35 | Cornflakes, milk, bread and margarine | 104.0 |
| 36 | Oatmeal, milk, bread and margarine | 62.0 |
| 37 | Barley with tomato and cheese | 68.0 |
| 38 | Oat cereal, milk, strawberry jam and orange juice breakfast | 69.0 |
| 39 | Fiber and fruit cereal, milk, rockmelon, pineapple | 50.0 |
| 40 | High fiber cereal, milk, strawberries, grapefruit | 42.0 |
| 41 | Egg omelet, bread, spinach, red capsicum, grilled tomato | 20.2 |
| 42 | Egg omelet, honey, bread, spinach, red capsicum | 15.5 |
| 43 | Bread, milk, brown sugar, banana, orange juice | 47.0 |
| 44 | Muffin, peanut butter | 27.3 |
| 45 | Candy bar, milk, ice-cream, heavy cream | 80.0 |
| 46 | Syrup, Skimmed milk, fat-free ice-cream | 80.0 |
| 47 | Biscuit, no-fat yogurt | 94.0 |
| 48 | Wheat flakes, fresh cheese, milk | 91.0 |
| 49 | Wheat-biscuit, low-fat milk, whole-meal bread, fruit, poultry, vegetable 1 | 123.0 |
| 50 | Wheat-biscuit, low-fat milk, whole-meal bread, fruit, poultry, vegetable 2 | 126.0 |
| 51 | Vegetable lasagna, cream dessert, orange drink | 27.0 |
| 52 | Vegetable lasagna, skim milk dessert, orange drink | 120.0 |
| 53 | White Rice | 75.0 |
| 54 | 100% rolled barley | 75.0 |
| 55 | 50% rolled barley | 75.0 |
| 56 | 30% rolled barley | 75.0 |
| 57 | White Wheat Bread | 50.0 |
| 58 | Whole Kernel Bread | 50.0 |
| 59 | B-glucan Rye Bread | 50.0 |
| 60 | Whole Meal Pasta | 50.0 |

Table 4.5: Library of mixed meals.

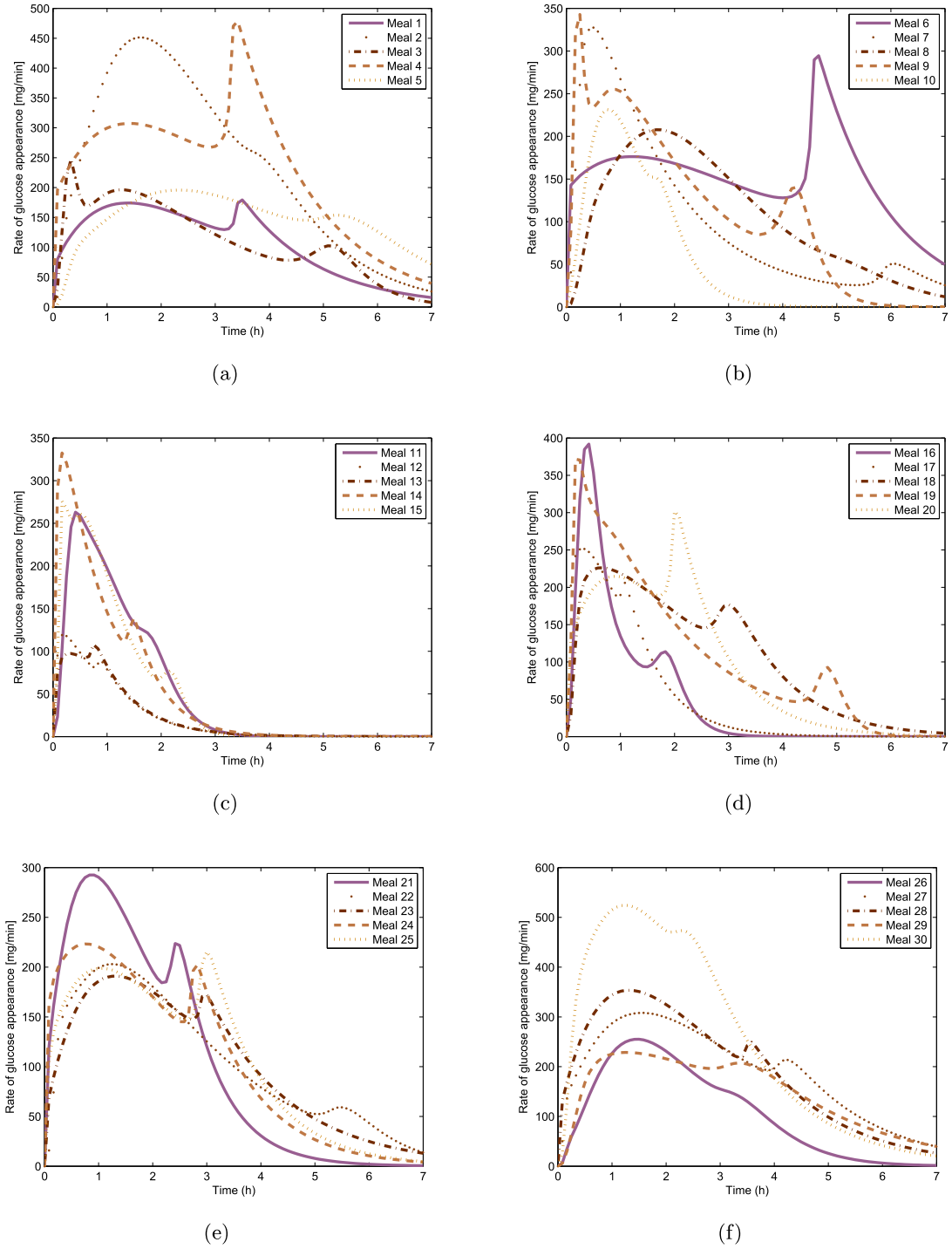


Figure 4.19: Time profile of rate glucose appearance for mixed meals (a) 1–5 (b) 6–10 (c) 11–15 (d) 16–20 (e) 21–25 and (f) 26–30.

to define scheduled modifications as amplitude or bias to the patterns. In this manner, the predefined variations of insulin sensitivity can be customised according to the requirements of the control testing. Figure 4.25 shows the customisable settings of insulin sensitivity variations

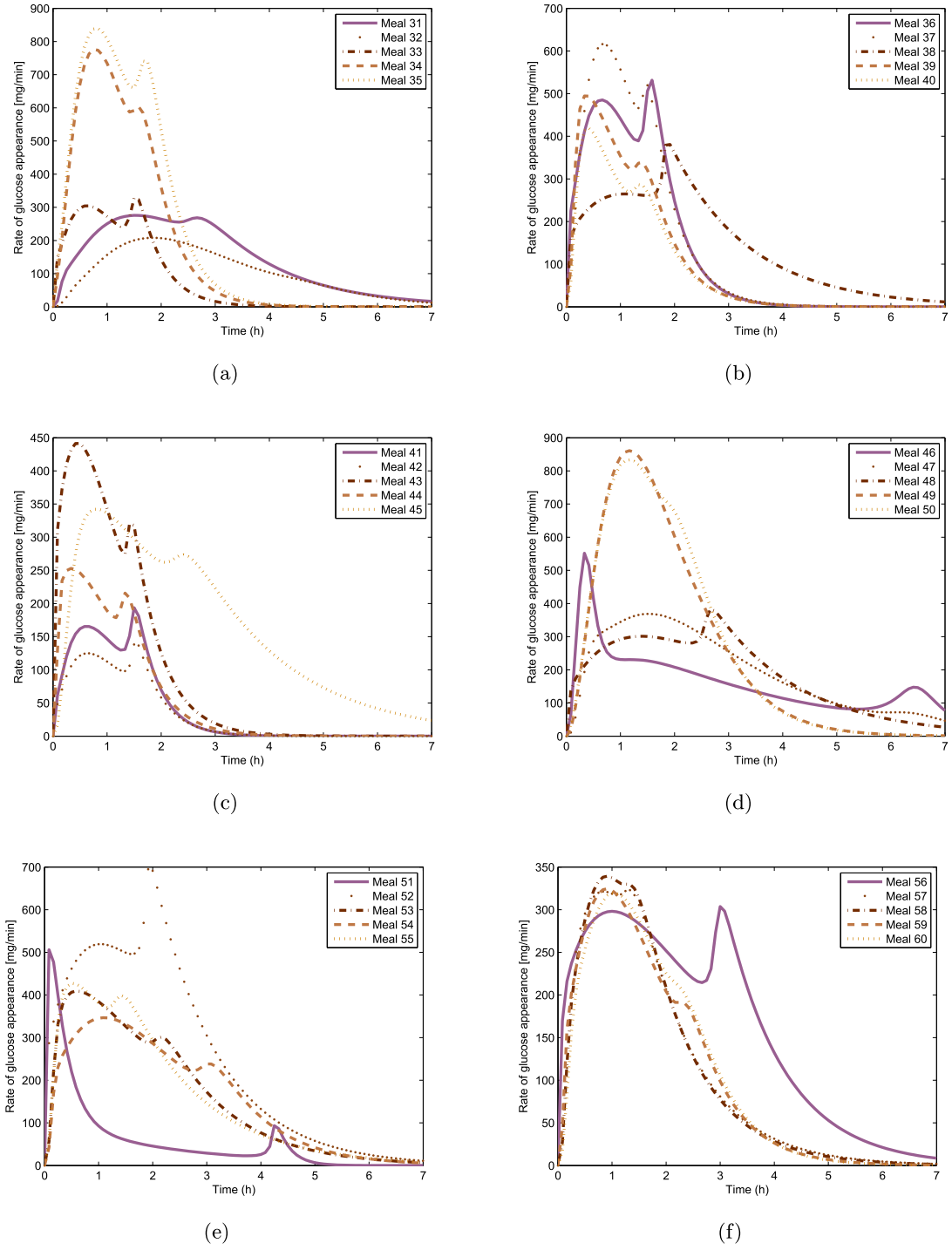


Figure 4.20: Time profile of rate glucose appearance for mixed meals (a) 31–35 (b) 36–40 (c) 41–45 (d) 46–50 (e) 51–55 and (f) 56–60.

from the virtual patient submenu.

In practice, four or five values of basal insulin are usually set in the insulin pump daily

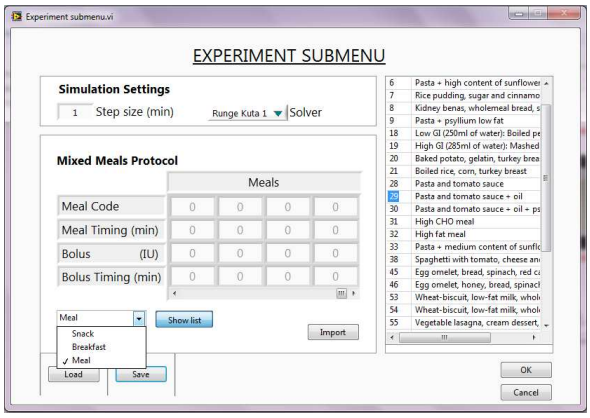


Figure 4.21: Experiment submenu when mixed meals option is on.

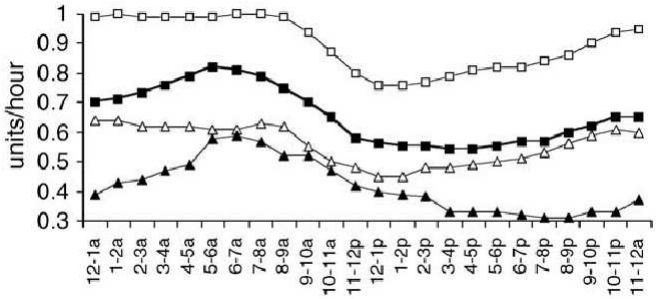


Figure 4.22: Average hourly basal rate values by age group. The open triangle represents ages 3–10 years of age, the open square depicts ages 11–20 years of age, the solid square represents ages 21–60 years of age, and the solid triangle depicts ages >60 years of age (taken from Scheiner and Boyer (2005)).

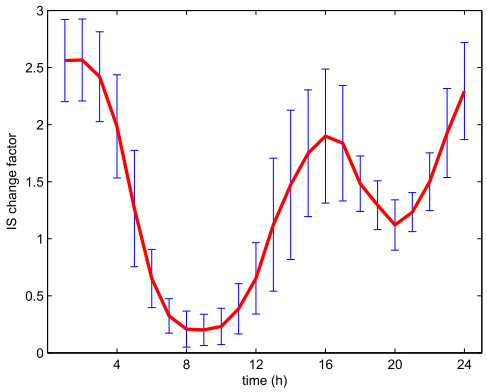


Figure 4.23: Mean and standard deviation of the variation profile of the insulin sensitivity parameter $V_{mx}$, which was applied to adult virtual patients in the Dalla Man *et al.* model.

to prevent glucose variations above 30 mg/dL (Scheiner et al., 2009). Figure 4.26 shows an

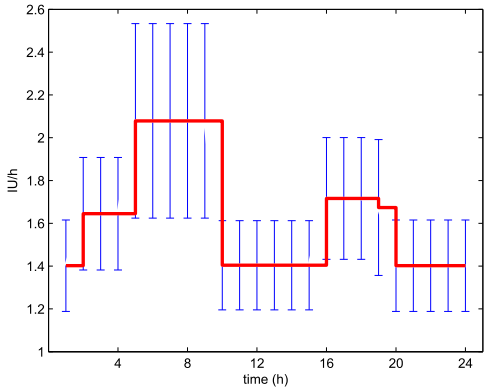


Figure 4.24: Mean and standard deviation of the basal insulin profile applied to adult virtual patients in the Dalla Man *et al.* model.

| Time \ Patient | 1 | 2 | 3 | 4 | 5 | 6 | 7 | 8 | 9 | 10 |
|---|---|---|---|---|---|---|---|---|---|---|
| 02:00 | 1.60 | 1.80 | 1.85 | 1.05 | 1.90 | 1.90 | 1.50 | 1.45 | 1.65 | 1.75 |
| 05:00 | 2.14 | 2.41 | 2.16 | 1.23 | 2.85 | 2.22 | 1.65 | 1.70 | 2.07 | 2.34 |
| 10:00 | 1.28 | 1.44 | 1.66 | 0.94 | 1.52 | 1.67 | 1.41 | 1.30 | 1.40 | 1.40 |
| 16:00 | 1.67 | 1.91 | 1.91 | 1.08 | 2.01 | 1.96 | 1.53 | 1.50 | 1.72 | 1.85 |
| 20:00 | 1.27 | 1.43 | 1.66 | 0.94 | 1.51 | 1.71 | 1.41 | 1.30 | 1.39 | 1.39 |

Table 4.6: Individualised basal insulin rate (IU/h) for each patient in the cohort.

| Time \ Patient | 1 | 2 | 3 | 4 | 5 | 6 | 7 | 8 | 9 | 10 |
|---|---|---|---|---|---|---|---|---|---|---|
| 00:00 | .100 | .100 | .100 | .050 | .125 | .075 | .050 | .075 | .150 | .175 |
| 12:00 | .0833 | .0833 | .075 | .0333 | .1166 | .05 | .025 | .055 | .1166 | .125 |
| 19:00 | .050 | .050 | .050 | .040 | .113 | .050 | .031 | .038 | .063 | .063 |

Table 4.7: Individualised insulin-to-carbohydrate ratio (IU/g) for each patient in the cohort.

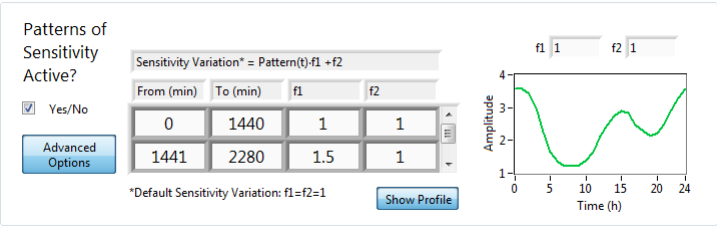


Figure 4.25: Advanced settings of patterns of sensitivity options from the virtual patient submenu.

example of the glucose concentration response when the default basal insulin profile is applied to the virtual patient. As a control, the platform includes an option in the experiment sub-

menu named default basal insulin that can be selected to obtain a corresponding daily basal insulin. This default profile substantially counteracts the effect of variation in insulin sensitivity.

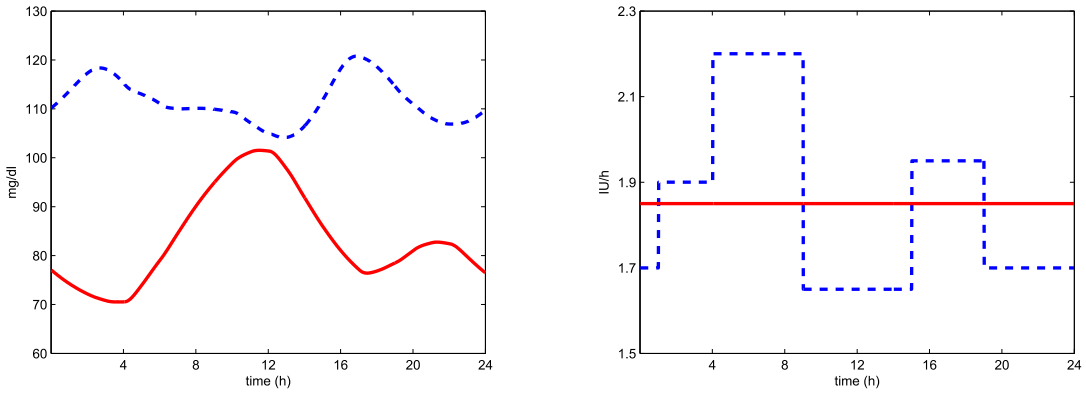


(a) (b)

Figure 4.26: Glucose concentration response of a virtual patient (a), including variation in insulin sensitivity, and (b), according to the basal insulin applied. The blue dashed line denotes a profile of basal insulin and the solid red line denotes a constant value of basal insulin.

The combination of sinusoidal variations in the platform, for varying any model parameter and the intra-patient variation of insulin sensitivity, enable the construction of numerous realistic control scenarios that contain diurnal and day-to-day variability.

### 4.3.4 Instrumentation models

**Glucose sensor model** The glucose sensor model is employed to estimate the behaviour of the measurement errors of continuous glucose monitoring (CGM) systems and enables a more realistic simulation of test scenarios. Several recent studies have been conducted on the accuracy of CGM systems (Gerritsen et al., 1999; Gross et al., 2000; Cheyne et al., 2002; Kovatchev et al., 2004; Clarke et al., 2005; Clarke and Kovatchev, 2007; Zisser et al., 2008b). The primary challenges of achieving accuracy are the sensitivity, the calibration stability and the inherent physiological lag between the blood glucose concentration and the interstitial glucose concentration.

The model suggested by Breton and Kovatchev (2008) represents the measurement behaviour of CGM systems and provides an improved description of sensor error dynamics than the Gaussian noise commonly included in control simulations (Chassin et al., 2004). Although this model demonstrates a sophisticated level of abstraction, Facchinetti *et al.* (Facchinetti et al., 2010) partially dismissed it due to the difficulty of achieving a perfect calibration when working with data collected in vivo. However, the Breton & Kovatchev model exhibits sufficient representativeness for use in realistic simulation tests.

The model comprises two components. The first component is related to the transport delay from the blood to the interstitial glucose concentration. The measurement is obtained from the

interstitial space. Eq. 4.29 describes this component as a first-order diffusion model as

$$\frac{\mathrm{d}IG(t)}{\mathrm{d}t} = -\frac{1}{\tau}(IG(t) - BG(t)) \tag{4.29}$$

where $IG(t)$ and $BG(t)$ are the interstitial and blood glucose concentration respectively, and $\tau$ is a rate constant for the two fluids.

The second component is related to the noise sensor, which does not constitute white noise, and is modelled by an autoregressive moving average (ARMA) model as shown in Eq. 4.30.

$$e_n = 0.7(e_{n-1} + v_n) \tag{4.30}$$

where $v_n \sim \phi(0, 1)$ is independent and identically distributed (i.i.d.), i.e., an error which is independent of previous errors and time and obtained from the same probability distribution. The sensor error $\varepsilon_n$ is calculated from the time series of normally distributed $e_n$ using a Johnson transformation Eq. 4.31.

$$\varepsilon_n = \xi + \lambda sinh(\frac{e_n - \gamma}{\delta}) \tag{4.31}$$

where $\xi$, $\lambda$, $\gamma$, and $\delta$ are fixed; their values are listed on Table 4.8.

| Parameter | Value |
|---|---|
| $\xi$ | -5.471 |
| $\lambda$ | 15.96 |
| $\gamma$ | -0.544 |
| $\delta$ | 1.689 |

Table 4.8: Parameter values used for Johnson transformation.

Commercial CGM systems have restrictions on measurement accuracy and technical features, such as the display period of glucose measurements or the minimum and maximum allowable glucose values, which are dependent on the manufacturer. Table 4.9 shows the display period of the CGM systems implemented on the platform.

| Model | Display period (min) |
|---|---|
| Dexcom | 3 |
| Guardian | 5 |
| Navigator | 1 |

Table 4.9: Display period of glucose measurements of implemented CGM systems.

The technical failure of loss of signal in the CGM systems has been implemented to evaluate the performance of glucose controllers under malfunctioning conditions. A failure schedule can be adjusted in the simulation setup of the hardware submenu.

**Insulin Pump Model** According to Hovorka (2006); Kovatchev et al. (2009), incorrect insulin delivery influences the performance of the glucose control algorithm. In this manner, deviations in the expected value of the insulin basal delivery or the insulin bolus must be considered in realistic simulations. The error model used for these deviations was assumed uncorrelated, with a zero mean and a constant coefficient of variation (CV) (Wilinska et al., 2010). According to the insulin pump, a specific CV can be set using data from the experimental tests in Zisser et al. (2010a).

The minimum basal and bolus increments and the maximum insulin delivery rate were implemented as technical features. These features are defined by the manufacturer and vary amongst devices. Table 4.10 presents the feature values for two commercial insulin infusion pumps.

| Model | Basal increment (IU) | Bolus increment (IU) | Maximum basal rate (IU/h) | Maximum bolus dose (IU/h) |
|---|---|---|---|---|
| Deltec Cozmo | 0.05 | 0.05 | 35 | 75 |
| Omnipod | 0.05 | 0.05 | 30 | 30 |

Table 4.10: Technical features of implemented insulin pumps.

Regarding the types of failures of insulin pumps in real-life scenarios, three effects were considered: constant delivery, partial delivery, and non-delivery of insulin. Each represents a different degree of pump occlusion. A constant delivery is a software failure in which the pump insulin does not respond to new values and maintains the current insulin delivery value. A partial delivery is a hardware failure in which the insulin pump occlusion prevents a full delivery rate. A non-delivery is a complete suspension of insulin delivery. To include this behaviour in the simulation, a failure schedule can be adjusted in the hardware submenu.

### 4.3.5 Outcome Measurements

The outcome measurements available in the platform are organised by graphical or numerical type. The following list briefly describes briefly the measurements used in the platform.

- One of the most useful measurements is the control variability grid analysis (CVGA), which is a graphical tool commonly used in closed-loop assessment. It locates the performance of a control algorithm in a given area according to an observation period. Each data point in CVGA represents the minimum/maximum values obtained during the glucose excursion (Magni et al., 2008).

- The risk trace is based on a data transformation that normalises the blood glucose scale (Kovatchev et al., 1998). Each blood glucose reading is transformed using the formula $f(BG) = 1.509([ln(BG)]^{1.084} - 5.381)$ for blood glucose (BG) measured in milligrams per deciliter.

- The Poincare plot is usually employed in time series analysis. In diabetes treatment, this plot evaluates the variability between consecutive blood glucose readings. A time spacing of 1 h is typically used.

- The grading system is another graphical outcome used to evaluate the efficacy and safety of closed-loop systems and glucose controllers. The grading outcome is the quantification

of time spent in each of six grades, A–F, to describe the level of control grade. This quantification is performed in the pre-prandial and post-prandial periods (Chassin et al., 2005).

- The aggregate blood glucose represents an hourly classification of hypoglycaemia, normoglycaemia or hyperglycaemia.
- The histogram displays a tabulated frequency graph of blood glucose readings by range.

The blood glucose signal displayed in Figure 4.27 was used to perform these graphical outcomes. The results are shown in Figure 4.28.

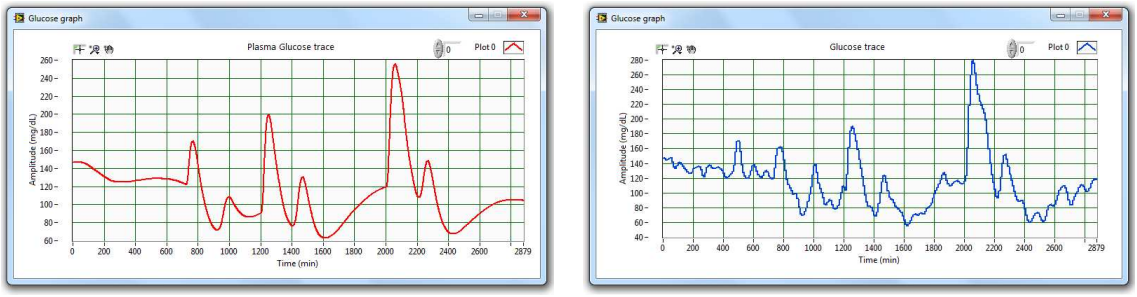


(a) (b)

Figure 4.27: Example of (a) blood glucose signal, and (b) corresponding sensor measure glucose signal.

The remaining outcomes consist of numerics, such as the low blood glucose index (LBGI) or the high blood glucose index (HBGI), which are used to evaluate variability and risk (Kovatchev et al., 1998, 2002). The blood glucose risk index is the sum of LBGI and HBGI. The standard deviation of the blood glucose rate of change is also included.

Numerical outcomes for measuring the average blood glucose and the deviation from a customised target range are also available.

## 4.4 Constructing a Simulation Scenario for Postprandial Control

A realistic and challenging simulated scenario is created to evaluate the robustness of the performance of the control algorithms introduced in this thesis. Concerns regarding the hypoglycaemic protection and its consequence on patient safety are evaluated with this scenario design.

Virtual patients of the Dalla man *et al.* model with individualised circadian variations, as previously introduced in section 4.3.3, are combined with daily sinusoidal variations of 20% amplitude with 19 h and 29 h periods of insulin sensitivity and insulin absorption, respectively. In the case of insulin sensitivity variation, the sinusoidal variation was performed using the parameter $V_{mx}$; in the case of insulin absorption, the sinusoidal variation was performed using

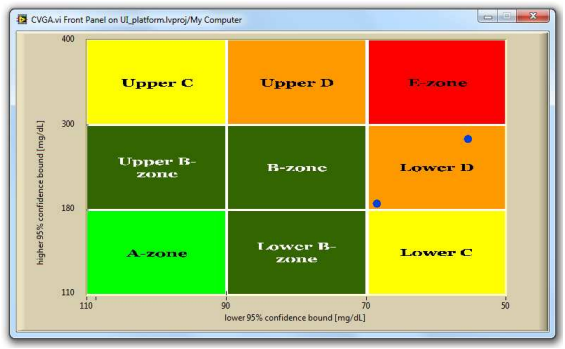


(a)

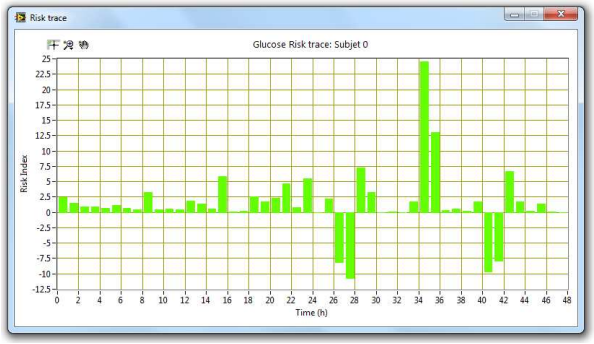


(b)

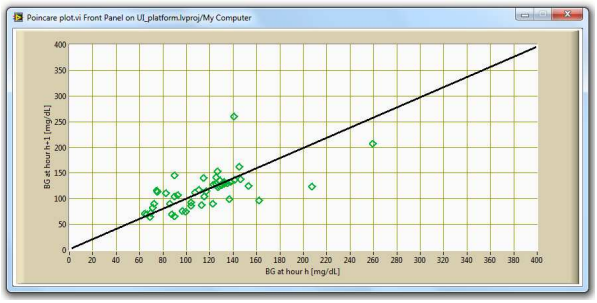


(c)

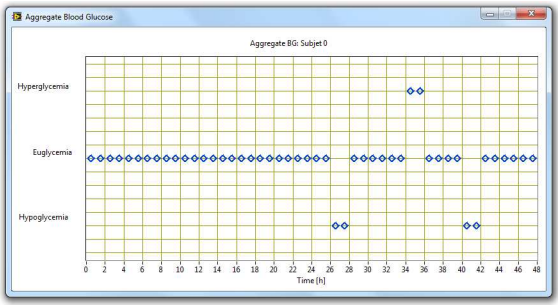


(d)

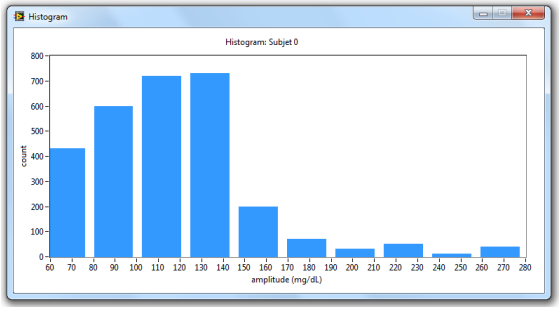


(e)

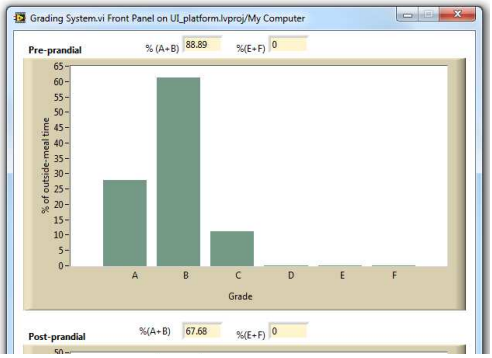


(f)

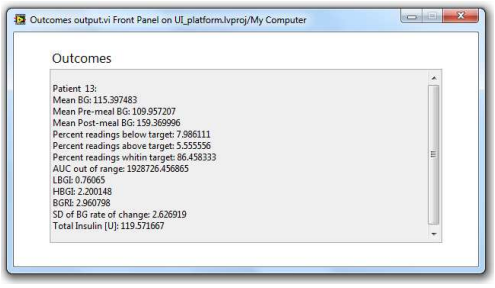


(g)

Figure 4.28: Outcomes metrics implemented in the *in silico* platform: (a) CVGA, (b) risk trace, (c) Poincare plot, (d) aggregate blood glucose, (e) histogram, (f) grading system, and (g) available numeric outcomes.

parameters $k_{a1}$, $k_{a2}$, and $k_d$.

Regarding the meal glucose, the rate of blood glucose appearance profile corresponding to six different meals from the library introduced in section 4.3.2 were selected in an 18-meal simulation trial per patient, for a total of 180 tests. The meals are approximately 60 g; this meal size is generally used in clinical trials. The nutritional composition is listed in Table 4.11, whereas their corresponding rate of blood glucose appearance profiles are shown in Figure. 4.29.

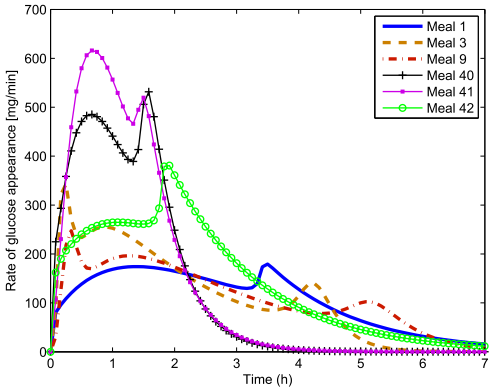


Figure 4.29: Rate of glucose appearance of mixed meals from Table 4.11.

| Meal code | $CHO$ | Fat | Protein | Fiber | Energy(kcal) |
|---|---|---|---|---|---|
| 1 | 52 | 10.5 | 14.5 | 1.7 | 300 |
| 3 | 52 | - | - | 2.6 | 240 |
| 9 | 52.5 | 10.5 | 14.5 | - | 300 |
| 40 | 62 | 17.0 | 12.0 | - | 120 |
| 41 | 68 | 8.0 | 12.0 | - | 120 |
| 42 | 69 | 12.8 | 13.1 | - | 300 |

Table 4.11: Nutritional composition of mixed meals (in grams) used for the test scenario.

The total simulation time is 28800 minutes, which corresponds to 20 days, in which the first day and the last day are used as transitory periods. A mixed meal is administered daily at 12:00; each meal is administered three times during the simulation execution but under different intra-patient variability conditions, according to the previously described sinusoidal variations. The protocol for meal intake corresponds to the meal-codes [1, 40, 9, 41, 3, 42], i.e., interleaving low and high rate of glucose appearance profiles.

## 4.5 Summary

In this chapter, a complete description of the *in silico* platform features are presented. This platform facilitates the simple and intuitive design of a broad range of realistic scenarios through customisation options in all components. The models that comprise the platform components are presented, with particular emphasis on the virtual patients and the instrumentation used in artificial pancreas development. A method for representing *in silico* a real cohort of patients

with T1D has been suggested, which can be beneficial to a process of control design intended for clinical trials. A realistic test scenario has been constructed and presented to address the challenge of control algorithms introduced in this thesis.

# Chapter 5

# Open-Loop Postprandial Control: A Set-Inversion-Based Approach

## 5.1 Introduction

This chapter presents a practical strategy designed to compute a solution in the basal-bolus space of an innovative and promising open-loop method for postprandial glycaemic control named iBolus (Rossetti et al., 2012). The objective is to optimise the computation time of the iBolus algorithm to enable integration of this bolus advisor in smart insulin pumps. This optimisation is performed by reducing the number of iterations performed with the set-inversion-based technology used in the previous non-optimised iBolus algorithm. A methodology based on the analysis of interval simulations, physiological assumptions, and search domain contractions was developed (León-Vargas et al., 2012b).

This chapter is organised as follows: First, a brief background on the mathematically guaranteed techniques (interval analysis) is used to calculate the interval simulations and the corresponding application in set-inversion problems is introduced in section of interval analysis and set inversion. Second, the section of prandial insulin delivery algorithm describes the methodology used by the non-optimal version of the iBolus algorithm. Third, the section about the optimisation method presents the target, the conditions governing the optimisation, the constraints used in the non-optimised and optimised versions of the iBolus algorithm, and the algorithm rationale about the implemented procedure. Last, the numerical results and discussion are presented to show the potential extent of the inclusion of this approach in commercial insulin infusion pumps.

## 5.2 Interval Analysis and Set Inversion

Interval analysis arose in the context of numerical analysis and the study of propagation of computational errors in finite number systems (Moore, 1966, 1979): if real numbers are substituted by compact subsets of the digital scale (intervals) which contain it, and real operators by interval operators, computations will lead to intervals that contain the actual solution, whose width is a measure of the approximation error. It is precisely this property of inclusion of the actual solution that makes interval analysis and methods derived very interesting when a mathematical guarantee is desired.

Inclusion functions are thus one of the fundamental tools in interval analysis. In the following, $[x]$ will denote a real interval, and $\underline{x}$ and $\overline{x}$ are its left and right endpoints, respectively. Interval vectors, or boxes, will be denoted in boldface, $[\mathbf{x}]$. The set of all real intervals will be denoted by $\mathbb{IR}$ and the set of $n$-dimensional boxes as $\mathbb{IR}^n$.

A formal definition follows.

*Definition 1*: Given a function $\mathbf{f} : \mathbb{R}^n \to \mathbb{R}^m$, the interval function $[\mathbf{f}] : \mathbb{IR}^n \to \mathbb{IR}^m$ is an inclusion function for $\mathbf{f}$ , if for any box $[\mathbf{x}] = [\underline{\mathbf{x}}, \overline{\mathbf{x}}] \in \mathbb{IR}^n$

$$[\mathbf{f}]([\mathbf{x}]) = [\min_{x \in [\mathbf{x}]} \mathbf{f}(\mathbf{x}), \max_{x \in [\mathbf{x}]} \mathbf{f}(\mathbf{x})].$$

The simplest way to get an inclusion function for $\mathbf{f}$ is replacing the real variable $x$ with an interval variable $[x]$ and the real arithmetic operations with corresponding interval operations. The result $[\mathbf{f}]$ is called a natural inclusion function of $\mathbf{f}$ (Moore, 1966). However, this may yield significant overestimation when multiple instances of a variable appear in the expression to evaluate (multiincidences problem). Other inclusion functions have been studied to reduce this problem like centered forms or Taylor expansion forms. See for instance Moore (1966, 1979); Alefeld and Herzberger (1983); Jaulin et al. (2001) for more details on this topic.

Currently, interval analysis is a mature technology that has been successfully applied in fields aside numerical analysis such as robotics, control, computer graphics, economy, global optimization, and fault detection, among others (Jaulin et al., 2001).

An important application of interval analysis is the solution of set inversion problems. Let $\mathbb{X} \subseteq \mathbb{R}^n$ and $\mathbb{Y} \subseteq \mathbb{R}^m$ be an input and output space, respectively. Given a set $Y \subseteq \mathbb{Y}$ and a map $\mathbf{f} : \mathbb{X} \to \mathbb{Y}$, the set $X := \mathbf{x} \in \mathbb{X} | \mathbf{f}(\mathbf{x}) \in Y$ is sought. The set $Y$ is usually defined through constraints on the output space. The Set Inversion via Interval Analysis (SIVIA) algorithm (Jaulin et al., 2001) makes use of a branch-and-bound technique together with interval analysis to get an approximation of the solution set $X$. This approximation is done in terms of subpavings (collection of boxes of the appropriate dimension with nonoverlapping interiors). An inner and outer subpaving, which will be denoted as $[X]_i$ and $[X]_o$ , respectively, are built so that $[X]_i \subseteq X \subseteq [X]_o$ . Hence, it is guaranteed that $[X]_i$ will contain only solutions while the complementary set of $[X]_o$, denoted as $\overline{[X]_o}$ , will contain only nonsolutions (see Figure 5.1).

Some definitions of interest for the SIVIA algorithm are below presented.

*Definition 2*: The width of a box $[\mathbf{x}] = [\underline{\mathbf{x}}, \overline{\mathbf{x}}] \in \mathbb{IR}^n$ is $w([\mathbf{x}]) := max_{i \in \{1,\dots,n\}}(\overline{x}_i - \underline{x}_i)$.

*Definition 3*: The midpoint of a box $[\mathbf{x}] = [\underline{\mathbf{x}}, \overline{\mathbf{x}}] \in \mathbb{IR}^n$ is $m([\mathbf{x}]) := \dfrac{(\underline{x}_i + \overline{x}_i)}{2}$.

*Definition 4*: The left and right children of a box $[\mathbf{x}] = [\underline{\mathbf{x}}, \overline{\mathbf{x}}] \in \mathbb{IR}^n$ are

$$L([\mathbf{x}]) := [\underline{x}_1, \overline{x}_1] \times \cdots \times [\underline{x_j}, m([x_j])] \times \cdots \times [\underline{x_n}, \overline{x_n}]$$
$$R([\mathbf{x}]) := [\underline{x}_1, \overline{x}_1] \times \cdots \times [m([x_j]), \overline{x_j}] \times \cdots \times [\underline{x_n}, \overline{x_n}]$$

where $j$ is the first component of $[\mathbf{x}]$ with maximum width, that is, $j = min\{i | w([x_i]) = w([\mathbf{x}])\}$.

*SIVIA algorithm* (Jaulin et al., 2001). Let $X$ be the solution set sought and $[X]_i$ and $[X]_o$ be two subpavings corresponding to inner and outer approximations of $X$ as defined earlier. Let

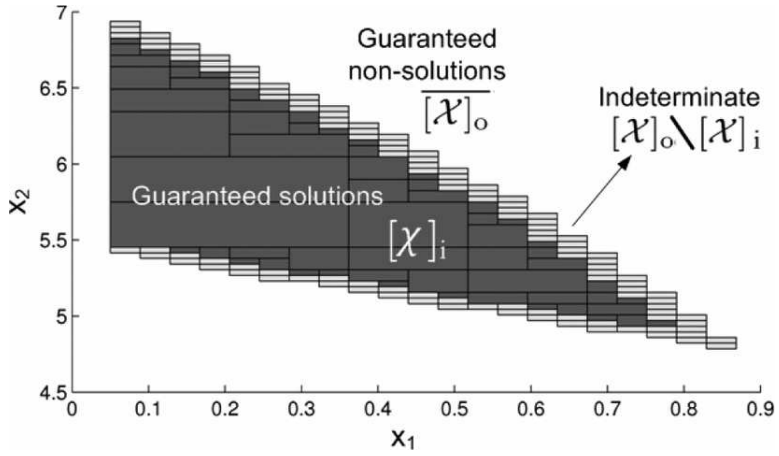


Figure 5.1: Plot that illustrates the concept of inner and outer subpaving. The dark rectangles represent the inner subpaving and guarantee the fulfillment of the constraints. The outer subpaving is made up of both the dark and the light rectangles. Its complementary set (in white) is guaranteed to contain only nonsolutions that violate some of the constraints. Results in the boundary (light rectangles) are unknown a priori.

$[t] : \mathbb{IR}^n \to \mathbb{IB}$ be a test interval function from the set of $n$-dimensional interval vectors (box in the input space) to the set of interval booleans, $\mathbb{IB} = 0, 1, [0, 1]$ (where 0 stands for false, 1 for true, and [0, 1] for indeterminate). Finally, let $[\mathbf{x}] \in \mathbb{IR}^n$ be an initial box in the input space and $\epsilon$ be a positive precision factor that can be chosen arbitrarily low. The SIVIA algorithm is as follows:

**SIVIA** $(in : [t], [\mathbf{x}], \epsilon, out : [X]_i, [X]_o)$

*if* $[t]([\mathbf{x}]) = 0$, return;
*if* $[t]([\mathbf{x}]) = 1$, then $\{[X]_i := [X]_i \cup [\mathbf{x}]; [X]_o := [X]_o \cup [\mathbf{x}]; return; \}$;
*if* $w([\mathbf{x}]) < \epsilon$, then $\{[X]_o := [X]_o \cup [\mathbf{x}]; return; \}$;
SIVIA$([t], L([\mathbf{x}]), \epsilon, [X]_i, [X]_o)$;
SIVIA$([t], R([\mathbf{x}]), \epsilon, [X]_i, [X]_o)$;

The inner subpaving will thus contains the boxes classified as true, while the outer subpaving contains the false and indeterminate boxes (of width smaller than the tolerance defined). Not small enough indeterminate boxes will be splitted in two subboxes by the midpoint of its largest dimension and the procedure repeated.

## 5.3 Prandial Insulin Delivery Algorithm

Set-Inversion-Based (SIB) prandial insulin delivery is a control strategy implementing the SIVIA algorithm to meet a set of predefined constraints. This is done through a recursive search of combinations of three components: namely, the bolus dose, the postprandial basal dose, and the time for basal-to-baseline restoration (the postprandial basal duration (PPBD)) (Revert et al., 2011).

SIB algorithm functionality can be summarized as follows. Given an interval vector (or box) of inputs [**x**], comprising the elements of bolus dose, basal dose, and PPBD, the SIB algorithm determines whether:

1. The full range of therapies contained in [**x**] meet the constraints.
2. None of them meet the constraints.
3. Some of them meet the constraints.

For the third case, the corresponding input box is partitioned and the resulting boxes are re-evaluated in an iterative way by the algorithm until getting a box that meets the constraints.

At each step in the algorithm, a patient's glucose-insulin model is used to predict the postprandial glycemia corresponding to the therapies contained in [**x**], using interval simulation techniques (Calm et al., 2011). After comparing the predicted postprandial glycemia with the constraint set, a 3-D plot of boxes meeting these constraints is obtained (see Figure 5.2(a)). A 2-D basal-bolus projection is then useful for showing the basal-bolus combinations space that will lead to a good performance for a particular patient and meal (see Figure 5.2(b)).

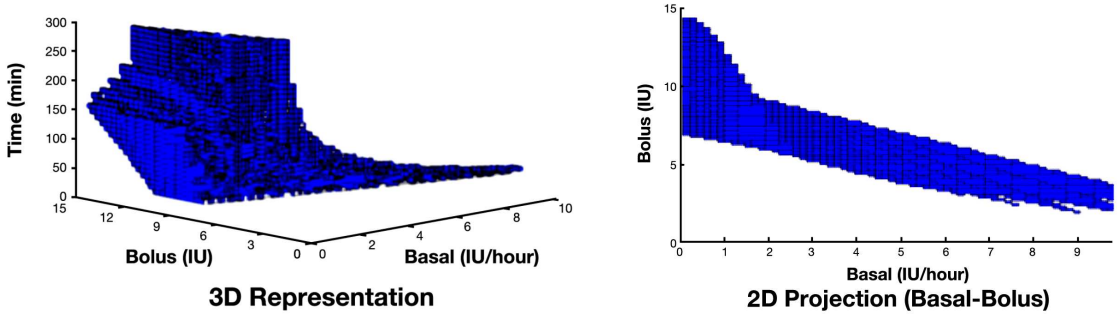


(a) (b)

Figure 5.2: Plot representing: (a) three-dimensional (basal dose, bolus dose, and PPBD) feasible set and (b) its corresponding basal-bolus two-dimensional projection.

It should be noted that, even when meeting all constraints, the postprandial behavior associated with each possible basal-bolus combination inside the paving of solutions is different.

## 5.4 Optimization Method

According to the results shown in Revert et al. (2010), the basal-bolus combination of interest within the paving of solutions corresponds to the box containing the maximum value for bolus dose as it successfully meets the constraints imposed, and accordingly, it was established as the optimization aim in this work.

The input space $\mathbb{X}$, as in the non-optimized version, corresponds to the standard capabilities found in commercial insulin pumps: 0–40 insulin units (IU) for the bolus dose; 0–10 IU/h for the basal dose; and 0–300 min for the PPBD. However, unlike the branch and bound method used by the SIVIA algorithm, in the optimization method the basal-bolus plane of the input space

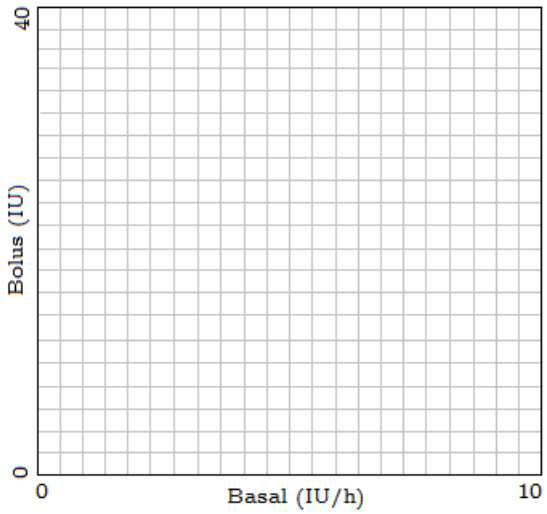


Figure 5.3: Basal-bolus space partitioned in a grid for the optimization method.

is partitioned into a grid of fixed granularity (see Figure 5.3), where the size of the basal-bolus components corresponds to the minimum width used in the non-optimized version of the SIB strategy. This size covers the range of inaccuracy present in insulin pumps (Zisser et al., 2010a). The PPBD component is treated as a single-value (real value) throughout the optimization process, and only at the last stage an upper and lower limit is computed to produce an interval output.

In essence, the optimization algorithm focuses on moving a box, $[\mathbf{x}]$, of fixed size from an starting point and cross the grid following a smart pathway to reach the target solution in few steps.

The set of constraints $\mathcal{C}$ used here correspond to those used by Revert and coauthors:

- 2 h postprandial glucose value below 140 mg/dl in a 5 h time horizon
- A maximum glucose slope of 10 mg/dl/h starting 4 h after the meal in order to avoid the late-term hyperglycemia.
- Hypoglycemic threshold of 70 mg/dl
- A 5 h postprandial glucose value above 90 mg/dl in order to avoid hypoglycemia.

The dynamic relationship between glucose and insulin was included implicitly in the algorithm proposed through the following physiological assumption: the more insulin delivered, the more blood sugar is lowered in the patient. Such physiological knowledge is useful for ruling out search areas according to the optimization aim.

Interval simulations (Calm et al., 2011), characterized by reflecting the collection of postprandial glucose profiles predicted for a set of therapies, were used. These interval simulations use a customized patient model which takes account different sources of uncertainty. The glucose-insulin model used in this optimization method was the same as that used in the non-optimized version. Model identification and validation was carried out from 6-day domiciliary data using a

continuous glucose monitor. For three days, the patient advanced or delayed bolus infusion with respect to mealtime at lunch according to an optimal experiment design to maximize sensitivity of identified parameters. Three additional days following the standard treatment were used for model validation. A detailed description about the model and its identification can be found in Laguna et al. (2010).

### 5.4.1 Algorithm Rationale

The optimization task was divided into two main stages: first finding the box containing the maximum bolus value that meets the hypoglycemia and hyperglycemia constraints (including the 5 h glucose above 90 mg/dl) and then verifying the slope constraints.

The optimization procedure is described by using a graphical example as follows. A typical search path in the basal-bolus plane is shown in Figure 5.4. In this figure, the blue squares represent "checkpoint" input boxes at algorithm steps where a certain condition is reached. Because we are seeking a solution with a maximum bolus value, the starting point (initial box) "$[\mathbf{x}_0]$" always corresponded to the maximum bolus dose possible and the minimum basal dose according to insulin pump capabilities. At this point, the hypoglycemia condition was always obtained because of the extreme bolus value (see Figure 5.5).

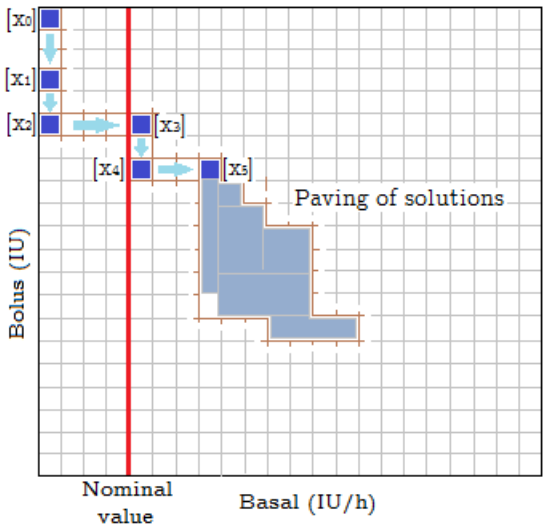


Figure 5.4: Smart search pathway used by the optimization algorithm. If the constraints are met by a basal value less than the nominal value, the solution may be found in checkpoints "$[\mathbf{x}_1]$" or "$[\mathbf{x}_2]$"; otherwise, it will be in "$[\mathbf{x}_4]$", "$[\mathbf{x}_5]$", or beyond.

To achieve a non-hypoglycemia condition, i.e., to reach checkpoint box "$[\mathbf{x}_1]$", a bolus decrement is required. In this procedure, the basal component was fixed at the minimum (0 IU/h) and the PPBD component to the maximum (300 min) (i.e., the minimum basal infusion, because the nominal basal dose $>$ 0 IU/h) to perform a domain-space contraction in the bolus component (see Figure 5.4) until the hypoglycemia constraint was met.

After reaching "$[\mathbf{x}_1]$", the hyperglycemia constraint is checked. If it is met, the algorithm verified that the slope constraints are met. If not, a change in PPBD can be conducted.

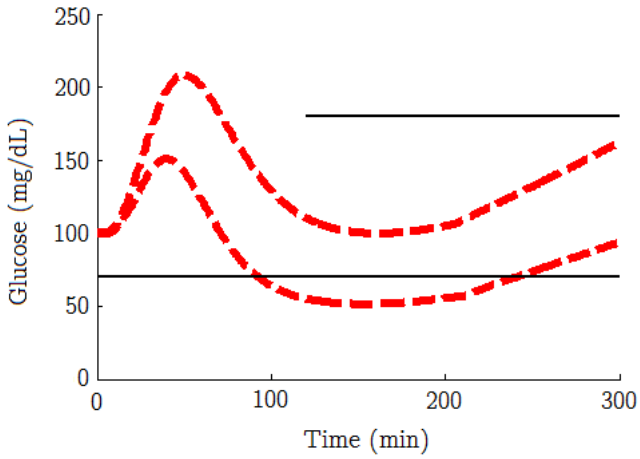


Figure 5.5: Typical interval glucose response when using the maximum bolus limit. The hypoglycemia constraint is always violated at the initial box "[$\mathbf{x}_0$]".

When the box is below the nominal basal dose, a longer PPBD implies a smaller basal infusion. Conversely, when the box is above the nominal basal dose, a longer PPBD implies a larger basal infusion. Figure 5.6 shows this behavior.

Two parameters, tHyper and tHypo, were used to discover if a PPBD variation could help meet the hyperglycemia constraint. When the box is below the nominal basal tHyper corresponds to the maximum time at which the hyperglycemia condition is no longer true, and tHypo corresponds to the minimum time at which the hypoglycemia condition is no longer true (see Figure 5.6(a)). In case the box is above the nominal basal, tHyper corresponds to the minimum time at which the hyperglycemia condition is no longer true and tHypo corresponds to the maximum time at which the hypo-glycemia condition is no longer true (see Figure 5.6(b)). Hence hypoglycemia and hyperglycemia constraints will be met simultaneously if

(1) tHyper $\geq$ PPBD $\geq$ tHypo, for below nominal-basal boxes or

(2) tHyper $\leq$ PPBD $\leq$ tHypo for above nominal-basal boxes.

Therefore, if condition (1) is not valid for the box "[$\mathbf{x}_1$]", it is still possible to modify the bolus value to affect the dynamics of tHyper and tHypo.

The next checkpoint box, "[$\mathbf{x}_2$]", is the bolus value when tHyper or tHypo is zero. If tHyper is zero for "[$\mathbf{x}_2$]", (1) is not fulfilled and a basal/bolus dose is not found. On the other hand, if tHypo is zero for "[$\mathbf{x}_2$]", (1) is fulfilled, and therefore it is a solution. Typical dynamics for tHyper and tHypo in reaching "[$\mathbf{x}_2$]" are shown graphically in Figure 5. Such dynamics are quite different. The trends can be explained based on the bolus reduction effect, whose action is mainly reflected on the hypoglycemia rather than the hyperglycemia condition. This behavior can also be treated as a "slopes" problem. When a bolus reduction occurs, tHypo starts with a slope "s0" and tHyper with a slope "s1". Both trends finalize with the same slope "sf" when reaching "[$\mathbf{x}_2$]" (see Figure 5.7). Therefore, (1) will or will not be fulfilled for "[$\mathbf{x}_2$]" according

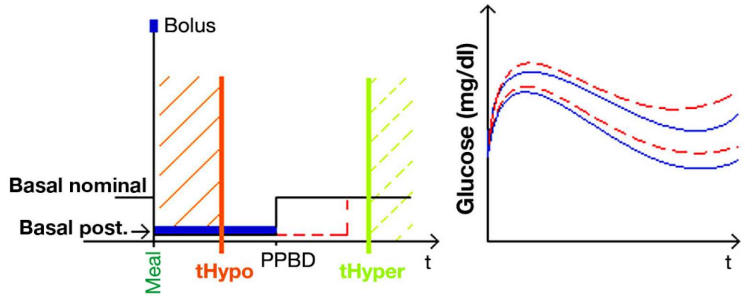


(a)

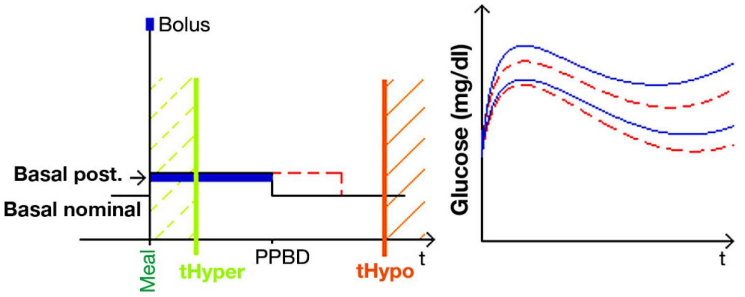


(b)

Figure 5.6: Insulin profiles (left) and their corresponding glucose responses (right) for two cases. (a) When a box is below the nominal basal, a shorter PPBD value produces a lower glucose response (blue solid curve) than a longer PPBD value (red dashed curve). (b) When a box is above the nominal basal, those PPBD values imply the opposite action. The dashed green lines area and the solid orange lines area indicates the values of PPBD at which hyperglycemia or hypoglycemia conditions are obtained, respectively.

to the distance between tHyper and tHypo for box "$[\mathbf{x}_1]$".

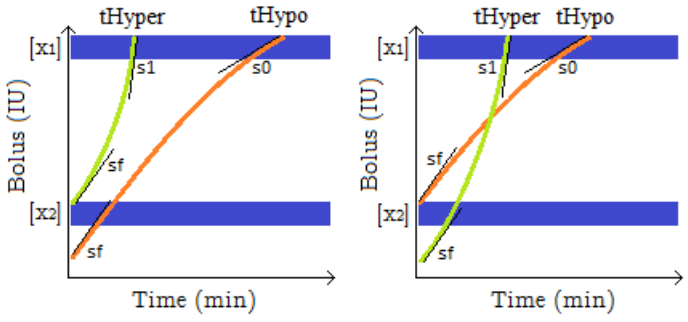


Figure 5.7: tHyper and tHypo dynamics observed in a bolus-PPBD plane. For some cases, no bolus reduction will achieve tHyper $\geq$ tHypo (left); for other cases, it can be achieved (right).

It is worth mentioning that basal value may be increased according to the patient needs, but there is a limit on how far the basal dose may be decreased in order to increase the bolus dose sufficiently to cover large carbohydrate meals. Up to this checkpoint, the most likely situation where no solution would be found will be for large carbohydrate intakes and foods with high

glycemic index.

If, when reaching "[$\mathbf{x}_2$]", (1) is not fulfilled, a further decrement in the bolus value will not be useful unless a new checkpoint with a different basal value is considered.

As (1) is not fulfilled for "[$\mathbf{x}_2$]", no value below the nominal basal will be part of the solution. Indirectly, all basal insulin values between the minimum and the nominal have been applied through the previous PPBD variation. Therefore, the next checkpoint box "[$\mathbf{x}_3$]" corresponds to the same bolus, but using the nominal basal value. Here, PPBD is again set at 300 min.

However, a value equal to the nominal basal implies a new and lower bolus value to meet the hypoglycemia constraint. This procedure corresponds to checkpoint box "[$\mathbf{x}_4$]".

In later checkpoints (e.g., "[$\mathbf{x}_4$]" and "[$\mathbf{x}_5$]"), iterative changes in bolus insulin to meet the hypoglycemia constraint followed by changes in basal insulin to meet the hyperglycemia constraint are performed until both constraints are met simultaneously. In this process, some changes in PPBD will be performed.

After the hypoglycemia and hyperglycemia constraints are met, PPBD should be changed to meet the slope constraints depending on the current basal value and on which slope was violated (upper or lower).

If this action is insufficient, with the slope violated being the lower slope, the algorithm will finish with no solution and a new process will need to be started using constraints more relaxed. However, if the upper slope is violated, a final option for improving the insulin action is to reduce the bolus component in an iterative way while the basal component is maximized. The flowchart of the optimized version of the SIB strategy is summarized in Figure 6.

The flowchart of the optimized version of the iBolus algorithm is summarized in Figure 5.8.

## 5.5 Numerical Results

To compare the optimization performance, responses of the non-optimized processing method (SIVIA algorithm) obtained for six real patients with T1D were used. The same patient model was used both in the optimized and non-optimized version. Continuous glucose monitoring data were used to obtain the respective patient model. Demographic characteristics of the subjects were as follows: six subjects (three males), age 41.8 ± 7.3 years, diabetes duration 20 ± 10 years, hemoglobin A1c 8.0% ± 0.6%, and body weight 68.7 ± 10 kg.

The comparison was carried out on a workstation Dell Precision T3500, Intel® Xeon Processor of 2.67 GHz and RAM memory of 4096 MB.

Results are presented in Table 5.1. As comparison metrics, the number of iterations and the total computation time was used (see Table 1). Iteration counting was based on how many interval simulations were performed during the corresponding algorithm steps.

Regarding the final solutions given by each strategy, once the solution box is found, the

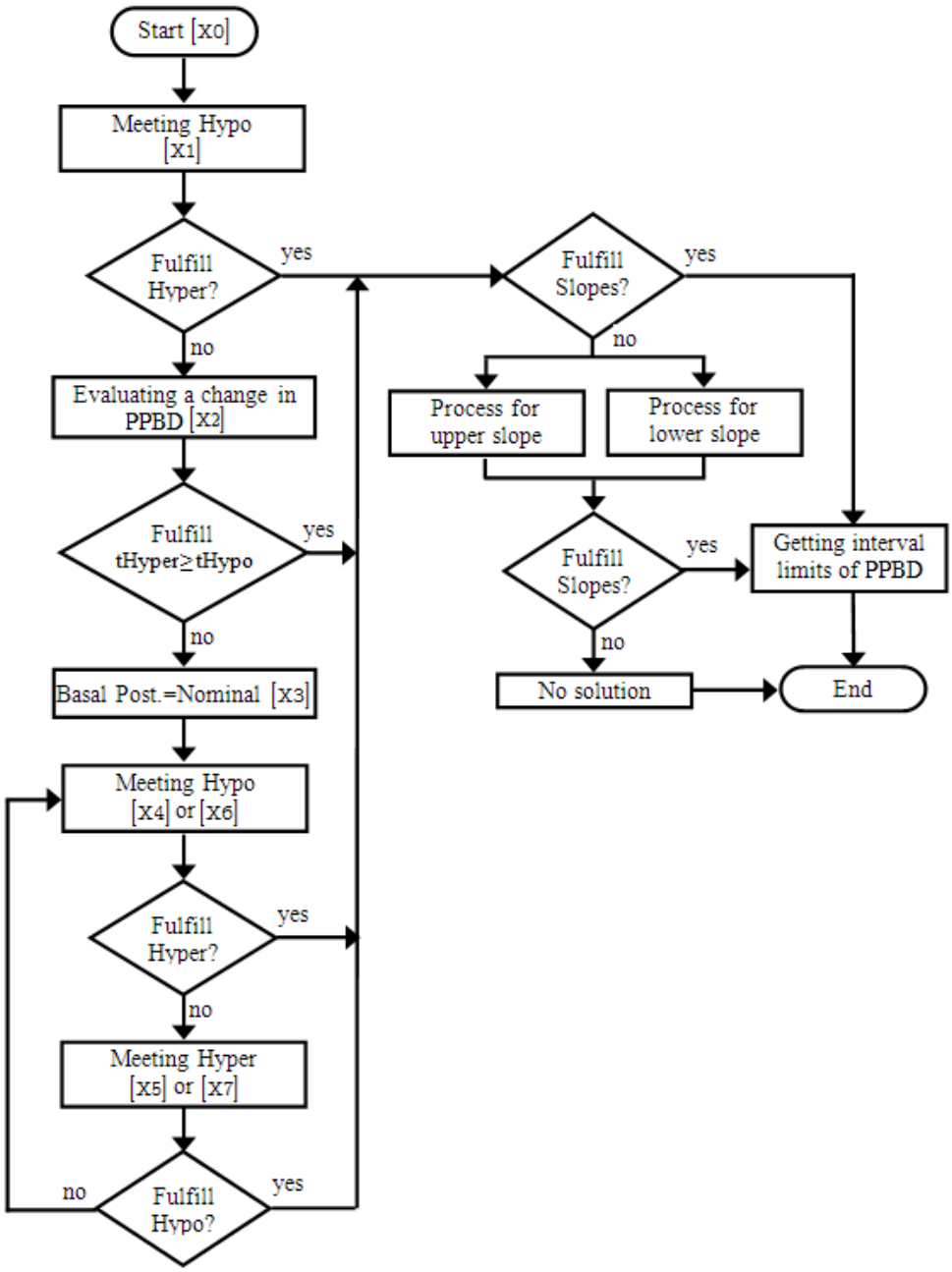


Figure 5.8: Flowchart of the optimized version of the iBolus algorithm. Hypo, hypoglycemia constraint; Hyper, hyperglycemia constraint; PPBD, postprandial basal duration.

insulin to be infused corresponds to the middle point $m([\mathbf{x}])$ of each component range (center of the box). The results show that the recommended basal/bolus doses found with this faster SIB method presented only minor differences from those of the non-optimized SIB strategy. Table 5.2 presents an statistical comparison about this issue.

LabVIEW software was used to estimate the computation time of the optimized iBolus algorithm when it is running at a very low processing rate. The results show that the mean of iterations for the optimized version requires approximately 3.59 s at 20 MHz processing.

| Patient | Iterations for non-optimized iBolus | Time (s) non-optimized iBolus | Iterations for optimized iBolus | Time (s) optimized iBolus |
|---|---|---|---|---|
| 01-1 | 277675 | 3098.38 | 30 | 0.406 |
| 01- 2 | 364653 | 4127.28 | 25 | 0.328 |
| 01- 3 | 333043 | 3266.38 | 34 | 0.468 |
| 01- 4 | 55735 | 540.04 | 67 | 0.889 |
| 02- 1 | 155781 | 1556.45 | 123 | 1.623 |
| 02- 2 | 277279 | 2833.72 | 69 | 0.936 |
| 02- 3 | 112321 | 1150.76 | 93 | 1.154 |
| 02- 4 | 587443 | 5946.55 | 168 | 2.153 |
| 03- 1 | 151707 | 1486.5 | 25 | 0.343 |
| 03- 2 | 711113 | 7133.46 | 24 | 0.328 |
| 04- 1 | 119139 | 1187.17 | 34 | 0.452 |
| 04- 2 | 274975 | 2735.84 | 33 | 0.452 |
| 04- 3 | 125455 | 1242.06 | 37 | 0.514 |
| 04- 4 | 240843 | 2384.65 | 62 | 0.842 |
| 05- 1 | 58335 | 601.87 | 46 | 0.593 |
| 05- 2 | 72971 | 745.05 | 96 | 1.217 |
| 05- 3 | 36977 | 379.51 | 44 | 0.577 |
| 05- 4 | 32263 | 368.36 | 75 | 0.967 |
| 06- 1 | 332203 | 3330.83 | 88 | 1.124 |
| 06- 2 | 992627 | 9929.81 | 90 | 1.154 |
| 06- 3 | 38929 | 384.01 | 90 | 1.108 |
| 06- 4 | 81337 | 831.82 | 73 | 0.952 |
| Mean | 246945.6 | 2617.7 | 64.8 | 0.844 |

Table 5.1: Performance Comparison between the Non- and Optimized iBolus algorithm. For each patient, several tests were conducted using different meal sizes.

| Error | Basal comparison (IU/h) | Bolus comparison (IU) | PPBD comparison (min) |
|---|---|---|---|
| *MAE±SD | 0.05±0.06 | 0.17±0.14 | 12.3±8.8 |
| 90th Percentile | 0.12 | 0.43 | 20.56 |
| Median | 0.028 | 0.13 | 8.87 |

*MAE stands for mean absolute error.

Table 5.2: Statistical comparison of the difference between solutions given from optimized and the non-optimized iBolus algorithm.

According to the Medical Solutions Guide (Maxim Integrated, 2011), a similar processing power is used in current smart insulin pumps.

## 5.6 Discussion

Parameter values of the patient model were set using data obtained from an ongoing clinical study about the performance of the iBolus algorithm in real patients (Rossetti et al., 2012). An

optimization strategy was implemented to compare its solutions with those of the non-optimized version. We found that the optimization version obtains similar solutions to the non-optimized iBolus, but in 0.032% of the time. However, it must be said that the baseline for the comparison time was the complete space of solutions of the non-optimized strategy. The new iBolus algorithm does not require the computation of such a global grid; therefore, a much lower computation time was expected.

In order to put the method into context, the accuracy and efficiency of the optimized version was compared against a Monte Carlo approach. A standard Monte Carlo test was developed with 1% and 5% of all possible combinations of basal, bolus, and PPBD at random. The best solution in each test was selected to calculate the mean absolute error with respect to the solution obtained using the non-optimized iBolus version (see Table 5.3). An important difference in accuracy was obtained compared with the one achieved by the optimized version (see Table 5.2). Moreover, given a total number of boxes of 320000 owing to the minimum size used, 1% and 5% of Monte Carlo correspond to 3200 and 16000 simulations, respectively. This means 50 and 250 times the number of simulations required by the optimized iBolus version.

| Monte Carlo test | Basal comparison (IU/h) | Bolus comparison (IU) | PPBD comparison (min) |
|---|---|---|---|
| MAE±SD for 1% | 0.31±0.3 | 1.03±0.6 | 53.08±46.3 |
| MAE±SD for 5% | 0.15±0.14 | 0.33±0.25 | 27.23±30 |

Table 5.3: Mean Absolute Error using best solution of Monte-Carlo technique for 1% and 5% of all possible with respect to solution of non-optimized iBolus algorithm.

The inclusion of physiological knowledge in the optimization strategy enables development of efficient search pathways to replace methods based on extensive search algorithms, where each possible combination is tested, whatever its physiological effects.

We acknowledge that this computing optimization is an ad hoc approach designed for an specific bolus insulin advisor. It must be pointed out that embedding this algorithm into an insulin pump may require modifications of the bolus-on-board computation as currently done. Although a temporal basal decrement at mealtime does not contribute to bolus on board, basal increments above baseline may be considered as combo boluses. In this case, the basal excess should compute as bolus on board.

It is worth noting that temporal basal decrements are related to super boluses as introduced by Walsh and Roberts (Walsh and Roberts, 2006). However, in this case, no constraints on total insulin administered exist. The algorithm automatically computes the required bolus dose and basal decrement (and for how long) to fulfill constraints on postprandial glucose based on the amount of carbohydrate intake and the prediction of the patient's behavior (considering intra-patient variability). Thus the algorithm may present an increment of total insulin dose if a patient changes his eating. Carbohydrate counting is used as input to the model, but not for a direct computation of the bolus size. An additional advantage of the method is that carbohydrate estimation error, as commonly done by the patients, can be naturally considered by the method as intervals in the meal intake.

As a limitation, the method relies on a mathematical model including meal absorption. Current models of carbohydrate digestion and absorption are limited due to the clinical data used for its development and may be representative of only a particular type of meal. Although variability in glucose absorption can be included in this methodology, more research is needed for the characterization of absorption profiles for different groups of meals.

In conclusion, a computationally efficient method for finding the maximum bolus-insulin solution of the iBolus algorithm using an smart search pathway has been presented and tested. The results indicate that an embedded version within modern insulin pumps is now feasible. Clinical studies are needed for a validation of the clinical efficiency of the method.

## 5.7 Summary

In this chapter, the theoretical background about interval analysis and set inversion are addressed. Those concepts are implemented in the new bolus advisor named iBolus using the set inversion via interval analysis (SIVIA) algorithm, which has presented acceptable results for postprandial glycaemic control. The optimisation method of the iBolus algorithm included in this chapter was designed to facilitate integration of this bolus advisor into modern insulin pumps. The results indicate that no significant differences with respect to the non-optimised version were found. In addition, simulation tests have proved that the computational performance of this new control algorithm is feasible for modern insulin pumps during the postprandial period.

# Chapter 6

# Closed-Loop Postprandial Control: Design and In silico Validation

## 6.1 Introduction

In this chapter, the problem of postprandial blood glucose control for T1D patients is treated using closed-loop control algorithms implementing insulin-on-board ($IOB$) constraints. The objective is to reduce hypoglycaemic events, which are usually presented as a result of overcorrection on the glucose-insulin system, in which a previous insulin administration is not considered. This reduction is mandatory, especially in black-box model-based control strategies, as detailed information about a patient's internal behaviour is not required. As mentioned previously in Chapter 3, this problem has been addressed for a PID controller by incorporating a term proportional to the expected plasma insulin level that inhibits the PID output or in the case of grey-box model-based control as model-predictive, $IOB$ adaptation is introduced into the control move calculations to constrain insulin delivery. These solutions are proven to be effective in reducing the risk of hypoglycaemia. Certain formulated approaches are not robust in the uncertainty of the glucose-insulin system, whereas other approaches are dependent on measurements of blood glucose or meal size, which may be susceptible to inaccuracies.

The formulation of a control scheme that can be intuitively understood and that simply and practically resolves these problems is a desirable contribution to postprandial blood glucose control. In this research, sliding mode control based techniques are used. This methodology enables the systematic inclusion of explicit constraints as it relies on the definition of a compensation loop, which is added to the control scheme to reduce adverse effects. The control schemes with sliding mode control addresses many constrained control problems regarding manipulated (input) and controlled (output) variables, as well as internal state limitations. The problem of overcorrection in postprandial control is addressed in this thesis by including bounds for the insulin-on-board signal. By taking an estimated $IOB$ value and conditioning a suitable variable structure, the maximum insulin delivery that is compatible with the $IOB$ safety constraint can be determined (León-Vargas et al., 2013b).

A model used to estimate the $IOB$ value is presented in the first part of this chapter. Subsequently, the new hybrid adaptive PD controller based on sliding mode control techniques is described. In this control scheme, the controller gain was used as the variable structure to fulfill the $IOB$ safety constraint. A practical methodology, which is based on clinical tests and validated *in silico*, is proposed here to determine an effective bound for the $IOB$ value.

This control scheme is compared with similar approaches to demonstrate the attractive features and the performance achieved with this new strategy. In the last part of this chapter, a new safety scheme designed with the sliding mode reference conditioning technology for reducing the risk of hypoglycaemia, especially in the postprandial period, was implemented and applied to several control approaches to evaluate its effect on behaviour, performance, and robustness under realistic test conditions. A method for optimal tuning, which demonstrates the potential offered by this safety scheme after inclusion in several glucose controllers, was also addressed (León-Vargas et al., 2013c).

## 6.2 Insulin-on-Board

The insulin-on-board can be defined as the amount of administered insulin that is still active in the body. In an attempt to reduce hypoglycemia events, some smart pumps estimate the $IOB$ to correct the boluses in order to prevent from excessive insulin stacking, particularly when boluses are given close together. Each patient exhibits its own insulin activity dynamics, which is usually characterized by the duration of insulin action (DIA), a parameter that clinicians are used to tune when setting up insulin pumps. A method to calculate the patient DIA is detailed in Walsh and Roberts (2006), and the test addressed is summarized as follows:

> The test begins with a high blood sugar (in range of hyperglycemia) and not much bolus on board acting. An accurate correction bolus and a correct DIA will return a high blood sugar to target by the end of the duration time period with no excess lowering of the blood sugar during the 2 hours beyond this time. This shows the speed of the insulin and the true patient DIA. However, two things may happen if it is not achieved:
>
> - If a low occurs before the end of patient DIA, the correction factor number is probably too small, resulting in a correction bolus that is too large (or the basal rate may be too high).
> - If a low occurs after the end of patient DIA, either the duration is too short (usually at least 4.5 to 6 hours is appropriate) or the basal rate may be too high and needs retesting. It is recommended to test the basal rate first to ensure it is accurate before testing the correction bolus.

Thus, the mentioned smart pumps estimate the actual $IOB$ from a set of time decay curves parameterized by DIA. The shape of the curves used by the pumps depends on the manufacturer and the type of insulin, but they are often linear function of time.

### 6.2.1 Estimation of Insulin-on-Board

Here, the insulin activity is represented by a two-compartment dynamical model based on Wilinska et al. (2005):

$$\begin{aligned} \frac{dC_1}{dt}(t) &= u(t) - K_{DIA}C_1(t) \\ \frac{dC_2}{dt}(t) &= K_{DIA}(C_1(t) - C_2(t)) \\ IOB(t) &= C_1(t) + C_2(t) \end{aligned} \tag{6.1}$$

where $C_1$ and $C_2$ are the two compartments and $u(t)$ is the insulin dose. The constant $K_{DIA}$ is tuned for each patient so as model (6.1) replicates its corresponding DIA. Because the way $K_{DIA}$ is calculated, (6.1) encompasses both the kinetics and dynamics of the insulin action. Fig. 6.1 shows the insulin activity curves obtained with model (6.1) for typical DIA values, while Table 6.1 shows the corresponding values of $K_{DIA}$ for several DIA values.

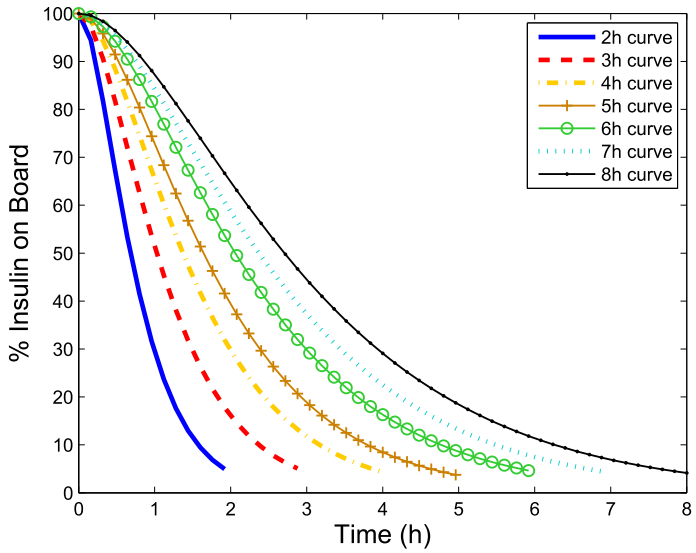


Figure 6.1: Estimated time profiles of insulin activity parameterized by DIA.

| $DIA$ (h) | 2 | 2.5 | 3 | 3.5 | 4 | 4.5 | 5 | 5.5 | 6 | 6.5 | 7 | 7.5 | 8 |
|---|---|---|---|---|---|---|---|---|---|---|---|---|---|
| $K_{DIA} \times 10^{-3}$ | 39 | 31.5 | 26 | 22.1 | 19.5 | 17.5 | 16.3 | 14.7 | 13 | 12.2 | 11.3 | 10.6 | 9.9 |

Table 6.1: IOB model parameter $K_{DIA}$ ($\text{min}^{-1}$) for different durations of insulin action.

## 6.3 Hybrid Adaptive PD Controller

An artificial pancreas for ambulatory purposes has to deal with the delays inherent to the subcutaneous route, the carbohydrate intakes, the metabolic changes, the glucose sensor errors and noise, and the insulin pump constraints. A hybrid adaptive PD controller is proposed in this thesis to overcome these problems. The control scheme adopted is depicted in Fig. 6.2. The

controller presents a hybrid structure combining open-loop and feedback control.

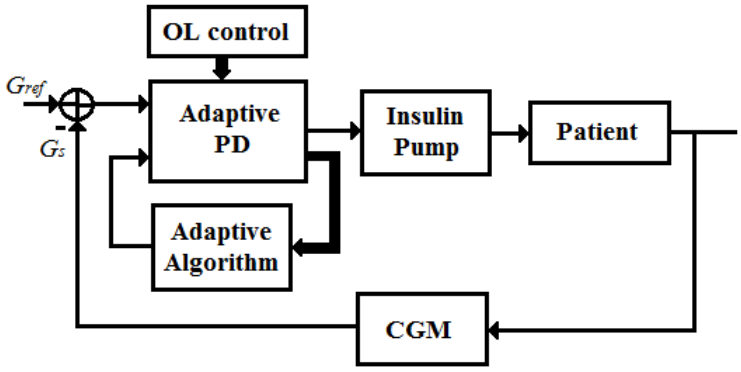


Figure 6.2: Hybrid control scheme for glucose regulation.

The basis for the feedback control is a PID-like controller. The controller gain and derivative time constant can be designed as usual. However, the integral action is replaced with an open-loop basal insulin profile. This integral action can eventually be switched on during the night. The main reason to remove the integral term during the postprandial period is that the control objective during this period is not to closely regulate glycemia at a given set-point but to reject a disturbance (the meal) without undershoots (hypoglycemia). An integral action strong enough, accumulating the error during the early postprandial period, will inevitable increase the risk of an overshoot in the glucose level unless a smoothed trajectory be implemented. On the other hand, a high integral time devised to reduce significantly the risk of late hypoglycemia is not capable of tracking the circadian variations in the insulin sensitivity. Note that this is not a limitation of the proposed algorithm but is inherent to the demanding realistic testing scenario used to evaluate the controller performance, which is described in section 4.4.

### 6.3.1 Control Structure

Fig. 6.3 shows the structure of the proposed hybrid controller. The closed-loop control output $u_{pd}$, which contains a term proportional to the blood glucose error $G_{ref} - G_s$ and a derivative term, is added to the basal insulin $I_{basal}$ provided by the open-loop control. This signal is multiplied by the time-varying adaptive gain $\gamma$, which takes values in the set $0 \leq \gamma \leq 1$, to give $u_\gamma$. Finally, the insulin dose administered to the patient $u_I$ is the sum of the bolus ($I_{bolus}$) and the control signal $u_\gamma$.

Note that the adaptation gain $\gamma$ not only affects the feedback action but also the basal insulin dose. The equations describing the hybrid control action are:

$$\begin{aligned} u_{pd} &= -K_p \left( (G_{ref} - G_s) - T_d \frac{dG_s}{dt} \right) \\ u_c &= u_{pd} + I_{basal} \\ u_\gamma &= \gamma(t) u_c \\ u_I &= u_\gamma + I_{bolus} \end{aligned} \tag{6.2}$$

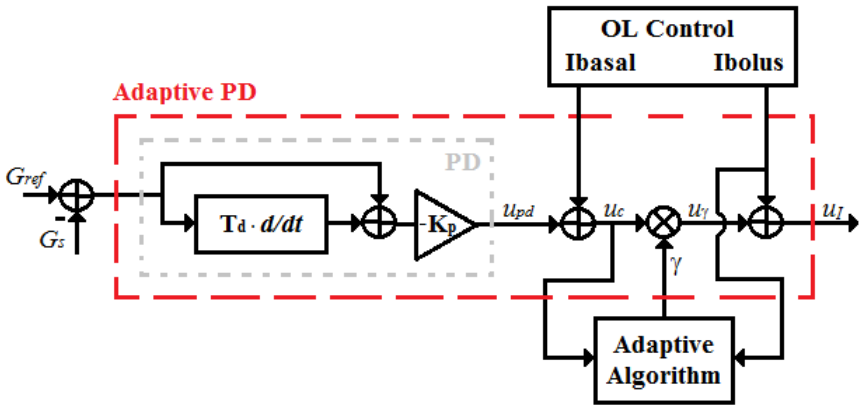


Figure 6.3: Structure of the hybrid PD controller.

The adaptive algorithm calculates on-line the maximum gain $\gamma$ compatible with the $IOB$ constraint so as to avoid excessive control action during the first postprandial period. This is described in the next subsection.

### 6.3.2 Switching Adaption Law

Fig. 6.4 displays the block diagram of the proposed adaptive algorithm for $\gamma$ on-line adjustment. It runs every sampling period of the pump just before pump insulin dose updating. It predicts the evolution of $IOB$ ($\widehat{IOB}$) during the following sampling period and determines, as explained next, the gain $\gamma$ used to calculate the insulin dose to be supplied during that period.

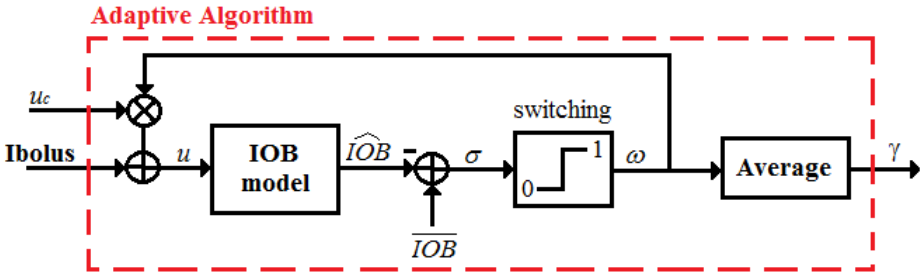


Figure 6.4: Block diagram of the adaptation law.

A variable structure algorithm based on sliding mode concepts previously developed by Garelli et al. (2011) is proposed in this adaptive scheme to determine the maximum gain compatible with the safety constraint. Note that system inversion techniques could alternatively be used. However, the variable structure approach allows a very simple and efficient implementation.

The switching function $\sigma$ is constructed with the $IOB$ estimator (6.1) and the $\overline{IOB}$ limit, which is determined using the procedure described in the next section.This signal $\sigma$ commands the comparator. Its output $\omega$ takes the value 1 for positive inputs and 0 otherwise. Finally, the gain $\gamma$ is obtained as the average value of $\omega$ during the pump updating period.

The mathematical equations describing the adaptation algorithm are:

$$\omega = \begin{cases} 1 & \text{if } \sigma \geq 0 \\ 0 & \text{otherwise} \end{cases}, \quad \sigma = \overline{IOB} - IOB \tag{6.3}$$

From (6.1) and (6.2), the time evolution of $\sigma$ is governed by the equation:

$$\frac{d\sigma}{dt} = K_{DIA}C_2 - I_{bolus} - u_c\omega \tag{6.4}$$

That is,

$$\begin{cases} \dfrac{d\sigma}{dt} = K_{DIA}C_2 - I_{bolus} - u_c & \text{if } \sigma \geq 0 \\ \dfrac{d\sigma}{dt} = K_{DIA}C_2 - I_{bolus} & \text{if } \sigma < 0 \end{cases} \tag{6.5}$$

The algorithm works as follows. Immediately after a bolus, the insulin-on-board increases largely surpassing the prescribed limit $\sigma = 0$, hence $\sigma < 0$. As a result, the signal $\omega$ switches to 0, so as to cancel the input to the $IOB$ estimator. Therefore, $IOB$ falls until crossing the surface $\sigma = 0$. Just when $\sigma$ becomes non-negative, $\omega$ switches to 1. Two things may happen then, depending on the sign of $\frac{d\sigma}{dt}$. If $\frac{d\sigma}{dt} > 0$, $\sigma$ increases further leaving the $\overline{IOB}$ and going to the interior of the safety region $\sigma > 0$. Conversely, if $\frac{d\sigma}{dt} < 0$, the constraint is reached again and $\omega$ switches to 0. In this case, a fast switching sequence occurs on the constraint $\sigma = 0$ until the insulin administered by the controller is not enough to compensate for the insulin decay term $K_{DIA}C_2$. In other words, after a transient following the bolus administration (called reaching mode in variable structure systems theory), a transitory sliding regime is established on the sliding surface $\sigma = 0$. During this mode, $\omega$ switches at very fast frequency between 0 and 1[1]. When the sliding existence condition does not hold anymore ($u_c < K_{DIA}C_2$), the sliding regime is left and the controller becomes fully operational. The discontinuous $\omega$ is averaged during the algorithm runtime, yielding $\gamma$. Fast switching at the pump command signal is thus avoided. Fig. 6.5 display the on-line performance of this adaptive algorithm for two consecutive control periods of 10 minutes each.

### 6.3.3 Operation Example

The operation of the adaptive controller is illustrated here. The postprandial period after a 60 g meal of patient 1 of the UVa cohort is displayed in Fig. 6.6. The responses obtained using the proposed hybrid PD controller with and without $\overline{IOB}$ limitation are shown in solid and dashed line, respectively. In the former case, it is seen that the adaptive gain is automatically switched to zero after the bolus, thus leading to a faster decrease in the $IOB$. Once the estimated $IOB$ reaches the safety constraint, a sliding regime is established on it, characterized by a fast switching of $\omega$ between the extreme values of $\gamma$ (0 and 1). Then, as the $IOB$ does

[1]This frequency depends basically on the minimum time step used for running the algorithm. It is desirable to have a much smaller time step than the control period.

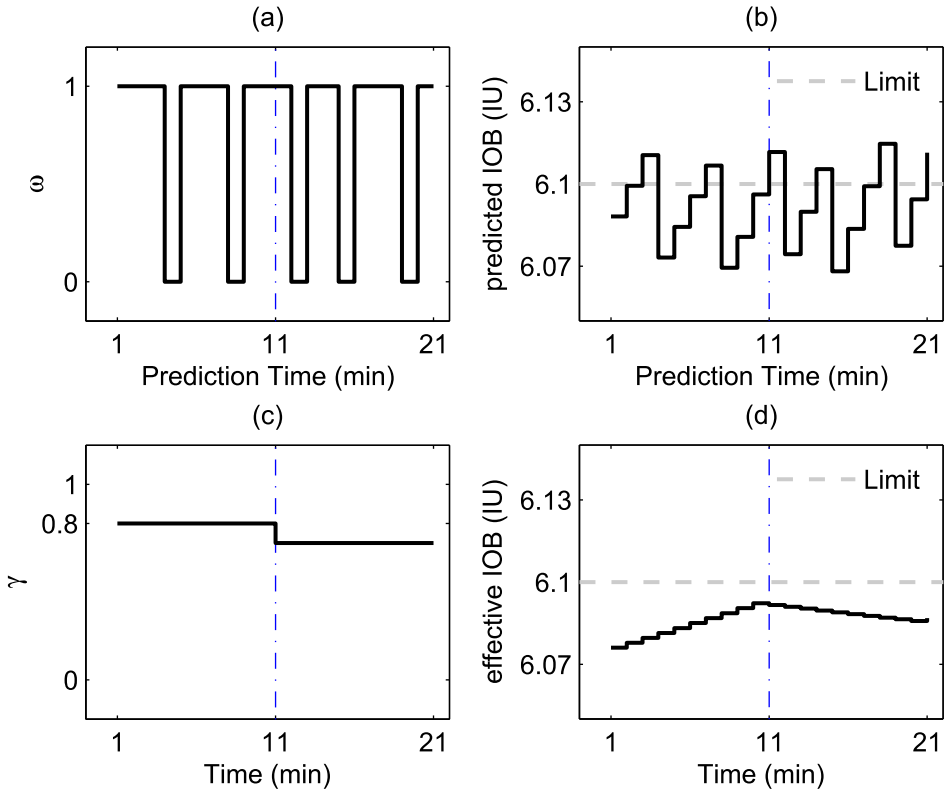


Figure 6.5: Two consecutive control periods 10 min each with an internal sample time of 1 min of the adaptive algorithm. (a) shows the switching behaviour of $\omega$ that avoids an excess in $IOB$ (limit fixed to 6.1 IU), and (b) shows the resulting $IOB$ prediction based on such $\omega$ dynamics. (c) shows the $\gamma$ value as the average of $\omega$ in each period, and (d) shows the effective $IOB$ obtained based on such $\gamma$ value. Note that the internal loop of the adaptive algorithm acts in a predictive way on each control period. The time step of this internal loop defines the maximum switching rate of $\omega$, the higher the maximum frequency of $\omega$, the higher the performance of the adaptive algorithm.

not try to go beyond its limit anymore, $\omega$ keeps constant at its maximum value and the $IOB$ falls below its constraint until the following meal. The gain $\gamma$ is the filtered version of $\omega$ in the way described in section 6.3.2. The insulin infusion profile and glucose response are also shown. It is observed that the proposed adaptive algorithm avoids the hypoglycemia event occurring with the unconstrained hybrid PD control. Note that this improvement in the late postprandial period does not entail an appreciable deterioration in the early one.

### 6.3.4 Determination of Insulin-on-Board Constraint

The determination of an appropriate, easy-to-find, and robust insulin-on-board limit is significatively sensitive for a safety scheme based on this constraint. Two experiments were considered to design and validate a feasible clinical test used to calculate the $\overline{IOB}$ limit required in (6.3) by the adaptive controller. In the first one, a cohort of ten virtual patients from Kovatchev et al. (2009) without parameters variation were used to develop the clinical test. In the second one,

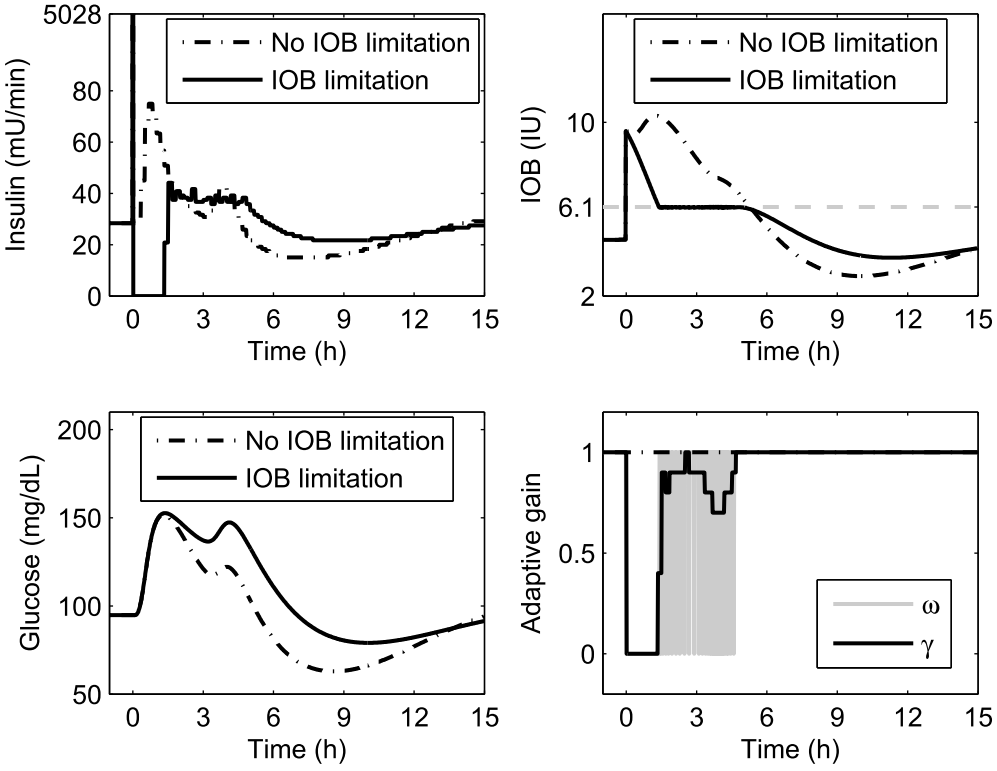


Figure 6.6: Time response of patient 1 to the hybrid PD controller with and without $\overline{IOB}$ constraint.

data from a clinical trial were used to contrast the results obtained *in silico*.

The *in silico* experiment starts from a conventional Basal/Bolus therapy with an optimal postprandial control performed on each virtual patient for meal tests of 40 g and 100 g. This optimal Basal/Bolus therapy is devised to achieve the minimum glucose excursion but also avoiding hypoglycemia. Fig. 6.7 depicts the time response of the blood glucose concentration during the postprandial period. A numeric summary of such optimal open-loop therapies is presented in Table 6.2.

| **Patient** | **1** | **2** | **3** | **4** | **5** | **6** | **7** | **8** | **9** | **10** |
|---|---|---|---|---|---|---|---|---|---|---|
| $I_{Basal}$(IU/h) | 1.6 | 1.8 | 1.85 | 1.07 | 1.9 | 1.89 | 1.5 | 1.44 | 1.63 | 1.73 |
| $Bolus40g$(IU) | 5 | 7.5 | 4.5 | 3.3 | 8.6 | 4.8 | 2.25 | 3.6 | 5.6 | 7.7 |
| $Bolus100g$(IU) | 6.3 | 9.4 | 7.1 | 5.6 | 13.7 | 8.8 | 3.7 | 4.4 | 8 | 11 |

Table 6.2: Optimal open-loop therapies used in conventional Basal/Bolus control

The optimal Basal/Bolus therapy and the corresponding patient's DIA are used to estimate the $IOB$ from (6.1). Fig. 6.8 displays the corresponding time response.

The *in silico* experiment ends with a closed-loop control using a PID tuned with techniques drawn from Steil et al. (2006). This control is performed to the same meal tests of 40 g and 100 g but adding the adaptive algorithm to the PID, and testing as $\overline{IOB}$ limit the $IOB$ values at the

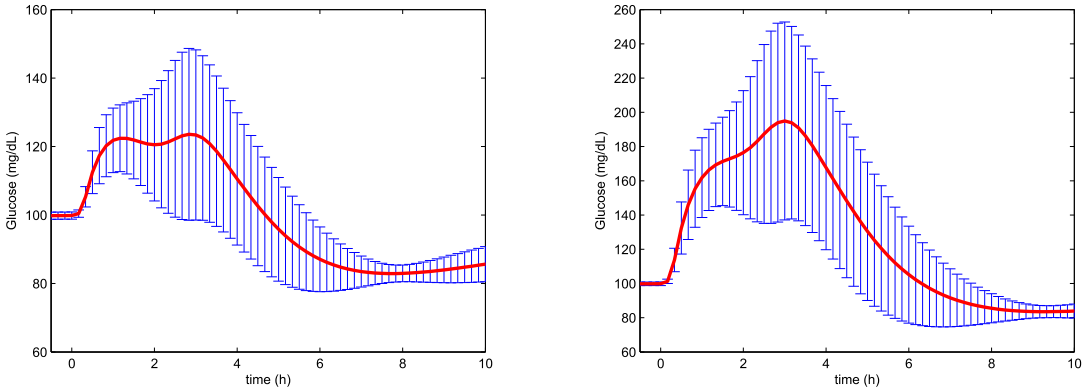


(a) (b)

Figure 6.7: Mean and standard deviation of blood glucose resulting from the optimal open-loop therapy in meal tests of (a) 40 g and (b) 100 g.

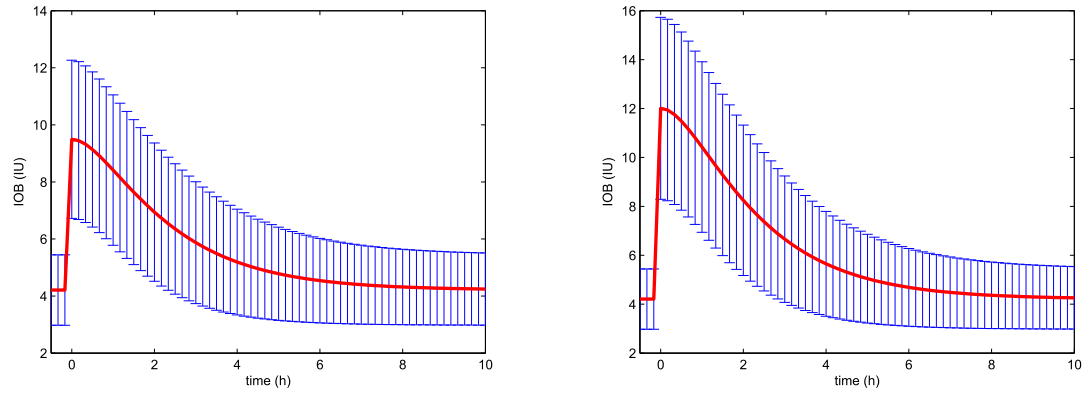


(a) (b)

Figure 6.8: Mean and standard deviation of $IOB$ from optimal open-loop therapy in meal tests of (a) 40g, and (b) 100g.

$2^{nd}$ and $3^{rd}$ postprandial hour from the preceding Basal/Bolus therapy. Table 6.3 contains the corresponding $IOB$ values at the $2^{nd}$ and $3^{rd}$ postprandial hour from the open-loop meal tests. Fig. 6.9 displays the blood glucose resulting from each $\overline{IOB}$ limit value tested in the closed-loop control.

Results of the closed-loop control are tabulated regarding to minimal glucose values and the time the safety scheme is used per patient and per meal, Tables 6.4 and 6.5. It is observed that the best results for meals of 40 g were obtained using an $\overline{IOB}$ limit corresponding to the $IOB$ value at the $2^{nd}$ postprandial hour, whereas for meals of 100 g an $\overline{IOB}$ limit corresponding to the $IOB$ value at the $3^{rd}$ postprandial hour was the best option. Others values for $\overline{IOB}$ limit either cause unacceptable hypoglycemia events or an excessive use of the safety scheme.

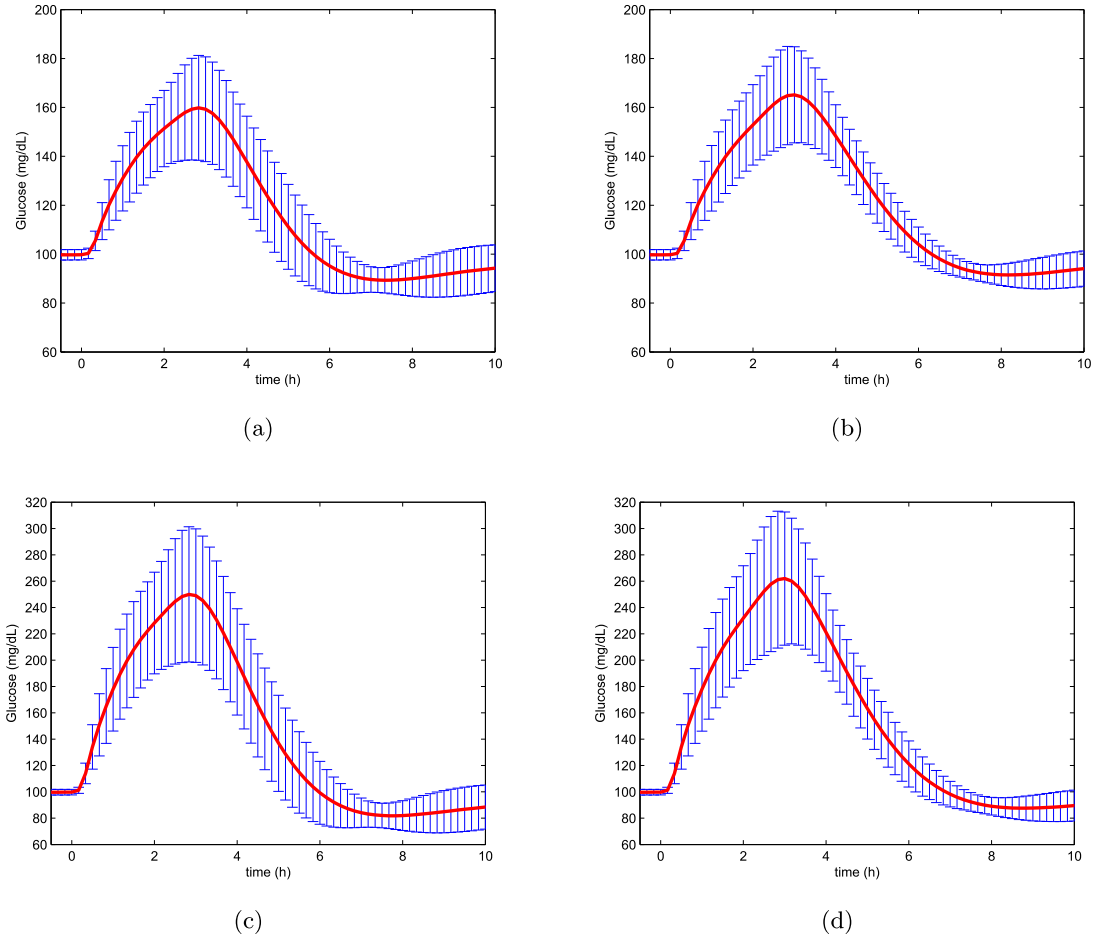


Figure 6.9: Mean and standard deviation of blood glucose resulting from closed-loop therapy using as $\overline{IOB}$ limit the $IOB$ value at the (a) $2^{nd}$ and (b) $3^{rd}$ postprandial hour of the optimal open-loop therapy for a meal test of 40 g; while as $\overline{IOB}$ limit the $IOB$ value at the (c) $2^{nd}$ and (d) $3^{rd}$ postprandial hour of the optimal open-loop therapy for a meal test of 100 g.

Analyzing the $IOB$ estimation from open-loop tests, it is observed that a strong linear relationship between the $IOB$ values at the $2^{nd}$ and $3^{rd}$ postprandial hour from meal test of 40 g and 100 g respectively, is presented with a correlation coefficient of $R = 0.99$.

This linear relationship found *in silico* is then compared against data from a clinical trial (Rossetti et al., 2012), where conventional open-loop therapies for postprandial control in meal tests of 40 g and 100 g were tested per patient. $IOB$ estimation for 9 patients from this clinical trial was calculated using the model (6.1), the patient DIA value, and the corresponding Basal/Bolus therapy administered. Resulting $IOB$ values at the $2^{nd}$ and $3^{rd}$ postprandial hour for each meal test of this clinical trial are listed in Table 6.6.

The same way as in the *in silico* experiment, results from clinical data reflected a similar behaviour between the $IOB$ values at the $2^{nd}$ and the $3^{rd}$ postprandial hour from meal test of 40 g and 100 g respectively. This case, a correlation coefficient of $R = 0.89$ continues to show

| Patient | Meal test of 40g | | Meal test of 100g | |
|---|---|---|---|---|
| | IOB at $2^{nd}$ pp* hour (IU) | IOB at $3^{rd}$ pp hour (IU) | IOB at $2^{nd}$ pp hour (IU) | IOB at $3^{rd}$ pp hour (IU) |
| 1 | 3.66 | 2.74 | 6.35 | 4.35 |
| 2 | 2.47 | 1.34 | 4.76 | 1.99 |
| 3 | 2.20 | 1.27 | 3.33 | 1.59 |
| 4 | 1.76 | 1.14 | 3.00 | 1.49 |
| 5 | 2.09 | 1.23 | 4.14 | 1.82 |
| 6 | 1.83 | 1.11 | 4.19 | 2.09 |
| 7 | 2.01 | 1.38 | 4.32 | 2.34 |
| 8 | 2.71 | 1.62 | 4.51 | 2.37 |
| 9 | 1.39 | 0.94 | 2.68 | 1.31 |

*pp states postprandial

Table 6.3: *IOB* values obtained *in silico* at the $2^{nd}$ and $3^{rd}$ postprandial hour from open-loop meal tests of 40g and 100g.

| Patient | Using as limit the IOB value at $2^{nd}$ pp hour | | Using as limit the IOB value at $3^{rd}$ pp hour | |
|---|---|---|---|---|
| | Min. Glucose (mg/dL) | Time on Safety (min) | Min. Glucose (mg/dL) | Time on Safety (min) |
| 1 | 84.5 | 0 | 86.7 | 10 |
| 2 | 91.3 | 0 | 95.5 | 35 |
| 3 | 82.0 | 22 | 92.6 | 60 |
| 4 | 86.3 | 12 | 95.9 | 66 |
| 5 | 86.7 | 0 | 86.7 | 0 |
| 6 | 79.8 | 23 | 87.7 | 55 |
| 7 | 85.4 | 18 | 93.7 | 51 |
| 8 | 87.1 | 0 | 87.1 | 0 |
| 9 | 76.2 | 21 | 81.5 | 50 |
| 10 | 81.0 | 0 | 87.1 | 25 |

Table 6.4: Minimum glucose values obtained *in silico* per patient for a meal test of 40g.

a high linear dependency. Fig. 6.10 shows the lineal regression obtained for each case, *in silico* and clinical data, between the *IOB* values mentioned.

| Patient | Using as limit the IOB value at $2^{nd}$ pp hour | | Using as limit the IOB value at $3^{rd}$ pp hour | |
|---|---|---|---|---|
| | Min. Glucose (mg/dL) | Time on Safety (min) | Min. Glucose (mg/dL) | Time on Safety (min) |
| 1 | 74.0 | 63 | 79.7 | 102 |
| 2 | 86.8 | 49 | 93.7 | 144 |
| 3 | 74.6 | 100 | 91.2 | 175 |
| 4 | 72.0 | 60 | 92.4 | 151 |
| 5 | **67.4** | 0 | 78.3 | 51 |
| 6 | **66.3** | 95 | 79.8 | 151 |
| 7 | 80.0 | 88 | 90.4 | 164 |
| 8 | 71.6 | 16 | 79.4 | 56 |
| 9 | **60.4** | 137 | **67.9** | 179 |
| 10 | 71.4 | 64 | 82.4 | 137 |

Table 6.5: Minimum glucose values obtained *in silico* per patient for a meal test of 100g.

| Patient | Meal test of 40g | | Meal test of 100g | |
|---|---|---|---|---|
| | IOB at $2^{nd}$ pp* hour (IU) | IOB at $3^{rd}$ pp hour (IU) | IOB at $2^{nd}$ pp hour (IU) | IOB at $3^{rd}$ pp hour (IU) |
| 1 | 3.66 | 2.74 | 6.35 | 4.35 |
| 2 | 2.47 | 1.34 | 4.76 | 1.99 |
| 3 | 2.20 | 1.27 | 3.33 | 1.59 |
| 4 | 1.76 | 1.14 | 3.00 | 1.49 |
| 5 | 2.09 | 1.23 | 4.14 | 1.82 |
| 6 | 1.83 | 1.11 | 4.19 | 2.09 |
| 7 | 2.01 | 1.38 | 4.32 | 2.34 |
| 8 | 2.71 | 1.62 | 4.51 | 2.37 |
| 9 | 1.39 | 0.94 | 2.68 | 1.31 |

*pp states postprandial

Table 6.6: Clinical $IOB$ value at the $2^{nd}$ and $3^{rd}$ postprandial hour from open-loop meal test of 40 g and 100 g.

Because data from open-loop tests of both, *in silico* experiment and clinical trial, share a very similar relationship about the appropriate candidate to use for $\overline{IOB}$ limit in the closed-loop control with the adaptive algorithm, one can say that this safety limit is supported indirectly by clinical data. Therefore, this methodology is adopted here to find a robust $\overline{IOB}$ limit.

It is worth noting that the $\overline{IOB}$ limit is not depending of the meal size. Therefore, the $\overline{IOB}$ limit proposed in this thesis as hypoglycemic protection is a constant value, although a time varying limit following the circadian variation of insulin sensitivity could also be a sensible choice. A procedure to find the $\overline{IOB}$ limit based in the above considerations is presented below.

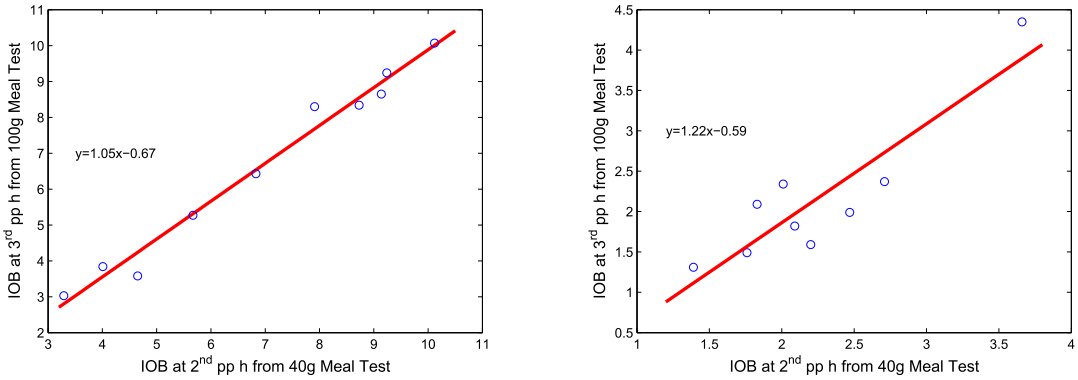


(a) (b)

Figure 6.10: Lineal regression between $IOB$ values at the $2^{nd}$ and $3^{rd}$ postprandial hour from meal tests of 40 g and 100 g respectively using (a) *in silico* experiment, and (b) clinical data.

### IOB limit determination procedure

The following procedure summarizes the open-loop postprandial clinical test proposed to obtain the $IOB$ limit:

1. Achieve an initial condition of preprandial blood glucose concentration between 80 and 120 mg/dL without insulin bolus administration during the previous 5 hours.
2. Administer a meal with 40g to 100 g of carbohydrates together with an insulin bolus.
3. Observe blood glucose evolution during the following 10 hours,
   - If minimum glucose is outside the set $(75, 90)$, then repeat step 2 adjusting the bolus. Alternatively the correction factor, for a retrospective calculation of bolus, can be used.
   - Else, calculate the $\overline{IOB}$ limit using (6.1) and the next formula:

$$\begin{aligned} \overline{IOB} &= IOB(T_{IOB}) \\ T_{IOB} &= \frac{CHO + 80g}{60g/h} \end{aligned} \tag{6.6}$$

where $CHO$(g) is the amount of carbohydrate intake. $T_{IOB}$ varies between 2 and 3 hours when $CHO$ changes between 40 g and 100 g. It is important to note that the $\overline{IOB}$ limit derived in this way is almost independent of the meal used in the test, as reflected the above *in silico* and real data experiments. Fig. 6.11 illustrates the method to obtain $\overline{IOB}$ from the insulin clearance curve and (6.6) for two different meals. It is verified that, although $T_{IOB}$ is significantly different for each meal, the corresponding limits are practically equal.

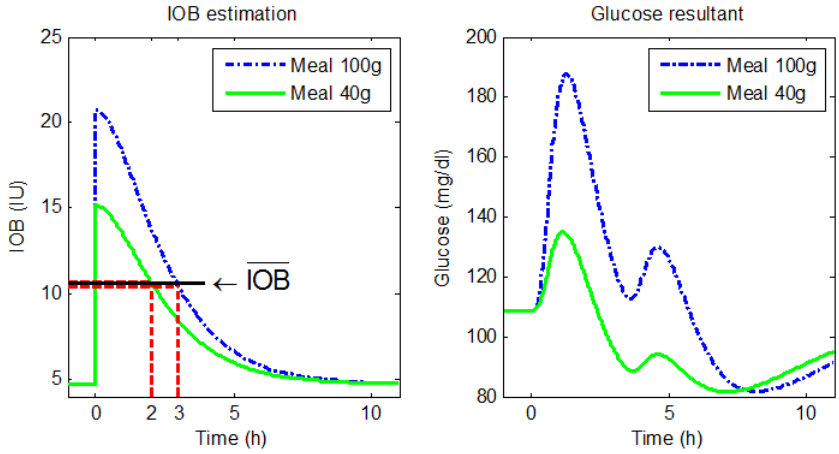


Figure 6.11: Calculation of $\overline{IOB}$ using $IOB$ and blood glucose response.

Note that the bound $\overline{IOB}$, calculated as suggested before or in any other way, can be intuitively adjusted with medical criteria according to the closed-loop response exhibited by the patient. For instance, the physician should decrease $\overline{IOB}$ in the case of frequent hypoglycemia, or increase it if the controller action is too conservative or the restriction is active during too long time.

### 6.3.5 Controller Tuning

Only three clinical trials are used to tune the adaptive PD controller. The proportional gain is tuned in proportion to the total daily dose insulin ($I_{TDD}$):

$$K_p = \frac{60}{T_d}\frac{I_{TDD}}{1500} \tag{6.7}$$

where $I_{TDD}$ is obtained using a protocol of 200g CHO distributed in 40g, 80g and 80g at 08:00, 13:00 and 19:00 respectively. The derivative gain is set to $T_d = 90$min for all patients. The $K_{DIA}$ parameter of the $IOB$ estimator is derived from the $DIA$, which is calculated following the trial described in section 6.2. Finally, the $\overline{IOB}$ limit is obtained following the procedure described in section 6.3.4. All the controller and relevant parameters are listed in Table 6.7.

### 6.3.6 Performance Results

The performance and robustness of the hybrid adaptive PD controller is assessed under the challenging and realistic test scenario described in section 4.4. It includes mixed meals, controller mistuning, circadian variations in the insulin sensitivity, discrete measurement and actuation, sensor errors and other disturbances. The focus of the analysis is on the 8 hour postprandial period. A night controller is switched on at midnight every day to achieve a preprandial glycemia near to 90 mg/dL before the meal.

| **Patient** | **1** | **2** | **3** | **4** | **5** | **6** | **7** | **8** | **9** | **10** |
|---|---|---|---|---|---|---|---|---|---|---|
| $I_{TDD}$(IU) | 51.2 | 56.4 | 57.7 | 33.2 | 68.9 | 54.6 | 42.2 | 43.4 | 59.7 | 63.2 |
| $I:CHO$(IU/g) | .0833 | .0833 | .0750 | .0333 | .1166 | .0500 | .0250 | .0550 | .1166 | .1250 |
| $DIA$(h) | 6.33 | 2.60 | 5.50 | 7.16 | 6.33 | 6.33 | 5.50 | 6.33 | 8.00 | 6.83 |
| $K_p$(IU/h per mg/dL) | .0227 | .0250 | .0256 | .0147 | .0306 | .0242 | .0187 | .0193 | .0265 | .0281 |
| $K_{DIA}(\text{min}^{-1})$ | .0122 | .0315 | .0147 | .0113 | .0122 | .0122 | .0147 | .0122 | .0099 | .0113 |
| $\overline{IOB}$(IU) | 6.1 | 1.9 | 5.7 | 3.9 | 7.8 | 6.1 | 3.8 | 5.3 | 8.9 | 8.1 |

Table 6.7: Controller and other relevant parameters

The same controller without gain adaptation is also evaluated to put in evidence the effect of $IOB$ limitation. Other two PID-like controllers found in the literature are implemented to have an additional baseline measure of performance and to emphasize the attractive features of the proposed gain adaptation algorithm. One of them is the fully automatic PID controller with insulin feedback (Steil et al., 2011) described in section 3.2.1, with a feedback parameter value of 5/6. The other, based on the proposal of Weinzimer et al. (2008b), is a hybrid PID controller with a 35% pre-bolus administered 15 min before the meal. The proportional and derivative gains are the same for all controllers, whereas the integral gain of the PID controllers is set to 450 min. The glucose set-point is also the same for all controllers as well as the initial condition.

Performance is compared, based on time responses and usual metrics such as the mean and standard deviation of the maximum glucose excursion, the number of hypoglycemia events, and the time the patients were in hyperglycemia and in hypoglycemia. Moreover, the graphical tool CVGA described in section 4.3.5 measures the performance of a control algorithm on an observation period is used.

The results and metrics obtained for the 180 meal tests are depicted in Figs. 6.12 and 6.13, and in Tables 6.8 and 6.9. Fig. 6.12 depicts the time response of the blood glucose concentration during the postprandial period. A very distinctive feature of the proposed controller is that the standard deviation decreases with time. Moreover, the time response obtained with the proposed controller does not exhibit the undershoot observed in the other cases.

Table 6.8 displays the numerical results. It is observed that only 2 hypoglycemia events occurred when using the hybrid adaptive PD controller, whereas more than 75 events occurred when using the other ones. Moreover, the time in hypoglycemia was significantly reduced from around 15% to 0.11% when using the proposed controller. It is also worthy to note that hypoglycemia avoidance is not achieved at the cost of an increase in severe hyperglycemia events. Meanwhile, the other metrics are very similar for all controllers.

Fig. 6.13 displays CVGA corresponding to the four controllers using an observation period of 8 hours postprandial glucose. A numeric assessment of the overall level of glucose regulation by the summary outcome of the CVGA is also tabulated by zones in Table 6.9.

It is observed that the hybrid adaptive PD controller avoids the cases of severe hypoglycemia present for the other controllers. After comparing with the same controller without gain adaptation, it can be concluded that this improvement is due to the IOB limitation. Furthermore,

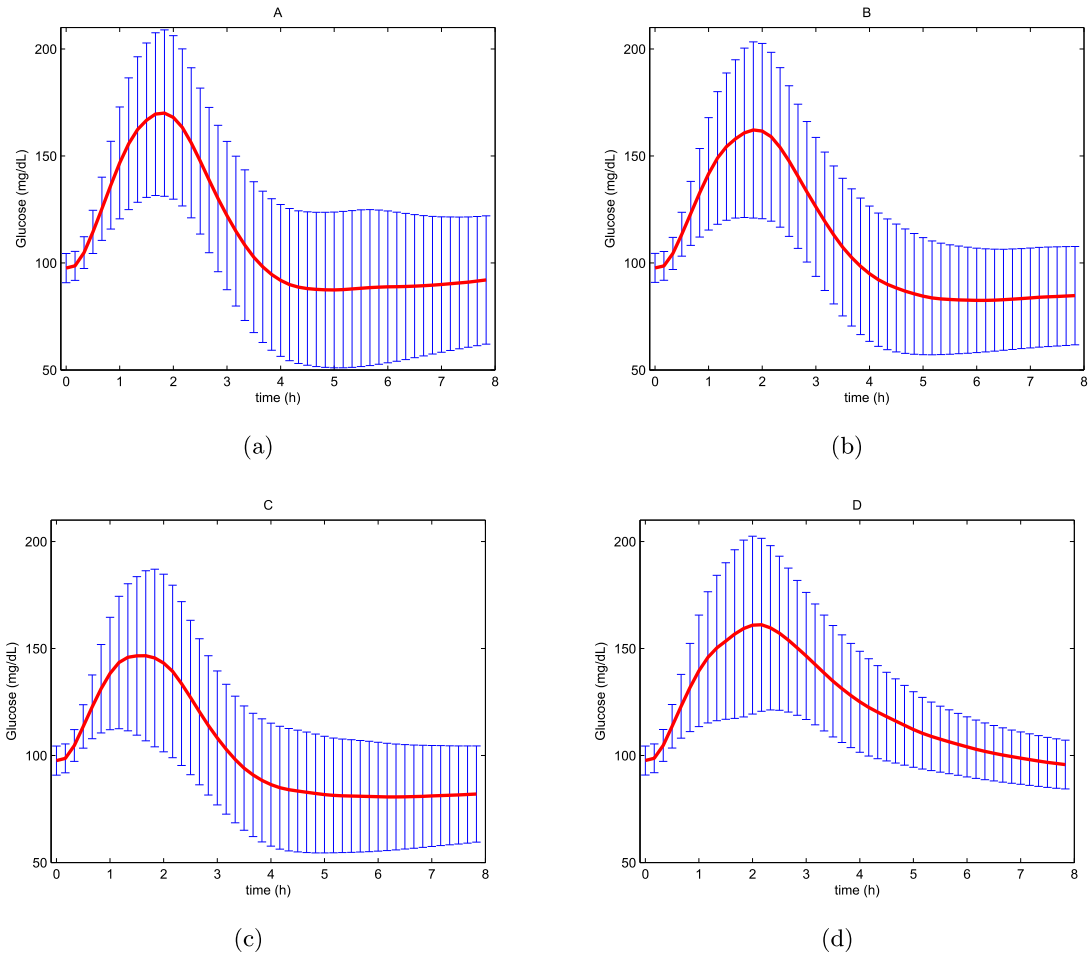


Figure 6.12: Mean and standard deviation of blood glucose for (a) PID with insulin feedback (PID-IFB), (b) PID controller with 35% pre-bolus, (c) PD controller with bolus, (d) Hybrid Adaptive PD controller.

| Metric / Controller | Excursions (mg/dL) | # hypos | Time hyper % | Time hypo % |
|---|---|---|---|---|
| PID-IFB | 79.13±36.36 | 76 | 5.84 | 15.55 |
| PID with 35% pre-bolus | 69.40±39.14 | 84 | 5.38 | 14.75 |
| PD with bolus | 56.35±36.58 | 92 | 3.58 | 16.72 |
| PD with bolus and $\overline{IOB}$ | 68.85±39.15 | 2 | 6.26 | 0.11 |

Table 6.8: Mean and standard deviation of maximum glucose excursion, number of hypoglycemia events (hypos) and time in hyper (¿180 mg/dL) and hypoglycemia (¡70 mg/dL)

it can be observed that the proposed controller achieves the largest amount of points in A and B zones, whereas there are only 4 points in the C-D-E zone. This behaviour states the susceptibility of the rest of controllers to overcorrection of hyperglycemia and hypoglycemia.

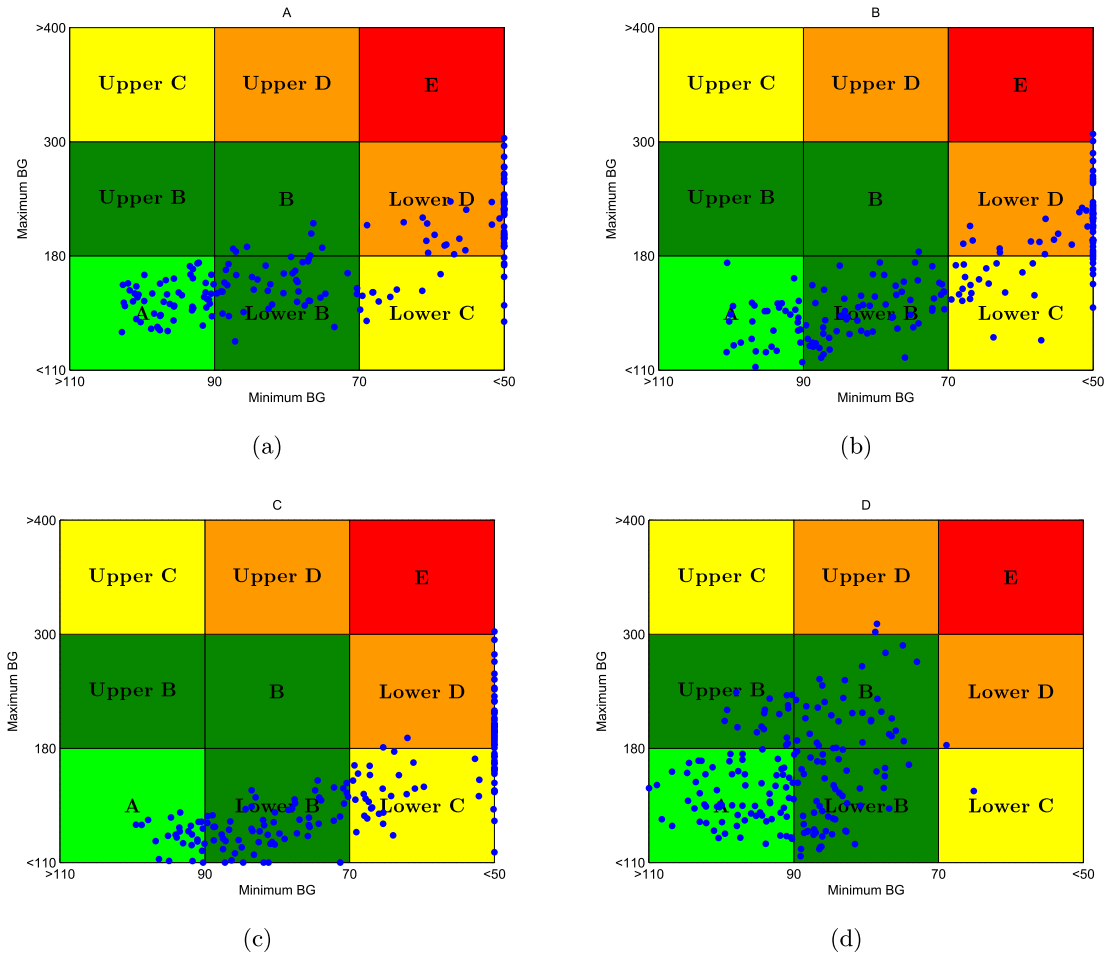


Figure 6.13: CVGA for (a) PID with insulin feedback (PID-IFB), (b) PID controller with 35% pre-bolus, (c) PD controller with bolus, (d) Hybrid Adaptive PD controller.

| Controller \ Zone | A | B | BU | BL | CL | CU | DL | DU | E |
|---|---|---|---|---|---|---|---|---|---|
| PID-IFB | 57 | 7 | 0 | 44 | 17 | 0 | 58 | 0 | 1 |
| PID with 35% pre-bolus | 30 | 1 | 0 | 65 | 27 | 0 | 55 | 0 | 2 |
| PD with bolus | 22 | 0 | 0 | 66 | 51 | 0 | 40 | 0 | 1 |
| PD with bolus and $\overline{IOB}$ | 65 | 34 | 17 | 60 | 1 | 0 | 1 | 2 | 0 |

Table 6.9: Control variability grid analysis for the different controllers

## 6.4 Safety Auxiliary Feedback Element Evaluation

This section presents an extensive performance evaluation of several closed-loop glucose controllers for T1D, with and without a novel safety layer, based on sliding mode reference conditioning technology known as the safety auxiliary feedback element (SAFE) (Revert et al., 2013). Traditional therapies are prone to poor glucose regulation, especially in the postprandial period, due to both physiological and technological limitations. Uncertainty is present throughout the

control system, namely, significant errors in glucose measurement, variability in the metabolic system related to kinetic and dynamic insulin action, or uncertainty in the glucose absorption and utilisation. This uncertainty entails strong limitations for the development of a practical and individualised model of the glucose-insulin system for each patient. The SAFE method controls the amount of insulin-on-board according to a unique constraint that can be adjusted with clinical criteria. The primary advantage of this scheme is that it does not affect the design of the main controller, which could be independently designed in advance.

### 6.4.1 SAFE Method

The SAFE method is briefly presented as follows [2].

Figure 6.14 presents a block diagram of a general glucose control loop to which the SAFE layer has been added. In the main control loop, the control action $u_c$ is the pump's insulin infusion rate, whereas $u_f$ represents the feed-forward action of priming bolus in meal announcement schemes. The glucose controller can be of any type, even nonlinear. For simplicity, the controller is assumed biproper (i.e., with a direct path from the error to the control action), which is of practical significance.

The SAFE algorithm implements an outer safety loop for glucose control with the main objective of reducing the number and severity of postprandial hypoglycaemic events. The algorithm automatically adjusts the desired glucose reference $G_d$ to a safety reference $G_{d_S}$ when the residual insulin in the subcutaneous tissue, the $IOB$, exceeds a given upper limit $\overline{IOB}$. That is, the outer control loop is only active when the $IOB$ changes to undesirable values beyond the imposed constraints, which in this case limits the main controller action.

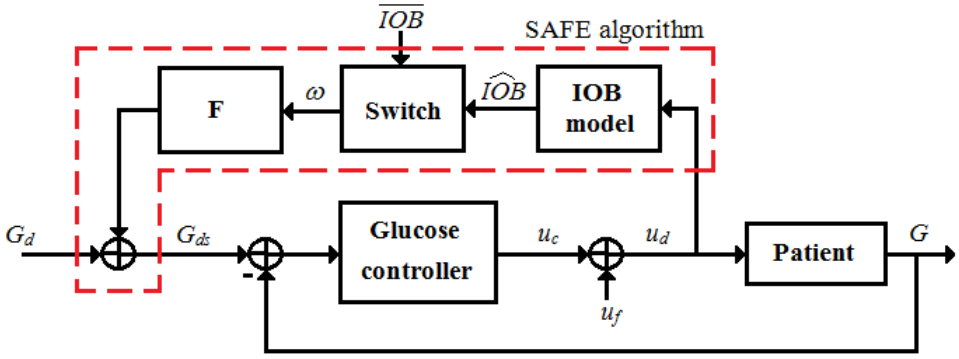


Figure 6.14: Basic scheme of a glucose control loop with the SAFE algorithm.

As the $IOB$ is inaccessible, it must be estimated. The $IOB$ estimation model presented in section 6.2.1 is employed in this evaluation. From the estimated $\widehat{IOB}$, a switching law is defined to generate the correct signal for the glucose reference $G_d$, which prevents surpassing $\overline{IOB}$. The main advantage of this approach is that it is applicable to any main control loop controller and thus provides a generalised method to address the over-reaction problem. The following paragraph describes how the switching function of the SAFE layer is implemented in this study.

[2] The reader is referred to Revert et al. (2013) for further details.

### 6.4.2 Switching SAFE Law

Only the upper constraint $\overline{IOB}$ for $IOB$ is considered as the main objective is to mitigate the problem of postprandial hypoglycaemic incidence. To fulfil this constraint, the following switching law is proposed.

$$w(t) = \begin{cases} w^+ & if\ \sigma(t) > 0 \\ 0 & otherwise, \end{cases} \tag{6.8}$$

with

$$\sigma(t) = IOB - \overline{IOB} + \tau(\dot{IOB} - \dot{\overline{IOB}}) \tag{6.9}$$

When the upper bound is violated (or about to be violated), the $w$ switches to $w^+ \neq 0$ to increase the safety reference $G_{d_S}$ and reduce the control action $u_c$, with the aim of preventing hypoglycaemia due to excess insulin.

The resulting discontinuous signal $w$ during the $IOB$ limitation is smoothed out by the first-order filter represented in the block $F$ previously to being added to $G_d$ to produce $G_{d_S}$[3].

### 6.4.3 Glucose Controllers

Two PID-like glucose controllers, with and without the SAFE method, are evaluated. The first controller is the classical PID algorithm, in which the integrative term is replaced by the basal insulin from the open-loop therapy and a prandial bolus defined by the patient's insulin-to-carbohydrate ratio and the corresponding meal size is implemented. This scheme is referred to as the PDBasal Hybrid controller, as shown in Figure 6.15.

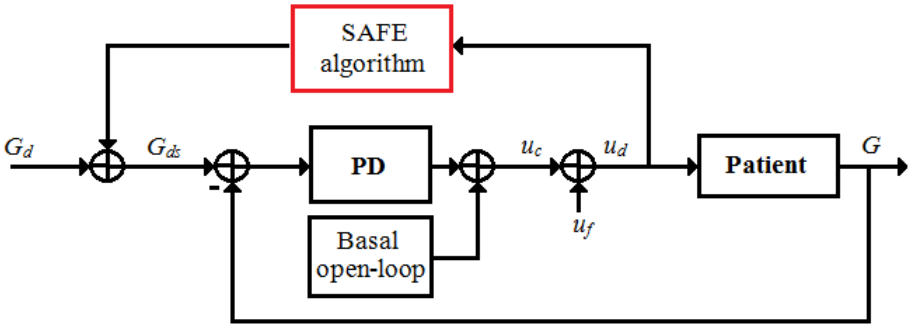


Figure 6.15: PDBasal Hybrid scheme with implementation of the SAFE method.

[3]Note that the filter $F$ has been replaced with respect to Revert et al. (2013) as we assume $G_d$ is constant.

The second controller is the well-established fully closed-loop PID-IFB algorithm presented in section 3.2.1, as shown in Figure 6.16. The control law is as follows:

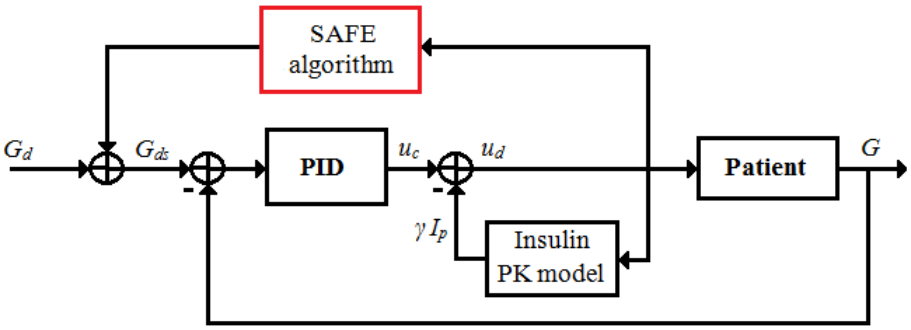


Figure 6.16: PID-IFB scheme with implementation of the SAFE method. The prandial Bolus insulin was not employed in this realisation.

$$u(t) = k_p \left[ e(t) + \frac{1}{\tau_I} \int e(t)dt + \tau_D \frac{de(t)}{dt} \right] - \gamma I_p(t) \tag{6.10}$$

where $\gamma I_p$ is the feedback component. The estimated plasma insulin $I_p$ is a two-compartment model assumed for the pharmacokinetics of insulin, with a bi-exponential impulse response given by

$$I_p(t) = \frac{I_B}{K_{cl}(\tau_2 - \tau_1)} (e^{-t/\tau_2} - e^{-t/\tau_1}) \tag{6.11}$$

where $\tau_1$ and $\tau_2$ are time constants (in min) associated with the subcutaneous absorption of insulin, $K_{cl}$ is the insulin clearance, and $I_B$ is the magnitude of the impulse (bolus) of insulin delivered at time t=0.

This insulin pharmacokinetic model is represented by the following equations

$$\begin{aligned} \frac{\mathrm{d}L(t)}{dt} &= u_d(t) - a_2 L(t) \\ \frac{\mathrm{d}I_p(t)}{dt} &= \frac{a_1 a_2}{K_{cl}} L(t) - a_1 I_p(t) \end{aligned} \tag{6.12}$$

where $L$ is an intermediate compartment, $a_1 = 1/\tau_1$ and $a_2 = 1/\tau_2$. The values for the model time constants are $\tau_1 = 55$ min and $\tau_2 = 70$ min and for insulin clearance $K_{cl} = 1$ L/min. According to Palerm (2011), the PID algorithm with insulin feedback must deliver the same

insulin-infusion rate to the subject as for the case without insulin feedback (i.e., $\gamma = 0$). Therefore, for a given controller gain selected for the case without insulin feedback, such as the nominal value given in Eq. 6.10, it can be adjusted by multiplying it by the factor

$$f = \left(1 + \frac{\gamma}{K_{cl}}\right) \tag{6.13}$$

### 6.4.4 Performance Results

The challenging test scenario designed in section 4.6, which implements realistic conditions, including different types of uncertainties and disturbances, and considers mixed meals, diurnal and day-to-day time-varying metabolic changes in insulin sensitivity and insulin absorption; controller mistuning; discrete measurement and actuation; and sensor errors, is also employed in this evaluation methodology. The resulting performance with and without the SAFE method is compared based on time responses and certain metrics.

#### Improvement in the performance of nominal-tuning controllers

To evaluate the control performance when the SAFE layer is added, the PDBasal Hybrid and the PID-IFB controllers were tuned based on default parameters values. Both cases use the same gain, and were tuned in proportion to the total daily dose insulin ($I_{TDD}$), as presented in section 6.3.5. The derivative gain was set to $T_d = 90$ min for all patients in both controllers. The basal insulin profile from the open-loop control designed to counteract the variation in insulin sensitivity was used in the PDBasal Hybrid controller whereas the integrative gain was set to $T_i = 450$ min and the feedback term $\gamma$ was set to 5/6 in the PID-IFB algorithm.

The practical procedure based on *in silico* experiments and clinical data presented in section 6.3.4 to determine the $\overline{IOB}$ limit was employed instead of the provisional method suggested by Revert et al. (2013). The filter cut-off frequency was set to 0.1 $\text{min}^{-1}$ and unity gain. The $w^+$ value was set to 350 mg/dl, and $\tau$ was set to 10 min. All other controller and relevant parameters are listed in Table 6.7. The performance results for nominal tuning according to the number of hypoglycaemic events and the mean blood glucose excursion are presented in Table 6.10.

The addition of the SAFE layer results in enhanced performance of hypoglycaemic events despite a moderate increment in the mean blood glucose excursion in both controllers.

### 6.4.5 Optimal Tuning

Extensive controller tunings were evaluated for the PDBasal Hybrid and the PID-IFB to obtain the best achievable performance with and without the SAFE layer. Based on the preceding nominal-tuning, the controller gain $K_p$ was changed to -60%, -40%, -20%, 0%, +20%, +40%, +60%; whereas the $I : CHO$ and the $\gamma$ term of the PDBasal Hybrid and PID-IFB, respectively, were changed to -60%, -30%, 0%, +30%, +60%. Therefore, 35 different tuning combinations were evaluated in each case with and without the SAFE layer. Figs. 6.17 and 6.18 graphically illustrate the resulting number of hypoglycaemic events and the mean excursion obtained with

| | PDBasal Hybrid | | | | PID-IFB | | | |
|---|---|---|---|---|---|---|---|---|
| | With SAFE | | Without SAFE | | With SAFE | | Without SAFE | |
| Patient | Hypos | Excursion | Hypos | Excursion | Hypos | Excursion | Hypos | Excursion |
| 1 | 1 | 64.6 | 10 | 60.2 | 0 | 74.2 | 7 | 72.4 |
| 2 | 0 | 52.0 | 6 | 39.7 | 0 | 87.2 | 3 | 72.0 |
| 3 | 0 | 68.7 | 9 | 54.7 | 3 | 107.8 | 8 | 93.9 |
| 4 | 0 | 67.0 | 8 | 46.4 | 3 | 102.5 | 12 | 87.6 |
| 5 | 0 | 63.1 | 6 | 51.1 | 1 | 90.6 | 6 | 86.7 |
| 6 | 0 | 69.6 | 8 | 46.2 | 3 | 111.8 | 10 | 96.3 |
| 7 | 0 | 63.5 | 8 | 41.2 | 1 | 96.5 | 9 | 74.8 |
| 8 | 0 | 62.1 | 12 | 54.2 | 0 | 75.1 | 6 | 72.7 |
| 9 | 1 | 121.7 | 18 | 108.6 | 0 | 134.9 | 10 | 129.3 |
| 10 | 0 | 78.6 | 8 | 68.4 | 1 | 108.1 | 7 | 103.1 |

Table 6.10: Performance results of PDBasal Hybrid and PID-IFB with and without the SAFE layer using nominal-tuning.

and without the SAFE layer. Note the additional arrow from the best tuning case without SAFE to the best case with SAFE.

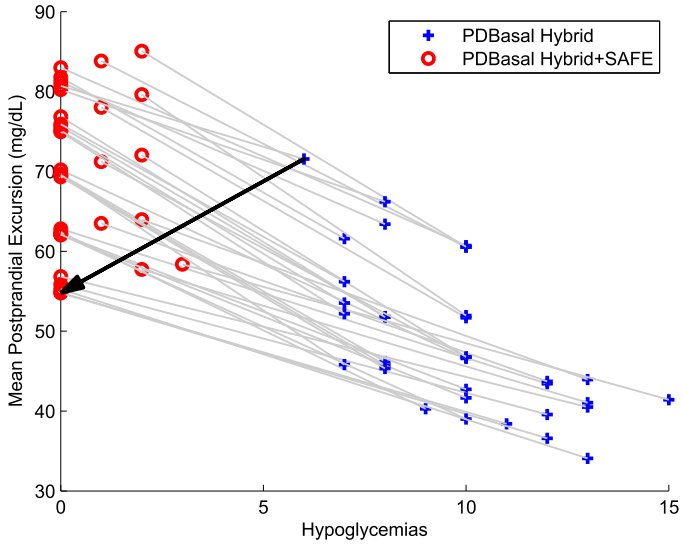


Figure 6.17: Performance results of patient six of the PDBasal Hybrid with (circle) and without (cross) the SAFE layer using several combinations of the control gain and the size of the prandial bolus.

Tables 6.11 and 6.12 display the best performances for each patient for the PDBasal Hybrid and the PID-IFB controller, respectively. The number of hypoglycaemic events, the mean blood glucose excursion, and the best tuning combination are listed as a percentage change from the nominal-tuning.

An improved performance is achieved not only for hypoglycaemic events but also for the

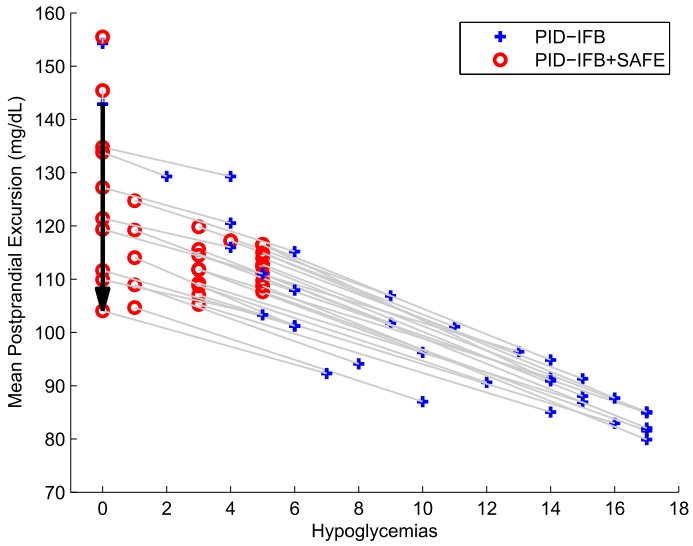


Figure 6.18: Performance results of patient six of the PID-IFB algorithm with (circle) and without (cross) the SAFE layer using several combinations of the control gain and the insulin feedback term gamma.

| | With SAFE | | | | Without SAFE | | | |
|---|---|---|---|---|---|---|---|---|
| Patient | Hypos | Excursion | Gain Kp | Gain I:CHO | Hypos | Excursion | Gain Kp | Gain I:CHO |
| 1 | 0 | 69.1 | -40 | -30 | 1 | 72.9 | -60 | -60 |
| 2 | 0 | 35.9 | -60 | 60 | 0 | 49.3 | -60 | -30 |
| 3 | 0 | 52.9 | 20 | 60 | 6 | 73.9 | -60 | -60 |
| 4 | 0 | 50.4 | -40 | 60 | 6 | 45.3 | -60 | 0 |
| 5 | 0 | 52.1 | -60 | 30 | 2 | 74.3 | -60 | -60 |
| 6 | 0 | 54.8 | -40 | 60 | 6 | 71.5 | -60 | -60 |
| 7 | 0 | 51.4 | -40 | 60 | 6 | 36.9 | -40 | 0 |
| 8 | 0 | 53.0 | -60 | 60 | 0 | 67.0 | -60 | -60 |
| 9 | 0 | 115.5 | -40 | 30 | 6 | 128.4 | -60 | -60 |
| 10 | 0 | 68.7 | -60 | 30 | 3 | 92.34 | -60 | -60 |

Table 6.11: Performance results of the PDBasal Hybrid with and without the SAFE layer regarding to minimal hypoglycaemic events and glucose excursion using the best-tuning. The best tuning of $Kp$ and $I:CHO$ in each case is presented as a percentage change with respect to the nominal value.

mean blood glucose excursion when the SAFE layer is added to the controllers. In the case of the PID-IFB controller, patient two performs better when the SAFE layer is not added.

### 6.4.6 SAFE in other control schemes (MPC)

One way to illustrate the adaptability of the SAFE layer to control schemes other than schemes based on PID controllers is to evaluate its effect on predictive controllers. In this case, model predictive control (MPC) is used. One class of MPC is the constrained type, in which constraints are explicitly included in the objective function. However, this test is implemented illustratively

| | With SAFE | | | | Without SAFE | | | |
|---|---|---|---|---|---|---|---|---|
| Patient | Hypos | Excursion | Gain Kp | Gain $\gamma$ | Hypos | Excursion | Gain Kp | Gain $\gamma$ |
| 1 | 0 | 71.3 | 40 | 0 | 0 | 77.4 | -40 | -30 |
| 2 | 0 | 83.8 | -60 | -60 | 0 | 72.9 | -40 | -60 |
| 3 | 0 | 104.1 | 0 | -60 | 0 | 114.5 | -60 | -20 |
| 4 | 0 | 97.4 | -20 | -60 | 0 | 128.0 | -60 | 30 |
| 5 | 0 | 89.5 | -20 | -60 | 0 | 94.6 | -60 | -60 |
| 6 | 0 | 104.1 | -40 | -60 | 0 | 142.9 | -60 | 30 |
| 7 | 0 | 86.5 | -60 | -60 | 0 | 106.7 | -60 | 0 |
| 8 | 0 | 73.3 | 0 | -60 | 0 | 75.3 | -40 | -30 |
| 9 | 0 | 134.1 | -20 | -60 | 0 | 140.2 | -40 | 60 |
| 10 | 0 | 109.9 | -40 | -60 | 0 | 115.5 | -60 | -30 |

Table 6.12: Performance results of PID-IFB with and without the SAFE layer regarding to minimal hypoglycemia events and glucose excursion using the best-tuning. The best tuning of $Kp$ and $\gamma$ in each case is presented as a percentage change with respect to the nominal value.

to demonstrate attractive SAFE features. As the MPC is a model-based controller, a model representing glucose-insulin dynamics based on ARX models is used (Magni et al., 2009b; Ellingsen et al., 2009). The ARX model identification implemented in this proof uses the meal glucose and the variation in insulin delivered with respect to basal rate as inputs and uses the variation in blood glucose concentration with respect to basal as an output.

To adequately represent glucose-insulin dynamics, a 1-day open-loop experiment with hypoglycaemia, normoglycaemia and hyperglycaemia was performed. The identification protocol includes breakfast1, lunch, dinner, and breakfast2 at 08:00, 13:00, 21:00, and 08:00, respectively. However, insulin is not administered during breackfast1, meal glucose is not administered during lunch but insulin is given, and the insulin delivered during breackfast2 was four times higher than a typical dosage. The prediction performance was enhanced by transforming the inputs with a first-order-order transfer function (Finan et al., 2007) and by the "recursively estimate ARX model" function included in the LabVIEW system identification toolkit.

The validation data were obtained from several variations of an open-loop experiment, including three meals during which the insulin delivered to each patient was modified using different pre-meal and post-meal bolus sizes (Magni et al., 2009a). The ARX parameter values used in the system identification toolkit were A[B1 B2][d1 d2], where A=15, B1=B2=15, d1=10 and d2=0. The sampling period was 1 min.

Constant MPC tuning parameters were maintained during the simulation. The prediction horizon and the control horizon were set to 250 time steps and 50 time steps, respectively. The weight for the change in delivered insulin rate was set to 200, whereas the weight for the glucose set point tracking was set to 1. The set point was set to 140 mg/dl for the first four postprandial hours and was set to 100 mg/dl for the remaining time. Fig. 6.19 shows the blood glucose response, the delivered insulin, and the $IOB$ estimation obtained for patient 5 with and without the SAFE layer added to the MPC.

Note that six meals are prone to present hypoglycaemic events without the SAFE layer. In addition, the blood glucose excursion is not significantly affected by the addition of the SAFE

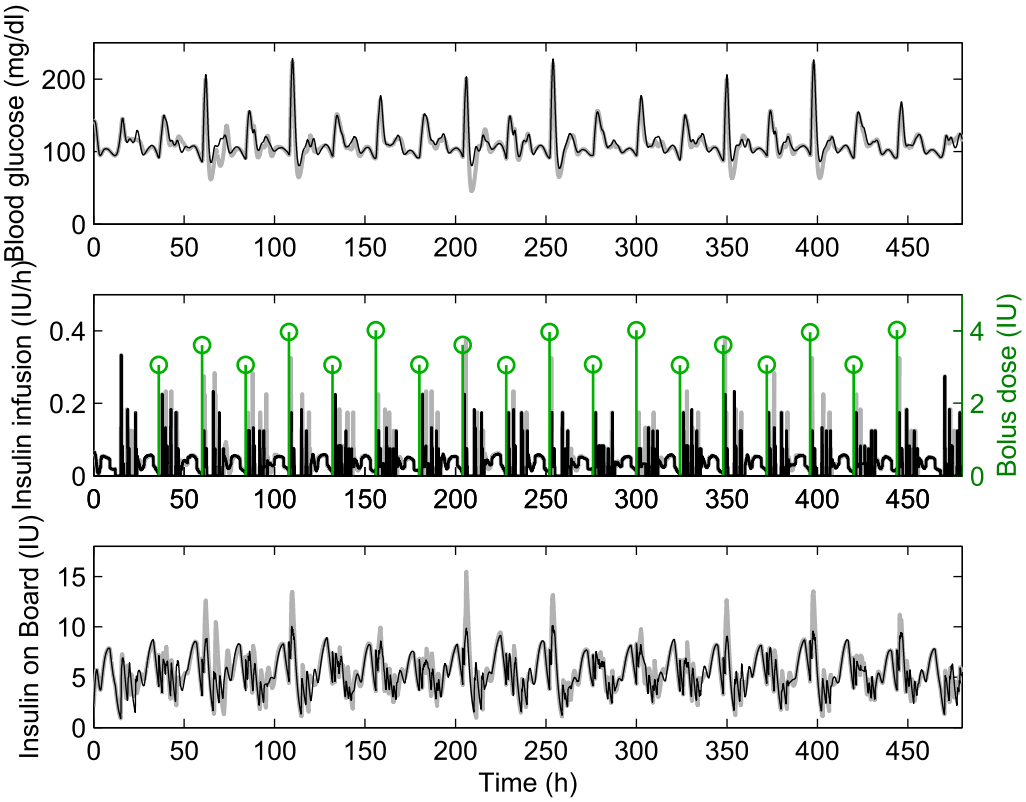


Figure 6.19: Blood glucose, insulin infusion, and IOB calculation of the MPC (gray) and the MPC-SAFE (black) response for patient five.

layer is added.

## 6.5 Summary

In this chapter, two safety schemes designed to prevent late hypoglycaemia under postprandial control are addressed. The two schemes are the specific hybrid adaptive PD controller strategy and the SAFE method envisioned to improve the safety of any glucose controller. To guarantee a robust performance, both strategies are based on sliding mode control techniques. The inclusion of a soft insulin-on-board constraint enables regulation of the insulin delivered to the patient in a practical and easy-to-implement manner. The major differences between these approaches is the variable structure used to modify the main control action, the switching function defined in the commutation law, and the updating procedure of the main control action. Although the safety scheme based on gain conditioning was designed for a specific control algorithm, this methodology could be implemented to additional glucose controllers. A practical procedure to determine a feasible insulin-on-board limit for the safety constraint was obtained after *in silico* experiments and a clinical data analysis. The safety schemes that supervise the normal performance of glucose controllers in this thesis have proven to be effective for reducing the risk of late hypoglycaemic events and have shown the potential for enhanced postprandial control with aggressive controller actions without jeopardising patient safety.

# Chapter 7

# Control Software Application: Implementation and Validation for use in Clinical Trials

## 7.1 Introduction

The Department of Endocrinology of the Hospital Clínico Universitario de Valencia, the Hospital Clínic i Universitari de Barcelona, the Institute of Control Systems and Industrial Computing at the Universitat Politècnica de València and the Institute of Informatics and Applications at the Universitat de Girona are part of an interdisciplinary research group that clinically validated the novel blood glucose control algorithm for closed-loop glycaemic control, which implements the SAFE layer as presented in the previous chapter.

Standardised meal tests are performed in T1D subjects treated with CSII therapy to compare the administration of a classical bolus (open-loop study) with a controller-driven prandial insulin delivery (closed-loop study) based on continuous subcutaneous glucose monitoring (CGM). Significant advances in postprandial control in terms of reduction of postprandial glucose variability and of the incidence of hypoglycaemia are expected.

In this chapter, the software application designed to validate and test the robustness of the control algorithms outlined. First, a protocol summary about the planned study is presented. Second, an overview of the main features related to the control software application is provided. Last, implementation and validation of the generated control device (software with embedded control algorithm) are briefly presented. Introductory information regarding technical documentation required by the regulatory agency for the control device to be used in clinical trials is also presented (León-Vargas et al., 2013a).

## 7.2 Study Protocol Summary

**Title**

Improving postprandial glycaemia by a new developed closed-loop control system (Closed-loop4meals)

**Investigators**

Hospital Clínico Universitario de Valencia (study site), Hospital Clínic i Universitari de Barcelona (study site), Universidad Politécnica de Valencia, and Universitat de Girona (Engineering team).

**Objective**

Clinical validation of a new algorithm for closed-loop control of postprandial glucose in comparison with a standard bolus (open-loop control), in T1D subjects using insulin pump therapy.

**Design**

Randomized, prospective, multicentric (Hospital Clínico Universitario de Valencia y Hospital Clínic de Barcelona), single-blind, one-way, repeated measures (four periods, two sequences) crossover study on T1D subjects under insulin pump therapy.

**Population**

Eligible subjects will be patients with T1D for more than one year, aged between 18 and 60 years and with a body mass index (BMI) between 18 and 30 kg/m2 intensive insulin therapy by means of continuous subcutaneous insulin infusion (CSII) for at least 6 months before screening, glycosylated haemoglobin between 6.0% and 8.5%; without advanced chronic micro- and macroangiopathic diabetic complications.

**Sample size**

Twenty subjects with T1D under CSII therapy.

**Treatments**

Closed-loop insulin administration (with an engineering-developed glucose controller) will be tested and compared with standard insulin treatment (Open-loop) in the postprandial state. Assessment and validation of the Closed-loop will be carried out through the execution of four 8-hour mixed meal tests. Each subject will undergo two mixed meals with Open-loop control and the other two meals with Closed-loop controlled insulin administration.

**Study variables**

**Primary variable**

The primary variable will be the coefficient of variation of the area under the curve (AUC) of plasma glucose (PG) during the postprandial period (CV AUC-PG0-8h).

**Secondary variables**

Secondary variables will be the following:

1. CV of PG during the early (CV AUC-PG0-3h) and the late (CV AUC-PG3-8h) postprandial phases.
2. AUC0-8h, AUC0-3h and AUC3-8h of PG.
3. Time spent in an acceptable glycaemic range (70-180 mg/dl), during the 0-8h, 0-3h and the 3-8h postprandial period.
4. Maximum (Cmax) and time to maximum (Tmax) of PG.

**Safety data**

- Physical examination Haematology, clinical chemistry, and urine analysis.
- Standard 12-lead electrocardiogram.
- Monitoring of any adverse event rose during experiments.

**Study duration and dates**

The expected duration of this study will be 12 months, with subject recruitment planned to start in September 2013 and ending of experiments projected until October 2014.

## 7.3 Software Description

The investigational control device comprised the software application that implemented the control algorithm. This control algorithm implements the safety auxiliary feedback element (SAFE), which was evaluated in the previous chapter. The main controller in this study is based on a PID algorithm that includes information from conventional open-loop therapy. The software application includes a graphical interface for the input and display of data and contains the required modules for implementation and execution of the control algorithm for use in clinical trials. The main characteristics of the software application are described in the next section.

### 7.3.1 System Requirements

The following requirements must be fulfilled to install the software application:

| | |
|---|---|
| Operating system | Preinstalled versions of Windows 7, 32-bit Home Basic / Home Premium / Professional / Enterprise / Ultimate (SP 1) |
| Processor | 32-bit (x86) at 1 GHz or higher |
| RAM | 1 GB minimum |
| Hard drive | 200 MB required for installation |
| Screen resolution | 1360 x 768 pixels recommended |

### 7.3.2 Software Framework

The software framework is illustrated in Figure 7.1. The framework begins with the login user request, which limits the use of the application to users that previously registered in a database that maintains a tracking log, see Figure 7.2.

This software must be simultaneously run on two computers. One computer serves as the **principal** computer and the other computer serves as a **backup**. Thus, in the event of failure or abnormal operation, a suspension of control activity or loss of historical data are prevented. As different functions are performed by each computer, two modes of execution are available in the software: in the *principal*, the application is used to perform control actions and log procedures; in the *backup*, the application waits for a recovery request to act in *principal* mode, as shown in Figure 7.3.

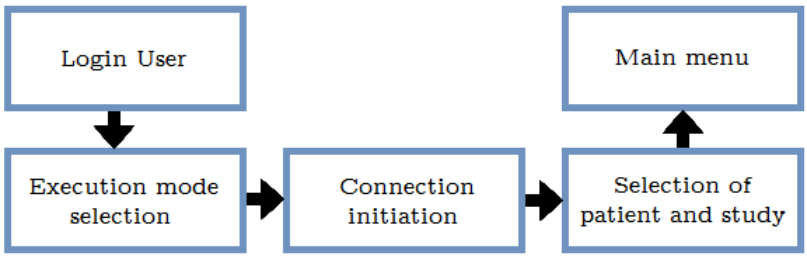


Figure 7.1: Software framework.

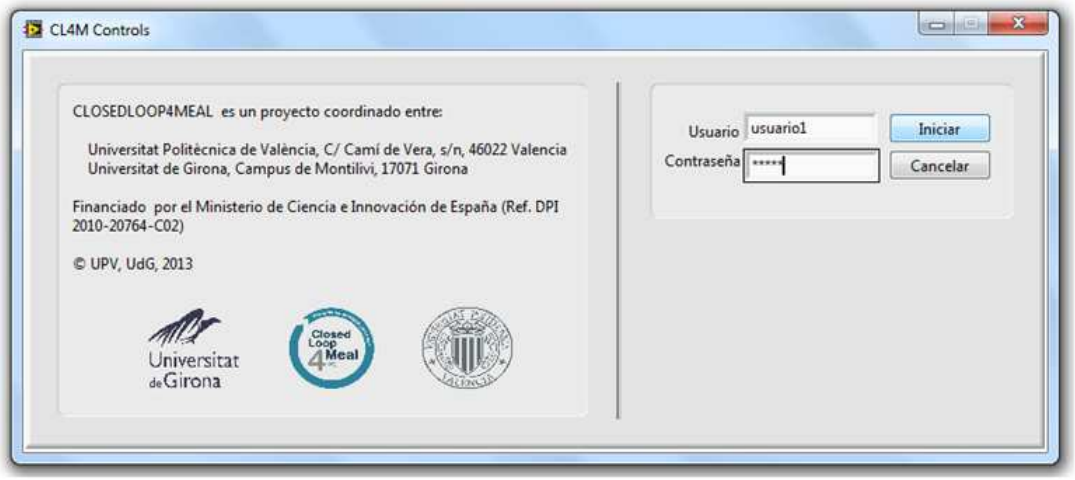


Figure 7.2: Login user.

The establishment of the connection between the computers is performed using the specified file paths of two shared folders; one previously created folder on each computer. This connection setup evaluates whether proper communication is performed by verifying reading and writing options on both folders. When this procedure is verified, the user interface is updated, as shown in Figure 7.3.

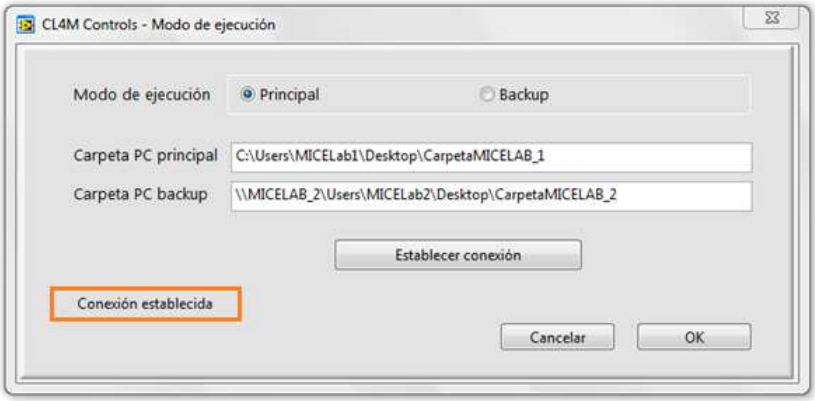


Figure 7.3: Execution mode and Connection confirmation.

The patient is selected from a dropdown list of all available patients who have been previously

incorporated in the data folder of the application. The patient information can be subsequently visualised in an additional table from the main menu, see Figure 7.4. The options displayed in the main user interface are dependent on the type of study to be performed, i.e., if it is an open- or closed-loop test, as shown in Figure 7.5.

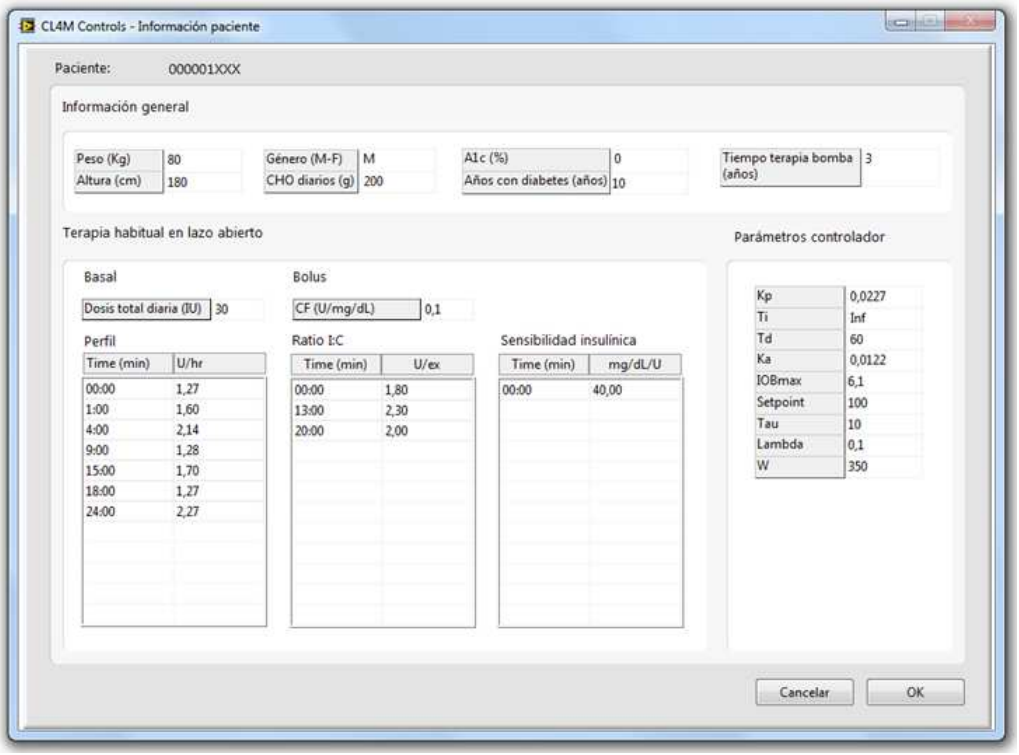


Figure 7.4: Information chart of clinical parameters for the patient selected and respective settings of the control algorithm.

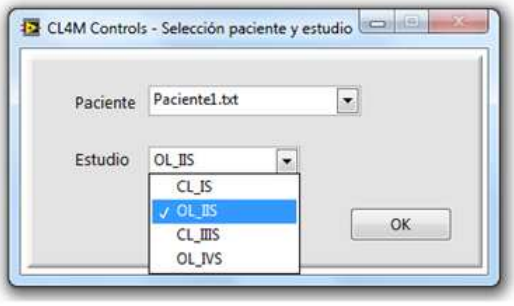


Figure 7.5: Selection of patient and type of study.

The main function of the software is performed in the main menu of the user interface. This menu include options for enabling the start/stop record, start/stop control, introduction of glucose measurements and visualisation of ARD errors, confirmation of suggested and effective insulin values, confirmation of the intake event, input of rescue CHO, and visualisation of glucose and insulin trace, as shown in Figure 7.6. In the registration process, all information about the test (glucose and insulin values, incidences, and events), is stored in each sampling period

in two files, with one for each shared folder to successfully retrieve the information in the event of error or failures.

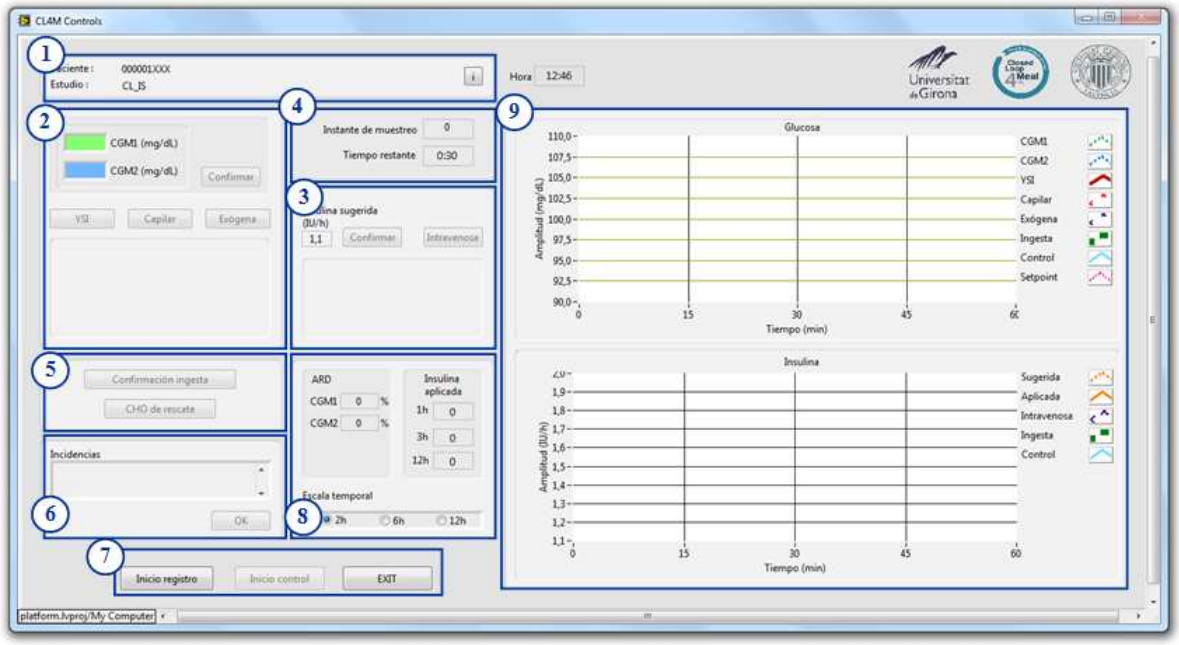


Figure 7.6: Main menu: (1) Patient and study information, (2) glucose data, (3) insulin data, (4) data on sampling times, (5) intake data, (6) incidents, (7) registration, control, and exit options, (8) numeric outputs and temporal scale options of the charts, and (9) glucose and insulin charts.

## 7.4 Implementation and Validation

The closed-loop blood glucose control algorithm used in the control software application is illustrated in Figure 7.7. The SMRC block corresponds to the SAFE layer described previously in section 6.4.1, and the main controller is designed as a hybrid scheme. This block is based on a PID algorithm, in which the derivative component is directly calculated from the glucose measured (approach typically used in industry to prevent control malfunctions of set-point changes). The integrative component is replaced by the basal insulin profile obtained from the open-loop adjustment. The prandial bolus is calculated from the patient' insulin-to-carbohydrate ratio and is incremented to create a super bolus by adding the amount of insulin corresponding to the first hour of postprandial basal insulin. This control scheme is referred as the PDBasal Hybrid SAFE algorithm.

The controller was designed and implemented in the software application and manually performed every 15 min. The platform employed to develop the control software was LabVIEW, which enables a rapid prototyping design. All code implemented in LabVIEW during the design stage of the controller was directly embedded into the software application, which accelerated the process of implementation and validation. Figure 7.8 displays screen shots obtained from the software code implemented in LabVIEW.

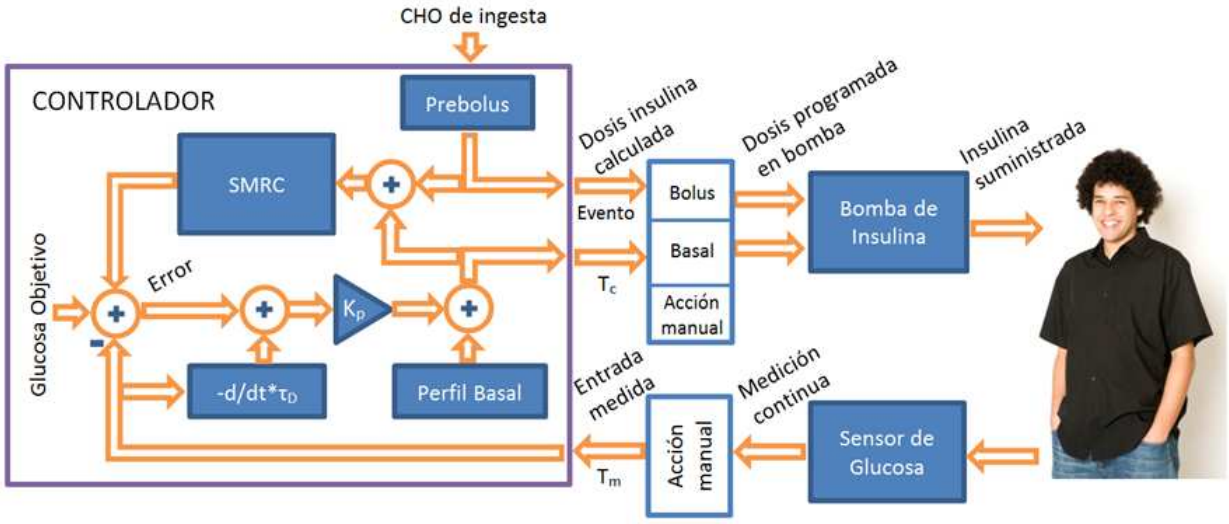


Figure 7.7: General scheme of the controller which will be clinically validated in the multicenter trial: the PDBasal Hybrid SAFE algorithm.

In the validation process, both the PDBasal Hybrid SAFE algorithm and the control software application were validated according to a specific requirement set. Regarding the control algorithm, the following requirements were considered:

- Demonstrate robustness with different nutritional composition of meals, variation in insulin sensitivity, errors in the CGM system readings, delays in the CGM system, delays in the control action, and with variation in insulin action.
- Minimise mid-hypoglycaemia and prevent inducing of severe hypoglycaemia.
- Evaluation with a representative virtual population of the target cohort.

Regarding the software application, the following requirements were considered:

- Specific interface requirements: correct import patient, study and protocol information, start/stop data logging and control, management of inputs, and display and recording of data.
- Correct performance in backup mode operation.

All requirements were successfully accomplished and validated. In the case of the control algorithm, the validation was performed based on the realistic scenario test used in the previous chapter. For the software validation, several tests were conducted to check all the elements that integrate the user interface. Figures 7.9 and 7.10 show graphical outcomes from particular results of these validation tests.

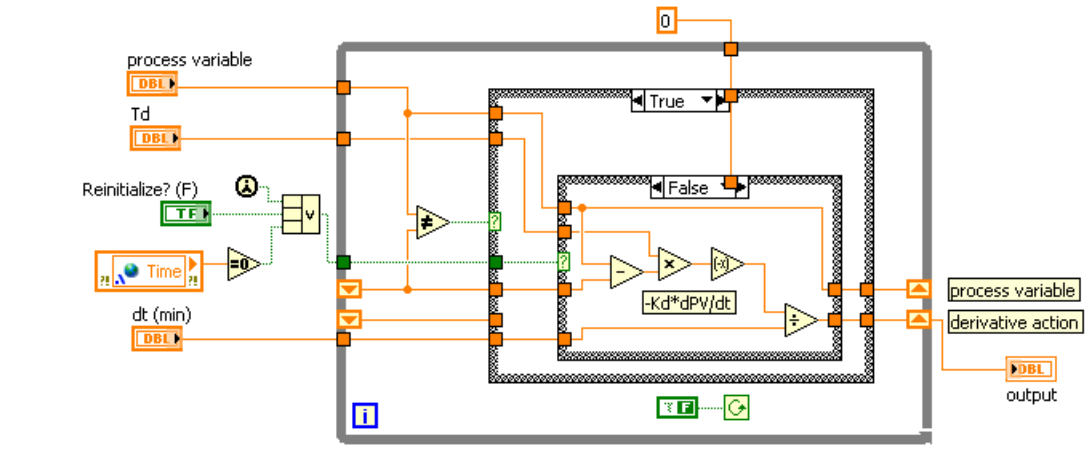


(a)

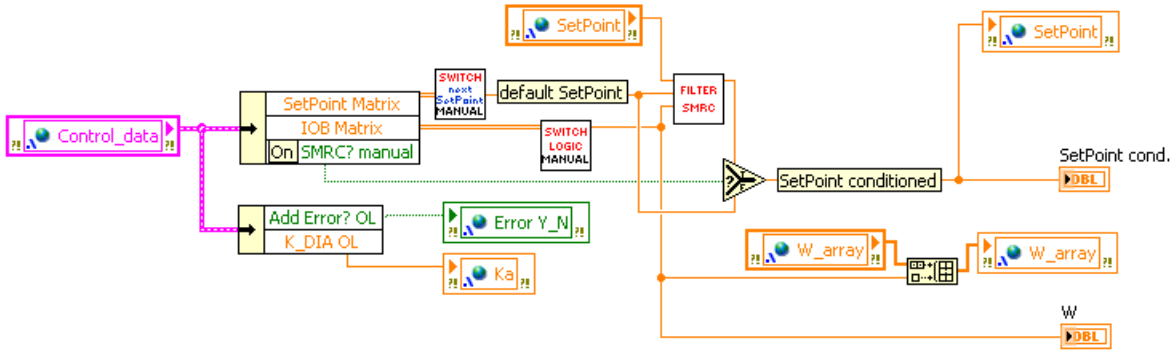


(b)

Figure 7.8: Graphical code in LabVIEW used to implement the (a) derivative action, and the (b) SMRC scheme.

## 7.5 Technical Documentation

Required documents were prepared for approval by the national regulatory agency AEMPS (Agencia Española de Medicamentos y Productos Sanitarios). An outline of the contents of these documents is presented as follows:

1. **Risk Management**: In this document, a risk analysis is performed to identify potential undesirable side effects in normal use of the device (control software) and to assess whether they constitute risks in relation to performance. This analysis includes the identification of hazards and potential risks associated with the manufacture and use of the product and a description of the actions that have been performed to minimise or eliminate the identified risks in conformance with standard technique UNE-EN 14971 (AEMPS).

2.1 **Controller Requirements**: In this document, the requirements to develop and validate this control device were defined. These requirements provide the basis for the development of the controller, its robustness and security properties and the *in silico* validation required for approval by the AEMPS.

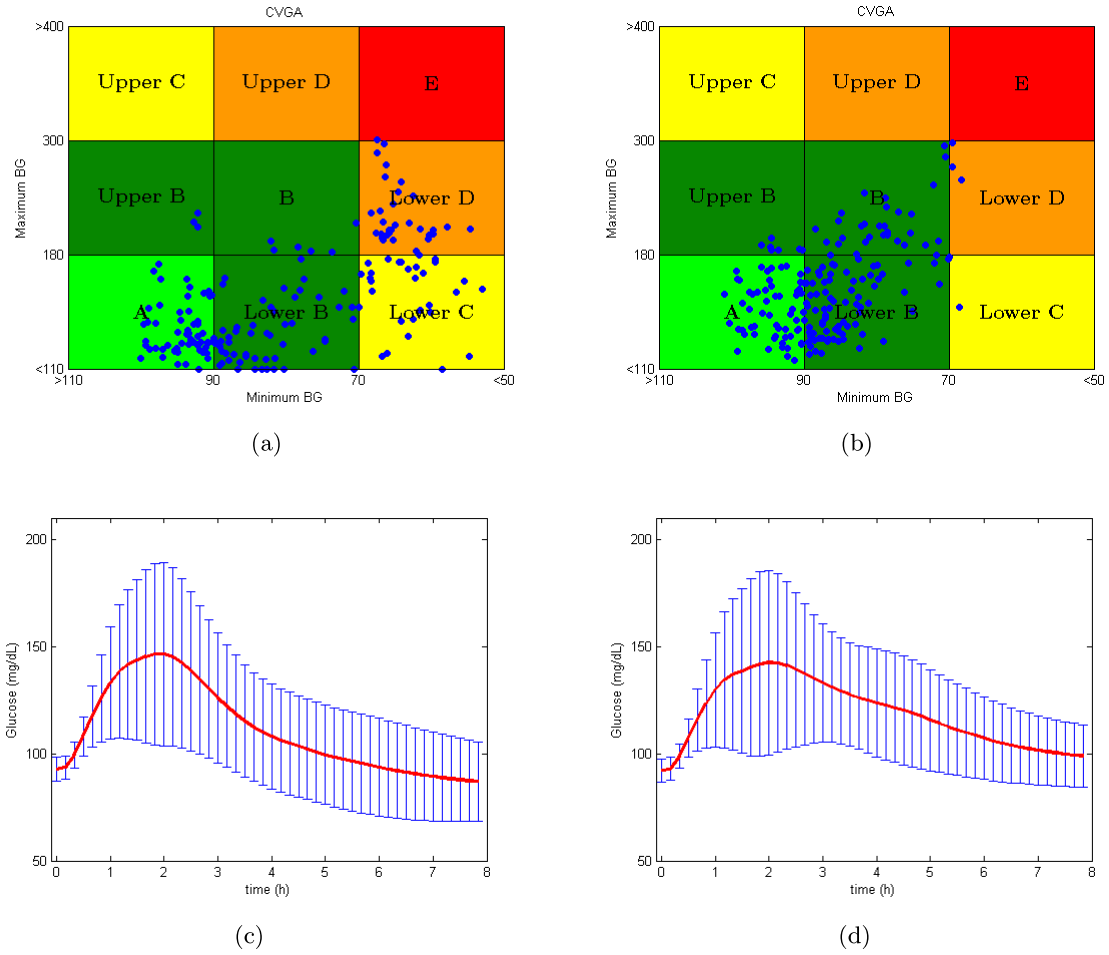


Figure 7.9: CVGA from the test in the (a) open-loop control and (b) closed-loop control; corresponding blood glucose response from the (c) open-loop control and (d) closed-loop control. These results demonstrate better performance of the PDBasal Hybrid SAFE algorithm according to safety and postprandial responses in conventional open-loop therapy.

2.2 **Controller Design**: The design of the device is defined in this document. It describes the control algorithm approach and the visualisation scheme of the software application.

2.3 **Controller Validation**: The validation of the device is defined in this document. It describes a set of validation tests that are performed by the device for strict compliance with the defined requirements.

2.4 **Controller Implementation**: In this document, the implementation of the device is described. All graphical codes regarding the software application and the control algorithm are also presented.

3. **User Manual of the control software application**: This document includes a user manual for the device. It details each of the steps to be performed during the software initial-

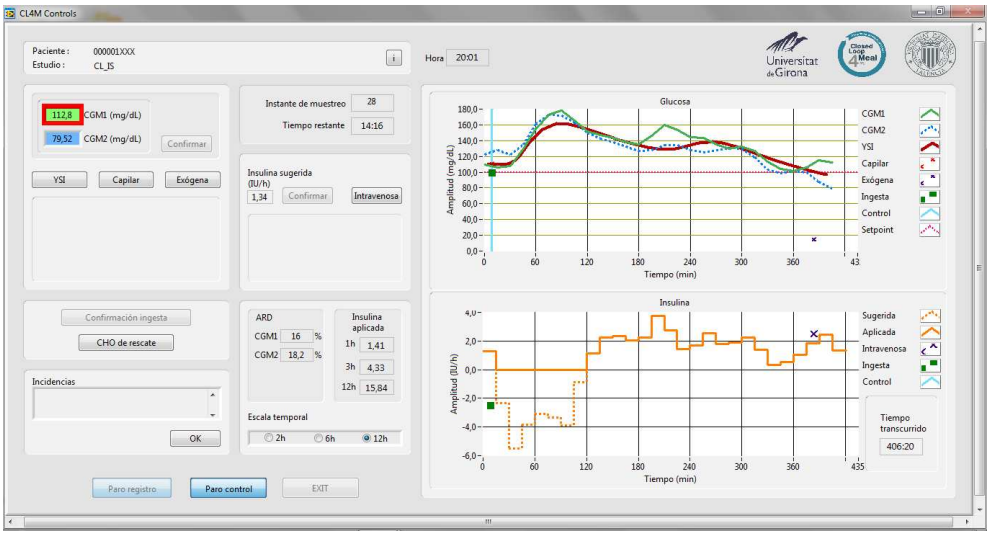


Figure 7.10: Real-time validation test of the software application.

isation and execution process and also describes each element included in the graphical user interface.

# Chapter 8

# Conclusions and Future Work

This thesis concludes by noting the contributions presented in the previous chapters. Potential future research on the subject of this thesis is also discussed.

## 8.1 Contributions

The main contribution of this thesis is the development of efficient and safe open- and closed-loop strategies for postprandial glucose control in Type 1 diabetic patients. A closed-loop blood glucose control algorithm, which was designed and developed in this thesis, is expected to be validated in a multicentre clinical trial. The contributions of the thesis are summarised as follows:

- A virtual environment for intensive and realistic preclinical testing and validation of blood glucose controllers was developed. Realistic scenarios can be simply performed in this virtual environment. The main options include intra-patient circadian variation of insulin sensitivity, customised dynamics for patient model parameters, estimated rate of glucose appearance profiles from a sizable library of mixed meals, real features and failures of insulin pumps and continuous glucose monitoring systems, and several numerical and graphical outcome metrics. The virtual environment was designed to facilitate a flexible definition of the control scenario from a unique graphical user interface and was implemented based on a graphical system design approach using the LabVIEW platform.

- An innovative and efficient postprandial control algorithm based on basal-bolus coordination for implementation in smart insulin pumps was developed and tested. Analyses of interval simulations, physiological assumptions, and search domain contractions were completed. As a limitation, the method relies on a mathematical model including meal absorption. Studies to validate the clinical efficiency of the control algorithm are needed.

- Closed-loop postprandial control algorithms that exhibit acceptable postprandial responses were developed and extensively tested. In these algorithms, the risk of late hypoglycaemic events was limited by insulin-on-board constraints to maintain safety. Sliding mode techniques were employed to gain robustness against parameter uncertainty and variability (which may cause severe hypoglycaemic events) by implementing a secondary loop without affecting the main control design. The results from the *in silico* evaluation indicate that the proposed controllers were successful in reducing the number of hypoglycaemic events without increasing the period of hyperglycaemia. They also demonstrate robustness with regards to overcorrection of hyper- and hypoglycaemia. The results suggest

that additional improvement in the controller response can be accomplished by lowering the set-point, providing a larger bolus or aggressively tuning the control gains. This evidence resulted in the development of the control algorithm to be employed in clinical trials.

- The new closed-loop postprandial glucose control algorithm designed and developed in this thesis was implemented and extensively evaluated *in silico* as a form of preclinical testing for future use in clinical trials. The control algorithm was embedded in a real-time software application that was specifically designed according to medical and engineering requirements in concordance with the national regulatory agency for the development of investigational devices (Agencia Española de Medicamentos y Productos Sanitarios, AEMPS). A limitation of this control device for clinical trial use is the lack of automation of the closed-loop system, which requires the input of CGM readings into the computer and subsequent manual alteration of pump settings every 15 minutes by medical staff.

## 8.2 Future Research

To continue the research initiated by this thesis, several improvements should be made to the developed control system to develop a practical application. The first aim is to evaluate the PDBasal Hybrid SAFE blood glucose control algorithm in real T1D patients to validate its performance in the postprandial period.

The second aim is to expand the control algorithm operation to day and night performances, including three "large" meals. In this thesis, a closed-loop control in the postprandial period was addressed; however, in a practical application of the system, diurnal dynamics must be considered. The development of strategies to evaluate dynamical $IOB$ limitations according to patient variability is also proposed.

A third aim is to develop autotuning capabilities in the control algorithm through smart learning approaches, which consider daily variability and adapt system performance according to long-term changes.

Last, a supervisory scheme for the control system that implements additional real-time information about the patient, such as heart rate, body temperature, and qualitative health signs, should be developed to govern and adapt different operation modes of the control algorithm according to a patient's current condition (physical activity, stress, and illness).

# Bibliography


Abu-Rmileh, A., Garcia-Gabin, W., and Zambrano, D. (2010). Internal model sliding mode control approach for glucose regulation in type 1 diabetes. *Biomedical Signal Processing and Control*, 5(2):94 – 102.

Agar, B. U., Eren, M., and Cinar, A. (2005). Glucosim: Educational software for virtual experiments with patients with type 1 diabetes. *Proc. IEEE eng. med. biolo. soc.*, pages 845–848.

Alamaireh, M. (2006). A predictive neural network control approach in diabetes management by insulin administration. *Proceedings of the 2nd IEEE International Conference on Information and Communication Technologes*, pages 1618–1623.

Alefeld, G. and Herzberger, J. (1983). *Interval Analysis*.

American Diabetes Association (2012). Diagnosis and classification of diabetes mellitus. *Diabetes Care*, 35(Supplement 1):S64–S71.

Atlas, E., Nimri, R., Miller, S., Grunberg, E. A., and Phillip, M. (2010). Md-logic artificial pancreas systems. *Diabetes care*, 33(5):1072–1076.

Barajas-Solano, C., Bondia, J., Calm, R., Herrero, P., and Vehí, J. (2012). A review of absorption models for mixed meals. In *5th International Conference on Advanced Treatments & Technologies for Diabetes*.

Barrett, P. H., Bell, B. M., Cobelli, C., Golde, H., Schumitzky, A., Vicini, P., and Foster, D. (1998). Saam ii: Simulation, analysis, and modeling software for tracer and pharmacokinetic studies. *Metabolism*, 47:484–492.

Bell, D. and Ovalle, F. (2000). Improved glycemic control with use of continuous subcutaneous insulin infusion compared with multiple insulin injection therapy. *Endocr Pract*, 6:357–360.

Bellazzi, R., Nucci, G., and Cobelli, C. (2001). The subcutaneous route to insulin-dependent diabetes therapy. *IEEE Engineering in Medicine and Biology Magazine*, 20(1):54–64.

Bequette, B. (2005). A critical assessment of algorithms and challenges in the development of a closed-loop artificial pancreas. *Diabetes technology & therapeutics*, 7(1):28–47.

Berger, M. and Rodbard, D. (1989). Computer simulation of plasma insulin and glucose dynamics after subcutaneous insulin injection. *Diabetes Care*, 12(10):725–736.

Bliss, M. (2007). *The discovery of insulin. 25th anniversary ed.* The University of Chicago Press.

Bode, B. (2011). Comparison of pharmacokinetic properties, physicochemical stability, and pump compatibility of 3 rapid-acting insulin analogues-aspart, lispro, and glulisine. *Endocrine Practice*, 17(2):271–280.

Bondia, J., Dassau, E., Zisser, H., Calm, R., Vehí, J., Jovanovic, L., and III, F. D. (2009). Coordinated basal-bolus infusion for tighter postprandial glucose control in insulin pump therapy. *J. Diabetes Sci. Technol.,*, 3 (1):89–97.

Brazeau, A. S., Mircescu, H., Desjardins, K., Leroux, C., Strychar, I., Ekoé, J., and Rabasa-Lhoret, R. (2013). Carbohydrate counting accuracy and blood glucose variability in adults with type 1 diabetes. *Diabetes Research and Clinical Practice*, 99(1):19–23.

Breton, M., Farret, A., Bruttomesso, D., Anderson, S., Magni, L., Patek, S., Dalla Man, C., Place, J., Demartini, S., Del Favero, S., et al. (2012). Fully integrated artificial pancreas in type 1 diabetes modular closed-loop glucose control maintains near normoglycemia. *Diabetes*, 61(9):2230–2237.

Breton, M. and Kovatchev, B. (2008). Analysis modeling and simulation of the accuracy of continuous glucose sensors. *Journal of Diabetes Science and Technology*, 2(5):853–862.

Bruttomesso, D., Farret, A., Costa, S., Marescotti, M., Vettore, M., Avogaro, A., Tiengo, A., Dalla Man, C., Place, J., Facchinetti, A., Guerra, S., Magni, L., De Nicolao, G., Cobelli, C., Renard, E., and Maran, A. (2009). Closed-loop artificial pancreas using subcutaneous glucose sensing and insulin delivery and a model predictive control algorithm: preliminary studies in padova and montpellier. *Journal of diabetes science and technology*, 3(5):1014–1021. cited By (since 1996) 30.

Buckingham, B., Chase, H., Dassau, E., Cobry, E., Clinton, P., Gage, V., Caswell, K., Wilkinson, J., Cameron, F., Lee, H., Bequette, B., and Doyle, F. r. (2010). Prevention of nocturnal hypoglycemia using predictive alarm algorithms and insulin pump suspension. *Diabetes Care*, 33:1013–1017.

Buse, J., Dailey, G., Ahmann, A., Bergenstal, R., Green, J., Peoples, T., Tanenberg, R., and Yang, Q. (2011). Baseline predictors of a1c reduction in adults using sensor-augmented pump therapy or multiple daily injection therapy: the star 3 experience. *Diabetes Technology and Therapeutics*, 13(6):601–606.

Calm, R., García-Jaramillo, M., Bondia, J., Sainz, M. A., and Vehí, J. (2011). Comparison of interval and monte carlo simulation for the prediction of postprandial glucose under uncertainty in type 1 diabetes mellitus. *Computer Methods and Program in Biomedicine*, 104 (3):325–332.

Camacho, E. and Bordons, C. (1999). *Model Predictive Control*.

Cameron, F., Bequette, B. W., Wilson, D. M., Buckingham, B. A., Lee, H., and Niemeyer, G. A. (2011). Closed-loop artificial pancreas based on risk management. *Journal of Diabetes Science and Technology*, 5(2):368–379.

Cameron, F., Niemeyer, G., and Bequette, B. W. (2012). Extended multiple model prediction with application to blood glucose regulation. *Journal of Process Control*, 22(8):1422–1432.

Campbell, N., Williamson, B., and Heyden, R. (2006). *Biology Exploring Life*. Pearson Prentice Hall.

Campos-Delgado, D., Hernandez-Ordonez, M., Femat, R., and Gordillo-Moscoso, A. (2006). Fuzzy-based controller for glucose regulation in type-1 diabetic patients by subcutaneous route. *IEEE Transactions on Biomedical Engineering*, 53(11):2201–2210.

Castle, J., Engle, J., Youssef, J., Massoud, R., Yuen, K., Kagan, R., and Ward, W. (2010). Novel use of glucagon in a closed-loop system for prevention of hypoglycemia in type 1 diabetes. *Diabetes Care*, 33(6):1282–1287.

Cengiz, E. and Tamborlane, W. V. (2009). A tale of two compartments: Interstitial versus blood glucose monitoring. *Diabetes Technology and Therapeutics*, 11:S11–S16.

Chase, H. P., Saib, S. Z., MacKenzie, T., Hansen, M. M., and Garg, S. K. (2002). Post-prandial glucose excursions following four methods of bolus insulin administration in subjects with type 1 diabetes. *Diabetic Med*, 19 (4):317–321.

Chassin, L. (2005). *In silico testing of glucose controllers: Methodology and sample application.* PhD thesis, City University London.

Chassin, L., Wilinska, M., and Hovorka, R. (2005). Grading system to assess clinical performance of closed-loop glucose control. *Diabetes Technology and Therapeutics*, 7(1):72–82.

Chassin, L. J., Wilinska, M. E., and Hovorka, R. (2004). Evaluation of glucose controllers in virtual environment: methodology and sample application. *Artificial Intelligence in Medicine*, 32:171–181.

Chee, F., Savkin, A., Fernando, T., and Nahavandi, S. (2005). Optimal $h_\infty$ insulin injection control for blood glucose regulation in diabetic patients. *IEEE Transactions on Biomedical Engineering*, 52(10):1625–1631.

Chen, J., Cao, K., Sun, Y., Xiao, Y., and Su, X. (2008). Continuous drug infusion for diabetes therapy: a closed-loop control system design. *Journal on Wireless Communications and Networking*, 2008:10.

Cheyne, E., Cavan, D., and Kerr, D. (2002). Performance of continuous glucose monitoring system during controlled hypoglycemia in healthy volunteers. *Diabetes Technology and Therapeutics*, 4:607–613.

Clarke, W., Anderson, S., Breton, M., Patek, S., Kashmer, L., and Kovatchev, B. (2009). Closed-loop artificial pancreas using subcutaneous glucose sensing and insulin delivery and a model predictive control algorithm: the virginia experience. *Journal of Diabetes Science and Technology*, 3(5):1031–8.

Clarke, W., Anderson, S., Farhy, L., Breton, M., Gonder-Frederick, L., Cox, D., and Kovatchev, B. (2005). Evaluating the clinical accuracy of two continuous glucose sensors using continuous glucose-error grid analysis (cg-ega). *Diabetes Care*, 28:2412–2417.

Clarke, W. and Kovatchev, B. (2007). Continuous glucose sensors: continuing questions about clinical accuracy. *Journal of Diabetes Science and Technology*, 1(5):669–675.

Clemens, A. (1979). Feedback control dynamics for glucose controlled insulin infusion system. *Medical Progress Through Technology*, 6(3):91–98.

Cobelli, C., Renard, E., and Kovatchev, B. (2011). Artificial pancreas: past, present, future. *Diabetes*, 60(11):2672–2682.

Cobelli, C., Renard, E., Kovatchev, B., Keith-Hynes, P., Ben Brahim, N., Place, J., Del Favero, S., Breton, M., Farret, A., Bruttomesso, D., Dassau, E., Zisser, H., Doyle, F. r., Patek, S., and Avogaro, A. (2012). Pilot studies of wearable outpatient artificial pancreas in type 1 diabetes. *Diabetes Care*, 35(9):65–67.

Dalla Man, C., Rizza, R., and Cobelli, C. (2007). Meal simulation model of the glucose-insulin system. *IEEE Transactions on Biomedical Engineering*, 54(10):1740–1749. cited By (since 1996) 118.

Dalla Man, C., Breton, M., and Cobelli, C. (2009). Physical activity into the meal glucose-insulin model of type 1 diabetes: In silico studies. *Journal of Diabetes Science and Technology*, 3(1):56–67.

Dalla Man, C., Camilleri, M., and Cobelli, C. (2006). A system model of oral glucose absorption: Validation on gold standard data. *IEEE Transactions on Biomedical Engineering*, 53:2472–2478.

Dalla Man, C., Raimondo, D., Rizza, R., and Cobelli, C. (2007). Gim, simulation software of meal glucose-insulin model. *Journal of Diabetes Science and Technology*, 1(3):323–330.

Dassau, E., Palerm, C., Zisser, H., Buckingham, B., Jovanovic, L., and Doyle, F. (2009). In silico evaluation platform for artificial pancreatic beta-cell development–a dynamic simulator for closed-loop control with hardware-in-the-loop. *Diabetes Technology and Therapeutics*, 11(3):187–194.

Dassau, E., Zisser, H., Harvey, R. A., Percival, M. W., Grosman, B., Bevier, W., Atlas, E., Miller, S., Nimri, R., Jovanovic, L., and Doyle, F. J. (2013). Clinical evaluation of a personalized artificial pancreas. *Diabetes Care*, 36(4):801–809.

Davidson, P., Hebblewhite, H., Steed, R., and Bode, B. (2008). Analysis of guidelines for basal-bolus dosing: basal insulin, correction factor, and carbohydrate-to-insulin ratio. *Endocrine Practice*, 14(9):1095–1101.

Dazzi, D., Taddei, F., Gavarini, A., Uggeri, E., Negro, R., and Pezzarossa, A. (2001). The control of blood glucose in the critical diabetic patient: a neuro-fuzzy method. *J Diabetes Complications*, 15(2):80–87.

de Canete, J. F., Gonzalez-Perez, S., and Ramos-Diaz, J. (2012). Artificial neural networks for closed loop control of in silico and ad hoc type 1 diabetes. *Computer Methods and Programs in Biomedicine*, 106(1):55 – 66.

Devries, J. H., Avogaro, A., Benesch, C., Bruttomesso, D., Caldwell, K., and Cobelli, C. (2012). On behalf of the ap@home consortium. comparison of two closed loop algorithms with open loop control in type 1 diabetes. *Diabetes*, 61(Suppl. 1):A60.

Diabetes Control and Complications Trial Research Group (1993). The effect of intensive treatment of diabetes on the development and progression of long-term complications in insulin-dependent diabetes mellitus. *The New England Journal of Medicine*, 329:977–986.

Doyle (Boland), E. A., Weinzimer, S. A., Steffen, A. T., Ahern, J. A. H., Vincent, M., and Tamborlane, W. V. (2004). A randomized, prospective trial comparing the efficacy of continuous subcutaneous insulin infusion with multiple daily injections using insulin glargine. *Diabetes Care*, 27(7):1554–1558.

Dua, P., Doyle III, F. J., and Pistikopoulos, E. N. (2006). Model-based blood glucose control for type 1 diabetes via parametric programming. *IEEE Trans. Biomed. Eng.*, 53(6):1478–1491.

Eddy, D. and Schlessinger, L. (2003). Archimedes: a trial-validate model of diabetes. *Diabetes Care*, 26:3093–3101.

El-Jabali, A. (2005). Neural network modeling and control of type 1 diabetes mellitus. *Bioprocess Biosyst Eng*, 27(2):75–79.

El-Khatib, F., Russell, S., Nathan, D., Sutherlin, R., and Damiano, E. (2010). A bihormonal closed-loop artificial pancreas for type 1 diabetes. *Science Translational Medicine*, 2(27):27ra27.

El-Khatib, F. H., Jiang, J., and Damiano, E. R. (2007). Adaptive closed-loop control provides blood-glucose regulation using dual subcutaneous insulin and glucagon infusion in diabetic swine. *Journal of Diabetes Science and Technology*, 1(2):181–192.

El-Khatib, F. H., Jiang, J., and Damiano, E. R. (2009). A feasibility study of bihormonal closed-loop blood glucose control using dual subcutaneous infusion of insulin and glucagon in ambulatory diabetic swine. *Journal of Diabetes Science and Technology*, 3(4):789–803.

El Youssef, J., Castle, J., Branigan, D., Massoud, R., Breen, M., Jacobs, P., Bequette, B., and Ward, W. (2011). A controlled study of the effectiveness of an adaptive closed-loop algorithm to minimize corticosteroid-induced stress hyperglycemia in type 1 diabetes. *Journal of Diabetes Science and Technology*, 5(6):1312–1326.

Elleri, D., Allen, J., Kumareswaran, K., Leelarathna, L., Grainger, S., Caldwell, K., Wilinska, M., Nodale, M., Acerini, C., Dunger, D., and Hovorka, R. (2011a). Day-and-night closed loop (cl) glucose control in adolescents with type 1 diabetes (t1d). *Diabetes*, 60(Suppl 1):A41.

Elleri, D., Allen, J., Kumareswaran, K., Leelarathna, L., Nodale, M., Caldwell, K., Cheng, P., Kollman, C., Haidar, A., Murphy, H., Wilinska, M., Acerini, C., Dunger, D., and Hovorka, R. (2013). Closed-loop basal insulin delivery over 36 hours in adolescents with type 1 diabetes: randomized clinical trial. *Diabetes Care*, 36(4):838–844.

Elleri, D., Allen, J. M., Nodale, M., Wilinska, M. E., Mangat, J. S., Larsen, A. M. F., Acerini, C. L., Dunger, D. B., and Hovorka, R. (2011b). Automated Overnight Closed-Loop Glucose Control in Young Children with Type 1 Diabetes. *Diabetes Technology & Therapeutics*, 13(4):416–424.

Ellingsen, C., Dassau, E., Zisser, H., Grosman, B., Percival, M., Jovanovic, L., and Doyle 3rd., F. (2009). Safety constraints in an artificial pancreatic beta cell: an implementation of model predictive control with insulin on board. *Journal of diabetes science and technology*, 3(3):536–544.

El Youssef, J., Castle, J., and Kenneth Ward, W. (2009). A review of closed-loop algorithms for glycemic control in the treatment of type 1 diabetes. *Algorithms*, 2(1):518–532.

Eren-Oruklu, M., Cinar, A., Quinn, L., and Smith, D. (2009). Adaptive control strategy for regulation of blood glucose levels in patients with type 1 diabetes. *Journal of Process Control*, 19:1333–1346.

Facchinetti, A., Sparacino, G., and Cobelli, C. (2010). Modeling the error of continuous glucose monitoring sensor data: critical aspects discussed through simulation studies. *Journal of Diabetes Science and Technology*, 4(1):4–14.

Fatourechi, M., Kudva, Y., Murad, M., Elamin, M., Tabini, C., and Montori, V. (2008). Hypoglycemia with intensive insulin therapy: a systematic review and meta-analyses of randomized trials of continuous subcutaneous insulin infusion versus multiple daily injections. *Journal of Clinical Endocrinology & Metabolism*, 94(3):729–740.

Finan, D., Zisser, H., Jovanovic, L., Bevier, W., and Seborg, D. (2007). Practical issues in the identification of empirical models from simulated type 1 diabetes data. *Diabetes Technology & Therapeutics*, 9(5):438–450.

Gantt, J., Rochelle, K., and Gatzke, E. (2007). Type 1 diabetic patient insulin delivery using asymmetric pi control. *Chemical Engineering Communications*, 194(5):586–602.

García-Jaramillo, M. (2011). *Prediction of postprandial blood glucose under intra-patient variability and uncertainty and its use in the design of insulin dosing strategies for type 1 diabetic patients*. PhD thesis, Universitat de Girona.

Garelli, F., Mantz, R., and De Battista, H. (2011). *Advanced control for constrained processes and systems (Control Engineering)*. The Institution of Engineering and Technology.

Gerritsen, M., Jansen, J., and Lutterman., J. (1999). Performance of subcutaneously implanted glucose sensors for continuous monitoring. *The Netherlands Journal of Medicine*, 54:167–179.

Gopakumaran, B., Duman, H., Overholser, D., Federiuk, I., Quinn, M., Wood, M., and Ward, W. (2005). A novel insulin delivery algorithm in rats with type 1 diabetes: the fading memory proportional-derivative method. *Artificial Organs*, 29(8):599–607.

Graff, M. R., Gross, T. M., Juth, S. E., and Charlson, J. (2000). How well are individuals on intensive insulin therapy counting carbohydrates? *Diabetes Research and Clinical Practice*, 50:S238.

Gross, T., Bode, B., Einhorn, D., Kayne, D., Reed, J., White, N., and Mastrototaro, J. (2000). Performance evaluation of the minimed continuous glucose monitoring system during patient home use. *Diabetes Technology and Therapeutics*, 2(1):49–56.

Guilhem, I., Leguerrier, A., Lecordier, F., Poirier, J. Y., and Maugendre, D. (2006). Technical risks with subcutaneous insulin infusion. *Diabetes and Metabolism*, 32(3):279–284.

Haidar, A., Legault, L., Dallaire, M., Alkhateeb, A., Coriati, A., Messier, V., Cheng, P., Millette, M., Boulet, B., and Rabasa-Lhoret, R. S. (2013). Glucose-responsive insulin and glucagon delivery (dual-hormone artificial pancreas) in adults with type 1 diabetes: a randomized crossover controlled trial. *Canadian Medical Association Journal*, 185(4):297–305.

Hanas, R. (2007). *Type 1 Diabetes in Children, Adolescents, and Young Adults: How to Become an Expert on Your Own Diabetes*. Class Publishing Ltd.

Heinemann, L. (2002). Variability of insulin absorption and insulin action. *Diabetes Technology and Therapeutics*, 4(5):673–682.

Heinemann, L. (2009). Insulin pump therapy: what is the evidence for using different types of boluses for coverage of prandial insulin requirements? *Journal of Diabetes Science and Technology*, 3(6):1490–1500.

Heinemann, L., Benesch, C., and DeVries, J. (2011). Ap@home: a novel european approach to bring the artificial pancreas home. *Journal of Diabetes Science and Technology*, 5:1363–1372.

Hernandez-Ordonez, M. and Campos-Delgado., D. U. (2006). Modelling light and moderate exercise in type 1 biadetic patints with glycogen depletion and replenishment. In *In 6th IFAC Symposium*, pages 465–470.

Hernández-Ordoñez, M., Montano, O., Campos-Delgado, D., and Palacios, E. (2007). Development of an educational simulator and graphical user interface for diabetic patients. In *4th International Conference on Electrical and Electronics Engineering*.

Herrero, P., Bondia, J., Palerm, C. C., Vehí, J., Georgiou, P., Oliver, N., and Toumazou, C. (2012). A simple robust method for estimating the glucose rate of appearance from mixed meals. *Journal of diabetes science and technology*, 6(1):153–162.

Hirsch, I. (2005). Insulin analogues. *The New England Journal of Medicine*, 352(2):174–183.

Holmes, G., Galitz, L., Hu, P., and Lyness, W. (2005). Pharmacokinetics of insulin aspart in obesity, renal impairment, or hepatic impairment. *Journal of Clinical Pharmacology*, 60:469–476.

Hovorka, R. (2006). Continuous glucose monitoring and closed-loop systems. *Diabetic Medicine*, 23(1):1–12.

Hovorka, R. (2011). Closed-loop insulin delivery: from bench to clinical practice. *Nature Reviews Endocrinology*, 7:385–395.

Hovorka, R., Allen, J., Elleri, D., Chassin, L., Harris, J., Xing, D., Kollman, C., Hovorka, T., Larsen, A., Nodale, M., De Palma, A., Wilinska, M., Acerini, C., and Dunger, D. (2010). Manual closed-loop insulin delivery in children and adolescents with type 1 diabetes: a phase 2 randomised crossover trial. *The Lancet*, 375(9716):743–751.

Hovorka, R., Canonico, V., Chassin, L. J., Haueter, U., Massi-Benedetti, M., Federici, M. O., Pieber, T. R., Schaller, H., Schaupp, L., Vering, T., and Wilinska, M. E. (2004a). Nonlinear model predictive control of glucose concentration in subjects with type 1 diabetes. *Physiological Measurement*, 25:905–920.

Hovorka, R., Chassin, L. J., Wilinska, M. E., Canonico, V., Akwi, J. A., and Federici, O. (2004b). Closing the loop: The adicol experience. *Diabetes Technology and Therapeutics*, 6:307–318.

Hovorka, R., Kremen, J., Blaha, J., Matias, M., Anderlova, K., Bosanska, L., Roubicek, T., Wilinska, M., Chassin, L. J., and Svacina, S. (2007). Blood glucose control by a model predictive control algorithm with variable sampling rate versus a routine glucose management protocol in cardiac surgery patients: a randomized controlled trial. *The Journal of Clinical Endocrinology Metabolism*, 92(8):2960–2964.

Hovorka, R., Kumareswaran, K., Harris, J., Allen, J. M., Elleri, D., Xing, D., Kollman, C., Nodale, M., Murphy, H. R., Dunger, D. B., Amiel, S. A., Heller, S. R., Wilinska, M. E., and Evans, M. L. (2011). Overnight closed loop insulin delivery (artificial pancreas) in adults with type 1 diabetes: crossover randomised controlled studies. *BMJ*, 342:d1855.

Hovorka, R., Shojaee-Moradie, F., Carroll, P., Chassin, L., Gowrie, I., Jackson, N., Tudor, R., Umpleby, A., and Jones, R. (2002). Partitioning glucose distribution/transport, disposal, and endogenous production during ivgtt. *American Journal of Physiology Endocrinology and Metabolism*, 282:992–1007.

International Diabetes Federation (2007). *Guideline for management of postmeal glucose.*

International Diabetes Federation (2011). *IDF Diabetes Atlas 5th edition.*

Jackson, M. A., Caputo, N., Castle, J. R., David, L. L., Jr., C. T. R., and Ward, W. K. (2012). Stable liquid glucagon formulations for rescue treatment and bi-hormonal closed-loop pancreas. *Current Diabetes Reports. December 2012, Volume 12, Issue 6, pp 705-710.*, 12(6):705–710.

Jaulin, L., Kieffer, M., Didrit, O., and E.Walter (2001). *Applied Interval Analysis.*

Kaveh, P. and Shtessel, Y. (2008). Blood glucose regulation via double loop higher order sliding mode control and multiple sampling rate. *Modern Sliding Mode Control Theory*, pages 427–445.

Kienitz, K. and Yoneyama, T. (1993). A robust controller for insulin pumps based on h-infinity theory. *IEEE Trans Biomed Eng*, 40(11):1133–1137.

Klonoff, D. (2012). The current status of bolus calculator decision-support software. *Journal of Diabetes Science and Technology*, 6(5):990–994.

Koschinsky, T., Jungheim, K., and Heinemann, L. (2003). Glucose sensors and the alternate site testing-like phenomenon: relationship between rapid blood glucose changes and glucose sensor signals. *Diabetes Technology and Therapeutics*, 5(5):829–842.

Kovacs, L., Szalay, P., Almassy, Z., and Barkai, L. (2013). Applicability results of a nonlinear model-based robust blood glucose control algorithm. *Journal of Diabetes Science and Technology*, 7(3):708–716.

Kovatchev, B. (2011). Closed loop control for type 1 diabetes. *BMJ*, 342:d1911.

Kovatchev, B., Breton, M., Dalla Man, C., and Cobelli, C. (2009). In silico preclinical trials: a proof of concept in closed-loop control of type 1 diabetes. *Journal of Diabetes Science and Technology*, 3(1):44–55.

Kovatchev, B., Cobelli, C., Renard, E., Anderson, S., Breton, M., Patek, S., Clarke, W., Bruttomesso, D., Maran, A., Costa, S., Avogaro, A., Dalla Man, C., Facchinetti, A., Magni, L. De Nicolao, G., Place, J., and Farret, A. (2010). Multinational study of subcutaneous model-predictive closed-loop control in type 1 diabetes mellitus: Summary of results. *Journal of Diabetes Science and Technology*, 4(6):1374–1381.

Kovatchev, B., GonderFrederick, L., Cox, D., and Clarke, W. (2004). Evaluating the accuracy of continuous glucose monitoring sensors: Continuous glucose error-grid analysis (cg-ega) illustrated by therasense freestyle navigator data. *Diabetes Care*, 27(8):1922–1928.

Kovatchev, B., Raimondo, D. M., Breton, M., Patek, S. D., and Cobelli, C. (2008). In silico testing and in vivo experiments with closed-loop control of blood glucose in diabetes world congress. In *Proceedings of the 17th IFAC World Congress*, volume 17, pages 4234–4239.

Kovatchev, B. P., Cox, D. J., Gonder-Frederick, L. A., and Clarke, W. L. (2002). Methods for quantifying self-monitoring blood glucose profiles exemplified by an examination of blood glucose patterns in patients with type 1 and type 2 diabetes. *Diabetes Technology and Therapeutics*, 4:295–303.

Kovatchev, B. P., Cox, D. J., Gonder-Frederick, L. A., Young-Hyman, D., Schlundt, D., and Clarke, W. L. (1998). Assessment of risk for severe hypoglycemia among adults with iddm: validation of the low blood glucose index. *Diabetes Care*, 21:1870–1875.

Laguna, A., Rossetti, P., Ampudia-Blasco, F., Vehí, J., and Bondia, J. (2010). Optimal design for individual model identification based on ambulatory continuous glucose monitoring in patients with type 1 diabetes. In *UKACC International Conference on CONTROL 2010.*

Lee, H. and Bequette, B. (2009). A closed-loop artificial pancreas based on model predictive control: Human-friendly identification and automatic meal disturbance rejection. *Biomedical Signal Processing and Control*, 4(4):347 – 354.

Lee, H., Buckingham, B., Wilson, D., and Bequette, B. (2009). A closed-loop artificial pancreas using model predictive control and a sliding meal size estimator. *Journal of Diabetes Science and Technology*, 3(5):1082–1090.

Lehmann, E. and Deutsch, T. (1992a). Aida: an automated insulin dosage advisor. In *Annual Symposium on Computer Application in Medical Care*, pages 818–819.

Lehmann, E. and Deutsch, T. (1992b). A physiological model of glucose-insulin interaction in type 1 diabetes mellitus. *Journal of Biomedical Engineering*, 14:235–242.

Lehmann, E., Tarín, C., Bondia, J., Teufel, E., and Deutsch, T. (2009). Incorporating a generic model of subcutaneous insulin absorption into the aida v4 diabetes simulator: (3) early plasma insulin determinations. *Journal of Diabetes Science and Technology*, 3(1):190–201.

Lehmann, E. D. (1999). Experience with the internet release of aida v4.0 - http://www.diabetic.org.uk/aida.htm - an interactive educational diabetes simulator. *Diabetes Technology and Therapeutics*, 1:41–54.

Lehmann, E. D. (2001). The freeware aida interactive educational diabetes simulator - http://www.2aida.org-(1)adownload survey for aida v4.0. *Diagnostics an Medical Technology*, 7:504–515.

León-Vargas, F. (2009). Prototipo de plataforma tecnológica para control en tiempo real de glucemia en pacientes con diabetes tipo 1. Master's thesis, Universitat de Girona.

León-Vargas, F., Bondía, J., and Vehí, J. (2012a). Metodología para generación de pacientes virtuales con diabetes tipo 1. In *14th International Conference on Energy Efficiency ans Sustainability in Ambient Intelligence. June 25-27, Tarragona, Spain.*

León-Vargas, F., Calm, R., Bondia, J., and Vehí, J. (2012b). Improving the computational effort of set-inversion-based prandial insulin delivery for its integration in insulin pumps. *Journal Diabetes Science and Technology*, 6(6):1420–1428.

León-Vargas, F., Carreras, A., Bondia, J., and Vehí, J. (2012c). In-silico evaluation for the outpatient artificial pancreas: emulating day-by-day living. In *5th International Conference on Advanced Treatments & Technologies for Diabetes. February 8-11, Barcelona, Spain.*

León-Vargas, F., Carreras, A., García-Jaramillo, M., Bondia, J., and Vehí, J. (2013a). *Documentación presentada ante la Agencia Española de Medicamentos y Productos Sanitarios (AEMPS) para la validación del controlador a usar en la investigación clínica "Mejora de glicemia postprandial mediante un nuevo sistema de control en lazo cerrado". Esta investigación está enmarcado dentro del proyecto CLOSEDLOOP4MEAL.*

León-Vargas, F., Garelli, F., de Battista, H., and Vehí, J. (2013b). Adaptive pd controller with insulin-on-board limitation. *Biomedical Signal Processing and Control*, 8:724–732.

León-Vargas, F., Garelli, F., de Battista, H., and Vehí, J. (2013c). Safe tuning and improvement of the postprandial response in closed-loop blood glucose controllers. *Biomedical Signal Processing and Control*, Submitted.

León-Vargas, F., Prados, G., Bondia, J., and Vehí, J. (2010). Integrating closed loop algorithms development, in- silico validation and hardware implementation in a single framework. In *3rd International Conference On Advanced Technologies and Treatments For Diabetes. February 10-13, Basel, Switzerland.*

León-Vargas, F., Prados, G., Bondia, J., and Vehí, J. (2011a). A new virtual environment for testing and hardware implementation of closed-loop control algorithms in the artificial pancreas. In *Proceedings of the Annual International Conference of the IEEE Engineering in Medicine and Biology Society, EMBS*, pages 385–388.

León-Vargas, F., Prados, G., Bondia, J., and Vehí, J. (2011b). Platform for rapid prototyping design of closed-loop glycemic controllers in virtual patients of type 1 diabetes mellitus. In *Workshop on Control, Dynamics, Monitoring and Applications. February 7-9, Caldes de Montbui, Spain.*

Magni, L., Forgione, M., Toffanin, C., Dalla Man, C., Kovatchev, B., De Nicolao, G., and Cobelli, C. (2009a). Run-to-run tuning of model predictive control for type 1 diabetes subjects: In silico trial. *Journal of Diabetes Science and Technology*, 3(5):1091–1098.

Magni, L., Raimondo, D., Bossi, L., Dalla Man, C., De Nicolao, G., Kovatchev, B., and Cobelli, C. (2007). Model predictive control of type 1 diabetes: an in silico trial. *Journal of Diabetes Science and Technology*, 1(6):804–812.

Magni, L., Raimondo, D., Dalla Man, C., Breton, M., Patek, S., Nicolao, G., Cobelli, C., and Kovatchev, B. (2008). Evaluating the efficacy of closed-loop glucose regulation via control-variability grid analysis. *Journal of Diabetes Science and Technology*, 2(4):630–635.

Magni, L., Raimondo, D., Man, C. D., Nicolao, G. D., Kovatchev, B., and Cobelli, C. (2009b). Model predictive control of glucose concentration in type 1 diabetic patients: An in silico trial. *Biomedical Signal Processing and Control*, 4(4):338 – 346.

Makroglou, A., Li, J., and Kuang, Y. (2006). Mathematical models and software tools for the glucose-insulin regulatory system and diabetes: an overview. *Applied Numerical Mathematics*, 56:559–573.

Mang, A., Pill, J., Gretz, N., Kranzlin, B., Buck, H., Schoemaker, M., and Petrich, W. (2005). Biocompatibility of an electrochemical sensor for continuous glucose monitoring in subcutaneous tissue. *Diabetes Technology and Therapeutics*, 7:163–173.

Marchetti, G., Barolo, M., Jovanovič, L., Zisser, H., and Seborg, D. (2008a). A feedforward–feedback glucose control strategy for type 1 diabetes mellitus. *Journal of Process Control*, 18(2):149–162.

Marchetti, G., Barolo, M., Jovanovic, L., Zisser, H., and Seborg, D. (2008b). An improved PID switching control strategy for type 1 diabetes. *IEEE Transactions on Biomedical Engineering*, 55(3):857–865.

Mari, A. (2002). Mathematical modeling in glucose metabolism and insulin secretion. *Current Opinion in Clinical Nutrition and Metabolic Care*, 5(5):495–501.

Mauseth, R., Wang, Y., Dassau, E., Kircher, R., Matheson, D., Zisser, H., Jovanovic, L., and Doyle III, F. (2010). Proposed clinical application for tuning fuzzy logic controller of artificial pancreas utilizing a personalization factor. *Journal of Diabetes Science and Technology*, 4(4):913–922.

Maxim Integrated (2011). *Medical solutions guide.*

Mazze, R. S., Strock, E., Borgman, S., Wesley, D., Stout, P., and Racchini, J. (2009). Evaluating the accuracy, reliability, and clinical applicability of continuous glucose monitoring (cgm): is cgm ready for real time? *Diabetes Technology and Therapeutics*, 11(1):11–18.

Miller, S., Nimri, R., Atlas, E., Grunberg, E. A., and Phillip, M. (2011). Automatic learning algorithm for the md-logic artificial pancreas system. *Diabetes Technology and Therapeutics*, 13(10):983–990.

Moore, R. (1966). *Interval Analysis.* Prentice-Hall.

Moore, R. (1979). *Methods and Applications of Interval Analysis.* SIAM.

Murphy, H., Elleri, D., Allen, J., Harris, J., Simmons, D., Rayman, G., Temple, R., Dunger, D., Haidar, A., Nodale, M., Wilinska, M., and R, H. (2011a). Closed-loop insulin delivery during pregnancy complicated by type 1 diabetes. *Diabetes Care*, 34:406–411.

Murphy, H., Kumareswaran, K., Elleri, D., Allen, J., Caldwell, K., Biagioni, M., Simmons, D., Dunger, D., Nodale, M., Wilinska, M., Amiel, S., and Hovorka, R. (2011b). Safety and efficacy of 24 h closed-loop insulin delivery in well-controlled pregnant women with type 1 diabetes: a randomized crossover case series. *Diabetes Care*, 34(12):2527–2529.

Niederreiter, H. (1978). Quasi-monte carlo methods and pseudo-random numbers. *Bulletin of the American Mathematical Society*, 84(6):957–1041.

Nimri, R., Atlas, E., Ajzensztejn, M., Miller, S., Oron, T., and M, P. (2012). Feasibility study of automated overnight closed-loop glucose control under md-logic artificial pancreas in patients with type 1 diabetes: the dream project. *Diabetes Technology and Therapeutics*, 14:728–735.

Nimri, R., Weintrob, N., Benzaquen, H., Ofan, R., Fayman, G., and Phillip, M. (2006). Insulin pump therapy in youth with type 1 diabetes: A retrospective paired study. *Pediatrics*, 117(6):2126–2131.

Nucci, G. and Cobelli, C. (2000). Models of subcutaneous insulin kinetics. a critical review. *Computer Methods and Programs in Biomedicine*, 62:249–257.

Oliver, N. S., Toumazou, C., Cass, A. E. G., and Johnston, D. G. (2009). Glucose sensors: a review of current and emerging technology. *Diabetic Medicine*, 26(3):197–210.

Palerm, C. (2011). Physiologic insulin delivery with insulin feedback: A control systems perspective. *Computer Methods and Programs in Biomedicine*, 102(2):130–137.

Palerm, C., Zisser, H., Jovanovic, L., and Doyle, F. (2008). A run-to-run control strategy to adjust basal insulin infusion rates in type 1 diabetes. *Journal of Process Control*, 18(3-4):258–265.

Palerm, C. C., Zisser, H., Bevier, W. C., Jovanovic, L., and Doyle III, F. J. (2007). Prandial insulin dosing using run-to-run control: application of clinical data and medical expertise to define a suitable performance metric. *Diabetes Care*, 30(5):1131–1136.

Parker, R., Doyle III, F., Ward, J., and Peppas, N. (2000). Robust $H_\infty$ glucose control in diabetes using a physiological model. *AIChE Journal*, 46(12):2537–2549.

Percival, M., Wang, Y., Grosman, B., Dassau, E., Zisser, H., Jovanovič, L., and III, F. D. (2011). Development of a multi-parametric model predictive control algorithm for insulin delivery in type 1 diabetes mellitus using clinical parameters. *Journal of Process Control*, 21(3):391–404.

Peterson, D., Jones, D., Dupuis, A., Bernstein, R., and OŚhea, M. (1978). Feasibility of tight control of juvenile diabetes mellitus through patient-monitored glucose. *Diabetes*, 27(S2):437.

Pickup, J., Mattock, M., and Kerry, S. (2002). Glycaemic control with continuous subcutaneous insulin infusion compared with intensive insulin injections in patients with type 1 diabetes: meta-analysis of randomised controlled trials. *BMJ*, 324:705–708.

Puckett, W. (1992). *Dynamic Modeling of Diabetes Mellitus*. PhD thesis, University of Wisconsin-Madison, Department of Chemical Engineering.

Reichard, P., Nilsson, B., and Rosenqvist, U. (1993). The effect of long-term intensified insulin treatment on the development of microvascular complications of diabetes mellitus. *New England Journal of Medicine*, 329(5):304–309.

Renard, E., Costalat, G., Chevassus, H., and Bringer, J. (2006). Closed loop insulin delivery using implanted insulin pumps and sensors in type 1 diabetic patients. *Diabetes Research and Clinical Practice*, 74(2):S173–S177.

Renard, E., Place, J., Cantwell, M., Chevassus, H., and Palerm, C. (2010). Closed-loop insulin delivery using a subcutaneous glucose sensor and intraperitoneal insulin delivery: feasibility study testing a new model for the artificial pancreas. *Diabetes Care*, 33(1):121–127.

Retnakaran, R., Hochman, J., DeVries, J. H., Hanaire-Broutin, H., Heine, R. J., Melki, V., and Zinman, B. (2004). Continuous subcutaneous insulin infusion versus multiple daily injections: The impact of baseline a1c. *Diabetes Care*, 27(11):2590–2596.

Revert, A., Calm, R., Vehí, J., and Bondia, J. (2011). Calculation of the best basal-bolus combination for postprandial glucose control in insulin pump therapy. *IEEE Trans Biomed Eng., vol. 58, no. 2, pp. 274-271, 2011.*, 58 (2):274–281.

Revert, A., Garelli, F., Picó, J., Battista, H. D., Rossetti, P., Vehi, J., and Bondia, J. (2013). Safety auxiliary feedback element for the artificial pancreas in type 1 diabetes. *IEEE Trans Biomed Eng.*, In press.

Revert, A., Rossetti, P., Calm, R., Vehí, J., and Bondia, J. (2010). Combining basal-bolus insulin infusion for tight postprandial glucose control: An in silico evaluation in adults, children, and adolescents. *J. Diabetes Sci. Technol*, 4 (6):1424–1437.

Rossetti, P., Ampudia-Blasco, F. J., Laguna, A., Revert, A., Vehí, J., Ascaso, J. F., and Bondia, J. (2012). Evaluation of a novel continuous glucose monitoring-based method for mealtime insulin dosing the ibolus in subjects with type 1 diabetes using continuous subcutaneous insulin infusion therapy: a randomized controlled trial. *Diabetes Technology and Therapeutics*, 14(11):1043–1052.

Ruiz, J. L., Sherr, J. L., Cengiz, E., Carria, L., Roy, A., Voskanyan, G., Tamborlane, W. V., and Weinzimer, S. A. (2012). Effect of insulin feedback on closed-loop glucose control: A crossover study. *Journal of Diabetes Science and Technology*, 6(5):1123–1130.

Ruiz-Velázquez, E., Femat, R., and Campos-Delgado, D. U. (2004). Blood glucose control for type 1 diabetes mellitus: A robust tracking $h_\infty$ problem. *Control Engineering Practice*, 12(9):1179–1195. Cited By (since 1996): 74.

Schaller, H. C., Schaupp, L., Bodenlenz, M., Wilinska, M. E., Chassin, L. J., Wach, P., Vering, T., Hovorka, R., and Pieber, T. R. (2006). On-line adaptive algorithm with glucose prediction capacity for subcutaneous closed loop control of glucose: Evaluation under fasting conditions in patients with type 1 diabetes. *Diabetic Medicine*, 23:90–93.

Scheiner, G. and Boyer, B. A. (2005). Characteristics of basal insulin requirements by age and gender in type-1 diabetes patients using insulin pump therapy. *Diabetes Research and Clinical Practice*, 69:14–21.

Scheiner, G., Sobel, R. J., Smith, D. E., Pick, A. J., Kruger, D., King, J., and Green, K. (2009). Insulin pump therapy: Guidelines for successful outcomes. *The Diabetes Educator*, 35(2 suppl):29S–41S.

Schlessinger, L. and Eddy, D. (2002). Archimedes: a new model for simulating health care systems: the mathematical formulation. *Journal Biomedical Informatics*, 35:37–50.

Scholtz, H. E., Pretorius, S. G., Wessels, D. H., and Becker, R. H. A. (2005). Pharmacokinetic and glucodynamic variability: assessment of insulin glargine, nph insulin and insulin ultralente in healthy volunteers using a euglycaemic clamp technique. *Diabetologia*, 48(10):1988–1995.

Scully, T. (2012). Diabetes in numbers. *Nature*, 485:S2–S3.

Senior, P. A., Kin, T., Shapiro, J., and Koh, A. (2012). Islet transplantation at the university of alberta: Status update and review of progress over the last decade. *Canadian Journal of Diabetes*, 36(1):32–37.

Shashaj, B., Busetto, E., and Sulli, N. (2008). Benefits of a bolus calculator in pre- and postprandial glycaemic control and meal flexibility of paediatric patients using continuous subcutaneous insulin infusion (csii). *Diabetic Medicine*, 25(9):1036–1042.

Shaw, J. E., Sicreea, R. A., and Zimmeta, P. Z. (2010). Global estimates of the prevalence of diabetes for 2010 and 2030. *Diabetes Research and Clinical Practice*, 87(1):4–14.

Sherr, J. L., Cengiz, E., Palerm, C. C., Clark, B., Kurtz, N., Roy, A., Carria, L., Cantwell, M., Tamborlane, W. V., and Weinzimer, S. A. (2013). Reduced hypoglycemia and increased time in target using closed-loop insulin delivery during nights with or without antecedent afternoon exercise in type 1 diabetes. *Diabetes Care*.

Shetty, G. and Wolpert, H. (2010). Insulin pump use in adults with type 1 diabetes. *Diabetes Technol. Ther.*, 12 (Supp 1):S11–S16.

Shimoda, S., Nishida, K., Sakakida, M., Konno, Y., Ichinose, K., Uehara, M., Nowak, T., and Shichiri, M. (1997). Closed-loop subcutaneous insulin infusion algorithm with a short-acting insulin analog for long-term clinical application of a wearable artificial endocrine pancreas. *Frontiers of Medical and Biological Engineering*, 8(3):197–211.

Sorensen, J. T. (1985). *A physiological model of glucose metabolism in man and its use to design and assess improved insulin therapies for diabetes.* PhD thesis, Massachusetts Institute of Technology.

Soria, B., Skoudy, A., and Martín, F. (2001). From stem cells to beta cells: new strategies in cell therapy of diabetes mellitus. *Diabetologia*, 44(4):407–415.

Soru, P., De Nicolao, G., Toffanin, C., Dalla Man, C., Cobelli, C., and Magni, L. (2012). Mpc based artificial pancreas: Strategies for individualization and meal compensation. *Annual Reviews in Control*, 36:118–128.

Steil, G., Palerm, C., Kurtz, N., Voskanyan, G., Roy, A., Paz, S., and Kandeel, F. (2011). The effect of insulin feedback on closed loop glucose control. *Journal of Clinical Endocrinology & Metabolism*, 96(5):1402–1408.

Steil, G., Panteleon, A., and Rebrin, K. (2004). Closed-loop insulin delivery-the path to physiological glucose control. *Advanced Drug Delivery Reviews*, 56(2):125–144.

Steil, G., Rebrin, K., Darwin, C., Hariri, F., and Saad, M. (2006). Feasibility of automating insulin delivery for the treatment of type 1 diabetes. *Diabetes*, 55(12):3344–3350.

Stout, P., Racchini, J., and Hilgers, M. (2004). A novel approach to mitigating the physiological lag between blood and interstitial fluid glucose measurements. *Diabetes Technology and Therapeutics*, 6(5):635–644.

Takahashi, D., Xiao, Y., Hu, F., and Lewis, M. (2008). A survey of insulin-dependent diabetes - part i: Therapies and devices. *International Journal of Telemedicine and Applications.*

Tarin, C., Teufel, E., Pico, J., Bondia, J., and Pfleiderer, H. (2005). Comprehensive pharmacokinetic model of insulin Glargine and other insulin formulations. *IEEE Transactions on Biomedical Engineering*, 52(12):1994–2005.

Tavris, D. and Shoaibi, A. (2004). The public health impact of the minimed continuous glucose monitoring system (cgms)-an assessment of the literature. *Diabetes Technology and Therapeutics*, 6(4):518–522.

Trajanoski, Z. and Wach, P. (1996). Fuzzy filter for state estimation of a glucoregulatory system. *Comput Methods Programs Biomed*, 50(3):265–273.

Trajanoski, Z. and Wach, P. (1998). Neural predictive controller for insulin delivery using the subcutaneous route. *IEEE Transactions on Biomedical Engineering*, 45(9):1122–1134.

Turksoy, K., Bayrak, E. S., Quinn, L., Littlejohn, E., and Cinar, A. (2013a). Adaptive multivariable closed-loop control of blood glucose concentration in patients with type 1 diabetes [paper number tua19.1]. *Accepted to the American Control Conference, Washington, DC.*

Turksoy, K., Bayrak, E. S., Quinn, L., Littlejohn, E., and Cinar, A. (2013b). Multivariable Adaptive Closed-Loop Control of an Artificial Pancreas Without Meal and Activity Announcement. *Diabetes Technology & Therapeutics*, pages 386–400.

Valla, V. (2010). Therapeutics of diabetes mellitus: Focus on insulin analogues and insulin pumps. *Experimental Diabetes Research*, 2010:14 pages.

Walsh, J. and Roberts, R. (2006). *Pumping insulin: everything you need for success on a smart insulin pump.* Torrey Pines Pr.

Walsh, J., Roberts, R., and Bailey, T. (2010). Guidelines for insulin dosing in continuous subcutaneous insulin infusion using new formulas from a retrospective study of individuals with optimal glucose levels. *Journal of Diabetes Science and Technology*, 4(5):1174–1181.

Walsh, J., Roberts, R., and Bailey, T. (2011). Guidelines for optimal bolus calculator settings in adults. *Journal of Diabetes Science and Technology*, 5(1):129–135.

Wang, Y., Dassau, E., and Doyle III, F. J. (2010a). Closed-loop control of artificial pancreatic b-cell in type 1 diabetes mellitus using model predictive iterative learning control. *IEEE Transactions on Biomedical Engineering*, 57(2):211–219.

Wang, Y., Dassau, E., Zisser, H., Jovanovic, L., and Doyle III, F. (2010b). Automatic bolus and adaptive basal algorithm for the artificial pancreatic $\beta$-cell. *Diabetes Technology & Therapeutics*, 12(11):879–887.

Wang, Y., Percival, M., Dassau, E., Zisser, H., Jovanoviè, L., , and III, F. D. (2009). A novel adaptive basal therapy based on the value and rate of change of blood glucose. *J. Diabetes Sci. Technol*, 3 (5):1099–1109.

Ward, W., Castle, J., and El, Y. (2011). Safe glycemic management during closed-loop treatment of type 1 diabetes: the role of glucagon, use of multiple sensors and compensation for stress hyperglycemia. *Journal of Diabetes Science and Technology*, 5:1373–1380.

Ward, W., Wood, M., Casey, H., Quinn, M., and Federiuk, I. (2005). An implantable subcutaneous glucose sensor array in ketosis-prone rats: Closed loop glycemic control. *Artificial Organs*, 29:131–143.

Weinstock, R. S. (2011). Closing the loop: Another step forward. *Diabetes Care*, 34(9):2136–2137.

Weinzimer, S., Steil, G., Swan, K., Dziura, J., Kurtz, N., and Tamborlane, W. (2008a). Fully automated closed-loop insulin delivery versus semiautomated hybrid control in pediatric patients with type 1 diabetes using an artificial pancreas. *Diabetes Care*, 31(5):934–939.

Weinzimer, S., Steil, G., Swan, K., Dziura, J., Kurtz, N., and Tamborlane, W. (2008b). Fully automated closed-loop insulin delivery versus semiautomated hybrid control in pediatric patients with type 1 diabetes using an artificial pancreas. *Diabetes Care*, 31(5):934–939.

Whiting, D., Guariguata, L., Weil, C., and Shaw, J. (2011). Global estimates of the prevalence of diabetes for 2011 and 2030. *Diabetes Research and Clinical Practice*, 94(3):311–321.

Wilinska, M., Chassin, L., Acerini, C., Allen, J., Dunger, D., and Hovorka, R. (2010). Simulation environment to evaluate closed-loop insulin delivery systems in type 1 diabetes. *Journal of diabetes science and technology*, 4(1):132.

Wilinska, M., Chassin, L., Schaller, H., Schaupp, L., Pieber, T., and Hovorka, R. (2005). Insulin kinetics in type-1 diabetes: continuous and bolus delivery of rapid acting insulin. *IEEE Transactions on Biomedical Engineering*, 52(1):3–12.

Wilinska, M. E. and Hovorka, R. (2008). Simulation models for in silico testing of closed-loop glucose controllers in type 1 diabetes. *Drug Discovery Today: Disease Models*, 5(4):289–298.

Wilson, D. (1999). Diabetes simulators: Ready for prime time? *Diabetes Technology & Therapeutics*, 1(1):55–56.

Zisser, H., Bevier, W., Dassau, E., and Jovanovic, L. (2010a). Siphon effects on continuous subcutaneous insulin infusion pump delivery performance. *Journal of Diabetes Science and Technology*, 4 (1):98–103.

Zisser, H., Jovanovic, L., Doyle III, F. J., Ospina, P., and Owens, C. (2005). Run-to-run control of meal-related insulin dosing. *Diabetes Technology and Therapeutics*, 7(1):48–57.

Zisser, H., Robinson, L., Bevier, W., Dassau, E., Ellingsen, C., Doyle III, F., and Jovanovic, L. (2008a). Bolus calculator: a review of four "Smart" insulin pumps. *Diabetes Technology & Therapeutics*, 10(6):441–444.

Zisser, H., Shwartz, S., Rather, R., Wise, J., and Bailey, T. (2008b). Accuracy of a seven-day continuous glucose sensor compared to ysi blood glucose values. In *In Proceedings of the 27th workshop of the AIDPIT Study Group*.

Zisser, H., Wagner, R., Pleus, S., Haug, C., Jendrike, N., Parkin, C., Schweitzer, M., and Freckmann, G. (2010b). Clinical performance of three bolus calculators in subjects with type 1 diabetes mellitus: A head-to-head-to-head comparison. *Diabetes Technol. Ther.*, 12 (2):955–961.